

# **Carbon–Hydrogen Bond and Carbon–Carbon Bond Activation of Alkanes with Rhodium Porphyrins**

CHAN, Yun Wai

A Thesis Submitted  
in Partial Fulfilment of the Requirements for the Degree of  
Doctor of Philosophy  
in  
Chemistry

The Chinese University of Hong Kong

August 2010

UMI Number: 3483858

All rights reserved

**INFORMATION TO ALL USERS**

The quality of this reproduction is dependent upon the quality of the copy submitted.

In the unlikely event that the author did not send a complete manuscript and there are missing pages, these will be noted. Also, if material had to be removed, a note will indicate the deletion.



UMI 3483858

Copyright 2011 by ProQuest LLC.

All rights reserved. This edition of the work is protected against unauthorized copying under Title 17, United States Code.



ProQuest LLC  
789 East Eisenhower Parkway  
P.O. Box 1346  
Ann Arbor, MI 48106-1346

Thesis/Assessment Committee

Professor MAK, Thomas Chung Wai (Chair)

Professor CHAN, Kin Shing (Thesis Supervisor)

Professor CHOW, Hak Fun (Committee Member)

Professor LAU, Tai-Chu (External Examiner)

# Table of Contents

|   | Page     |
|---|----------|
| Table of Contents   | i        |
| Acknowledgements  | v        |
| Abbreviations   | vi       |
| Structural Abbreviations for Porphyrin Complexes                        | vii      |
| Abstract  | viii     |
| <b>Chapter 1 General Introduction</b>                                   | <b>1</b> |
| 1.1 General Introduction to Alkanes                                     | 1        |
| 1.1.1 Bond Strength   | 1        |
| 1.1.2 Steric Strain   | 2        |
| 1.2 Activation and Functionalization of Alkanes by Transition Metals    | 2        |
| 1.2.1 Importance of Alkane Activation                                   | 3        |
| 1.2.2 Challenges of CHA and CCA   | 5        |
| 1.2.2.1 Difficulties of Alkane CHA                                      | 5        |
| 1.2.2.2 Difficulties of Alkane CCA                                      | 6        |
| 1.3 Carbon-Hydrogen Activation of Alkanes by Transition Metal Complexes | 7        |
| 1.3.1 Stoichiometric CHA of Alkane by Transition Metal Complexes        | 7        |
| 1.3.1.1 Electrophilic Activation  | 7        |
| 1.3.1.2 Oxidation Addition  | 8        |
| 1.3.1.3 $\sigma$ -Bond Metathesis                                       | 10       |
| 1.3.1.4 Homolytic Cleavage (Radical Pathway)                            | 10       |
| 1.3.1.5 1,2-Addition of C-H Bond across M=X                             | 11       |
| 1.3.2 Catalytic CHA of Alkane with Transition Metal Complexes           | 12       |
| 1.4 Carbon-Carbon Activation by Transition Metal Complexes              | 14       |
| 1.4.1 Ring Strain Relief  | 14       |
| 1.4.2 Aromaticity Driven CCA  | 15       |
| 1.4.3 Intramolecular CCA in Pincer-Type System                          | 15       |
| 1.4.4 Chelation-Assisted Intermolecular CCA of Imine                    | 16       |
| 1.4.5 Intermolecular CCA of Carbonyl                                    | 17       |
| 1.4.6 Intramolecular $\beta$ -Alkyl Elimination                         | 18       |
| 1.4.6.1 Intramolecular $\beta$ -Alkyl Elimination of Metal Alkyl        | 18       |
| 1.4.6.2 Intramolecular $\beta$ -Alkyl Elimination of Metal Alkoxide     | 19       |
| 1.4.6.3 Intramolecular $\beta$ -Alkyl Elimination of Metal Amido        | 19       |
| 1.4.7 CCA by Alkane Metathesis  | 20       |
| 1.4.8 CCA by Nucleophilic Attack  | 22       |
| 1.4.9 Catalytic CCA of Alkane with Transition Metal Complexes           | 23       |
| 1.5 Porphyrins and Metalloporphyrins                                    | 24       |
| 1.5.1 Porphyrin Ligands   | 24       |
| 1.5.2 Metalloporphyrins   | 25       |

|                  |         |  |           |
|------------------|---------|--|-----------|
|                  | 1.5.3   | Structural Features of Metalloporphyrins   | 27        |
|                  | 1.5.4   | Vacant Coordination Sites of Metalloporphyrins   | 28        |
|                  | 1.5.5   | Chemistry of Metalloporphyrins   | 28        |
| 1.6              |         | Chemistry of Rhodium Porphyrin Complexes   | 30        |
|                  | 1.6.1   | Rh <sup>I</sup> (por) Chemistry  | 30        |
|                  | 1.6.2   | Rh <sup>II</sup> (por) Chemistry   | 31        |
|                  | 1.6.3   | Rh <sup>III</sup> (por) Chemistry  | 34        |
| 1.7              |         | Scope of Thesis  | 36        |
| <b>Chapter 2</b> |         | <b>Base-promoted Carbon–Hydrogen Bond Activation of Alkanes with Rhodium(III) Porphyrin Complexes</b>                        | <b>45</b> |
| 2.1              |         | Carbon–Hydrogen Bond Activation of Alkanes with Rhodium(III) Porphyrin Complexes   | 45        |
| 2.2              |         | Objectives of the Work   | 46        |
| 2.3              |         | Preparation of Starting Materials  | 46        |
|                  | 2.3.1   | Preparation of Porphyrins  | 46        |
|                  | 2.3.2   | Preparation of Rhodium Porphyrin Complexes   | 47        |
|                  | 2.3.2.1 | Synthesis of Rh(tpp)Cl, Rh(tpp)Cl and Rh(bocp)Cl   | 47        |
|                  | 2.3.2.2 | Synthesis of Rh(tpp)H  | 47        |
|                  | 2.3.2.3 | Synthesis of Rh <sub>2</sub> (tpp) <sub>2</sub>  | 47        |
|                  | 2.3.2.4 | Synthesis of Rh(tpp) <sup>-</sup> Na <sup>+</sup>  | 47        |
| 2.4              |         | Optimization of Reaction Conditions  | 48        |
|                  | 2.4.1   | Temperature Effect   | 48        |
|                  | 2.4.2   | Base Effect  | 48        |
|                  | 2.4.3   | Ligand Effect  | 50        |
| 2.5              |         | Base-promoted CHA of Alkanes   | 51        |
| 2.6              |         | Stability of Rh(tpp)Alkyls   | 52        |
|                  | 2.6.1   | Stability of Rh(tpp)( <i>c</i> -pentyl) with Base  | 52        |
|                  | 2.6.2   | Stability of Rh(tpp)( <i>c</i> -hexyl) with Base   | 56        |
|                  | 2.6.3   | Stability of Rh(tpp)( <i>n</i> -hexyl) with Base   | 57        |
| 2.7              |         | X-ray Structure Determination  | 58        |
| 2.8              |         | Mechanistic Studies  | 63        |
|                  | 2.8.1   | Proposed Mechanism for CHA   | 63        |
|                  | 2.8.2   | Alkyl CHA in the Absence of Base   | 63        |
|                  | 2.8.3   | Base-promoted CHA  | 64        |
|                  | 2.8.4   | Kinetic Isotope Effect of Alkyl CHA  | 67        |
|                  | 2.8.5   | Reactivity Studies of Proposed Intermediates   | 68        |
|                  | 2.8.6   | Recent Finding in Rh(tpp)OH  | 71        |
| 2.9              |         | Conclusion   | 71        |
| <b>Chapter 3</b> |         | <b>Metalloradical-promoted Functionalization of Cycloheptane to Rhodium Porphyrin Benzyl via C–H and C–C Bond Activation</b> | <b>76</b> |
| 3.1              |         | Introduction   | 76        |
|                  | 3.1.1   | Properties of Cycloheptane   | 76        |
|                  | 3.1.2   | CHA of Cycloheptane  | 77        |
|                  | 3.1.3   | CCA of Cycloheptane  | 77        |
| 3.2              |         | Objectives of the Work   | 78        |
| 3.3              |         | Discovery of CCA of <i>c</i> -Heptane  | 78        |
| 3.4              |         | Mechanistic Investigation  | 79        |

|                  |       |  |     |
|------------------|-------|--|-----|
|                  | 3.4.1 | Reaction Time Profile  | 79  |
|                  | 3.4.2 | Reactivity of $\text{Rh}_2(\text{ttp})_2$ and $\text{Rh}(\text{ttp})\text{H}$ with <i>c</i> -Heptane                           | 81  |
|                  | 3.4.3 | Conversion of $\text{Rh}(\text{ttp})(c\text{-heptyl})$ to $\text{Rh}(\text{ttp})\text{Bn}$                                     | 81  |
| 3.5              |       | Proposed Mechanistic Pathways  | 88  |
|                  | 3.5.1 | Conversion of $\text{Rh}(\text{ttp})(c\text{-heptyl})$ to $\text{Rh}(\text{ttp})\text{Bn}$ via $\gamma\text{-H}^+$ Elimination | 88  |
|                  | 3.5.2 | Conversion of $\text{Rh}(\text{ttp})(c\text{-heptyl})$ to $\text{Rh}(\text{ttp})\text{Bn}$ via $\beta$ -Alkyl Migration        | 90  |
|                  | 3.5.3 | Conversion of $\text{Rh}(\text{ttp})(c\text{-heptyl})$ to $\text{Rh}(\text{ttp})\text{Bn}$ via $\beta\text{-H}^+$ Elimination  | 90  |
| 3.6              |       | Mechanistic Studies of Conversion of $\text{Rh}(\text{ttp})(\text{cycloheptatrienyl})$ to $\text{Rh}(\text{ttp})\text{Bn}$     | 95  |
|                  | 3.6.1 | $^1\text{H}$ NMR Kinetics  | 95  |
|                  | 3.6.2 | Determination of Reaction Order and Rate Constant  | 95  |
|                  | 3.6.3 | Activation Parameters  | 98  |
|                  | 3.6.4 | Promoting Effects of Additives   | 102 |
| 3.7              |       | Overall Proposed Mechanism   | 107 |
| 3.8              |       | Conclusion   | 109 |
| <b>Chapter 4</b> |       | <b>Metalloradical-Catalyzed Aliphatic Carbon–Carbon Bond Activation of Cyclooctane</b>   | 112 |
|                  | 4.1   | Introduction   | 112 |
|                  | 4.1.1 | Properties of Cyclooctane  | 112 |
|                  | 4.1.2 | CHA of <i>c</i> -Octane  | 113 |
|                  | 4.1.3 | CCA of <i>c</i> -Octane  | 113 |
|                  | 4.2   | Objectives of the Work   | 114 |
|                  | 4.3   | Discovery of CCA of <i>c</i> -Octane   | 114 |
|                  | 4.4   | Mechanistic Investigation  | 116 |
|                  | 4.4.1 | Conversion of CHA Product $\text{Rh}(\text{ttp})(c\text{-octyl})$ to CCA Product $\text{Rh}(\text{ttp})(n\text{-octyl})$       | 116 |
|                  | 4.4.2 | Reaction Time Profile  | 121 |
|                  | 4.4.3 | Reactivity of Intermediates $\text{Rh}(\text{ttp})\text{H}$ and $\text{Rh}_2(\text{ttp})_2$ towards <i>c</i> -Octane           | 126 |
|                  | 4.5   | Proposed Mechanism of $\text{Rh}^{\text{II}}(\text{ttp})$ -Catalyzed CCA of <i>c</i> -Octane                                   | 127 |
|                  | 4.5.1 | Synergetic Effect of $\text{Rh}(\text{ttp})\text{H}/\text{Rh}_2(\text{ttp})_2$ in CCA of <i>c</i> -Octane                      | 131 |
|                  | 4.5.2 | Steric of Porphyrin  | 132 |
|                  | 4.6   | Conclusion   | 133 |
| <b>Chapter 5</b> |       | <b>Comparison of CHA and CCA of Various Cycloalkanes</b>   | 137 |
|                  | 5.1   | Thermodynamics Consideration of CHA and CCA of Cycloalkanes  | 138 |
|                  | 5.2   | Kinetic Consideration of CHA and CCA of Cycloalkanes   | 141 |
|                  | 5.3   | Consideration of $\text{Rh}(\text{ttp})\text{Bn}$ Formation  | 144 |
|                  | 5.4   | Thermodynamic Consideration of CHA and CCA of <i>n</i> -Alkanes  | 145 |
|                  | 5.5   | Kinetic Consideration of CHA and CCA of <i>n</i> -Alkanes  | 147 |

|                  |                              |     |
|------------------|------------------------------|-----|
| 5.6              | Conclusion                   | 149 |
| <b>Chapter 6</b> | <b>Experimental Sections</b> | 151 |
|                  | Appendix                     | 191 |
|                  | List of Spectra              | 213 |
|                  | Spectra                      | 215 |

## Acknowledgement

First and foremost, I would like to express my most sincere gratitude to my supervisor, Professor Kin Shing Chan, for his invaluable advice, patient guidance, enthusiasm and continuous encouragement throughout my research work. He inspired me much in applying fundamental chemical knowledge in my research.

Thanks are also given to all my dear former group members: Dr. Siu Kwan Yeung, Dr. Lirong Zhang, Dr. Xinzhu Li, Dr. Tsz Ho Lai, Dr. Yin Ki Jenkins Tsang, Ms. Cheuk Man Lau, Mr. Peng Fai Chiu, Ms. Xu Song and Mr. Man Ho Lee. I also thank my current group members in Chan's group for helpful discussion and encouragement, especially Dr. Bao Zhu Li, Mr. Chi Wai Cheung, Mr. Kwong Shing Choi, Mr. Hong Sang Fung, Ms. Ching Chi Au, Ms. Siu Yin Lee, Ms. Ying Ying Qian, Mr. Ching Tat To and Mr. Chun Sum Chan.

I appreciate so much the selfless help from all members of the Department of Chemistry and technical support in all circumstances, especially Ms. Hoi Shan Chan for X-ray crystallographic determination, and Mr. Chi Chun Lee and Ms. Hau Yan Ng for mass spectrometric analysis.

I have to express my thanks to my family for their unfailing support and care. Without their love and understanding, I would not be able to finish the course of my study.

May, 2010.

Yun Wai Chan

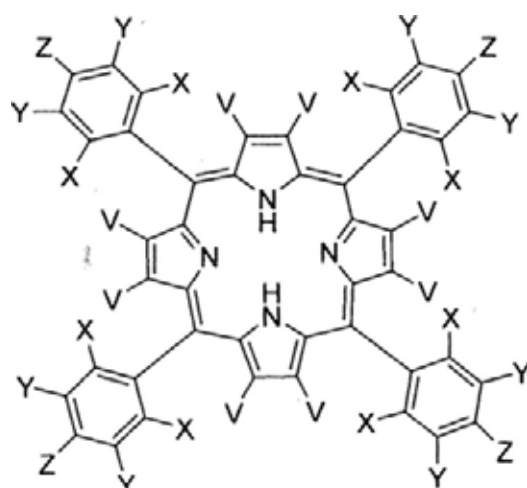
Department of Chemistry

The Chinese University of Hong Kong

## Abbreviations

|                 |   |                 |                              |
|-----------------|---|-----------------|------------------------------|
| $\delta$        | : chemical Shift                          | m               | : multiplet (NMR)            |
| Anal            | : analytical                              | M <sup>+</sup>  | : molecular ion              |
| Ar              | : Aryl                                    | M               | : molarity                   |
| Bn              | : benzyl                                  | Me              | : methyl                     |
| BDE.            | : bond dissociation energy                | mg              | : milligram (s)              |
| br              | : broad singlet (NMR)                     | min             | : minute (s)                 |
| <sup>t</sup> Bu | : <i>tert</i> -butyl                      | mL              | : milliliter (s)             |
| Bz              | : benzyl                                  | mmol            | : milimole (s)               |
| Calcd.          | : calculated                              | MS              | : mass spectrometry          |
| CCA             | : carbon carbon bond activation           | NBS             | : <i>N</i> -bromosuccinimide |
| CHA             | : carbon hydrogen bond activation         | nm              | : nanometer                  |
| COD             | : 1,5-cyclooctadiene                      | NMR             | : nuclear magnetic resonance |
| Cp              | : cyclopentadienyl                        | OAc             | : acetate anion              |
| d               | : day (s)                                 | Por             | : porphyrin dianion          |
| d               | : doublet (NMR)                           | ppm             | : part per million           |
| DMF             | : <i>N,N</i> -dimethylformamide           | Ph              | : phenyl                     |
| <i>e.e.</i>     | : enantiomeric excess                     | PhCN            | : benzonitrile               |
| E               | : enthalpy                                | <sup>i</sup> Pr | : isopropyl                  |
| Et              | : ethyl                                   | Py              | : pyridine                   |
| FABMS           | : fast atom bombardment mass spectrometry | q               | : quartet (NMR)              |
| ESI             | : Electrospray ionization                 | qu              | : quintet (NMR)              |
| g               | : gram (s)                                | R               | : alkyl group                |
| G               | : Gibbs free energy                       | r.t.            | : room temperature           |
| h               | : hour (s)                                | s               | : second (s)                 |
| HRMS            | : highest resolution mass spectrometry    | s               | : singlet (NMR)              |
| Hz              | : Hertz                                   | S               | : entropy                    |
| IR              | : infrared                                | TEMPO           | : tetramethylpiperidinoxy    |
| <i>J</i>        | : coupling constant                       | THF             | : tetrahydrofuran            |
| K               | : equilibrium constant                    | t               | : triplet (NMR)              |
|                 |   | TLC             | : thin-layer chromatography  |
|                 |   | TMS             | : tetramethylsilane          |

## Structural Abbreviations for Porphyrins

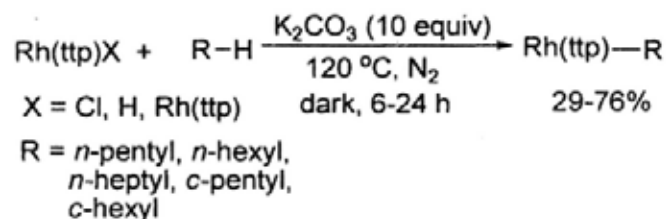


Nomenclature of Porphyrins

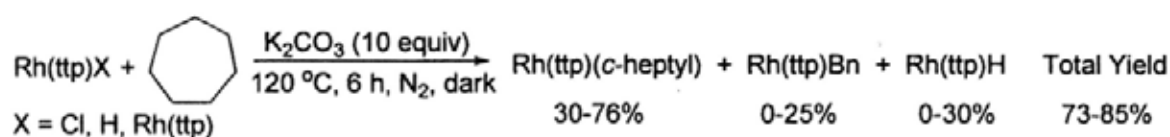
| Abbreviations         | Porphyrin   | Substituents |    |   |                 |
|-----------------------|---|--------------|----|---|-----------------|
|                       |   | V            | X  | Y | Z               |
| H <sub>2</sub> (ttp)  | 5,10,15-20-tetratolylporphyrin  | H            | H  | H | Me              |
| H <sub>2</sub> (tpp)  | 5,10,15-20-tetraphenylporphyrin   | H            | H  | H | H               |
| H <sub>2</sub> (btp)  | 5,10,15-20-tetrakis( <i>p-t</i> -butylphenyl)porphyrin                                | H            | H  | H | <sup>t</sup> Bu |
| H <sub>2</sub> (bocp) | 2,3,7,8,12,13,17,18-Octachloro-5,10,15-20-tetrakis( <i>p-t</i> -butylphenyl)porphyrin | Cl           | H  | H | <sup>t</sup> Bu |
| H <sub>2</sub> (oep)  | 2,3,7,8,12,13,17,18-octaethylporphyrin  | Et           | H  | H | H               |
| H <sub>2</sub> (tmp)  | 5,10,15-20-tetramesitylporphyrinato   | H            | Me | H | Me              |

## Abstract

The objectives of this research focus on the investigation of carbon-hydrogen bond activation (CHA) and carbon-carbon bond activation (CCA) of alkanes by rhodium porphyrin complexes as well as the mechanistic understanding.

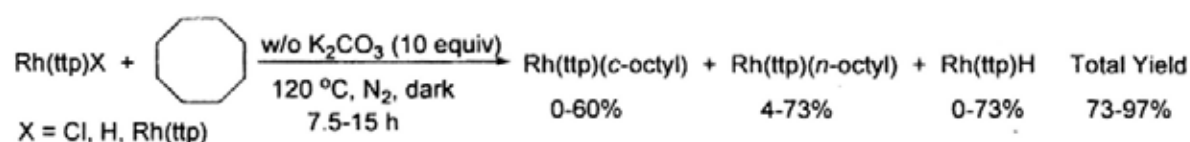


Base-promoted CHA of unstrained alkanes with 5,10,15,20-tetratolylporphyrinorhodium complexes,  $\text{Rh}(\text{ttp})\text{X}$  ( $\text{X} = \text{Cl, H, Rh}(\text{ttp})$ ), has been achieved.  $\text{Rh}(\text{ttp})\text{Cl}$ , reacted with *n*-pentane, *n*-hexane, *n*-heptane, *c*-pentane and *c*-hexane in the presence of potassium carbonate at 120 °C in 6 to 24 h to give rhodium porphyrin alkyls,  $\text{Rh}(\text{ttp})\text{R}$ , in 29-76% yields. Mechanistic investigations suggested that  $\text{Rh}_2(\text{ttp})_2$  and  $\text{Rh}(\text{ttp})\text{H}$  are key intermediates for the parallel CHA step. The roles of base are (i) to facilitate the formation of  $\text{Rh}(\text{ttp})\text{Y}$  ( $\text{Y}^- = \text{OH}^-, \text{KCO}_3^-$ ), (ii) to enhance the CHA rate with alkane and generate  $\text{Rh}(\text{ttp})\text{H}$  by a  $\text{Rh}(\text{ttp})\text{Y}$  species which is more reactive than  $\text{Rh}(\text{ttp})\text{Cl}$ , and (iii) to provide a parallel CHA pathway by  $\text{Rh}_2(\text{ttp})_2$ .



$\text{K}_2\text{CO}_3$ -promoted CHA of the ring-strained cycloheptane with  $\text{Rh}(\text{ttp})\text{Cl}$  at 120 °C in 6 h gave the CHA product  $\text{Rh}(\text{ttp})(c\text{-heptyl})$  and together with, unexpectedly, the CCA product  $\text{Rh}(\text{ttp})\text{Bn}$ , in 30% and 24% yields, respectively. Mechanistic studies revealed that  $\text{Rh}(\text{ttp})(c\text{-heptyl})$  undergoes  $\beta$ -hydride elimination in neutral condition or  $\beta$ -proton elimination in basic condition followed by reprotonation to give rhodium(III) porphyrin hydride,  $\text{Rh}(\text{ttp})\text{H}$ , and *c*-heptene. Successive base-promoted CHA of *c*-heptene with  $\text{Rh}(\text{ttp})\text{H}$ , followed by  $\beta$ -proton elimination, generates cycloheptatriene. The CHA of cycloheptatriene with  $\text{Rh}(\text{ttp})\text{H}$  formed

Rh(ttp)(*c*-heptatrienyl), which underwent rearrangement with carbon-carbon cleavage at 120 °C in 16 d to yield Rh(ttp)Bn in 96% yield.



*c*-Octane reacted with Rh(ttp)Cl at 120 °C in 7.5 h in the presence of K<sub>2</sub>CO<sub>3</sub> to yield Rh(ttp)(*n*-octyl) and Rh(ttp)H in 33% and 58% yields, respectively. Mechanistic investigations indicate that the CCA product is generated from the Rh<sup>II</sup>(ttp)-catalyzed 1,2-addition of *c*-octane with Rh(ttp)H. Reaction of *c*-octane and Rh(ttp)H/Rh<sub>2</sub>(ttp)<sub>2</sub> (10:1) selectively yielded Rh(ttp)(*n*-octyl) in 73% at 120 °C in 15 h. The catalyst Rh<sup>II</sup>(ttp) radical cleaves the C-C bond of *c*-octane to form to a Rh(ttp)-alkyl radical, which then abstracts a hydrogen atom from Rh(ttp)H to generate the Rh(ttp)(*n*-octyl), and subsequently leading to regeneration of the Rh<sup>II</sup>(ttp) radical.

## 摘要

本論文主要研究了銻卟啉絡合物與烷烴進行碳-氫鍵和碳-碳鍵的活化反應，同時對反應過程的機理進行了探討。

在鹼的促進作用下，銻卟啉絡合物， $\text{Rh}(\text{ttp})\text{X}$  ( $\text{X} = \text{Cl}, \text{H}, \text{Rh}(\text{ttp})$ )，可與無張力的烷烴進行碳氫鍵活化反應。在  $120\text{ }^\circ\text{C}$ ，添加碳酸鉀的條件下， $\text{Rh}(\text{ttp})\text{X}$  可以與正戊烷，正己烷，正庚烷，環戊烷以及環己烷進行反應，經過 6-24 h 得到相應的銻卟啉烷基絡合物， $\text{Rh}(\text{ttp})\text{R}$ ，其產率為 29-76%。機理研究表明， $\text{Rh}_2(\text{ttp})_2$  及  $\text{Rh}(\text{ttp})\text{H}$  可以分別與烷烴進行碳氫鍵活化反應，因此它們都是關鍵的碳氫鍵活化的中間體。鹼的作用在於：(i) 促進  $\text{Rh}(\text{ttp})\text{Y}$  ( $\text{Y} = \text{OH}^-, \text{KCO}_3^-$ ) 的形成；(ii) 與  $\text{Rh}(\text{ttp})\text{Cl}$  相比， $\text{Rh}(\text{ttp})\text{Y}$  具有更高的反應活性，從而促進  $\text{Rh}(\text{ttp})\text{H}$  的產生，提高烷烴碳氫鍵活化的速度；(iii) 促進  $\text{Rh}_2(\text{ttp})_2$  的形成，為碳氫鍵活化反應提供一個平行過程。

碳酸鉀可以促進  $\text{Rh}(\text{ttp})\text{Cl}$  與具有環張力的環庚烷進行碳氫鍵活化反應，在  $120\text{ }^\circ\text{C}$  條件下，經過 6 h，得到碳氫鍵活化產物， $\text{Rh}(\text{ttp})(c\text{-heptyl})$ ，其產率為 30%；同時意外得到了碳碳鍵活化的產物  $\text{Rh}(\text{ttp})\text{Bn}$ ，其產率為 24%。機理研究顯示  $\text{Rh}(\text{ttp})(c\text{-heptyl})$  在中性條件下可進行  $\beta$ -氫消除，或者在鹼性條件下進行  $\beta$ -質子消除，隨後通過質子化作用，從而產生三價銻卟啉氫化物， $\text{Rh}(\text{ttp})\text{H}$ ，以及環庚烯。在鹼的促進作用下， $\text{Rh}(\text{ttp})\text{H}$  與環庚烯進行連續的碳氫鍵活化反應，隨後進行  $\beta$ -質子消除，產生環庚三烯。 $\text{Rh}(\text{ttp})\text{H}$  與環庚三烯進行碳氫鍵活化反應，形成  $\text{Rh}(\text{ttp})(c\text{-heptatrienyl})$ 。在  $120\text{ }^\circ\text{C}$  條件下， $\text{Rh}(\text{ttp})(c\text{-heptatrienyl})$  通過重排作用，發生碳碳鍵斷裂反應，經過 16 d，得到  $\text{Rh}(\text{ttp})\text{Bn}$ ，其產率為 96%。

在  $120\text{ }^\circ\text{C}$ ，添加碳酸鉀的條件下，環辛烷與  $\text{Rh}(\text{ttp})\text{Cl}$  反應，經過 7.5 h，得到  $\text{Rh}(\text{ttp})(n\text{-octyl})$  以及  $\text{Rh}(\text{ttp})\text{H}$ ，其產率分別為 33% 及 58%。機理研究表明， $\text{Rh}(\text{ttp})\text{H}$  與環辛烷在  $\text{Rh}^{\text{II}}(\text{ttp})$  的催化作用下可以進行 1, 2-加成反應，從而得到碳碳鍵活化的產物。在  $120\text{ }^\circ\text{C}$  條件下，環辛烷與  $\text{Rh}(\text{ttp})\text{H}/\text{Rh}_2(\text{ttp})_2$  (10:1) 進行反應，經過 15 h，選擇性的得到了  $\text{Rh}(\text{ttp})(n\text{-octyl})$ ，其產率為 73%。環辛烷的碳碳鍵在催化劑  $\text{Rh}^{\text{II}}(\text{ttp})$  游離基的作用下斷裂，從而形成銻卟啉烷基游離基。然後銻卟啉烷基游離基從  $\text{Rh}(\text{ttp})\text{H}$  上得到一個氫原子，形成  $\text{Rh}(\text{ttp})(n\text{-octyl})$ ，並再次產生銻卟啉游離基。

## Chapter 1 General Introduction

### 1.1 General Introduction to Alkanes

#### 1.1.1 Bond Strength

Alkanes are non-polar saturated hydrocarbons which are made of either strong C–H or C–C single bonds with bond dissociation energy over  $80 \text{ kcal mol}^{-1}$  (Tables 1.1 and 1.2).<sup>1,2</sup> As a result, they are usually chemically inert.

Table 1.1 C–H Bond Dissociation Energies (BDE) of Some Alkane Molecules<sup>2</sup>

| C–H bond of Alkane                          | BDE ( $\text{kcal mol}^{-1}$ ) | C–H bond of Alkane                          | BDE ( $\text{kcal mol}^{-1}$ ) |
|---|--------------------------------|---|--------------------------------|
| CH <sub>3</sub> –H                          | 105.0                          | <i>c</i> -C <sub>3</sub> H <sub>5</sub> –H  | 106                            |
| CH <sub>3</sub> CH <sub>2</sub> –H          | 100.5                          | <i>c</i> -C <sub>4</sub> H <sub>7</sub> –H  | 96.8                           |
| <i>n</i> -C <sub>3</sub> H <sub>7</sub> –H  | 100.9                          | <i>c</i> -C <sub>5</sub> H <sub>9</sub> –H  | 95.6                           |
| <i>n</i> -C <sub>4</sub> H <sub>9</sub> –H  | 100.7                          | <i>c</i> -C <sub>6</sub> H <sub>11</sub> –H | 99.5                           |
| <i>n</i> -C <sub>5</sub> H <sub>11</sub> –H | 100.2                          | <i>c</i> -C <sub>7</sub> H <sub>13</sub> –H | 94.0                           |
| <i>n</i> -C <sub>6</sub> H <sub>13</sub> –H | 99.0                           | <i>c</i> -C <sub>8</sub> H <sub>15</sub> –H | 95.7                           |
| <i>n</i> -C <sub>7</sub> H <sub>15</sub> –H | 98.0                           |   |                                |

Table 1.2 C–C Bond Dissociation Energies of Some Alkane Molecules<sup>2</sup>

| C–C bond of Alkane  | BDE ( $\text{kcal mol}^{-1}$ ) | C–C bond of Alkane  | BDE ( $\text{kcal mol}^{-1}$ ) |
|---|--------------------------------|---|--------------------------------|
| CH <sub>3</sub> –CH <sub>3</sub>                          | 90.2                           | C <sub>2</sub> H <sub>5</sub> –C <sub>2</sub> H <sub>5</sub>                      | 86.8                           |
| CH <sub>3</sub> –C <sub>2</sub> H <sub>5</sub>            | 88.5                           | C <sub>2</sub> H <sub>5</sub> –C <sub>3</sub> H <sub>7</sub>                      | 87.3                           |
| CH <sub>3</sub> – <i>n</i> -C <sub>3</sub> H <sub>7</sub> | 88.9                           | C <sub>2</sub> H <sub>5</sub> – <i>n</i> -C <sub>4</sub> H <sub>9</sub>           | 86.9                           |
| CH <sub>3</sub> – <i>n</i> -C <sub>4</sub> H <sub>9</sub> | 88.8                           | <i>n</i> -C <sub>3</sub> H <sub>7</sub> – <i>n</i> -C <sub>3</sub> H <sub>7</sub> | 87.5                           |

### 1.1.2 Steric Strain

Due to the non-bonding repulsions between adjacent atoms or like charges as well as also bond-angle strain, the structure of a molecule may be forced in a particular arrangement and lead to a sharp increase in the energy of the system. This is called strain energy. Unlike straight chain alkane which is relatively strain-free, the strain energy of cycloalkane is usually the driving force of reactions. There are three important sources of steric strain: (i) Prelog strain, which is caused by the intramolecular van der Waals repulsive forces of large atoms or groups crowding together; (ii) Baeyer strain, which is originated from bond-angle distortion; (iii) Pitzer strain, is caused from torsional deformation by  $\sigma$ -bond rotation from the most stable conformation. Table 1.3 lists the strain energy and the C–C BDE of some cycloalkanes.<sup>3</sup>

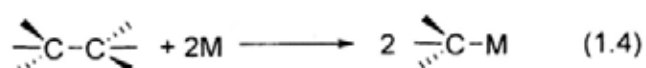
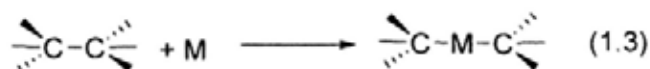
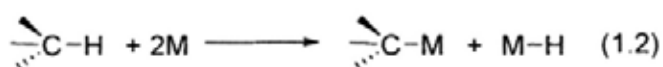
Table 1.3 Ring Strain and C–C BDE of Cycloalkanes<sup>3</sup>

| Cycloalkane  | Strain energy (kcal mol <sup>-1</sup> ) <sup>3a</sup> | BDE of C–C bond (kcal mol <sup>-1</sup> ) <sup>3b,c</sup> |
|--------------|---|---|
| Cyclopentane | 6.5   | 86.9 <sup>d</sup>   |
| Cyclohexane  | 0   | 87.3  |
| Cycloheptane | 6.3   | 86.6  |
| Cyclooctane  | 9.6   | 79.6  |

### 1.2 Activation and Functionalization of Alkanes by Transition Metals

Carbon–hydrogen activation (CHA) and carbon–carbon activation (CCA) of alkanes by transition metals involves the cleavage of the strong and inert alkyl C–H and C–C bonds, respectively and the subsequent formation of M–H or M–C bonds (eqs 1.1-1.4).<sup>1,4</sup> The ultimate goal in alkane activation is the catalytic conversion of hydrocarbons into more functionalized and potentially more useful chemicals. The initial C–H and C–C activations of

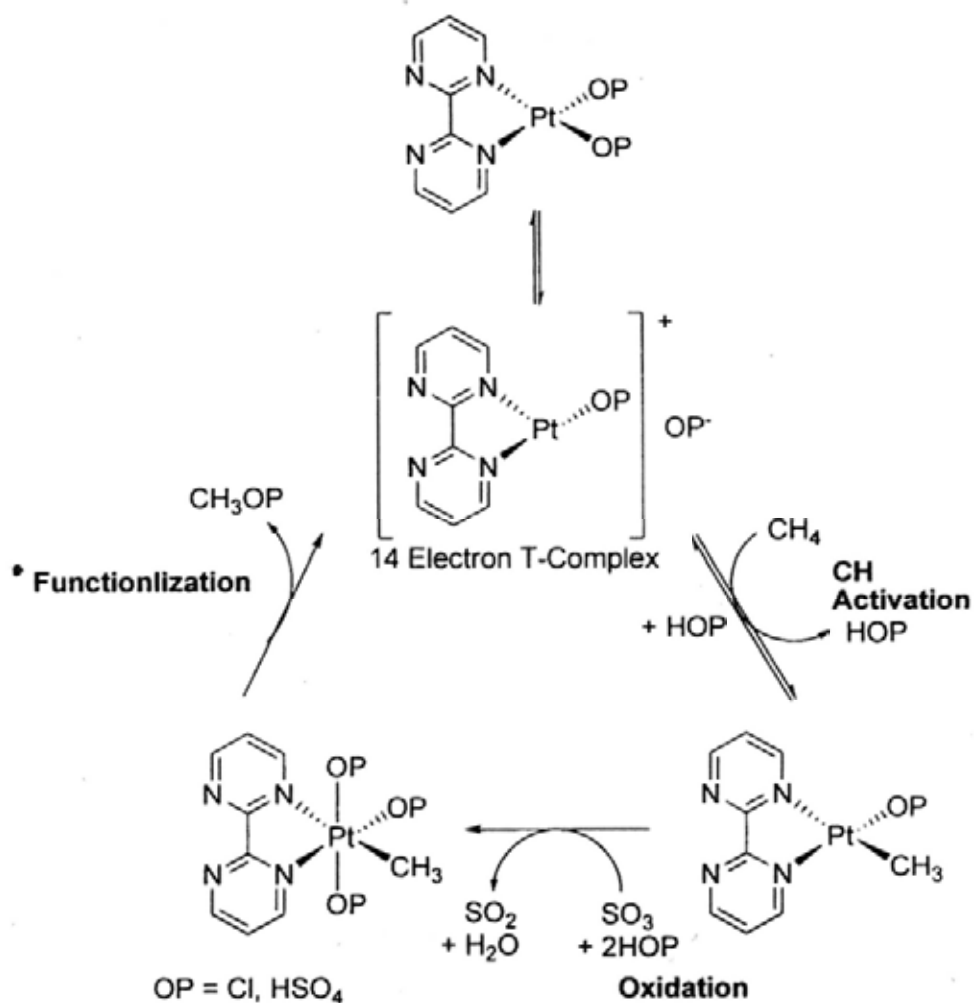
alkanes by metal-containing species can be viewed as the first step towards the conversion of alkanes into commodity chemicals.



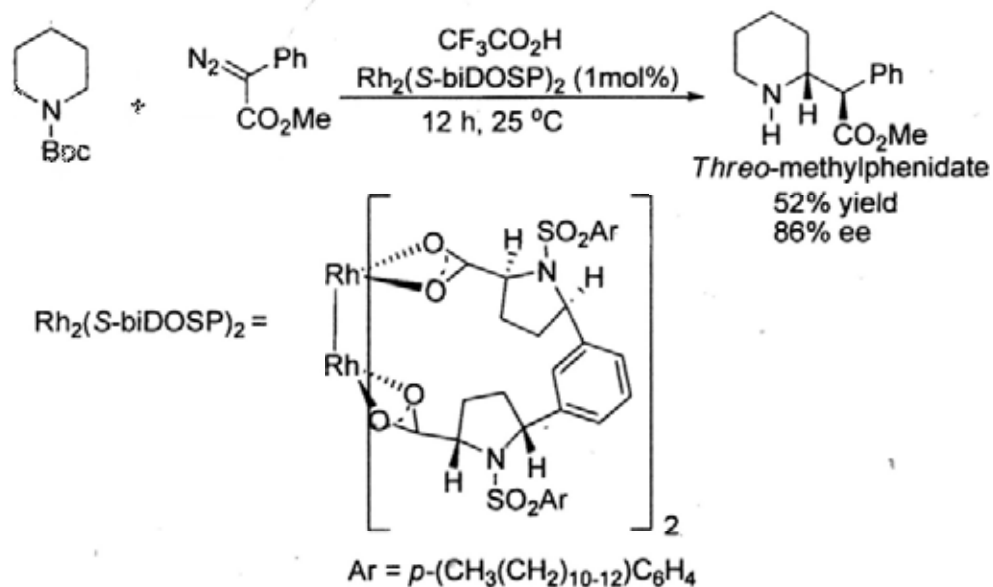
The functionalization of alkanes by transition metals consists of two essential steps: (1) activation of alkanes, and (2) conversion of the M-C bond to a functional group, for example C-O, C-N and C=C bonds.

### 1.2.1 Importance of Alkane Activation

CHA and CCA of alkane are potentially broadly applicable in the industrial synthesis of bulk chemical like methanol via syn-gas synthesis (Scheme 1.1),<sup>5a</sup> Transition metal complexes were also found to catalyze the transformation of natural product via alkyl CHA (Scheme 1.2).<sup>5b,c</sup>



Scheme 1.1 Catalytic Oxidation of Methane Potentially Applicable in Industry



Scheme 1.2 Synthesis of *Threo*-methylphenidate by  $\text{Rh}_2(\text{S-biDOSP})_2$

## 1.2.2 Challenges of CHA and CCA

In the course of alkane functionalization, the bond activation step is usually the most challenging step due to the inertness of alkane. Both alkyl CHA and CCA are difficult, it is commonly accounted by their high bond dissociation energies. Indeed, CHA and CCA encounter difficulties in different aspects.

### 1.2.2.1 Difficulties of Alkane CHA

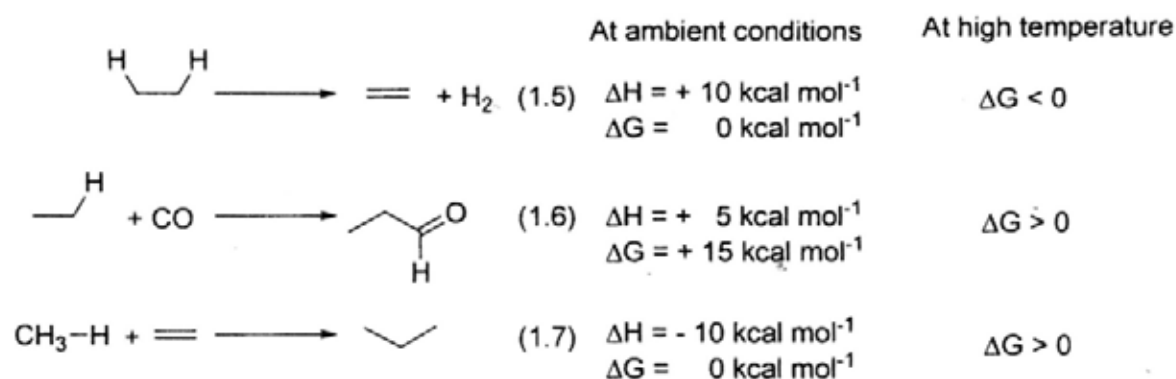
Generally, the CHA of alkanes faces challenges in the following aspects:

(1) Chemoselectivity: Vigorous reaction conditions and reactive reagents are usually employed for alkane functionalization as they are inert. The product of an alkane functionalization reaction is very likely more reactive than the starting material and so reacts faster with the functionalizing reagent.<sup>1</sup> It is called over-functionalization and can be a severe problem. For example, it is very difficult to stop the air oxidation of methane at the methanol stage. The methanol formed is more reactive than methane so that it preferentially reacts with the oxidizing agent. Many of the reactions in this section can only be run to give low or very low conversion in order to obtain a satisfactory selectivity.

(2) Regioselectivity: When there are more than one type of C–H bonds in an alkane molecule, an important selectivity issues arises (primary, secondary and tertiary C–H bonds). Tertiary radicals and carbonium ions are more stable than their secondary or primary analogs. Therefore, if carbon-centered radicals or carbonium ions are involved in the functionalization steps, an intrinsic selectivity pattern: tertiary > secondary > primary would happen. However, for very bulky reagents or in reactions in which the C–H bond to be broken is brought side-on to the functional group, for example S<sub>N</sub>2, primary position is favored due to steric effects.<sup>1</sup>

(3) Alkane dehydrogenation as well as carbonylation are classic examples of CHA, however, both transformation are not favorable at ambient conditions (eqs 1.5 and 1.6). However, dehydrogenation is favorable at high reaction temperature as hydrogen gas is

generated. Due to the decrease of entropy after transformation, the addition of a C–H bond across an olefin is endogonic at high reaction temperature (eq 1.7).<sup>6</sup>



### 1.2.2.2 Difficulties of Alkane CCA

Carbon–carbon bond activation of alkanes with transition metal complexes are more challenging than much carbon–hydrogen bond activation.<sup>7</sup> This is mainly accounted by two reasons: (i) kinetically inaccessibility of the C–C bonds of alkanes due to the surrounding C–H bonds (Figure 1.1), and (ii) steric repulsion between the ligands surrounding the metal and the alkyl group bound to it.<sup>8</sup> As a result, CCA is much more difficult and less reported than CHA.

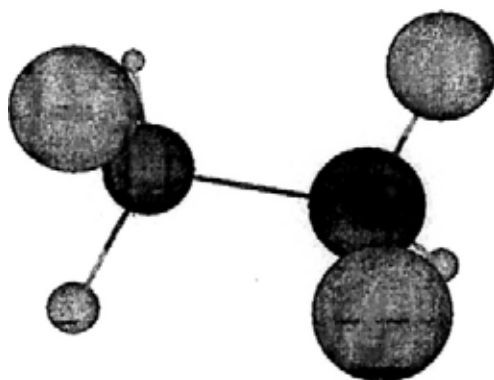


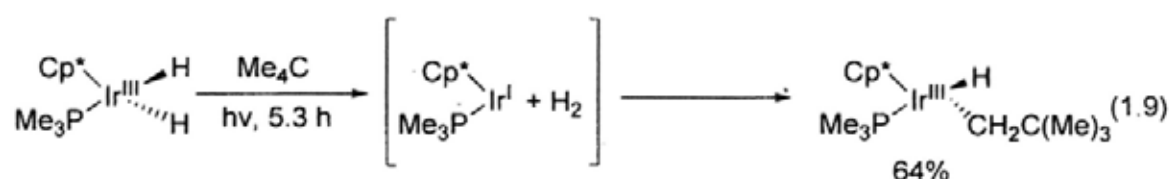
Figure 1.1 Structure of an Ethane Molecule (Ball and Stick Model)



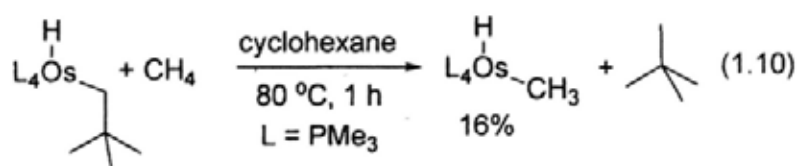
### 1.3.1.2 Oxidative Addition

In oxidative addition, a metal complex, with vacant-sites and a relatively low oxidation state, is oxidized by the metal insertion of C–H bond. Both the formal oxidation state of the metal and the electron count of the metal complex increase by two. As oxidative addition is a bimolecular process, it follows the second order rate law ( $\text{rate} = k [\text{M}][\text{Sub}]$ ).<sup>9</sup>

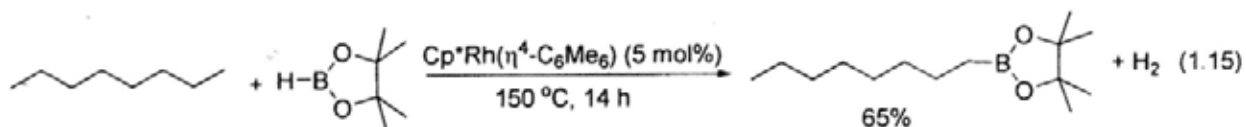
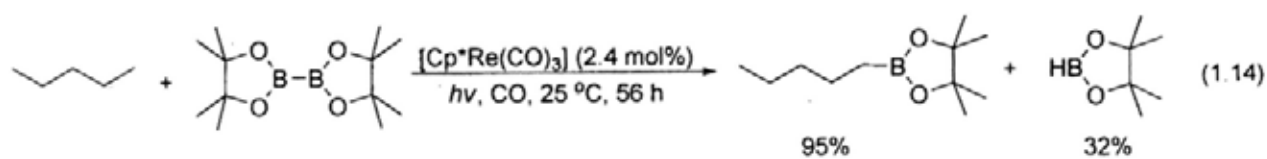
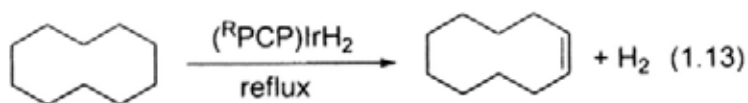
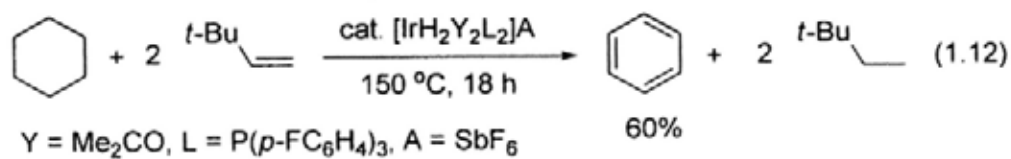
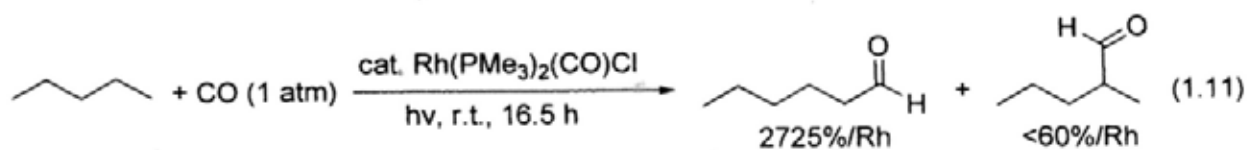
In the late 1980s, Bergman demonstrated the intermolecular CHA of neopentane with iridium dihydride complex via oxidation addition of the iridium(I) intermediate to give hydridoalkyl iridium(III) complex (eq 1.9).<sup>10</sup>



Stoichiometric alkyl CHA reactions were later found to be successful in other transition metal systems like Os (eq 1.10).<sup>11</sup>



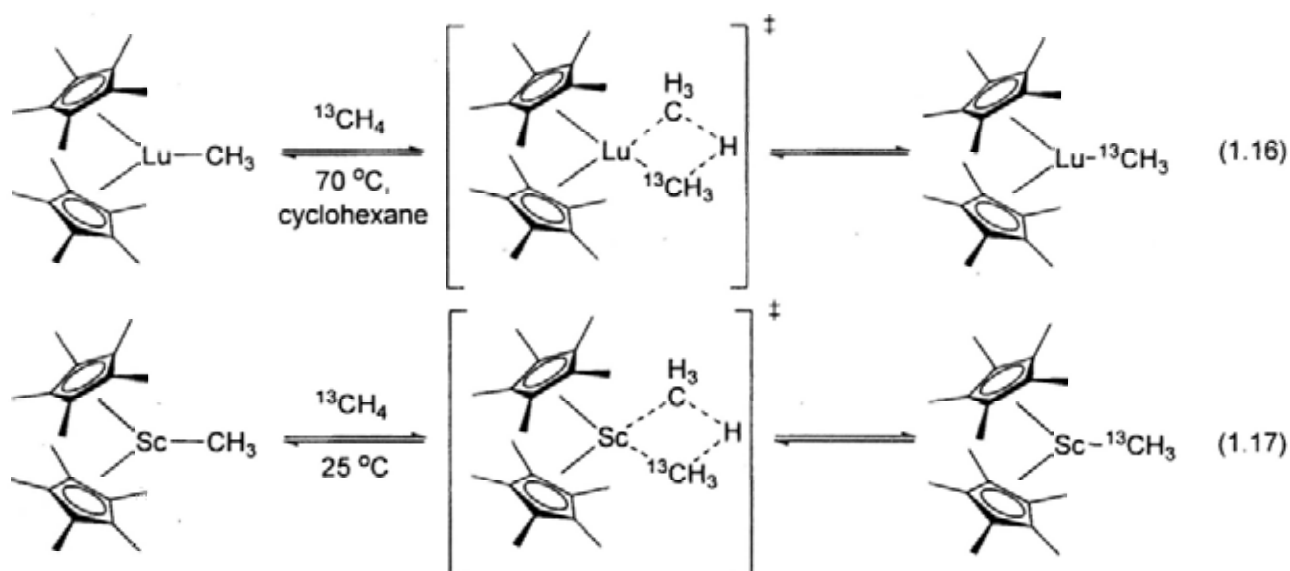
Some of the above examples laid down a good foundation for the development of catalytic functionalization of alkane. Photochemical carbonylation of *n*-pentane was catalyzed by  $\text{Rh}(\text{PMe}_3)_2(\text{CO})\text{Cl}$  to give aldehydes (eq 1.11).<sup>12</sup> The first well-characterized catalytic dehydrogenation system was reported by Crabtree. However, such a system required either a sacrificial hydrogen acceptor or irradiation (eq 1.12).<sup>13a</sup> Acceptorless dehydrogenation was later reported to be successfully catalyzed by Ir pincer complex (eq 1.13).<sup>13b</sup> Borylation of alkane was also catalyzed by  $\text{Cp}^*\text{Re}(\text{CO})_3$  and  $\text{Cp}^*\text{Rh}(\eta^4\text{-C}_6\text{Me}_6)$  (eq 1.14 and 1.15).<sup>14a,b</sup> Indeed, catalytic borylation of aromatic C–H bonds was achieved by  $[\text{IrCl}(\text{COD})]$  with 2,2'-bipyridine<sup>14c</sup> and  $\text{Cp}^*\text{IrH}_2(\text{BPin})_2$  (where HBPIn = pinacolborane).<sup>14d</sup>



### 1.3.1.3 $\sigma$ -Bond Metathesis

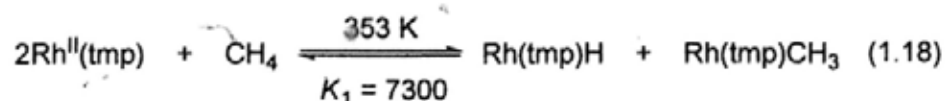
$\sigma$ -Bond metathesis is also a bimolecular process. Different from oxidative addition, the oxidation state of the transition metal involved  $\sigma$ -bond metathesis remains unchanged. A number of examples were reported in which  $d^0$  metal alkyls underwent  $\sigma$ -bond metathesis with alkanes. A four-centered transition state is generally accepted.

In 1983, Waston reported that  $\text{Cp}^*_2\text{LuMe}$  underwent exchange with  $^{13}\text{CH}_4$  to give  $\text{Cp}^*_2\text{Lu}^{13}\text{CH}_3$  at  $70^\circ\text{C}$  in cyclohexane solvent (eq 1.16).<sup>15</sup> Bercaw also reported the methyl exchange reaction between  $\text{Cp}^*\text{ScMe}$  and  $^{13}\text{CH}_4$  (eq 1.17).<sup>16</sup>



### 1.3.1.4 Homolytic Cleavage (Radical Pathway)

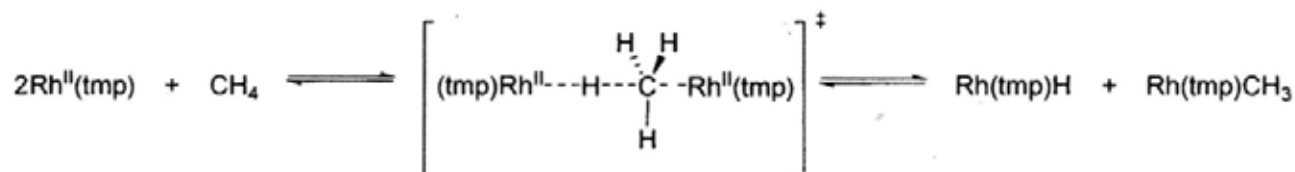
One of the most remarkable classes of organometallic CHA system is based on porphyrin complexes. Wayland et al. demonstrated the CHA of methane with metalloradical  $\text{Rh}^{\text{II}}(\text{tmp})$  ( $\text{tmp}$  = tetramesitylporphyrinato dianion) to give  $\text{Rh}(\text{tmp})\text{Me}$  and  $\text{Rh}(\text{tmp})\text{H}$  (eq 1.18).<sup>17a</sup>



Further mechanistic studies suggested that the CHA reaction is first order in methane and second order in  $\text{Rh}^{\text{II}}(\text{tmp})$  which follow:

$$\text{Rate} = k [\text{Rh}^{\text{II}}(\text{tmp})]^2 [\text{CH}_4]$$

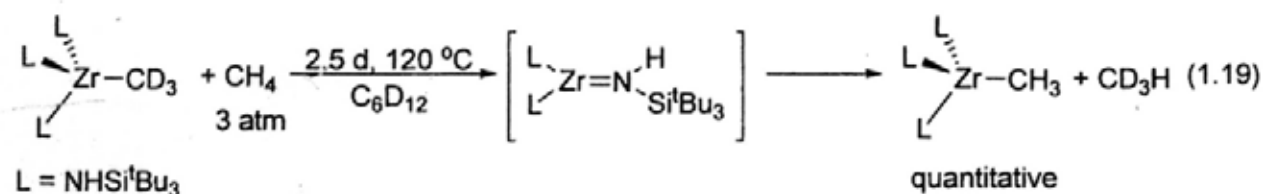
Temperature dependence of the forward rate constant  $k$  gives activation parameters for the methane CHA reaction ( $\Delta H^\ddagger = 7.1 \pm 1.0 \text{ kcal mol}^{-1}$ ;  $\Delta S^\ddagger = -39 \pm 5 \text{ cal mol}^{-1} \text{ K}^{-1}$ ). The large deuterium isotopic effects of the reaction ( $k_{\text{H}}/k_{\text{D}}$  (298 K) = 8.6; ( $k_{\text{H}}/k_{\text{D}}$  (353K) = 5.1) implicate that the rate-determining step involves a linear  $\text{C}^{\cdots}\text{H}^{\cdots}\text{Rh}$  fragment. The small activation enthalpy ( $\Delta H^\ddagger = 7.1 \pm 1.0 \text{ kcal mol}^{-1}$ ) indicates that the cleavage of  $\text{C}^{\cdots}\text{H}$  bond in the transition state is accompanied by the formation of both  $\text{Rh}^{\cdots}\text{C}$  and  $\text{Rh}^{\cdots}\text{H}$  bonds. Therefore, the methane activation was proposed to go through a linear 4-centered transition state (Scheme 1.4).<sup>17b</sup>



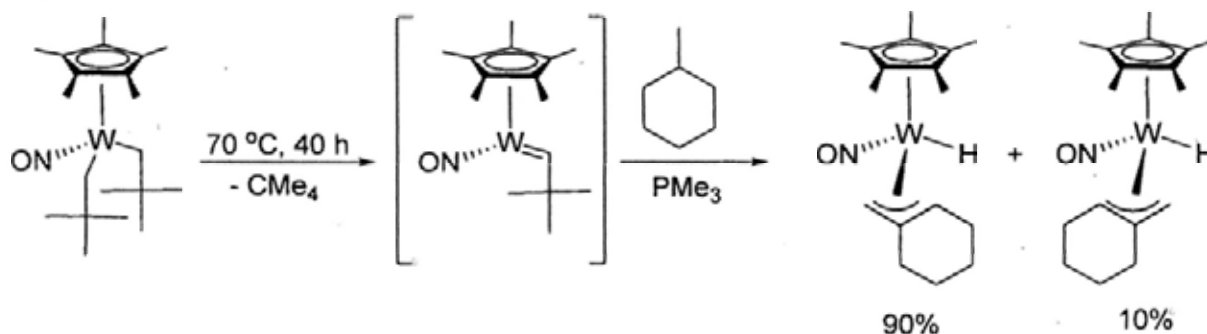
Scheme 1.4 Methane CHA via Termolecular Transition State

### 1.3.1.5 1,2-Addition of C–H bond across M=X

In 1988, Wolczanski<sup>18</sup> and Bergman<sup>19</sup> independently reported that Zr(IV) amido complexes could undergo 1,2-elimination of alkane to give the corresponding transient imido complexes. Wolczanski examined the reactivity of the newly-formed imido complex with methane and resulted in the formation of Zr-CH<sub>3</sub> complex via the 1,2-addition of alkyl C–H bond across the Zr=N bond (eq 1.19).



Legzdins reported a series of Mo and W systems which underwent CHA of hydrocarbons, including alkane, via the addition across the proposed M=C intermediates (Scheme 1.5).<sup>20</sup>



Scheme 1.5 Alkyl CHA by Cp\*W complexes

### 1.3.2 Catalytic CHA of Alkane with Transition Metal Complexes

The detailed studies of stoichiometric reactions of alkyl CHA with different transition metal complexes provided a basic understanding of the reaction mechanism. Some of the stoichiometric CHA had been developed into catalytic functionalization (Table 1.4).

Table 1.4 Selected Examples of Catalytic CHA with Transition Metal Complexes

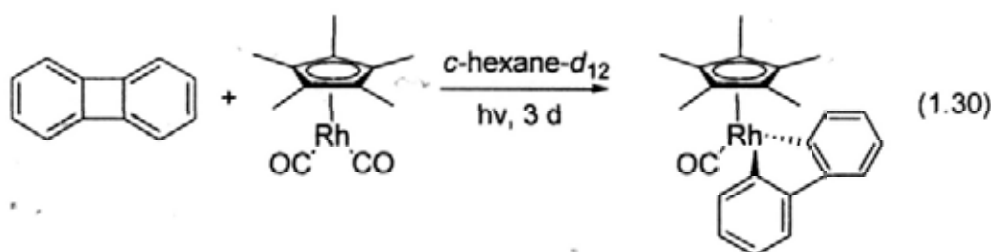
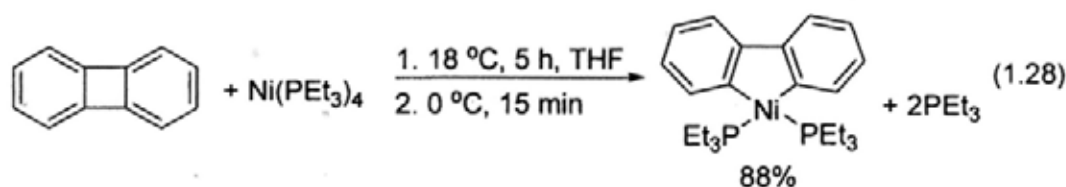
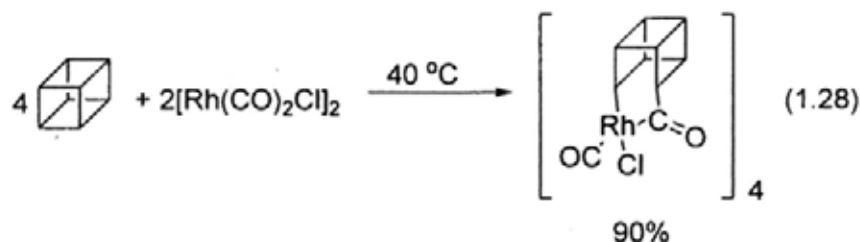
| Catalytic Reaction | Examples  |
|--------------------|---|
| Dehydrogenation    | $n\text{-octane} + 1\text{-decene} \xrightarrow[n\text{-octane, } 150\text{ }^\circ\text{C, } 120\text{ min}]{(t\text{-Bu}^i\text{PCP})\text{IrH}_2\text{ (1.0 mM)}} 1\text{-octene} + \text{decane} \quad (1.20)$ <p>                     1999 Goldman et al.<sup>21</sup><br/>                     (0.5 M) 97%<br/> <i>t</i>-Bu<sup>i</sup>PCP = 2,6-bis(di(<i>t</i>-butyl)phosphinomethyl)phenyl                 </p>  |
| H-D Exchange       | $n\text{-butane-}d_0 + \text{D}_2 \xrightarrow[100\text{ }^\circ\text{C, } 2\text{ d}]{[\text{Si}]\text{-ORh} \begin{matrix} \diagup \\ \text{H} \end{matrix} \text{ (4 mol\%)} } \text{mixture of } n\text{-butane-}d_{1-9} \quad (1.21)$ <p>                     1982 Schwartz et al.<sup>22</sup><br/>                     recovered 20% yield 79%                 </p>  |
| Carbonylation      | $\text{Cyclohexane} + \text{CO} \xrightarrow[1\text{-5 h}]{\text{Hg}^* (254\text{ nm})} \text{Cyclohexane-CHO} + \text{Cyclohexane-CO-Cyclohexane} \quad (1.22)$ <p>                     1991 Crabtree et al.<sup>23</sup><br/>                     total yield 10-70%                 </p>   |
| Methane Oxidation  | $\text{CH}_4 + 2\text{H}_2\text{SO}_4 \xrightarrow[220\text{ }^\circ\text{C, } 2.5\text{ h}]{\text{cat. (bypm)PtCl}_2} \text{CH}_3\text{OSO}_3\text{H} + 2\text{H}_2\text{O} + \text{SO}_2 \quad (1.23)$ <p>                     1998 Periana et al.<sup>5</sup><br/>                     bypm = 2,2'-bipyrimidine 72%                 </p>   |
| Amination          | $\text{Cyclohexane} + \text{PhI=NTs} \xrightarrow[80\text{ }^\circ\text{C, } 4\text{ h}]{5\text{ mol\% Tp}^*\text{BrAg}} \text{Cyclohexane-N-Ts} \quad (1.24)$ <p>                     2008 Perez et al.<sup>24</sup><br/>                     90%<br/>                     (Tp<sup>*</sup>Br = hydrotris(3,4,5-tribromo)pyrazolylborate ligand)                 </p>   |
| Chlorination       | $\text{CH}_4 + \text{Cl}_2 \xrightarrow[100\text{ }^\circ\text{C, } 11\text{ h}]{[\text{Si}]\text{-ORh} \begin{matrix} \text{Cl} \\ \diagup \\ \text{H} \end{matrix} \text{ (2 mol\%)} } \text{CH}_3\text{Cl} + \text{CH}_2\text{Cl}_2 + \text{CHCl}_3 + \text{CCl}_4 \quad (1.25)$ <p>                     1984 Schwartz et al.<sup>25</sup><br/>                     recovered yield 86.3%<br/>                     12.6% 1.1% trace trace                 </p> |
| Isomerization      | $\text{1-butane} \xrightarrow[150\text{ }^\circ\text{C, } <1\text{ min}]{\text{cat. H}_2\text{SO}_4\text{-SbF}_5/\text{ZrO}_2} \text{2-methylpropane} \quad (1.26)$ <p>                     1979 Arata et al.<sup>26</sup><br/>                     80% 20%                 </p>  |
| Boration           | $\text{Cp}^*\text{W(CO)}_3[\text{Bcat}(\text{Me})_2] + \text{1-pentene} \xrightarrow[>6\text{ h}]{\text{Hg lamp}} \text{1-pentene-Bcat}(\text{Me})_2 \quad (1.27)$ <p>                     2000 Hartwig et al.<sup>27</sup><br/>                     ([Bcat(Me)<sub>2</sub>] = B-1, 2-O<sub>2</sub>C<sub>6</sub>H<sub>2</sub>-3, 5-Me<sub>2</sub>) 85%                 </p>   |

## 1.4 Carbon–Carbon Activation by Transition Metal Complexes

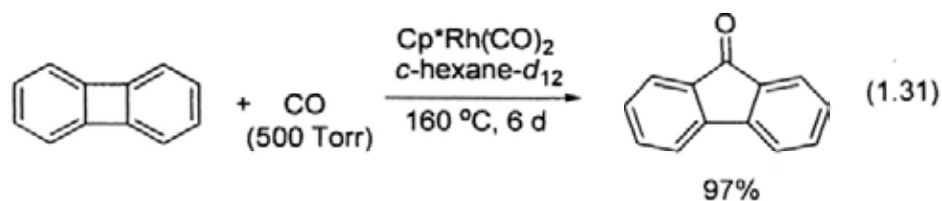
Carbon–carbon bond activation of alkanes with transition metal complexes are much less reported than carbon–hydrogen activation.<sup>7</sup> Several strategies have been commonly employed to realize CCA, including ring strain relief,<sup>28</sup> the aromaticity driven CCA from pre-aromatic system,<sup>29</sup> chelation assisted CCA,<sup>30</sup> intermolecular CCA of imine<sup>31</sup> and carbonyl,<sup>32,33</sup> intramolecular  $\beta$ -carbon-carbon bond cleavage<sup>34-37</sup> and alkane metathesis.<sup>38</sup> They will be discussed one by one in the following section.

### 1.4.1 Ring Strain Relief

Early CCA examples with transition metal complexes were focused on ring strained molecules as the cleavage of the highly strained system provided extra driving force for the reaction (eqs 1.28-1.30).<sup>28</sup>

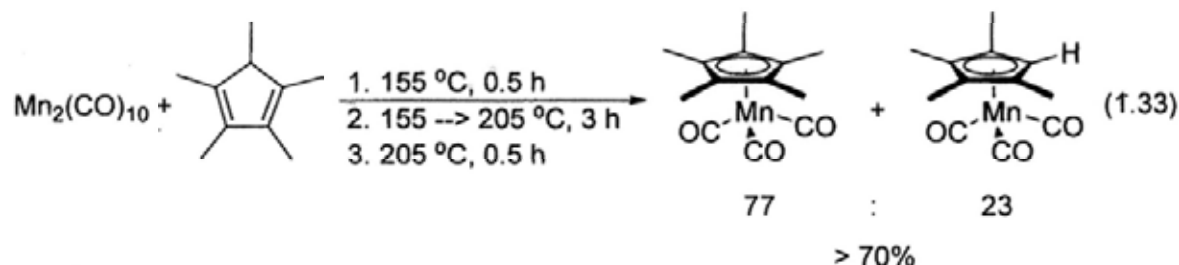
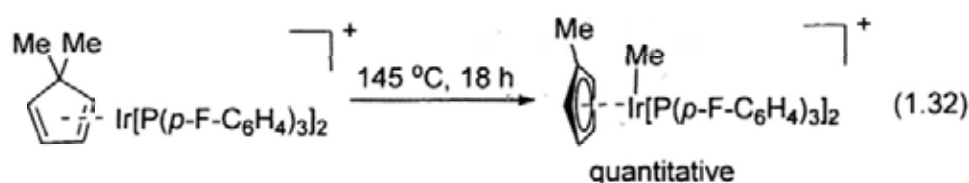


The above examples demonstrate the cleavage of ring strained C–C bond and meanwhile with the formation of M–C bond. Since M–C bond is relatively weak (30 to 70 kcal mol<sup>-1</sup>),<sup>2</sup> the organometallic compounds formed are easily further transformed to complete the functionalization (eq 1.31).<sup>28c</sup>



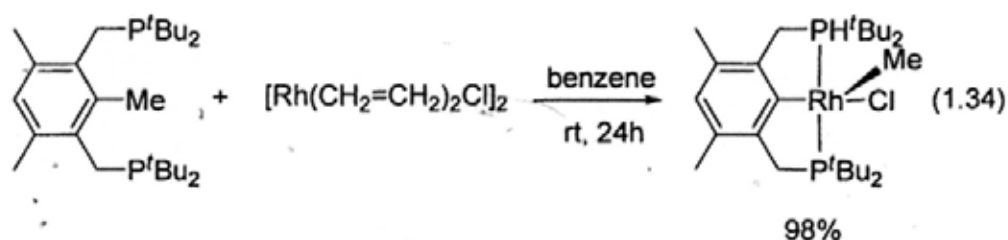
### 1.4.2 Aromaticity Driven CCA

The transformation of an aromatic compound from the corresponding pre-aromatic one provides an extra driving force. Crabtree et al. reported that the carbon-carbon bond of 1,1-dimethylcyclopentadiene was cleaved by Ir complexes to give the corresponding  $\eta^5$ -methylcyclopentadienyl(methyl)iridium (eq 1.32).<sup>29a</sup> Hughes also found that  $\text{Mn}_2(\text{CO})_{10}$  reacted with neat pentamethylcyclopentadiene to afford a mixture of CHA product,  $\text{Mn}(\eta^5\text{-C}_5\text{Me}_5)(\text{CO})_3$  and CCA product,  $\text{Mn}(\eta^5\text{-C}_5\text{Me}_4\text{H})(\text{CO})_3$  (eq 1.33).<sup>29b</sup>

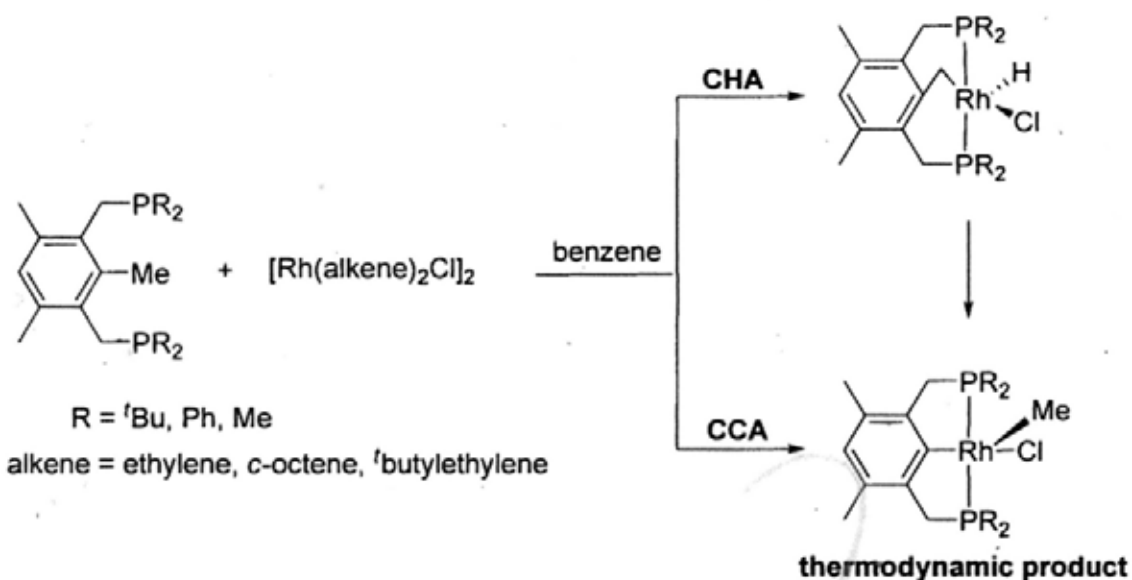


### 1.4.3 Intramolecular CCA in Pincer-Type System

Chelation assisted CCA makes use of a strategy in which the targeted carbon-carbon bond is brought close to the metal center by ligand coordination of the substrate so as to lower the activation barrier. Intramolecular  $\text{sp}^2\text{-sp}^3$  CCA in pincer type (PCP) system by Milstein et al. gave the best illustration (eq 1.34).<sup>30</sup>



The coordinating P ligands in the target molecule brings the Rh center into close proximity, and subsequently inserts into the aryl-Me bond. Mechanistic investigation of the CCA reaction revealed that the initial coordination of the diphosphine ligand to the rhodium olefin complex is the rate-determining step.<sup>30b</sup> The operating mechanism involves parallel benzylic CHA and aromatic CCA, the CHA product eventually converts to the thermodynamically favored CCA product (Scheme 1.6).

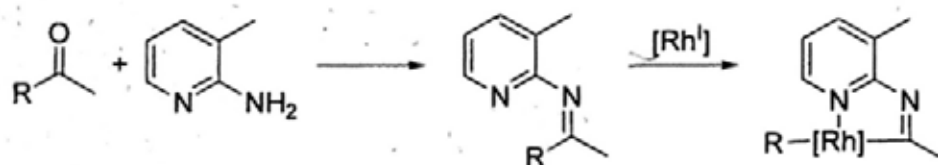


Scheme 1.6 Proposed Mechanism of Parallel CHA and CCA in PCP System

When less bulky dimethylphosphines was employed in the PCP ligand, the more stable CCA product formed. However, when less basic diphenylphosphine was used, CHA product became more stable and formed preferentially.<sup>30</sup>

#### 1.4.4 Chelation-Assisted Intermolecular CCA of Imine

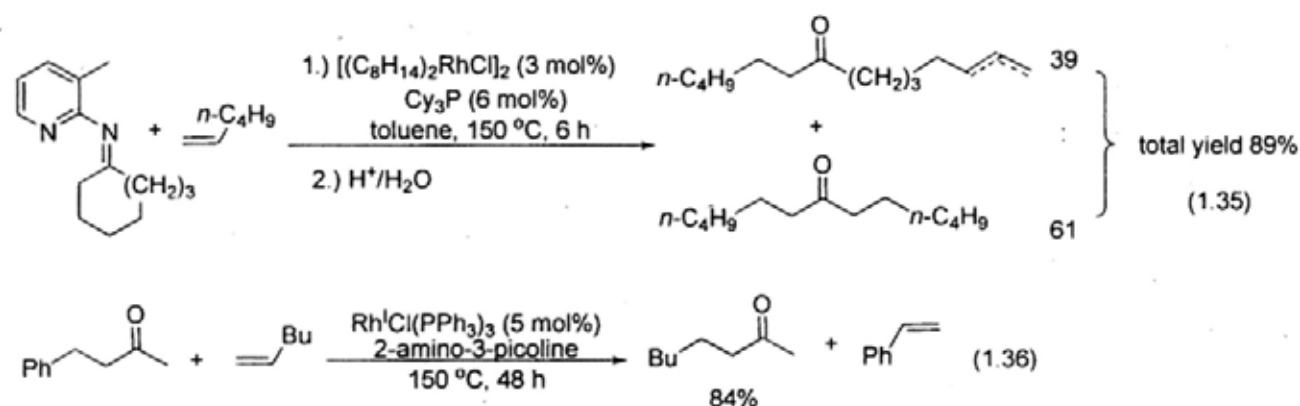
Jun et al. discovered that by using 2-amino-3-picoline, a temporary chelating auxiliary which reacted with ketone to form ketimine,  $\text{Rh}^{\text{I}}\text{Cl}(\text{PPh}_3)_3$  facilitated the CCA of unstrained ketone (Scheme 1.7).



Scheme 1.7 Chelation Assisted CCA of Imine

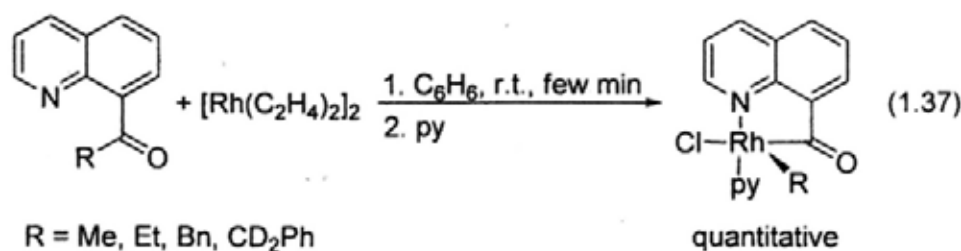
The C $\alpha$ -C $\beta$  bond of the newly formed ketimine is cleaved by Rh(PPh $_3$ ) $_3$ Cl with the generation of (iminoacyl)rhodium alkyl.<sup>31</sup>

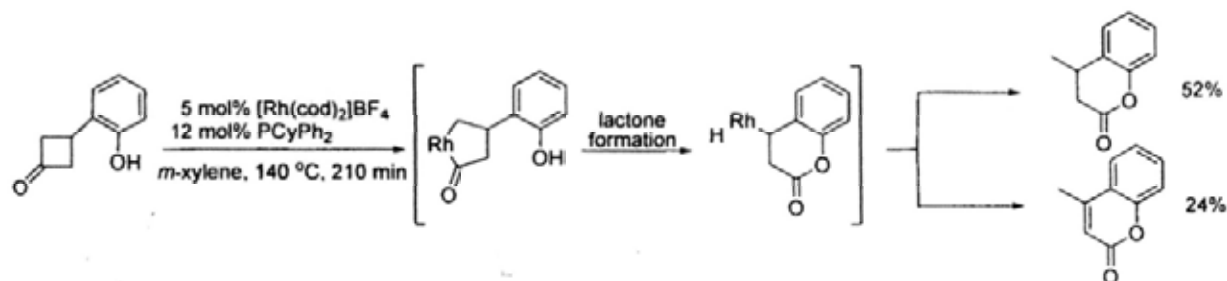
The nitrogen atom on the pyridine ring directed the rhodium center to the C $\alpha$ -C $\beta$  bond of the imine via a chelation-assisted strategy. This approach has also been applied to the C-C activation of primary amines,<sup>31c</sup> alkyne,<sup>31d-f</sup> cycloalkanone imine (eq 1.35)<sup>31g</sup> and catalytic CCA of unstrained ketone (eq 1.36).<sup>31h</sup>



#### 1.4.5 Intermolecular CCA of Carbonyl

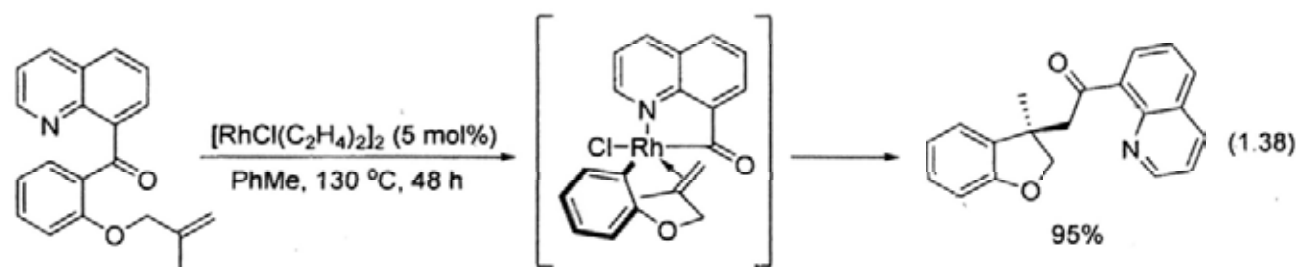
The C-C bond adjacent to a carbonyl group is more potent to be cleaved due to two reasons: (1) the C-C bond is weaker than alkyl C-C bond by around 5 kcal mol $^{-1}$  in general;<sup>2</sup> (2) the carbonyl group serves as a directing group to the metal center and brings the targeted C-C bond in close proximity. Suggs found that [Rh(C $_2$ H $_4$ ) $_2$ ] $_2$  cleaved the  $\beta$ -keto C-C bond of 8-quinolinyll alkyl ketones (eq 1.37).<sup>32</sup> Ito reported that [Rh(cod)]BF $_4$  catalyzed the transformation of substituted cyclobutanone to give the lactones via CCA (Scheme 1.8).<sup>33a,b</sup>





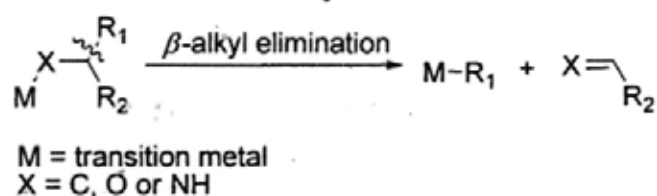
Scheme 1.8 Lactone formation catalyzed by  $Rh^I$  complex via CCA

More recently, Douglas et al. facilitated the intramolecular carbo-acylation with catalyst  $[RhCl(C_2H_4)_2]$  (1.38).<sup>33c</sup>



#### 1.4.6 Intramolecular $\beta$ -Alkyl Elimination

Intramolecular  $\beta$ -alkyl elimination of transition metal complexes like metal alkyl, alkoxide and amido complexes are mostly reported with highly Lewis acidic transition metals. The  $C_\alpha$ - $C_\beta$  bonds of the metal complexes are cleaved to give metal alkyl and the corresponding olefin, carbonyl or imine (Scheme 1.9).



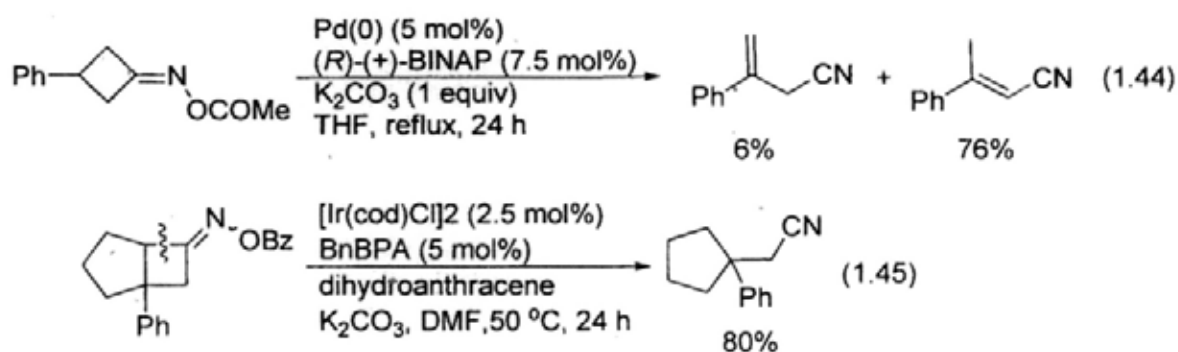
Scheme 1.9 General Expression of Intramolecular  $\beta$ -Alkyl Elimination

##### 1.4.6.1 Intramolecular $\beta$ -Alkyl Elimination of Metal Alkyl

The first example of  $\beta$ -alkyl elimination of metal alkyl was demonstrated by the thermal decomposition of coordinatively unsaturated lutetium isobutyl complex to yield lutetium methyl complex and propene via  $\beta$ -methyl elimination (eq 1.39).<sup>34a</sup> Bercaw later

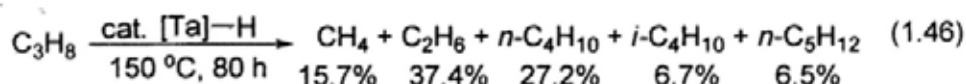


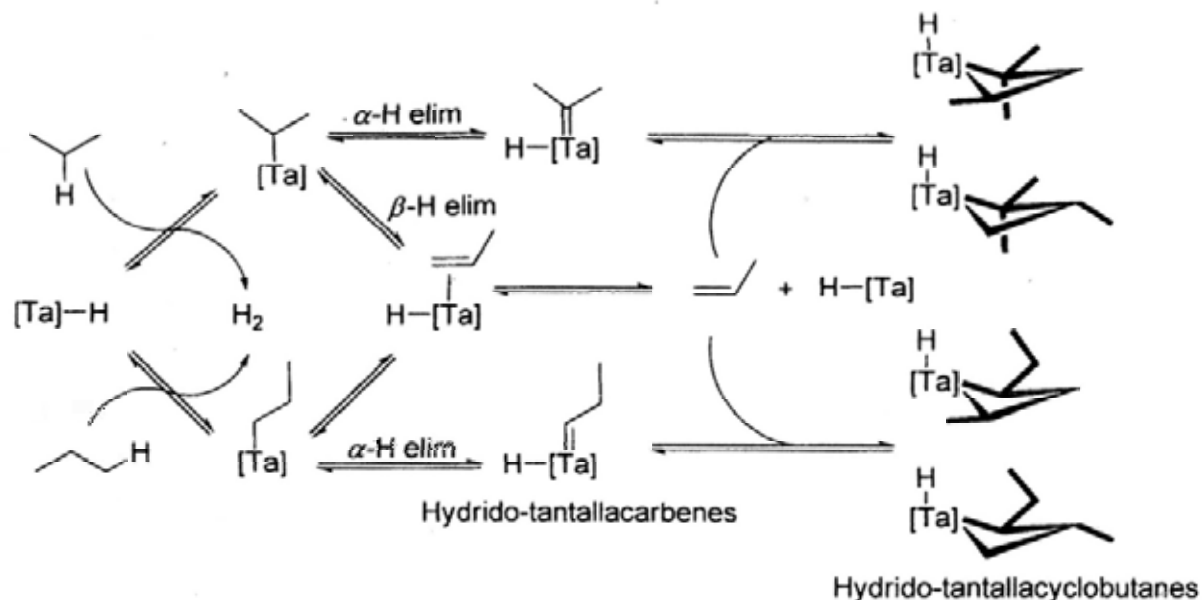
acyloximes to afford unsaturated nitriles (eq 1.44).<sup>37a</sup> Later, Ir complex was used to yield saturated nitriles where CCA occurred at the sterically less hindered site (eq 1.45).<sup>37b</sup>



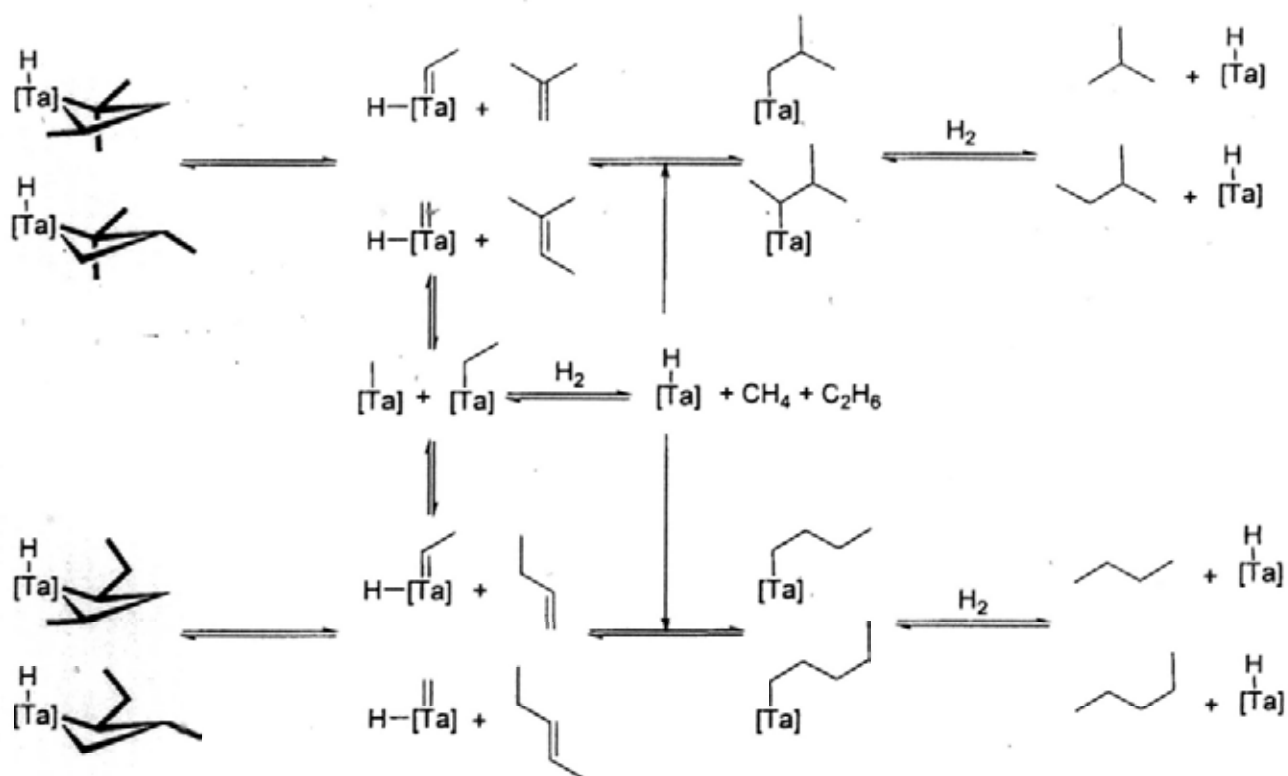
#### 1.4.7 CCA by Alkane Metathesis

Basset et al. developed a silica-supported tantalum hydride complex,  $(\equiv\text{Si}-\text{O}-\text{Si}\equiv)(\equiv\text{Si}-\text{O}-)_2\text{Ta}-\text{H}$  which catalyzed the transformation of linear or branched alkanes into the next higher and lower alkanes at 25 to 200 °C.<sup>38</sup> The Ta-H complex facilitated the conversion of propane to give a mixture of methane, ethane, *n*-butane, isobutene and *n*-pentane in 15.7%, 37.4%, 27.2%, 6.7% and 6.5% yields, respectively at 150 °C in 80 hours (eq 1.46).





Scheme 1.10a Mechanistic Scheme of the Formation of Hydrido-tantallacyclobutanes from [Ta]-H and Propane



Scheme 1.10b Transformation of Hydrido-tantallacyclobutanes to [Ta]-H and Various Alkanes via Hydrogenolysis

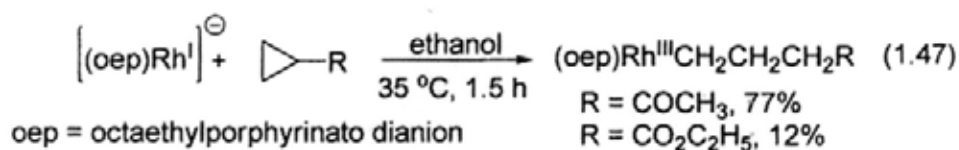
Basset et al. proposed a mechanism in which propane first reacts with Ta-H via CHA to give Ta-propyls and hydrogen. Ta-propyls then undergo  $\alpha$ -H elimination to give hydrido-

tantallacarbenes or  $\beta$ -H elimination to give Ta-H and propene via four possible tantallacyclobutanes (Scheme 1.10a). Subsequently, the tantallacyclobutanes transform to Ta-alkyls which further react with hydrogen to generate a mixture of alkane and regenerate [Ta]-H catalyst (Scheme 1.10b).

One of the major disadvantages of this type of CCA is poor selectivity problem. Even though propane has only one chemically equivalent C-C bond, the CCA of propane gave a mixture of methane, ethane, *n*-butane, *i*-butane, 2-methylbutane and *n*-pentane.<sup>38</sup>

#### 1.4.8 CCA by Nucleophilic Attack

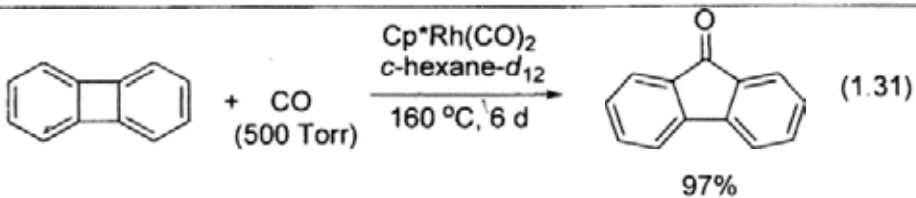
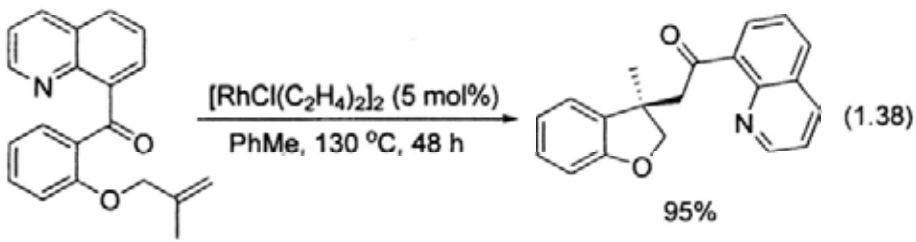
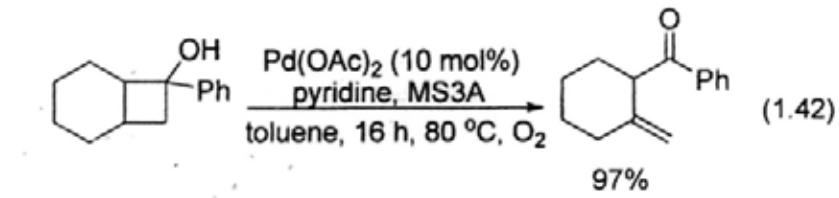
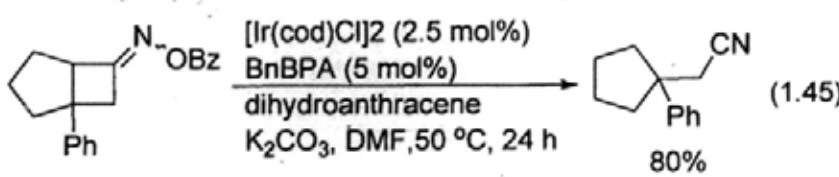
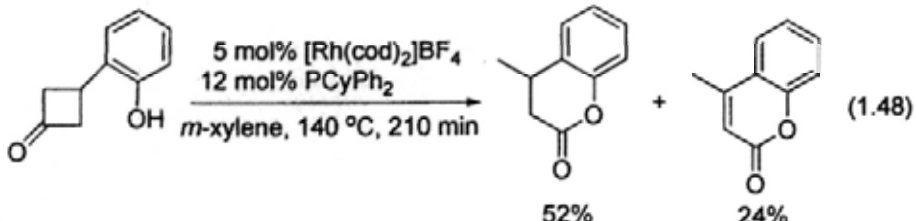
Ogoshi et al. reported that the C-C bond of cyclopropane was also cleaved by the nucleophilic attack of rhodium(I) porphyrin to the carbon center under mild conditions (eq 1.47).<sup>39</sup> An acyl or ester group on the cyclopropane ring facilitated the aliphatic CCA.



### 1.4.9 Catalytic CCA of Alkane with Transition Metal Complexes

Based on the above fundamental investigation of CCA, a few strategies have been applied to catalytic functionalization. The following table lists the selected examples (Table 1.5).

Table 1.5 Selected Examples of Transition Metal Catalyzed CCA

| Catalytic Reaction   | Examples   |
|--|--|
| Carbonylation<br>1997 Jones et al. <sup>28c</sup>  |  <p style="text-align: right;">(1.31)<br/>97%</p>  |
| Intramolecular<br>Carbo-Acylation<br>2009 Douglas et al. <sup>33c</sup>  |  <p style="text-align: right;">(1.38)<br/>95%</p>   |
| Dealkylation of<br>Alcohol and Imine<br>2003 Uemura et al. <sup>36</sup><br>and 2005 Uemura et al. <sup>37</sup> |  <p style="text-align: right;">(1.42)<br/>97%</p>  |
|  |  <p style="text-align: right;">(1.45)<br/>80%</p>  |
| Alkane Metathesis<br>1997 Basset et al. <sup>38</sup>  | $\text{C}_2\text{H}_6 \xrightarrow[150\text{ }^\circ\text{C, 80 h}]{\text{cat. [Ta]-H}} \text{CH}_4 + \text{C}_3\text{H}_8 + n\text{-C}_4\text{H}_{10} + i\text{-C}_4\text{H}_{10} \quad (1.46)$ <p style="text-align: center;">53%    44%    2.6%    0.4%</p> |
| Lactones Formation<br>2000 Ito et al. <sup>33</sup>  |  <p style="text-align: right;">(1.48)<br/>52%    24%</p>   |

## 1.5 Porphyrins and Metalloporphyrins

### 1.5.1 Porphyrin Ligands

Porphyrins are heterocyclic macrocycles which consist of four pyrrole subunits interconnected at their  $\alpha$  carbon atoms by methine bridges. They contain 22  $\pi$  electrons, with 18  $\pi$  electrons in the 16-membered ring conjugated system (Figure 1.3).<sup>40,41</sup> Porphyrins obey the Huckel's rule and therefore the macromolecules are aromatic and highly conjugated systems. Consequently, they have very intense absorption in the visible region. The diagonal radii of the cavity ( $C_t-N = 2.098 \text{ \AA}$ ) allow the coordination of various metal centers in the plane of the four nitrogen atoms.<sup>41</sup> When incorporated with metals, porphyrins serve as planar tetradentate, dianionic macrocyclic ligands to form stable complexes.  $^1\text{H}$  NMR spectroscopy confirms the aromaticity with a shielding effect on a nucleus which resides out of the porphyrin plane.<sup>41</sup>

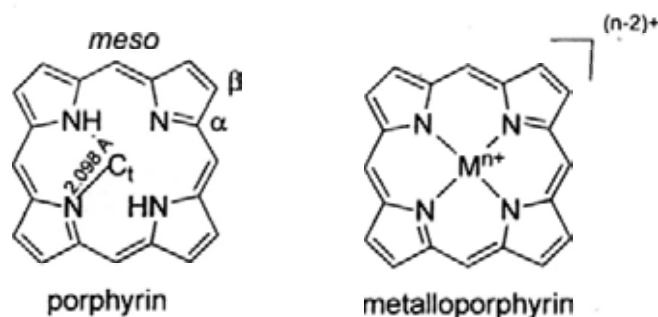
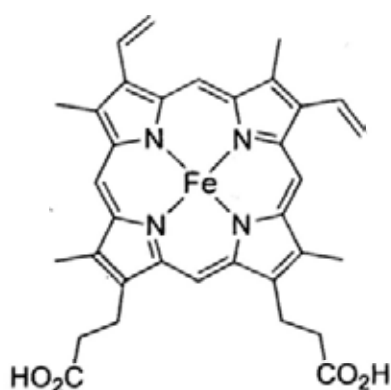


Figure 1.3 Structures of Porphyrin and Metalloporphyrin

A wide variety of porphyrin ligands can be easily synthesized by substitution of the peripheral positions of the porphyrin (*meso*- and  $\beta$ -). Substitution of the four *meso*-hydrogens with aryl groups gives *meso*-tetraarylporphyrins. The aryl groups are essentially orthogonal to the plane of the 18  $\pi$  aromatic porphyrin macrocycle. They are much easier to synthesize than the  $\beta$ -substituted ones and easily modified with a variety of functional groups.<sup>42</sup>

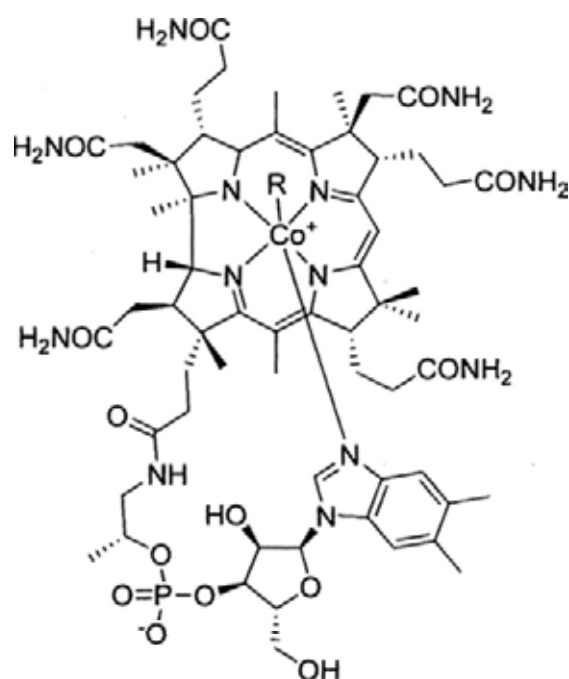
## 1.5.2 Metalloporphyrins

Metalloporphyrins, with the insertion of metal atoms/ions in the center cavity of porphyrins, are commonly found in nature. Iron porphyrin is one of the best known examples as it is found in the core of hemoglobin for oxygen carriers (Figure 1.4a).<sup>43</sup> Four Nobel Prizes were awarded to the scientists who studied the chemistry of coenzymes B<sub>12</sub> (Table 1.6),<sup>43b</sup> a substituted cobalt porphyrin working as rearrangement catalysts (Figure 1.4b).<sup>43</sup> They are important model compounds for understanding the chemical reactivities and relationships of several biologically important macromolecules.<sup>44</sup>



Heme group working as oxygen carriers

Figure 1.4a Structure of Heme



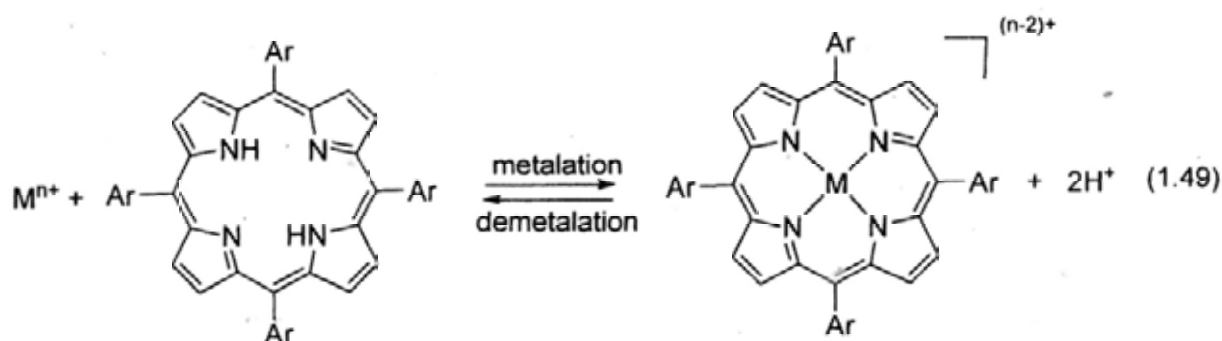
R = 5'-deoxyadenosyl, Me, OH, CN

Figure 1.4b Structure of Vitamin B<sub>12</sub>

Table 1.6 Nobel laureates and their work with vitamin B<sub>12</sub>

| Year | Nobel Laureates                                  | Contribution   |
|------|--|--|
| 1934 | Whipple, G. H.<br>Murphy, W. P.<br>Dam. H. C. P. | Discovery of vitamin B <sub>12</sub>                                       |
| 1957 | Lord Todd, A. R.                                 | Structure determination of vitamin B <sub>12</sub>                         |
| 1964 | Hodgkin, D. C.                                   | Structure determination of vitamin B <sub>12</sub> (X-ray crystallography) |
| 1965 | Woodward, R. B.                                  | Synthesis of vitamin B <sub>12</sub>                                       |

Replacing the two inner pyrrole protons by metal ions, porphyrins can serve as very stable tetradentate ligands to give metalloporphyrins (eq 1.49).



Porphyrin ligands are selective towards coordination in term of the size of metal ions. Due to the size of the central cavity of porphyrins, metals with ionic radii 60 – 70 pm, are optimally fit into the central cavity in planar coordination to give square-planar complexes.<sup>40b,45</sup> Therefore, the 1<sup>st</sup> row transition metal ions usually fit into the cavity. However, the 2<sup>nd</sup> and 3<sup>rd</sup> row transition metal ions have larger ionic radii and therefore form complexes with slightly out of plane structures upon coordination of porphyrins (Table 1.7, Figure 1.5). Metalloporphyrins are characterized with their intense colour (Soret band at 400 nm) and exhibit unique reactivities.<sup>46</sup>

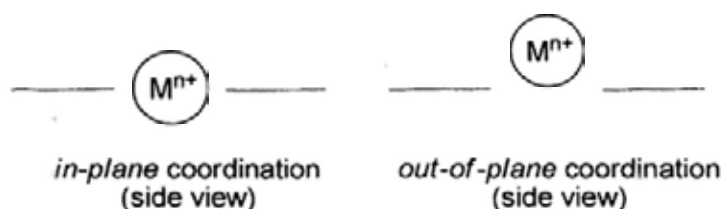


Figure 1.5 *In-plane* and *out-of-plane* coordination of metal ions with porphyrins

Table 1.7 Suitability of Various Transition Metal Ions with Porphyrin Coordination<sup>45</sup>

| Metal ion        | Ionic radius (pm) | Suitability of metal ion in complexes |
|------------------|-------------------|---------------------------------------|
| Co <sup>2+</sup> | 82                | Relatively large (out of plane)       |
| Co <sup>3+</sup> | 64                | Proper size                           |
| Rh <sup>2+</sup> | 86                | Too large, out of plane               |
| Rh <sup>3+</sup> | 75                | Relatively large (out of plane)       |
| Ir <sup>2+</sup> | 89                | Too large, out of plane               |
| Ir <sup>3+</sup> | 75                | Relatively large (out of plane)       |

### 1.5.3 Structural Features of Metalloporphyrins

Porphyrins are aromatic tetradentate ligands which prefer a planar or nearly planar arrangement, but it has also been found to be highly flexible. Introducing steric crowding of substituents at the *meso*- and  $\beta$ -positions of porphyrin would result in the deformation of porphyrin in either ruffle or saddle deformation or a mixture of these two deformations (Figure 1.6).<sup>47</sup> The deformation of porphyrin are known to cause significant changes in the chemical and spectroscopic properties including axial ligand affinities, redox potentials, transition dipoles and red shift.<sup>48</sup> The enantioselectivity of catalytic epoxidation can be fine-tuned by nonplanar deformations.<sup>48c</sup>

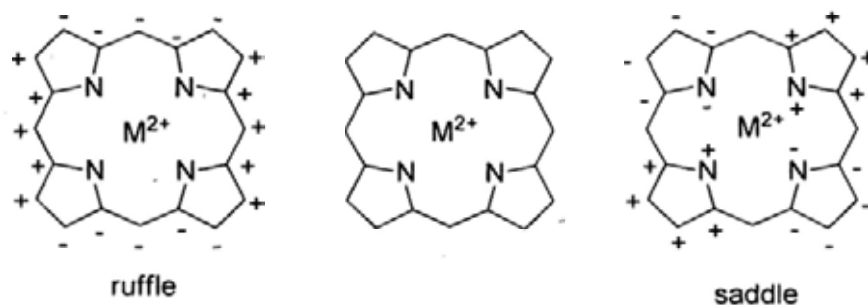


Figure 1.6 Schematic Depiction of Ruffled and Saddled Conformations. (The + and – indicate displacements on opposite sides of the mean plane of the porphyrin)

#### 1.5.4 Vacant Coordination Sites of Metalloporphyrins

As a tetradentate ligand, a porphyrin occupies the four equatorial coordination sites of a metal center, the two axial coordination sites of metalloporphyrin are available for further ligand coordination to form an octahedral complex. For a controlled stoichiometric or catalytic activation of substrates there is indeed a need for two such open coordination sites: one for substrate binding and another for the regulation of catalytic activity (e.g. using the *trans*-effect).<sup>46,49</sup> As *cis*- and *trans*- effects on axial coordination at the metal centre affect ligand reactivity, extensive efforts have been spent on this area.<sup>50,51</sup>

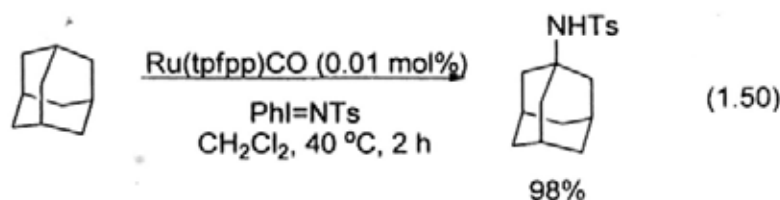
#### 1.5.5 Chemistry of Metalloporphyrins

Chemists have been interested in efficient and highly selective chemical transformations which are easily achieved in enzymatic reactions but almost impossible by conventional synthetic methods. Learning from nature, biomimic approach, is one of the most exciting fields in organometallic chemistry.<sup>45,52</sup>

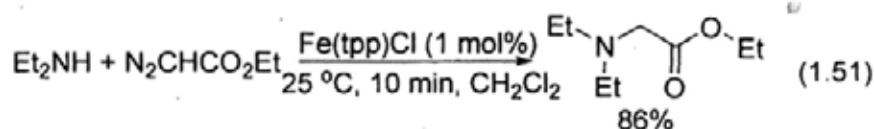
Since metalloporphyrins reversibly bind to small molecules, they are promising catalysts.<sup>52</sup> Metalloporphyrins have shown remarkable reactivity in various catalytic reactions, such as amidation of alkanes (eq 1.50),<sup>53</sup> N-H insertion of amine (eq 1.51),<sup>54</sup>

cyclopropanation of alkenes (eq 1.52),<sup>55</sup> epoxidation (eqs 1.53),<sup>56</sup> hydroxylation (eq 1.54)<sup>57</sup> and oxidation of alkenes (eq 1.55).<sup>58</sup>

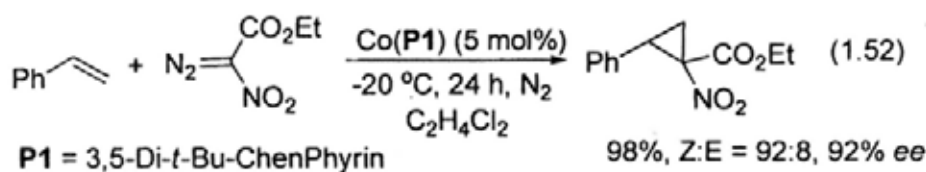
#### Amidation of Alkanes



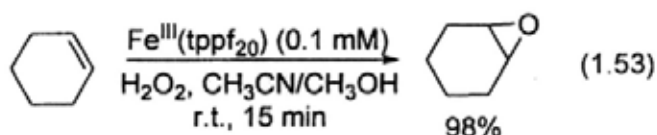
#### Amine N-H Insertion



#### Cyclopropanation

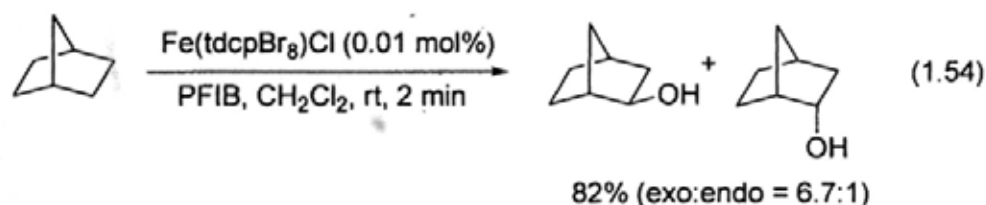


#### Epoxidation

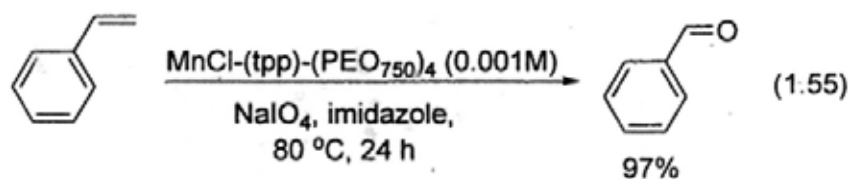


$\text{Fe}^{\text{III}}(\text{tppf}_{20}) = 5,10,15,20\text{-tetrakis-(2,3,4,5,6-pentafluorophenyl)porphyrinato iron(III)}$

#### Hydroxylation of Alkanes



#### Oxidation of Alkene



$\text{PEO}_{750} = \text{CH}_3(\text{OCH}_2\text{CH}_2)_{16}\text{O- group}$

## 1.6 Chemistry of Rhodium Porphyrin Complexes

Rhodium can be easily incorporated into the porphyrin cavities by refluxing free porphyrins with rhodium(III) halides in PhCN (eq 1.56).<sup>59,60</sup> The most common oxidation states of rhodium are +1 and +3 while +2 is less common.<sup>40b</sup> Figure 1.7 shows the energy level diagrams for  $\text{Rh}^{\text{I}}(\text{por})$ ,  $\text{Rh}^{\text{II}}(\text{por})$  and  $\text{Rh}^{\text{III}}(\text{por})$  and they exhibit the reactivities of nucleophile, radical and electrophile, respectively.

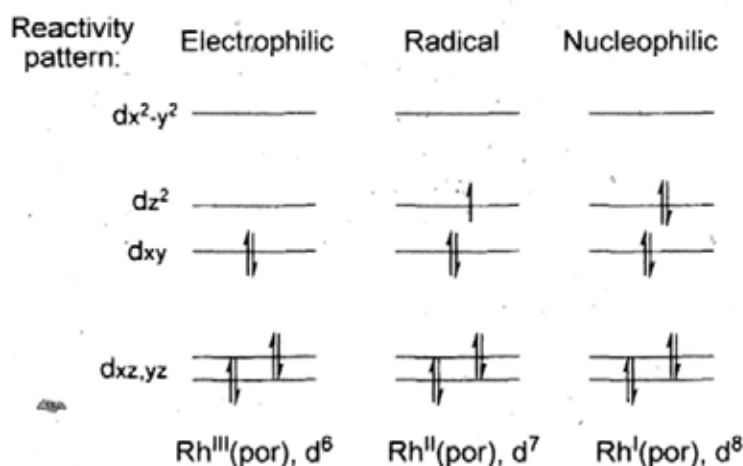
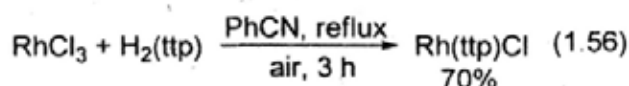
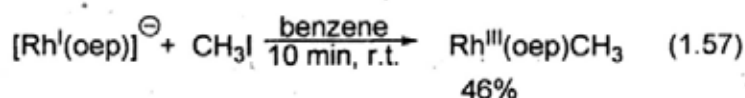


Figure 1.7 Energy Level Diagrams for Rh(por) at Various Oxidation States

### 1.6.1 $\text{Rh}^{\text{I}}(\text{por})$ Chemistry

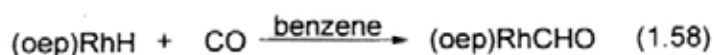
$\text{Rh}^{\text{I}}(\text{por})$  complexes are generally prepared by reduction of  $\text{Rh}^{\text{III}}(\text{por})$  chloride. The anionic complexes contain a pair of electron in the  $d_{z^2}$  orbital and therefore, react like strong nucleophiles.  $\text{Rh}^{\text{I}}(\text{por})$  are well known for addition reactions<sup>60</sup> and nucleophilic substitution.<sup>61</sup>  $\text{Rh}(\text{por})$  alkyl complexes are generally prepared by the nucleophilic substitution of alkyl halides with  $\text{Rh}^{\text{I}}(\text{por})$  complexes (eq 1.57).<sup>61</sup>



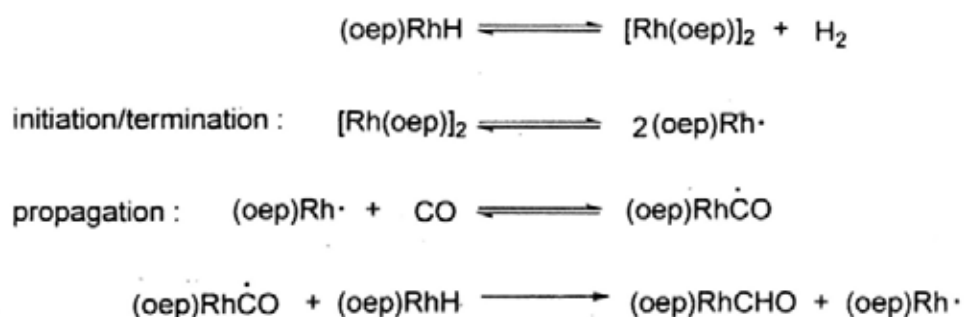
## 1.6.2 Rh<sup>II</sup>(por) Chemistry

Rh<sup>II</sup>(por) complexes have a half-filled dz<sup>2</sup> orbital which make them react like organic radicals and manifest unusually diverse reactions in chemistry.<sup>40b</sup> For less bulky porphyrins (such as ttp and oep), monomeric Rh<sup>II</sup>(por) complexes equilibrate to give Rh–Rh bonded complexes since (por)Rh–Rh(por) bonds range from 12-16 kcal mol<sup>-1</sup>.<sup>17b,62</sup> More bulky Rh<sup>II</sup>(por) complexes such as tmp hardly dimerize and essentially remain monomeric form.

Wayland et al. reported the preparation of a metalloformyl porphyrin complex Rh(oep)CHO from the insertion of CO into Rh(oep)H (eq 1.58).<sup>63</sup> At that time, there was a lack of precedence for the insertion of CO into metal-hydride bond.<sup>63</sup>



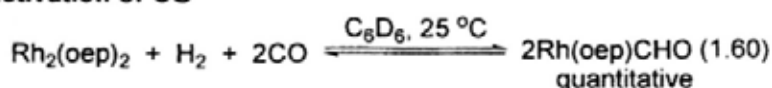
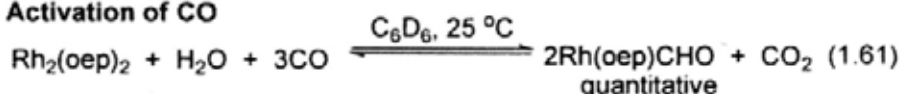
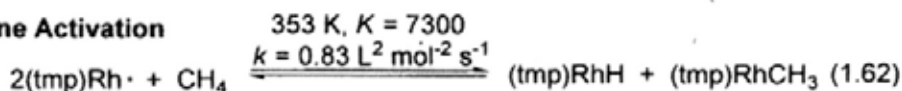
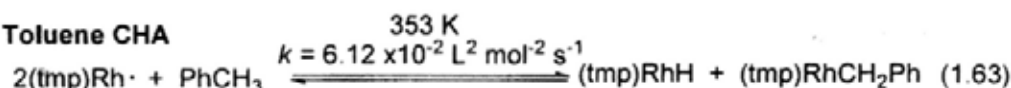
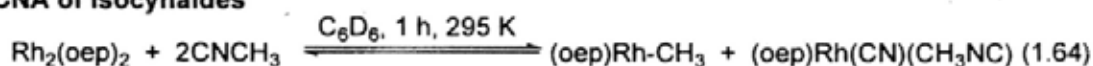
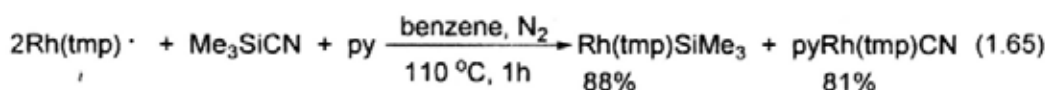
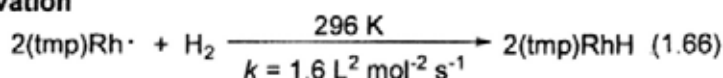
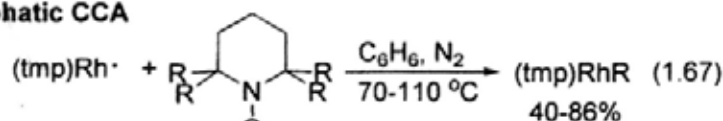
Mechanistic investigation of the CO insertion into Rh(oep)H was later carried out by Haplem et al..<sup>64</sup> A radical chain mechanism was proposed (Scheme 1.11). Rh<sub>2</sub>(oep)<sub>2</sub>, which forms from Rh(oep)H in equilibrium amount, gives Rh<sup>II</sup>(oep) radical as the Rh–Rh bond is weak. Rh<sup>II</sup>(oep) radical then attacks CO to generate a C-centered acyl rhodium radical and subsequent hydrogen atom abstraction from Rh(oep)H gives Rh(oep)CHO and regenerate Rh(oep) radical.



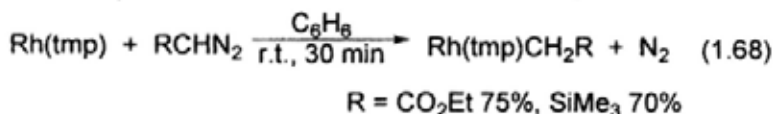
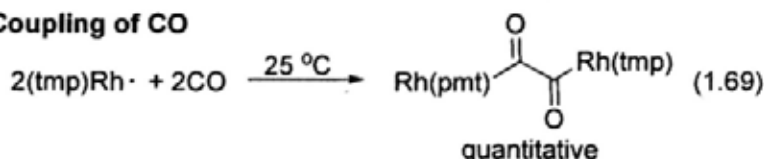
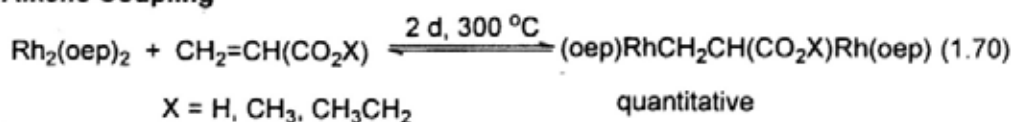
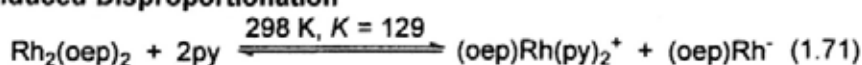
Scheme 1.11 Proposed Mechanism for CO insertion into Rh(oep)H

Monomeric Rh<sup>II</sup>(por) complexes are odd electron complexes and act like radicals in various reactions. A series of Rh<sup>II</sup>(por) chemistry has been reported by Wayland et al. and Chan et al.. Various chemical transformations of Rh<sup>II</sup>(por) are summarized by eqs 1.59-1.71,

including Rh-Rh homolysis/dimerization (eq 1.59),<sup>64</sup> activation of CO (eqs 1.60 and 1.61),<sup>65</sup> methane activation (eq 1.62),<sup>17b</sup> C-H activation of toluene (eq 1.63),<sup>17b</sup> isocyanide activation (eq 1.64),<sup>66</sup> silyl cyanide oxidation addition (eq 1.65),<sup>67</sup> H<sub>2</sub> activation (eq 1.66),<sup>68</sup> aliphatic C-C activation (eq 1.67),<sup>69a,b</sup> reaction with diazo compound (eq 1.68),<sup>69c</sup> reductive coupling of CO (eq 1.69),<sup>70</sup> alkene coupling (eq 1.70)<sup>71a</sup> and ligand induced disproportionation (eq 1.71).<sup>71b</sup>

**Rh-Rh Homolysis/Dimerization****Activation of CO****Activation of CO****Methane Activation****Toluene CHA****CNA of Isocyanides****Oxidative Addition of Silyl Cyanide****H<sub>2</sub> Activation****Aliphatic CCA**

R = Me, CD<sub>3</sub>, Et, Bn

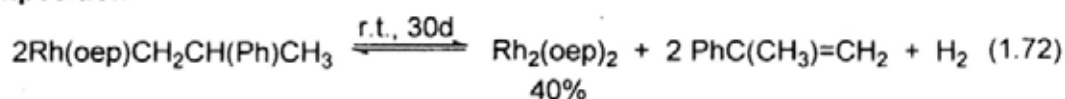
**Reaction with diazo complexes****Reductive Coupling of CO****Alkene Coupling****Ligand Induced Disproportionation**

### 1.6.3 Rh<sup>III</sup>(por) Chemistry

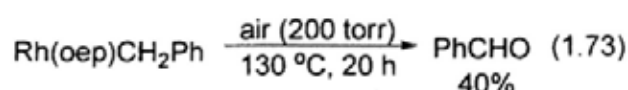
Rh<sup>III</sup>(por) complexes have full-filled d<sub>xy</sub> orbital at the outermost energy level and are diamagnetic. They are usually kinetically inert and air stable. This makes Rh<sup>III</sup>(por) complexes such as Rh(por) halides and alkyls serve as starting materials.

The chemistry of Rh<sup>III</sup>(por) is very fruitful and various examples are summarized in eqs 1.72-1.78 including thermal decomposition (eq 1.72),<sup>72</sup> oxidation (eq 1.73),<sup>72</sup> intermolecular reductive elimination (eq 1.74),<sup>73</sup> alkyl 1,2-rearrangement (eq 1.75),<sup>74</sup> aldehydic CHA (eq 1.76),<sup>75</sup> base-promoted BnCCA of toluene (eq 1.77)<sup>76</sup> and CCA of ether (eq 1.78).<sup>77</sup>

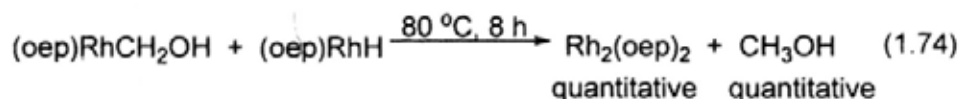
#### Thermal decomposition



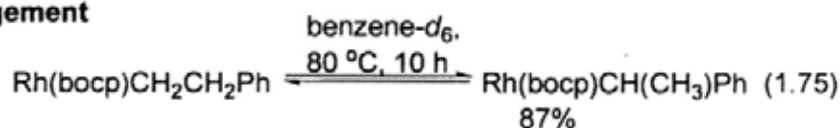
#### Oxidation



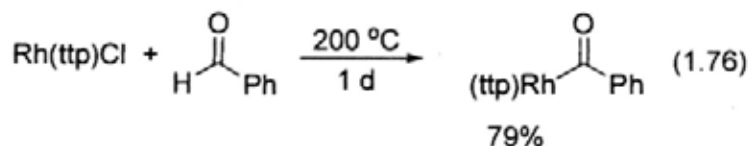
#### Intermolecular reductive elimination



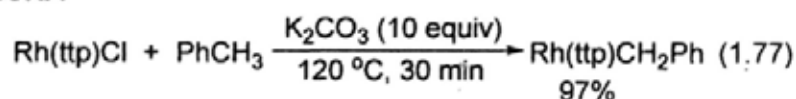
#### Alkyl 1,2-rearrangement



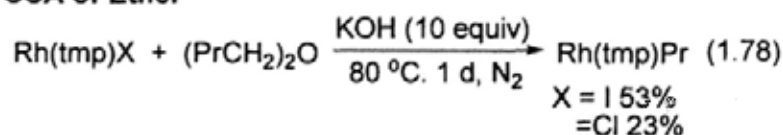
#### Aldehydic CHA



#### Base-promoted BnCHA

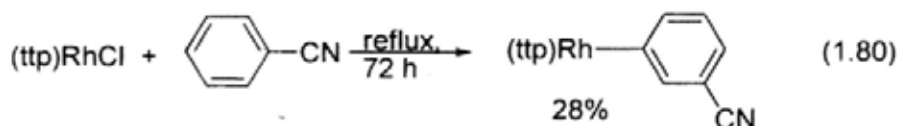
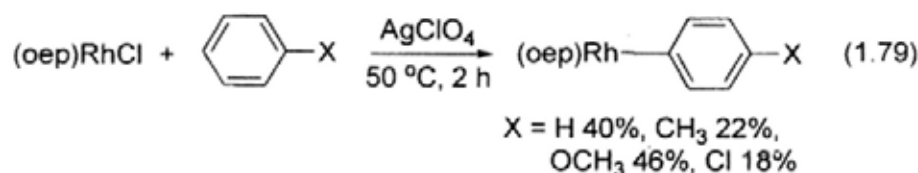


#### Base-Promoted CCA of Ether

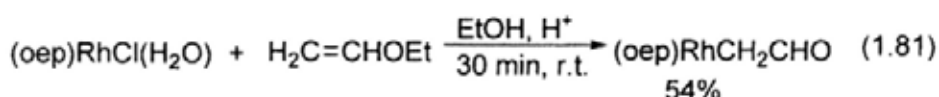


Since  $\text{Rh}^{\text{III}}(\text{por})$  has a empty  $d_z^2$  and electron deficient, four coordinated cationic  $\text{Rh}^{\text{III}}(\text{por})$  reacts like a Lewis acid or electrophile to undergo electrophilic aromatic substitution with arene (eqs 1.79 and 1.80),<sup>78,79</sup> electrophilic addition to alkene (eq 1.81)<sup>80</sup> and  $\alpha$ -metalation of ketone (eq 1.82).<sup>80</sup> Besides,  $\text{Rh}^{\text{III}}(\text{por})$  are well known for catalytic cyclopropanation of alkenes (eq 1.83)<sup>81</sup> and catalytic Aldol condensation (eq 1.84).<sup>80</sup>

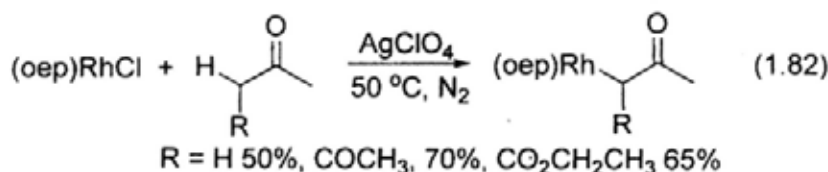
#### Electrophilic Aromatic Substitution



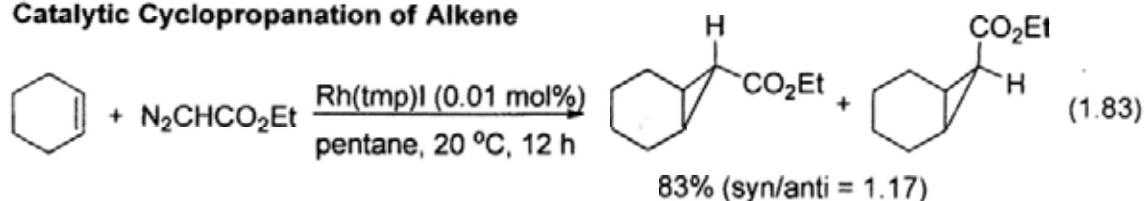
#### Electrophilic Addition



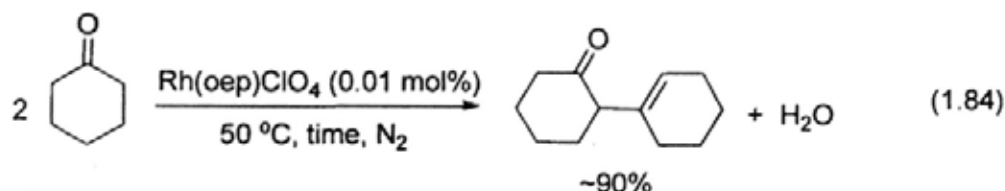
#### $\alpha$ -Metalation of Ketone



#### Catalytic Cyclopropanation of Alkene



#### Catalytic Aldol Condensation



## 1.7 Scope of Thesis

The objectives of the research focus on the studies of the C–H and C–C activation of alkanes with rhodium porphyrin complexes. The thesis is outlined in the following sections:

- (i) base-promoted C–H activation of aliphatic alkanes and non-strained cycloalkanes with rhodium(III) porphyrin complexes
- (ii) metalloradical-promoted functionalization of cycloheptane to rhodium(III) porphyrin benzyl via C–H and C–C activations
- (iii) metalloradical-promoted aliphatic C–C activation of cyclooctane
- (iv) summary of C–H and C–C activations of alkanes

## Reference

- (1) (a) *Comprehensive organic synthesis: selectivity, strategy & efficiency in modern organic chemistry*; Trost, B. M., Fleming, I., Eds.; Pergamon Press: New York 1991. (b) Crabtree, R. H. *Chem. Rev.* **1985**, *85*, 245-269. (c) Crabtree, R. H. *Dalton Trans.* **2001**, *17*, 2437-2450.
- (2) Luo, Y. R. *Comprehensive Handbook of Chemical Bond Energies*, CRC Press, Boca Raton, FL, 2007.
- (3) (a) Isaacs, N. S. *Physical Organic Chemistry*; Longman: Essex, 1987. (b) The BDE of C–C bonds are calculated based on the  $\Delta H_{\text{formation}}$ , see Stull, D. R.; Westrum, E. F. Jr.; Sinke, G. C. *The Chemical Thermodynamics of Organic Compounds*; John Wiley & Sons: New York 1969. (c) Exner, K.; Schleyer, P. V. R. *J. Phys. Chem. A* **2001**, *105*, 3407-3416. (d) The C–C BDE of *c*-hexane is calculated to be 82.7 kcal mol<sup>-1</sup> and the literature reported value is 87.3 kcal mol<sup>-1</sup>. The C–C BDE of *c*-pentane is calculated to be 82.9 kcal mol<sup>-1</sup>. So, the C–C BDE of *c*-pentane is corrected by 4 kcal mol<sup>-1</sup> to 86.9 kcal mol<sup>-1</sup>.
- (4) Goldberg, K. I.; Goldman, A. S., Eds. *Activation and Functionalization of C–H Bonds*; ACS Symposium Series 885; American Chemical Society: Washington, DC, 2004.
- (5) (a) Periana, R. A.; Taube, D. J.; Gamble, S.; Taube, H.; Satoh, T.; Fujii, H. *Science* **1998**, *280*, 560-564. (b) Davies, H. M. L.; Manning, J. R. *Nature* **2008**, *451*, 417-424. (c) Davies, H. M. L.; Hansen, T.; Hopper, D. W.; Panaro, S. A. *J. Am. Chem. Soc.* **1999**, *121*, 6509-6510.
- (6) Labinger, J. A.; Bercaw, J. E. *Nature* **2002**, *417*, 507-514.
- (7) (a) Jones, W. D. *Nature* **1993**, *364*, 676-677. (b) Murakami, M.; Ito, Y. *In Topics in Organometallic Chemistry, Vol. 3, Activation of Unreactive Bonds and Organic Synthesis*, Murai, S. Ed., Springer-Verlag: Berlin Heidelberg, 1999, 97-129.

- (8) Sen, A. *Acc. Chem. Res.* **1998**, *31*, 550-557.
- (9) Thayer, J. S. *Organometallic Chemistry. An Overview*, New York, N. Y., Weinheim: VCH Publishers, 1987.
- (10) Janowicz, A. H.; Bergman, R. G. *J. Am. Chem. Soc.* **1982**, *104*, 352-354.
- (11) (a) Harper, T. G. P.; Shinomoto, R. S.; Deming, M. A.; Flood, T. C. *J. Am. Chem. Soc.* **1988**, *110*, 7915-7916.
- (12) Sakakura, T.; Tanaka, M. *Chem. Lett.* **1987**, 249. Sakakura, T.; Tanaka, M. *J. Chem. Soc., Chem. Commun.*, **1987**, 758-759.
- (13) (a) Burk, M. J.; Crabtree, R. H.; Parnell, C. P.; Uriarte, R. J. *Organometallics* **1984**, *3*, 816-817. Burk, M. J.; Crabtree, R. H. *J. Am. Chem. Soc.* **1987**, *109*, 8025-8032. (b) Xu, W.; Rosini, G. P.; Gupta, M.; Jensen, C. M.; Kaska, W. C.; Krogh-Jespersen, K.; K.; Goldman, A. S. *Chem. Commun.* **1997**, 2273-2274.
- (14) (a) Chen, H.; Hartwig, J. F. *Angew. Chem., Int. Ed.* **1999**, *38*, 3391-3393. (b) Chen, H.; Schlecht, S.; Semple, T. C.; Hartwig, J. F. *Science* **2000**, *287*, 1995-1997. (c) Boller, T. M.; Murphy, J. M.; Hapke, M.; Ishiyama, T.; Miyaura, N.; Hartwig, J. F. *J. Am. Chem. Soc.* **2005**, *127*, 14263-14278. (d) Cho, J. Y.; Tse, M. K.; Holmes, D.; Maleczka, R. E.; Smith, M. R. *Science* **2002**, *295*, 305-308.
- (15) Waston, P. L. *J. Am. Chem. Soc.* **1983**, *105*, 6491-6493.
- (16) Thompson, M. E.; Bercaw, J. E. *Pure Appl. Chem.* **1984**, *56*, 1-10.
- (17) (a) Wayland, B. B.; Sherry, A. E. *J. Am. Chem. Soc.* **1990**, *112*, 1259-1261. (b) Wayland, B. B.; Ba, S.; Sherry, A. E. *J. Am. Chem. Soc.* **1991**, *113*, 5305-5311.
- (18) Cummins, C. C.; Baxter, S. M.; Wolczanski, P. T. *J. Am. Chem. Soc.* **1988**, *110*, 8731-8733.
- (19) Walsh, P. J.; Hollander, F. J.; Bergman, R. G. *J. Am. Chem. Soc.* **1988**, *110*, 8729-8731.

- (20) Wada, K.; Pamplin, C. B.; Legzdins, P.; Patrick, B. O.; Tsyba, I.; Bau, R. A. *J. Am. Chem. Soc.* **2003**, *125*, 7035-7048.
- (21) Liu, F.; Pak, E. B.; Singh, B.; Jensen, C. M.; Goldman, A. S. *J. Am. Chem. Soc.* **1999**, *121*, 4086-4087.
- (22) Ward, M. D.; Schwartz, J. *Organometallics* **1982**, *1*, 1030-1032.
- (23) Ferguson, R. R.; Crabtree, R. H. *J. Org. Chem.* **1991**, *56*, 5503-5510.
- (24) Gomez-Emeterio, B. P.; Urbano, J.; Diaz-Requejo, M. M.; Perez, P. J. *Organometallics* **2008**, *27*, 4126-4130.
- (25) Kitajima, N.; Schwartz, J. *J. Am. Chem. Soc.* **1984**, *106*, 2220-2222.
- (26) Hino, M.; Kobayashi, S.; Arata, K. *J. Am. Chem. Soc.* **1979**, *101*, 6439-6441.
- (27) Waltz, K. M.; Hartwig, J. F. *J. Am. Chem. Soc.* **2000**, *122*, 11358-11369.
- (28) (a) Cassar, L.; Eaton, P. E.; Halpern, J. *J. Am. Chem. Soc.* **1970**, *92*, 3515-3518. (b) Eisch, J. J.; Piotrowski, A. M.; Han, K. I.; Kruger, C.; Tsay, T. H. *Organometallics* **1985**, *4*, 224-231. (c) Perthuisot, C.; Edelbach, B. L.; Zubris, D. L.; Jones, W. D. *Organometallics* **1997**, *16*, 2016-2023.
- (29) (a) Crabtree, R. H.; Dion, R. P.; Gibboni, D. J.; McGrath, D. V.; Holt, E. M. *J. Am. Chem. Soc.* **1986**, *108*, 7222-7227. (b) Hemond, R. C.; Hughes, R. P.; Locker, H. B. *J. Am. Chem. Soc.* **1986**, *5*, 2391-2392.
- (30) (a) Gozin, M.; Weisman, A.; Ben-David, Y.; Milstein, D. *Nature* **1993**, *364*, 699-670. (b) Rybtchinski, B.; Vigalok, A.; Ben-David, Y.; Milstein, D. *J. Am. Chem. Soc.* **1996**, *118*, 12406-12415. (c) van der Boom, M. E.; Liou, S. Y.; Ben-David, Y.; Gozin, M.; Milstein, D. *J. Am. Chem. Soc.* **1998**, *120*, 13415-13421. (d) Rybtchinski, B.; Milstein, D. *Angew. Chem. Int. Ed.* **1999**, *38*, 870-883. (e) van der Boom, M. E.; Liou, S. Y.; Ben-David, Y.; Gozin, M.; Milstein, D. *J. Am. Chem. Soc.* **1998**, *120*, 13415-13421. (f) Rybtchinski, B.; Milstein, D.; *J. Am. Chem. Soc.* **1999**, *121*, 4528-4529.

- (31) (a) Jun, C. -H. *Chem. Soc. Rev.* **2004**, *33*, 610–618. (b) Jun, C. -H.; Moon, C. W.; Lee, D. -Y. *Chem. Eur. J.* **2002**, *8*, 2420-2428. (c) Jun, C.-H.; Chung, K.-Y.; Hong, J.-B. *Org. Lett.* **2001**, *3*, 785-787. (d) Lim, S.-G.; Lee, J. H.; Moon, C. W.; Hong, J.-B.; Jun, C.-H. *Org. Lett.* **2003**, *5*, 2759-2761. (e) Park, Y. J.; Kwon, B.-I.; Ahn, J.-A.; Lee, H.; Jun, C.-H. *J. Am. Chem. Soc.* **2004**, *126*, 13892-13893. (f) Jun, C.-H.; Lee, H.; Moon, C. W.; Hong, H.-S. *J. Am. Chem. Soc.* **2001**, *123*, 8600-8601. (g) Jun, C.-H.; Lee, H.; Lim, S.-G. *J. Am. Chem. Soc.* **2001**, *123*, 751-752. (h) Jun, C.-H.; Lee, H. *J. Am. Chem. Soc.* **1999**, *121*, 880-881.
- (32) (a) Suggs, J. W.; Jun, C. H. *J. Am. Chem. Soc.* **1984**, *106*, 3054-3056. (b) Suggs, J. W.; Jun, C. H. *J. Am. Chem. Soc.* **1986**, *108*, 4679-4681.
- (33) (a) Murakami, M.; Amii, H.; Ito, Y. *Nature* **1994**, *370*, 541-542. (b) Murakami, M.; Tsuruta, T.; Ito, Y. *Angew. Chem. Int. Ed.* **2000**, *39*, 2484-2486. (c) Dreis, A. M.; Douglas, C. J. *J. Am. Chem. Soc.* **2009**, *131*, 412-413.
- (34) (a) Waston, P. L.; Roe, D. C. *J. Am. Chem. Soc.* **1982**, *104*, 6471-6473. (b) Hajela, S.; Bercaw, J. E. *Organometallics* **1994**, *13*, 1147-1154.
- (35) Hartwig, J. F.; Bergman, R. G.; Andersen, R. A. *Organometallics* **1991**, *10*, 3344-3362.
- (36) (a) Nishimura, T.; Ohe, K.; Uemura, S. *J. Am. Chem. Soc.* **1999**, *121*, 2645-2646. (b) Nishimura, T.; Araki, H.; Maeda, Y.; Uemura, S. *Org. Lett.* **2003**, *5*, 2997-2999.
- (37) (a) Nishimura, T.; Uemura, S. *J. Am. Chem. Soc.* **2000**, *122*, 12049-12050. (b) Nishimura, T.; Yoshinaka, T.; Nishiguchi, Y.; Maeda, Y.; Uemura, S. *Org. Lett.* **2005**, *7*, 2425-2427.
- (38) (a) Vidal, V.; Theolier, A.; Thivolle-Cazat, J.; Basset, J. M. *Science* **1997**, *276*, 99-102. (b) Basset, J. M.; Coperet, C.; Lefort, L.; Maunders, B. M.; Maury, O.; Le Roux, E.; Saggio, G.; Soignier, S.; Soulivong, D.; Sunley, G. J.; Taoufik, M.; Thivolle-Cazat, J. *J. Am. Chem. Soc.* **2005**, *127*, 8604-8605.

- (39) Ogoshi, H.; Setsune, J. I.; Yoshida, Z. I. *J. Organomet. Chem.* **1980**, *185*, 95-104.
- (40) (a) Fleischer, E. B. *Acc. Chem. Res.* **1970**, *3*, 105-112. (b) *The Porphyrin Handbook Volume 3*; Kadish, K. M., Smith, K. M., Guilard, R., Eds.; Academic Press: Boston, 2000. (c) *Porphyrins and Metalloporphyrins*; Smith, K. M., Ed.; Elsevier Scientific Pub. Co.: New York, 1975. (d) Ogoshi, H. Mizutani, A. *Acc. Chem. Res.* **1998**, *31*, 81-89.
- (41) *Porphyrins and Metalloporphyrins*; Smith, K. M., Ed.; Elsevier Scientific Pub. Co.: New York, 1975.
- (42) Shanumgathasan, S.; Edwards, C.; Boyle, R. W. *Tetrahedron* **2000**, *56*, 1025-1046.
- (43) (a) *Chemistry and Biochemistry of B<sub>12</sub>*; Banerjee, R., Ed.; John Wiley: New York, 1999. (b) Hodgkin, D. C.; Kamper, J.; Mackay, M.; Pickworth, J. *Nature* **1956**, *178*, 64-66. (c) [http://nobelprize.org/nobel\\_prizes/medicine/articles/carpenter/table.html](http://nobelprize.org/nobel_prizes/medicine/articles/carpenter/table.html), Accessed on 13<sup>th</sup> March, 2010.
- (44) (a) Schrauzer, G. N. *Angew. Chem. Int. Ed. Engl.* **1976**, *15*, 414-426. (b) Schrauzer, G. N. *Acc. Chem. Res.* **1968**, *1*, 97-103. *B<sub>12</sub>*; Dolphin, D. Ed.; Wiley-Interscience: New York, 1982.
- (45) (a) *Bioinorganic Chemistry: Inorganic Elements In The Chemistry of Life: An Introduction and Guide*; Kaim, W.; Schwederski, B., Eds.; John Wiley: New York, 1994. (b) Emsley, J. *The Elements* 3<sup>rd</sup> Ed., Clarendon Press: Oxford, 1998.
- (46) (a) *The Porphyrins*; Dolphin, D., Ed.; Academic press: New York, 1979. (b) Dolphin, D.; Felton, R. H. *Acc. Chem. Res.* **1974**, *7*, 26-32.
- (47) (a) Haddad, R. E.; Gazeau, S.; Pecaut, J.; Marchon, J. C.; Medforth, C. J.; Shelnut, J. A. *J. Am. Chem. Soc.* **2003**, *125*, 1253-1268. (b) Ryeng, H.; Ghosh, A. *J. Am. Chem. Soc.* **2002**, *124*, 8099-8103.
- (48) (a) Shelnut, J. A.; Song, X.-Z.; Ma, J.-G.; Jia, S.-L.; Jentzen, W.; Medforth, C. J. *Chem. Soc. Rev.* **1998**, *27*, 31-41. (b) Ogura, H.; Yatsunyk, L.; Medforth, C. J.; Smith, K. M.;

- Barkigia, K. M.; Renner, M. W.; Melamed, D.; Walker, F. A. *J. Am. Chem. Soc.* **2001**, *123*, 6564-6578. (c) Gazeau, S.; Pecaut, J.; Haddad, R. E.; Shelnutt, J. A.; Marchon, J.-C. *Eur. J. Inorg. Chem.* **2002**, 2956-2960.
- (49) (a) *Chemistry and Biochemistry of B<sub>12</sub>*; Banerjee, R., Ed.; John Wiley: New York, 1999.  
(b) Hodgkin, D. C.; Kamper, J.; Mackay, M.; Pickworth, J. *Nature* **1956**, *178*, 64-66.
- (50) Gassman, P. G.; Ghosh, A.; Almlo, J. *J. Am. Chem. Soc.* **1992**, *114*, 9990-10000.
- (51) (a) Collman, J. P.; Brauman, J. I.; Doxsee, K. M.; Sessler, J. L.; Morris, R. M.; Gibson, Q. H. *Inorg. Chem.* **1983**, *22*, 1427-1432. (b) Collman, J. P.; Boulatov, R. *J. Am. Chem. Soc.* **2000**, *122*, 11812-11821.
- (52) *The Porphyrin Handbook Volume 6*; Kadish, K. M., Smith, K. M., Guilard, R., Eds.; Academic Press: Boston, 2000.
- (53) Liang, J. L.; Yuan, S. X.; Huang, J. S.; Yu, W. Y.; Che, C. M. *Angew. Chem. Int. Ed.* **2002**, *41*, 3468-3468.
- (54) Baumann, K. L.; Mbuvi, H. M.; Du, G.; Woo, L. K. *Organometallics* **2007**, *26*, 3995-4002.
- (55) Zhu, S.; Perman, J. A.; Zhang, X. P. *Angew. Chem., Int. Ed.* **2008**, *47*, 8460-8463.
- (56) Smeureanu, G.; Aggarwal, A.; Söll, C. E.; Arijeloye, J.; Malave, E.; Drain, C. M. *Chem. Eur. J.* **2009**, *15*, 12133-12140.
- (57) Traylor, T. G.; Hill, K. W.; Fann, W.-P.; Tsuchiya, S.; Bunlap, B. E. *J. Am. Chem. Soc.* **1992**, *114*, 1308-1312.
- (58) Liu, S. -T.; Reddy, V.; Lai, R. -Y. *Tetrahedron* **2007**, *63*, 1821-1825.
- (59) (a) Zhou, X.; Li, Q.; Mak, T. C. W.; Chan, K. S. *Inorg. Chim. Acta* **1998**, *270*, 551-554.  
(b) Zhou, X.; Tse, M. K.; Wu, D.-D.; Mak, T. C. W.; Chan, K. S. *J. Organomet. Chem.* **2000**, *598*, 80-86. (c) Mak, K. W.; Yeung, S. K.; Chan, K. S. *Organometallics* **2002**, *21*, 2362-2364.

- (60) Ogoshi, H.; Setsune, J.; Omura, T.; Yoshida, Z. *J. Am. Chem. Soc.* **1975**, *97*, 6461-6466.
- (61) Ogoshi, H.; Omura, T.; Yoshida, Z. *J. Am. Chem. Soc.* **1973**, *95*, 1666-1668.
- (62) (a) Wayland, B. B.; Coffin, V. L.; Farnos, M. D. *Inorg. Chem.* **1988**, *27*, 2745-2747. (b) Wayland, B. B. *Polyhedron* **1988**, *7*, 1545-1555.
- (63) Wayland, B. B.; Woods, B. A. *J. Chem. Soc., Chem. Commun.* **1981**, 700-701.
- (64) Paonessa, R. S.; Thomas, N. C.; Halpern, J. *J. Am. Chem. Soc.* **1985**, *107*, 4333-4335.
- (65) Wayland, B. B.; Woods, B. A.; Pierce, R. *J. Am. Chem. Soc.* **1982**, *104*, 302-303.
- (66) Poszmik, G.; Carroll, P. J.; Wayland, B. B. *Organometallics* **1993**, *12*, 3410-3417.
- (67) Chan, K. S.; Zhang, L. R.; Fung, C. W. *Organometallics* **2004**, *23*, 6097-6098.
- (68) Wayland, B. B.; Ba, S.; Sherry, A. E. *Inorg. Chem.* **1992**, *31*, 148-150.
- (69) (a) Tse, M. K.; Chan, K. S. *J. Chem. Soc., Dalton Trans.* **2001**, 510-511. (b) Chan, K. S.; Li, X. Z.; Dzik, W. I.; de Bruin, B. *J. Am. Chem. Soc.* **2008**, *130*, 2051-2061. (c) Zhang, L. R.; Chan, K. S. *Organometallics* **2007**, *26*, 679-684.
- (70) Wayland, B. B.; Sherry, A. E.; Poszmik, G.; Bunn, A. G. *J. Am. Chem. Soc.* **1992**, *114*, 1673-1681.
- (71) (a) Wayland, B. B.; Poszmik, G. *Organometallics* **1992**, *11*, 3534-3542. (b) Wayland, B. B.; Balkus, K. J., Jr.; Farnos, M. D. *Organometallics* **1989**, *8*, 950-955.
- (72) De Rossi, K. J.; Wayland, B. B. *J. Am. Chem. Soc.* **1985**, *107*, 7941-7944.
- (73) Van Voorhees, S. L.; Wayland, B. B. *Organometallics* **1985**, *4*, 1887-1888.
- (74) Mak, K. W.; Chan, K. S. *J. Am. Chem. Soc.* **1998**, *120*, 9689-9687.
- (75) Chan, K. S.; Lau, C. M. *Organometallics* **2006**, *25*, 260-265.
- (76) Chan, K. S.; Chiu, P. F.; Choi, K. S. *Organometallics* **2007**, *26*, 1117-1119.
- (77) Lai, T. H.; Chan, K. S. *Organometallics* **2009**, *28*, 6845-6846.
- (78) Aoyama, Y.; Yoshida, T.; Sakurai, K.; Ogoshi, H. *Organometallics* **1986**, *5*, 168-173.

- (79) (a) Zhou, X.; Li, Q.; Mak, T. C. W.; Chan, K. S. *Inorg. Chim. Acta* **1998**, *270*, 551-554.  
(b) Zhou, X.; Tse, M. K.; Wu, D.-D.; Mak, T. C. W.; Chan, K. S. *J. Organomet. Chem.* **2000**, *598*, 80-86.
- (80) Aoyama, Y.; Tanaka, Y.; Yoshida, T.; Toi, H.; Ogoshi, H. *J. Organomet. Chem.* **1987**, *329*, 251-266.
- (81) (a) Callot, H. J.; Piechocki, C. *Tetrahedron Lett.* **1980**, *21*, 3489-3492. (b) Callot, H. J.; Metz, F.; Piechocki, C. *Tetrahedron* **1982**, *38*, 2365-2369.

## Chapter 2 Base-promoted Carbon–Hydrogen Bond Activation of Alkanes with Rhodium(III) Porphyrin Complexes

### 2.1 Carbon–Hydrogen Bond Activation by Rhodium(III) Porphyrins

Carbon–hydrogen bond activation (CHA) of organic compounds by transition-metal complexes is an important area of research in organometallic chemistry.<sup>1</sup> The CHA of alkane is challenging, due to the lack of reactivity of alkanes.<sup>2</sup> Previous examples include low-valent transition-metal complexes, while more recent systems involve high-valent late-transition-metal complexes because of their added advantages of broader functional group compatibility.<sup>3</sup> Examples of high-valent late-transition-metal Rh(III) and Ir(III) complexes undergoing CHA are well-known.<sup>4</sup> Schwartz et al. demonstrated the Rh(III)-catalyzed chlorination of methane.<sup>4a,b</sup> Recently, iridium(III) pincer complexes were shown to catalyze the dehydrogenation of *c*-octane.<sup>4c,d</sup> Periana et al. worked on the alkyl CHA with *bis*-bidentate O-donor iridium(III) complexes.<sup>4e,f</sup>

The bond activation chemistry of Rh(III) and Ir(III) is commonly accepted to occur by either  $\sigma$ -bond metathesis or heterolysis. However, recent reports provided evidence for oxidative addition in which a Rh(V) or Ir(V) intermediate is formed.<sup>5</sup> Therefore, diverse mechanistic possibilities exist.

The Chan group have been interested in the CHA by rhodium(III) porphyrin complexes. Rhodium porphyrin chloride can activate the *meta* C–H bond of benzonitrile to give (*m*-cyanophenyl) rhodium porphyrin complexes selectively via an S<sub>E</sub>Ar mechanism.<sup>6</sup> Aryl and alkyl aldehydes also undergo selective aldehydic CHA to give rhodium porphyrin

aryl and alkyl acyls.<sup>7</sup> Recently, Chan et al. have reported the selective benzylic CHA of toluenes promoted by base.<sup>8</sup> These types of CHA are mechanistically puzzling, though a heterolytic or  $\sigma$ -bond metathesis pathway was suggested.

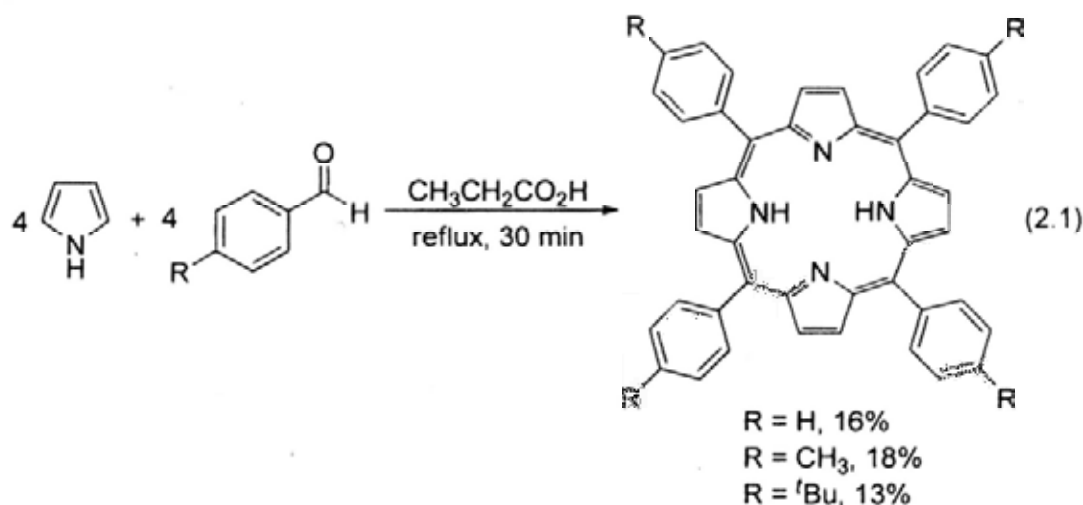
## 2.2 Objectives of the Work

The objectives of this work are to (i) broaden the synthetic scope and (ii) to gain further mechanistic understanding of the alkyl CHA with rhodium porphyrin complexes.

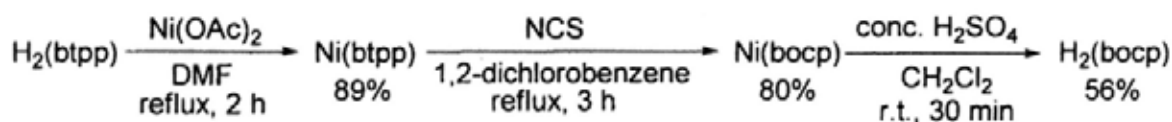
## 2.3 Preparation of Starting Materials

### 2.3.1 Preparation of Porphyrins<sup>9</sup>

Tetraphenylporphyrin ( $H_2tp$ ),<sup>9a-c</sup> tetratolylporphyrin ( $H_2ttp$ )<sup>9b,9d</sup> and tetra-(4-*tert*-butylphenyl)porphyrin ( $H_2(btp)$ )<sup>9c</sup> were directly synthesized from the co-tetramerization of the corresponding aldehydes and pyrrole in refluxing propanoic acid for 30 min in 16%, 18% and 13% yields, respectively according to the literatures (eq 2.1).<sup>9</sup>



An electron-deficient porphyrin,  $H_2(bocp)$ , which bears eight chlorine atoms at the  $\beta$ -positions, was synthesized in three steps from  $H_2(btp)$  (Scheme 2.1).<sup>9d,10</sup>

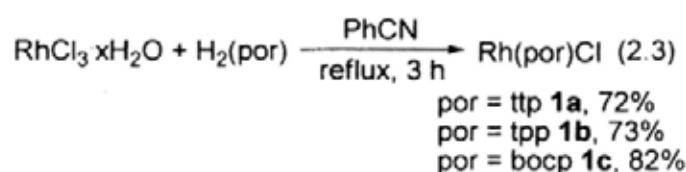


Scheme 2.1 Synthetic Procedures of  $H_2(bocp)$

## 2.3.2 Preparation of Rhodium Porphyrin Complexes

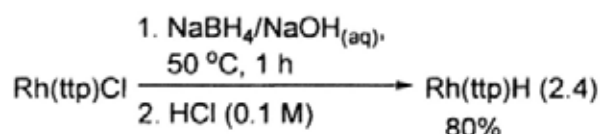
### 2.3.2.1 Synthesis of Rh(ttp)Cl, Rh(tpp)Cl and Rh(bocp)Cl

Rhodium porphyrin chlorides complexes  $\text{Rh}^{\text{III}}(\text{ttp})\text{Cl}$ ,  $\text{Rh}^{\text{III}}(\text{tpp})\text{Cl}$  and  $\text{Rh}^{\text{III}}(\text{bocp})\text{Cl}$  were synthesized by the metallation of corresponding free porphyrin with  $\text{RhCl}_3 \cdot x\text{H}_2\text{O}$  in refluxing PhCN (eq 2.2).<sup>11</sup>



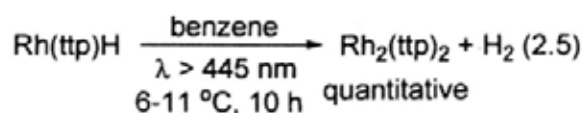
### 2.3.2.2 Synthesis of Rh(ttp)H

$\text{Rh}(\text{ttp})\text{H}$  **1d** was synthesized according to the literature method.<sup>12</sup>  $\text{Rh}(\text{ttp})\text{Cl}$  **1a** was first reduced by  $\text{NaBH}_4$  and then the reaction mixture was protonated by diluted HCl to give  $\text{Rh}(\text{ttp})\text{H}$  in 80% yield (eq 2.4).



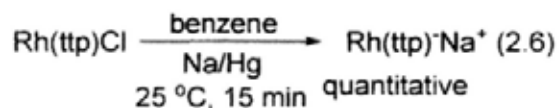
### 2.3.2.3 Synthesis of $\text{Rh}_2(\text{ttp})_2$

$\text{Rh}_2(\text{ttp})_2$  **1e** was synthesized according to the literature method.<sup>12</sup>  $\text{Rh}(\text{ttp})\text{H}$  **1d** was added into degassed benzene and the red solution was irradiated at  $\lambda > 445$  nm at 6-11 °C for 10 hours to give  $\text{Rh}_2(\text{ttp})_2$  **1e** in quantitative yield and presumably hydrogen (eq 2.5).



### 2.3.2.4 Synthesis of $\text{Rh}(\text{ttp})\text{Na}^+$

Rh(tpp)Na<sup>+</sup> **1e** was synthesized according to the literature method.<sup>13</sup> Rh(tpp)Cl **1a** was dissolved in degassed benzene and then Na/Hg was added (eq 2.6). The reaction mixture was stirred at room temperature for 15 min. The resultant deep reddish brown solution was transferred via cannular under nitrogen atmosphere for subsequent reaction.

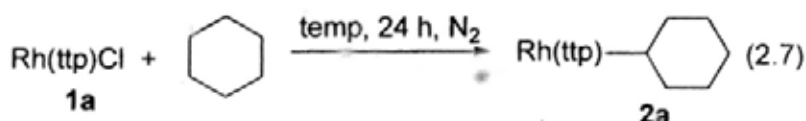


## 2.4 Optimization of Reaction Conditions

### 2.4.1 Temperature Effect

Initially, rhodium(III) tetrakis-(4-tolylporphyrin) chloride (Rh(tpp)Cl; **1a**) reacted with *c*-hexane at 80 °C and 100 °C for 24 hours to give a trace amount of Rh(tpp)(*c*-hexyl) (eq 2.7, Table 2.1, entries 1 and 2). At 120 °C for 24 hours, successful CHA of *c*-hexane occurred and Rh(tpp)(*c*-hexyl) **2a** was obtained in 31% yield (Table 2.1, entry 3). When the temperature was further increased to 150 °C or 200 °C, Rh(tpp)(*c*-hexyl) **2a** was obtained in lower yields of Rh(tpp)(*c*-hexyl) **2a** were obtained in 16% and 18%, respectively (Table 2.1, entries 4 and 5). Likely, Rh(tpp)(*c*-hexyl) **2a** is thermally unstable. Indeed, when Rh(tpp)(*c*-hexyl) **2a** was heated in *c*-hexane at 120 °C and 150 °C for 1 day, the recovery yields were 80% and 41%, respectively. Therefore, the optimal reaction temperature was selected to be 120 °C.

Table 2.1 Effect of Temperature on CHA of *c*-Hexane

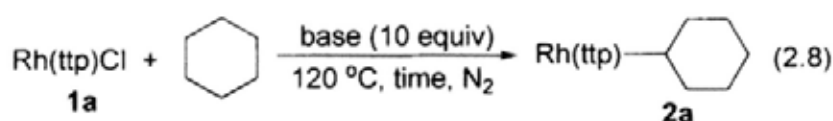


| Entry | Temp (°C) | Yield (%) |
|-------|-----------|-----------|
| 1     | 80        | Trace     |
| 2     | 100       | 3         |
| 3     | 120       | 31        |
| 4     | 150       | 16        |
| 5     | 200       | 18        |

### 2.4.2 Base Effect

With the reported base-promoted benzylic CHA of toluenes by  $\text{Rh}^{\text{III}}(\text{ttp})\text{Cl}$ <sup>8</sup> and other examples of base promoted CHA by transition-metal complexes,<sup>14</sup> we sought to examine the promoting effect of various base. Table 2.2 and eq 2.8 list the results of the screenings. The ligand,  $\text{PPh}_3$ , only gave coordination complex **3**, without any CHA product (Table 2.2, entry 2). On the other hand, non-coordinating bases of 2,2'-bipyridine, 2,6-di-*tert*-butylpyridine, and 2,6-diphenylpyridine gave higher yield of over 50% of  $\text{Rh}(\text{ttp})(c\text{-hexyl})$  in 1 day (eq 2.8, Table 2.2, entries 3-5). However, a shorter reaction time of 6 hours resulted in much lower yield of 23% (Table 2.2, entry 6).

Table 2.2 Base Effect in CHA



| Entry | Base                    | Time (h) | Yield (%)      |
|-------|-------------------------|----------|----------------|
| 1     | Nil                     | 24       | 31             |
| 2     | $\text{PPh}_3$          | 24       | 0 <sup>a</sup> |
| 3     | 2,2'-bpy <sup>b</sup>   | 48       | 50             |
| 4     | 2,6-dbpy <sup>c</sup>   | 24       | 50             |
| 5     | 2,6-dppy <sup>d</sup>   | 24       | 58             |
| 6     | 2,6-dppy <sup>d</sup>   | 6        | 23             |
| 7     | NaOH                    | 6        | 47             |
| 8     | NaOAc                   | 6        | 51             |
| 9     | $\text{K}_2\text{CO}_3$ | 6        | 59             |
| 10    | $\text{K}_2\text{CO}_3$ | 24       | 40             |

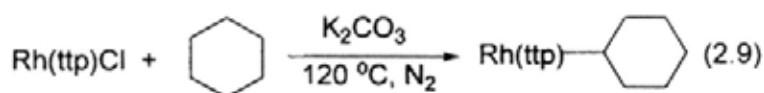
<sup>a</sup>  $\text{Rh}(\text{ttp})\text{Cl}(\text{PPh}_3)$  **3** was obtained in 83%

<sup>b</sup> 2,2'-bpy = 2,2'-bipyridine; <sup>c</sup> 2,6-dbpy = 2,6-di-*tert*-butylpyridine; <sup>d</sup> 2,6-dppy = 2,6-diphenylpyridine

To our delight, nucleophilic inorganic bases were found to promote both the yields and rates of CHA (Table 2.2, entries 7-9). When NaOH was added, the reaction only took 6 hours and the yield of **2a** was 47%. NaOAc gave a slightly higher yield of 51%, and  $\text{K}_2\text{CO}_3$

gave the highest yield of 59%. These nucleophilic bases required just 6 hours for the reaction to complete. Prolonged heating to 1 day with  $K_2CO_3$  resulted in a lower yield of 40% (Table 2.2, entry 10). From these results, the optimal reaction conditions were found to require  $K_2CO_3$  in 6 hours.

Table 2.3 Effect of  $K_2CO_3$  Loading in CHA of *c*-Hexane



| Entry | $K_2CO_3$ equiv | Time (h) | Yield (%) |
|-------|-----------------|----------|-----------|
| 1     | Nil             | 24       | 31        |
| 2     | 5               | 24       | 35        |
| 3     | 10              | 6        | 59        |
| 4     | 20              | 6        | 56        |

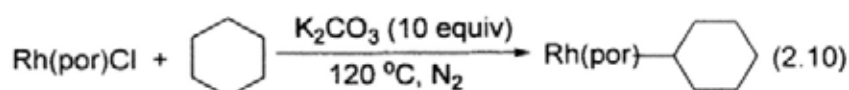
The loading of base was further optimized (eq 2.9, Table 2.3). Five equivalents of  $K_2CO_3$  increased the reaction yield slightly, but the reaction rate was not faster (Table 2.3, entry 2 vs 1). A higher loading of 10 equivalents of  $K_2CO_3$  increased both the reaction yield and rate (Table 2.3, entry 3). However, a further increase to 20 equivalents of  $K_2CO_3$  did not result in any further enhancement in yield (Table 2.3, entry 4). Therefore, the optimized reaction conditions were found to require 10 equiv of  $K_2CO_3$  at 120 °C. Visual inspection of the reaction mixture showed that even 5 equiv of  $K_2CO_3$  did not dissolve completely at 120 °C; therefore, the reaction mixture was heterogeneous.

### 2.4.3 Ligand Effect

The structures of porphyrin in the rhodium porphyrin chlorides affect the rates and yields of the CHA of *c*-hexane. The electronic effects of CHA were examined by three  $\text{Rh}(\text{por})\text{Cl}$  species, including  $\text{Rh}(\text{ttp})\text{Cl}$  **1a**,  $\text{Rh}(\text{tpp})\text{Cl}$  **1b** (tpp = 5,10,15,20-tetraphenylporphyrinato dianion) and  $\text{Rh}(\text{bocp})\text{Cl}$  **1c** (bocp = 2,3,7,8,12,13,17,18-octachloro-5,10,15,20-tetrakis(*p*-tert-butylphenyl)porphyrinato dianion) (Table 2.4, eq 2.10). The

reaction rates followed the order of electron-deficient Rh(por)Cl: Rh(bocp)Cl > Rh(tpp)Cl > Rh(ttp)Cl (Table 2.4, entries 1-3).

Table 2.4 CHA of *c*-Hexane with Rh(por)Cl

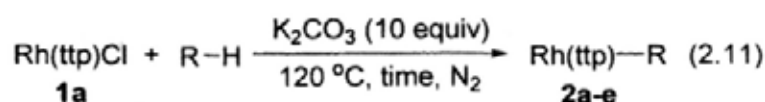


| Entry | por  | Time (h) | Yield (%)      |
|-------|------|----------|----------------|
| 1     | ttp  | 6        | <b>2a</b> (59) |
| 2     | tpp  | 5        | <b>4a</b> (52) |
| 3     | bocp | 1        | <b>4b</b> (61) |

## 2.5 Base-promoted CHA of Alkanes

The optimized K<sub>2</sub>CO<sub>3</sub>-promoted reaction conditions were successfully applied to other alkanes. *c*-Pentane and *c*-hexane gave the *c*-pentyl and *c*-hexyl complexes, in 76% and 59% yields, respectively in 6 hours (eq 2.11, Table 2.5, entries 1-2). The straight-chain alkanes reacted with Rh(tpp)Cl **1a** more slowly than *c*-hexane (Table 2.5, entries 3-5 vs 2). A longer time of 24 hours was required. The yields of Rh(tpp) alkyls increased with the chain length, presumably due to the observed increasing solubility of Rh(tpp)Cl **1a** in longer-chain hydrocarbons. Selective terminal CHA took place to give only the primary Rh(tpp) alkyls. While the thermal isomerization of Rh(tpp)CH<sub>2</sub>CH<sub>2</sub>CH<sub>3</sub> into Rh(tpp)CH(CH<sub>3</sub>)<sub>2</sub> has been reported, the time to establish equilibrium requires 10 days.<sup>15</sup> Therefore, the isomerization of these Rh(tpp) alkyls did not occur in 24 hours.

Table 2.5 Activation of Alkanes with Rh(tp)Cl



| Entry | Substrate         | Time (h) | Yield (%)                                |
|-------|-------------------|----------|--|
| 1     | <i>c</i> -pentane | 6        | Rh(tp)( <i>c</i> -hexyl) <b>2b</b> (76)  |
| 2     | <i>c</i> -hexane  | 6        | Rh(tp)( <i>c</i> -pentyl) <b>2a</b> (59) |
| 3     | <i>n</i> -pentane | 24       | Rh(tp)( <i>n</i> -pentyl) <b>2c</b> (29) |
| 4     | <i>n</i> -hexane  | 24       | Rh(tp)( <i>n</i> -hexyl) <b>2d</b> (40)  |
| 5     | <i>n</i> -heptane | 24       | Rh(tp)( <i>n</i> -heptyl) <b>2e</b> (58) |

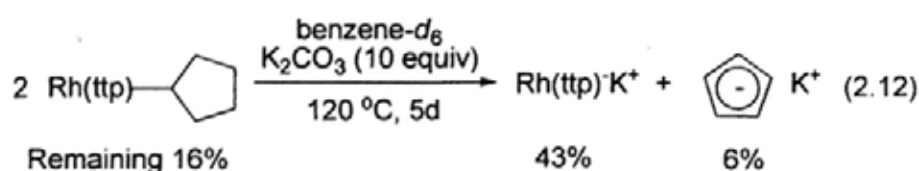
We were not able to detect any *c*-hexanol, *c*-hexyl chloride, *c*-hexene or *c*-hexanone by GC-MS analysis of the crude reaction mixture. It may be that the concentration of these species, if formed, was low in the presence of 1000 times more *c*-hexane.

## 2.6 Stability of Rh(tp)Alkyls

In order to understand the lower yield of Rh(tp) alkyl with longer reaction time (Table 2.3, entries 9 and 10), the thermal stability of Rh(tp) alkyls in the presence of K<sub>2</sub>CO<sub>3</sub> at 120 °C was examined and monitored by <sup>1</sup>H NMR spectroscopy.

### 2.6.1 Stability of Rh(tp)(*c*-pentyl) with Base

Rh(tp)(*c*-pentyl) **2b** and K<sub>2</sub>CO<sub>3</sub> (10 equiv) were added into benzene-*d*<sub>6</sub> and the reaction mixture was heated at 120 °C for 5 days (eq 2.12, Table 2.6, Figures 2.1 and 2.2).



After 30 minutes of heating, the pyrrole signal of Rh(tp)(*c*-pentyl) **2b** shifted up from δ 8.99 to δ 8.59 ppm and was assigned to Rh(tp)<sup>-</sup>. Rh(tp)<sup>-</sup> and Rh(tp)H were formed in 34% and

8% yields, respectively. Then after 13 hours, a small amount of cyclopentadienyl anion  $^1\text{H}$  NMR signal appeared ( $\delta$  5.69 ppm).<sup>11</sup> After 5 days, its yield increased to 6%. When dilute aqueous HCl was added into the reaction mixture, Rh(tp)H **1d** ( $\delta$  ( $\beta$ -pyrrole) =  $\delta$  9.03 ppm) was observed, further supporting the formation of Rh(tp) $^-$ .

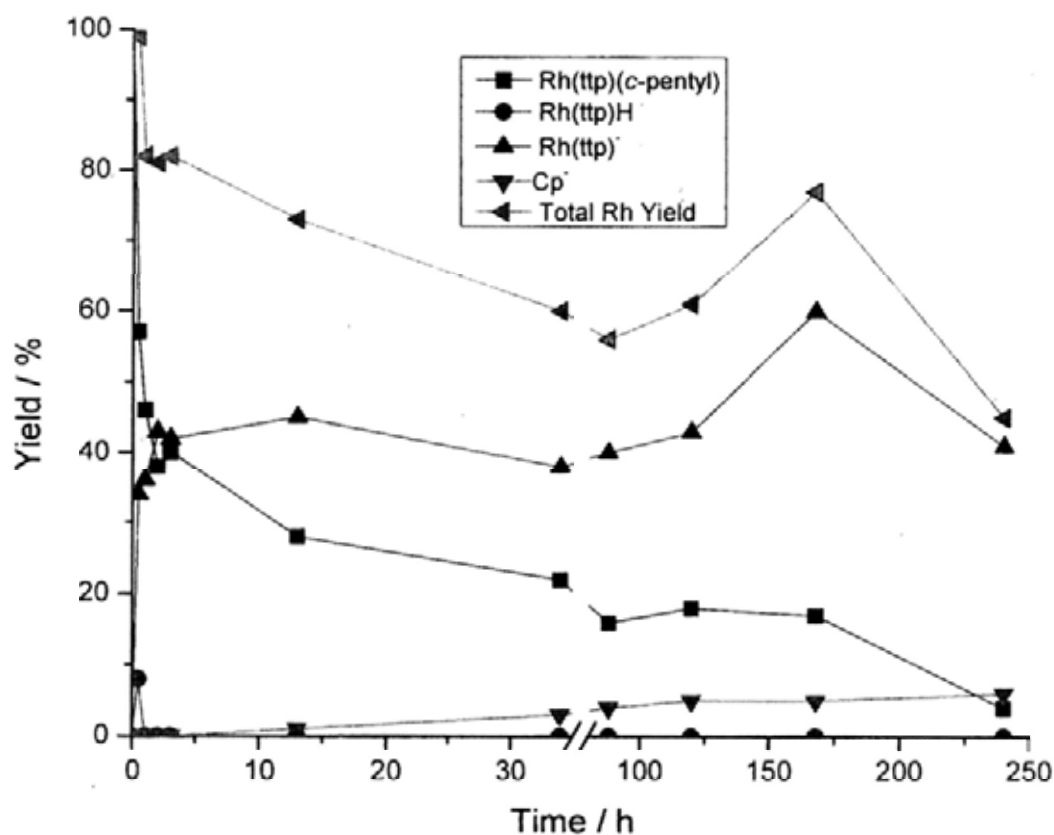


Figure 2.1 Reaction Time Profile of Decomposition of Rh(tp)(c-pentyl) **2b**

Table 2.6 Reaction Time Profile of the Decomposition of Rh(tp)(c-pentyl)

| Entry | Time / h | Yield / %        |         |        |    | Total Rh |
|-------|----------|------------------|---------|--------|----|----------|
|       |          | Rh(tp)(c-pentyl) | Rh(tp)H | Rh(tp) | Cp |          |
| 1     | 0        | 100              | 0       | 0      | 0  | 100      |
| 2     | 0.5      | 57               | 8       | 34     | 0  | 99       |
| 3     | 1        | 46               | 0       | 36     | 0  | 82       |
| 4     | 2        | 38               | 0       | 43     | 0  | 81       |
| 5     | 3        | 40               | 0       | 42     | 0  | 82       |
| 6     | 13       | 28               | 0       | 45     | 1  | 73       |
| 7     | 34       | 22               | 0       | 38     | 3  | 60       |
| 8     | 88       | 16               | 0       | 40     | 4  | 56       |
| 9     | 120      | 18               | 0       | 43     | 5  | 61       |
| 10    | 168      | 17               | 0       | 60     | 5  | 77       |
| 11    | 240      | 4                | 0       | 41     | 6  | 45       |

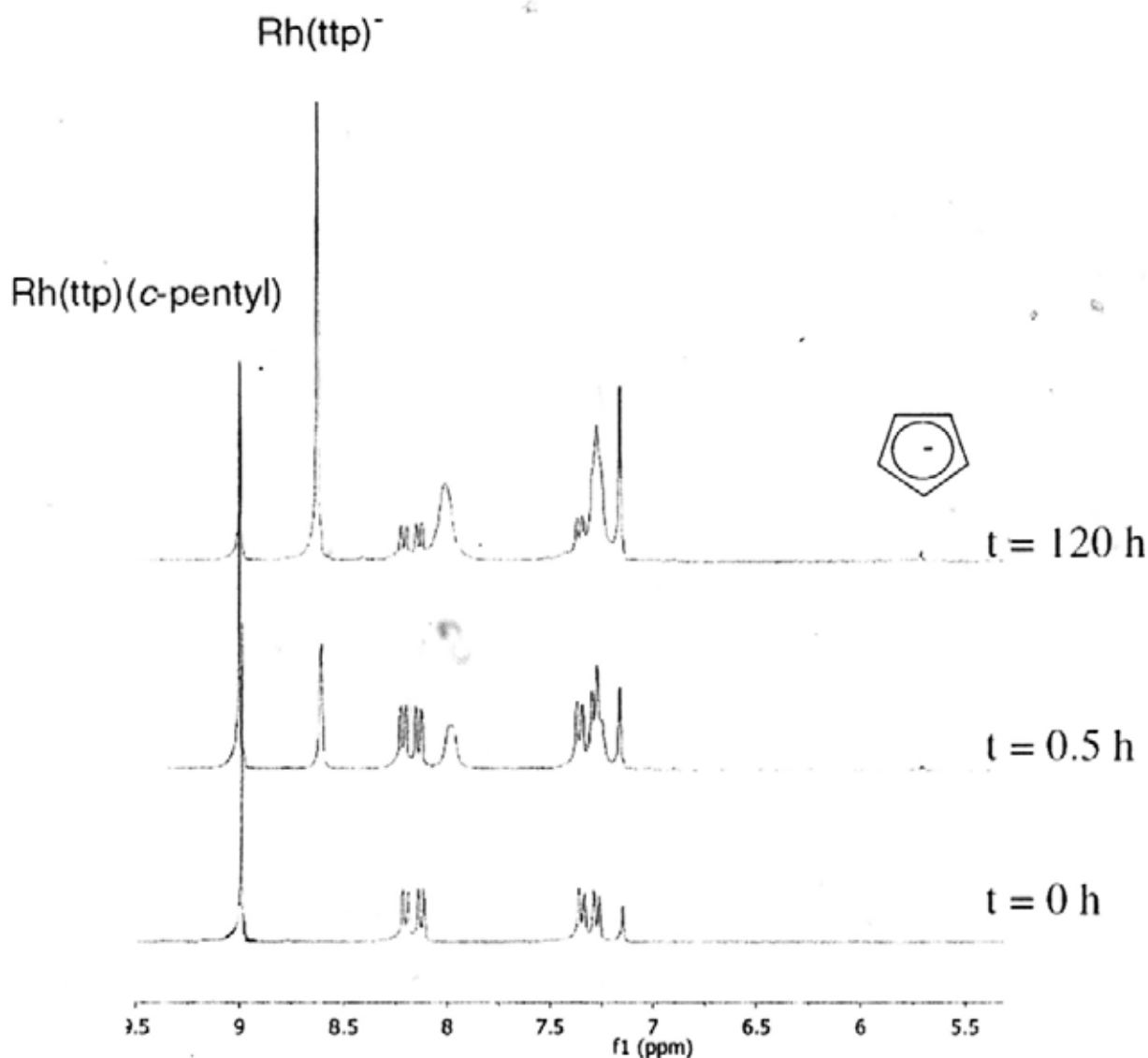
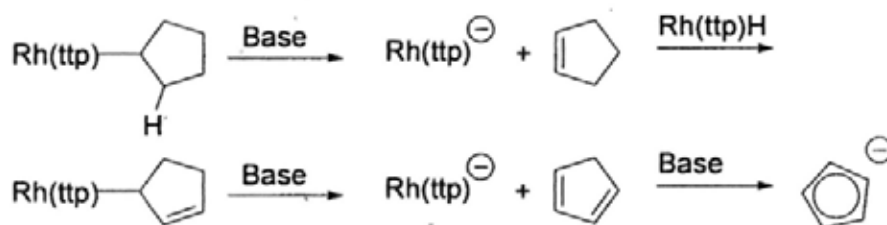


Figure 2.2  $^1\text{H}$  NMR Spectra of the Reaction  $\text{Rh}(\text{ttp})(c\text{-pentyl})$  with  $\text{K}_2\text{CO}_3$  in  $\text{Benzene-}d_6$



Scheme 2.2 Proposed Decomposition Pathway of  $\text{Rh}(\text{ttp})(c\text{-pentyl})$  **2b**

It is rationalized that  $\text{K}_2\text{CO}_3$  abstracts the  $\beta$ -alkyl proton of  $\text{Rh}(\text{ttp})(c\text{-pentyl})$  **2b** by an  $\text{E}_2$  elimination to give  $\text{Rh}(\text{ttp})^-$  **1e** and  $c\text{-pentene}$  (Scheme 2.2). As  $\text{Rh}(\text{ttp})\text{H}$  **1d** is a moderately strong acid with  $\text{p}K_a$  about 11,<sup>16</sup>  $\text{Rh}(\text{ttp})^-$  **1e** is therefore a good leaving group.



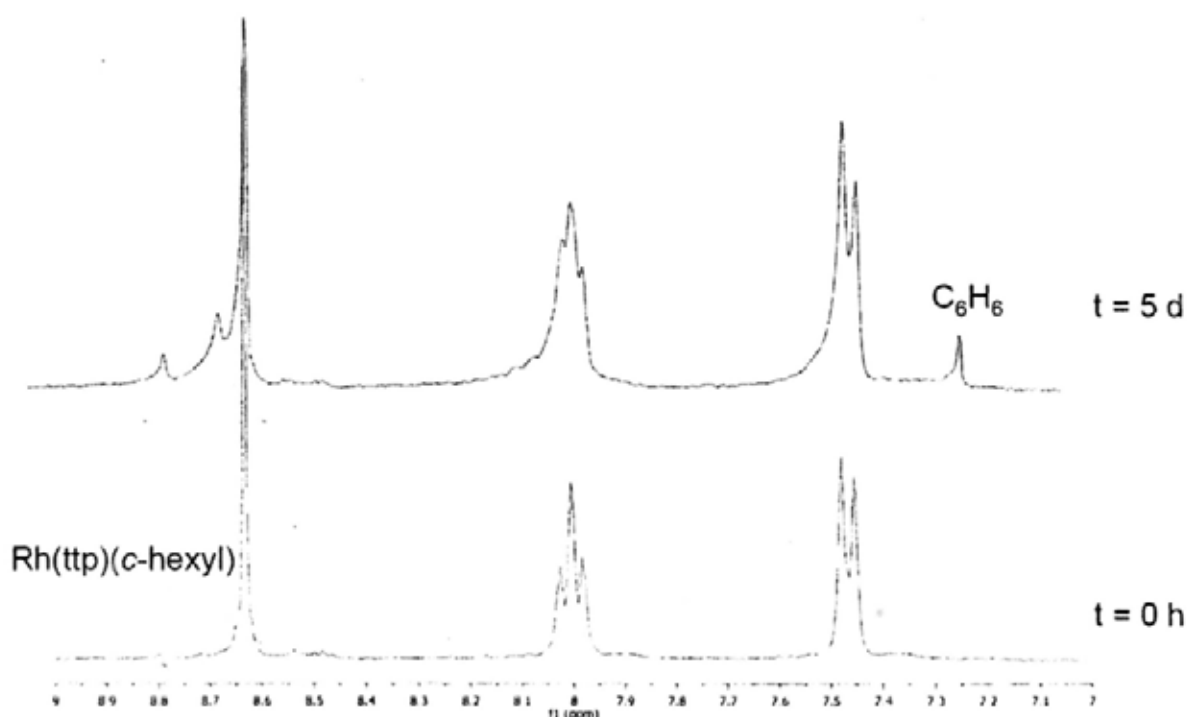
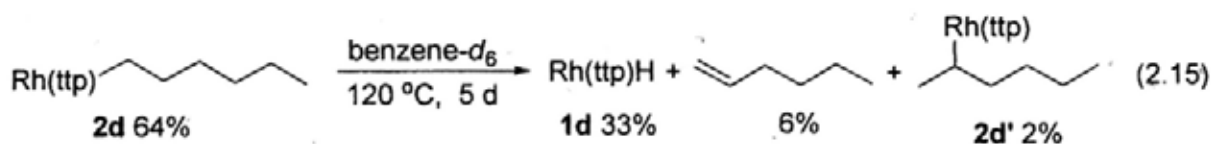


Figure 2.3  $^1\text{H}$  NMR Spectra of the Reaction  $\text{Rh}(\text{tp})(c\text{-hexyl})$  with  $\text{K}_2\text{CO}_3$  in  $c\text{-Hexane-}d_{12}$

The higher stability of  $\text{Rh}(\text{tp})(c\text{-hexyl})$  **2a** is likely due to the smaller dihedral angle of  $\text{Rh-C}_\alpha\text{-C}_\beta\text{-H}_\beta$  in disfavoring the anti-periplanar transition state of an  $\text{E}_2$  elimination.<sup>18</sup> (Dihedral angles of  $\text{Rh-C}_\alpha\text{-C}_\beta\text{-H}_\beta$  of  $\text{Rh}(\text{tp})(c\text{-pentyl})$  **2b**  $\text{Rh}(\text{tp})(c\text{-hexyl})$  **2a** are  $131^\circ$  and  $122^\circ$ , respectively. See X-ray crystallography section 2.7.)

### 2.6.3 Stability of $\text{Rh}(\text{tp})(n\text{-hexyl})$ with Base

$\text{Rh}(\text{tp})(n\text{-hexyl})$  **2d** is more stable than  $\text{Rh}(\text{tp})(c\text{-pentyl})$  **2b** and  $\text{Rh}(\text{tp})(c\text{-hexyl})$  **2a**.  $\text{Rh}(\text{tp})(n\text{-hexyl})$  **2d** underwent slower reaction to give  $\text{Rh}(\text{tp})\text{H}$  **1d** and  $n\text{-hexene}$  in 33% and 6% yields, respectively as well as the 1,2-rearrangement product **2d'** in 2% yield under the same reaction conditions (eq 2.15).<sup>9d,10</sup>



These CHA reactions further provide a facile, convenient synthesis of Rh(por) alkyls. For comparison, a previous synthesis of rhodium porphyrin alkyl was achieved by a two-step process via reductive alkylation (NaBH<sub>4</sub>/RBr) with yields from 48-97%.<sup>19</sup> This synthetic route can access a variety of rhodium porphyrin alkyls directly from alkanes in one step.

## 2.7 X-ray Structure Determination

Table 2.7 Selected Bond lengths (Å) and Angles (deg) for Rh(por)R

| Entry | Rh(tp)R                                | Rh-C length<br>(Å) | Dihedral angle<br>between phenyl<br>group and the<br>mean plane (deg) | Max. deviation<br>from 24-least<br>sq plane (Å) | Rh-<br>N <sub>average</sub><br>(Å) |
|-------|--|--------------------|---|---|------------------------------------|
| 1     | Rh(tp)( <i>c</i> -hexyl)<br><b>2a</b>  | 2.126(7)           | 80.79 (7)   | 0.465(4)  | 2.019                              |
| 2     | Rh(tp)( <i>c</i> -pentyl)<br><b>2b</b> | 2.073(7)           | 80.98 (3)   | 0.452(7)  | 2.017                              |
| 3     | Rh(tp)( <i>n</i> -heptyl)<br><b>2e</b> | 2.048(3)           | 82.25(5)  | 0.552(3)  | 2.019                              |
| 4     | Rh(oep)CH <sub>3</sub> <sup>16</sup>   | 1.970(4)           | ----  | ----  | 2.027                              |

Table 2.7 lists selected bond lengths and angles for complexes **2a,b,e**. Figures 2.4-2.6 show the molecular structures of **2a,b,e**, respectively (30% thermal ellipsoids). The Rh-C bond lengths of **2a,b,e** range from 2.07 to 2.13 Å (Table 2.7, entries 1-3) and are similar to the reported Rh-C bond lengths of Rh(oep)Me (oep = 2,3,7,8,12,13,17,18-

octaethylporphyrinato dianion) ( $1.97 \text{ \AA}$ )<sup>20</sup> (Table 2.7, entries 4). The Rh-N<sub>avg</sub> bond lengths do not vary significantly ( $2.017 \text{ \AA} - 2.019 \text{ \AA}$ ). The Rh-C bond lengths appear to follow the steric size of alkyls in the order: *c*-hexyl > *c*-pentyl > *n*-heptyl (Table 2.7, entries 1-3). The various alkyls do not cause large distortion of the mean porphyrin plane from planarity in these complexes **2a** ( $0.465 \text{ \AA}$ ), **2b** ( $0.452 \text{ \AA}$ ), and **2e** ( $0.552 \text{ \AA}$ ). The porphyrin structures of Rh(tpp)(*c*-hexyl) **2a**, Rh(tpp)(*c*-pentyl) **2b** and Rh(tpp)(*n*-hexyl) **2e** are slightly distorted to adopt a saddle form (Figures 2.7-2.9).

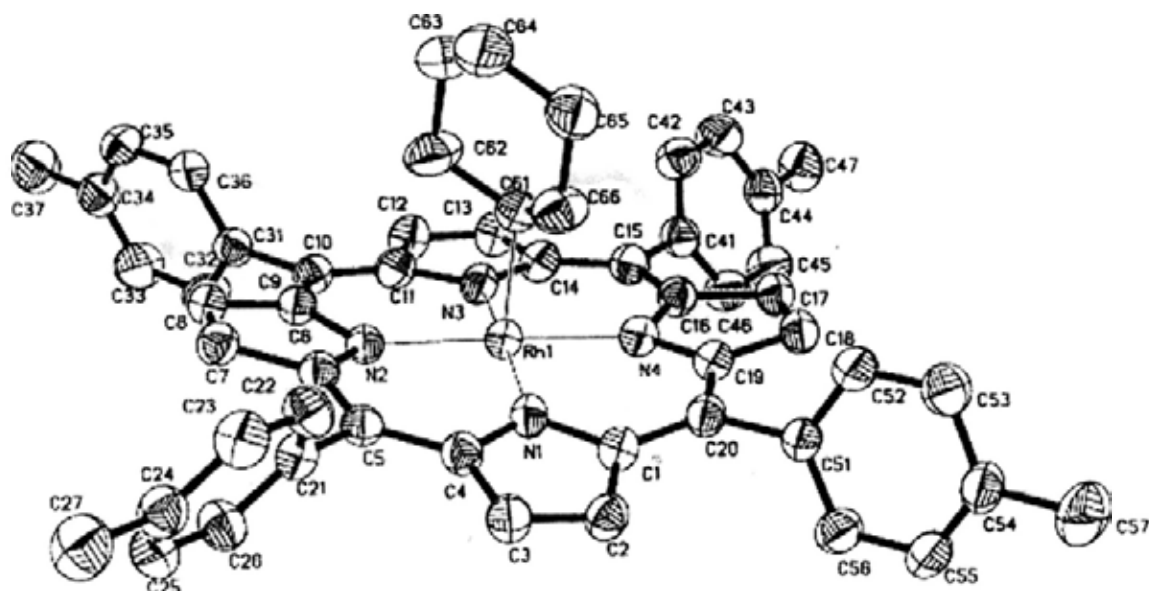


Figure 2.4 ORTEP Presentation of the Molecular Structure with Numbering Scheme for Rh(ttp)(c-hexyl) **2a** (30% Probability Displacement Ellipsoids).

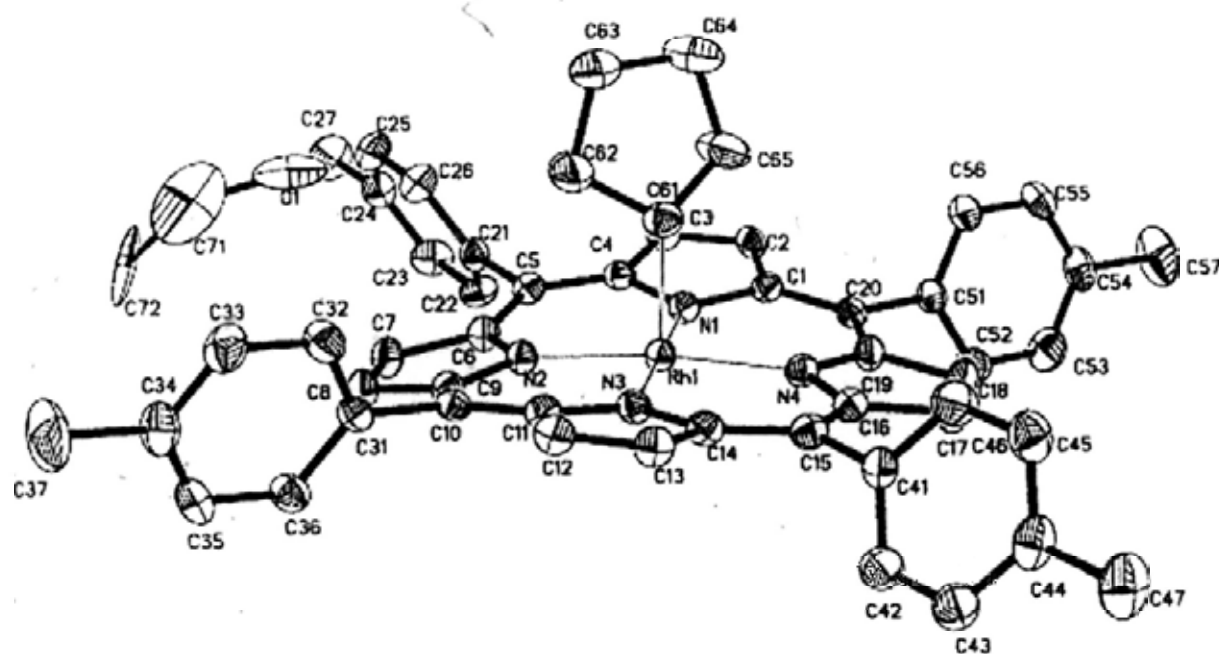


Figure 2.5 ORTEP Presentation of the Molecular structure with Numbering Scheme for Rh(ttp)(c-pentyl) · EtOH **2b** (EtOH omitted for clarity) (30% Probability Displacement Ellipsoids).

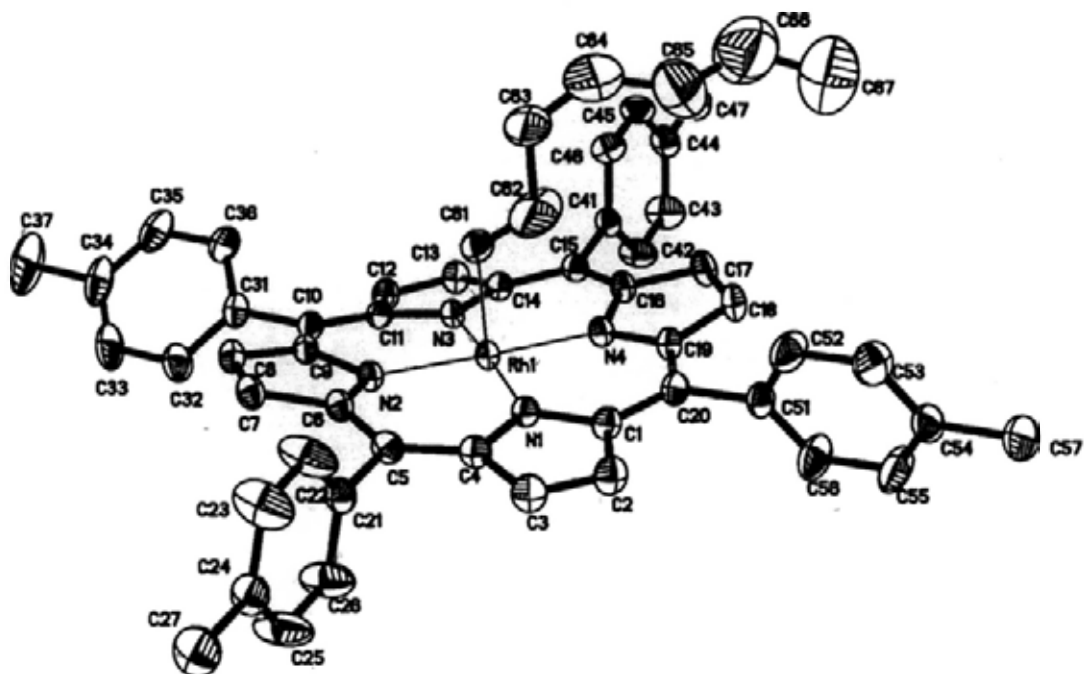


Figure 2.6 ORTEP Presentation of the Molecular Structure with Numbering Scheme for Rh(ttp)(*n*-heptyl) **2e** (30% Probability Displacement Ellipsoids).

Figures 2.7-2.9 The conformations of porphyrins showing the displacement of the core atoms and of Rh from the 24-atom least squares plane of porphyrin core (in pm; negative values correspond to displacement towards the alkyl group). Absolute values of the angles between pyrrole rings and the least-squares plane, and angles between pyrrole rings and the least-squares plane, and angles between phenyl substituents and the least-squares plane, are shown in bold.

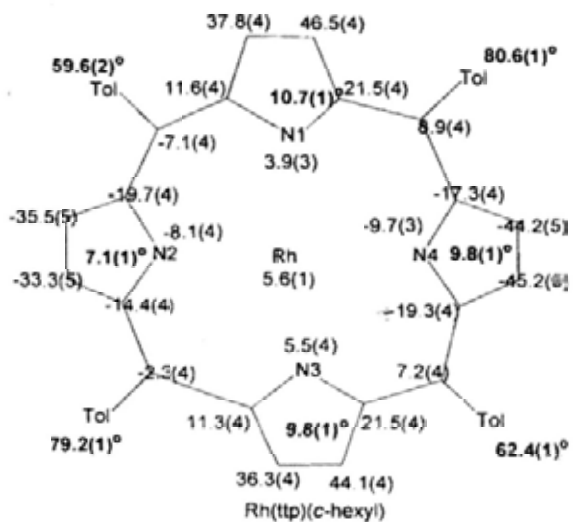


Figure 2.7a

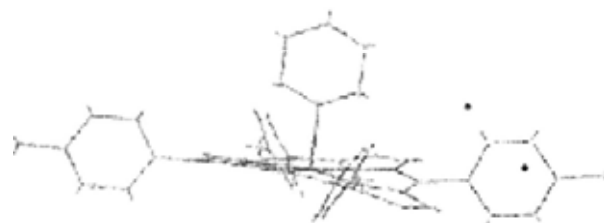


Figure 2.7b

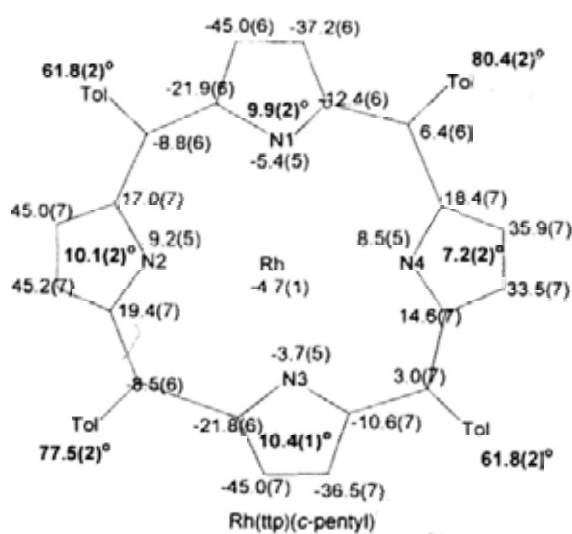


Figure 2.8a



Figure 2.8b

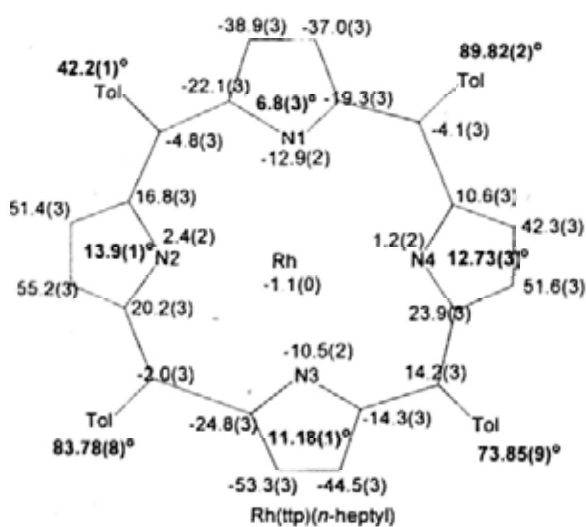


Figure 2.9a

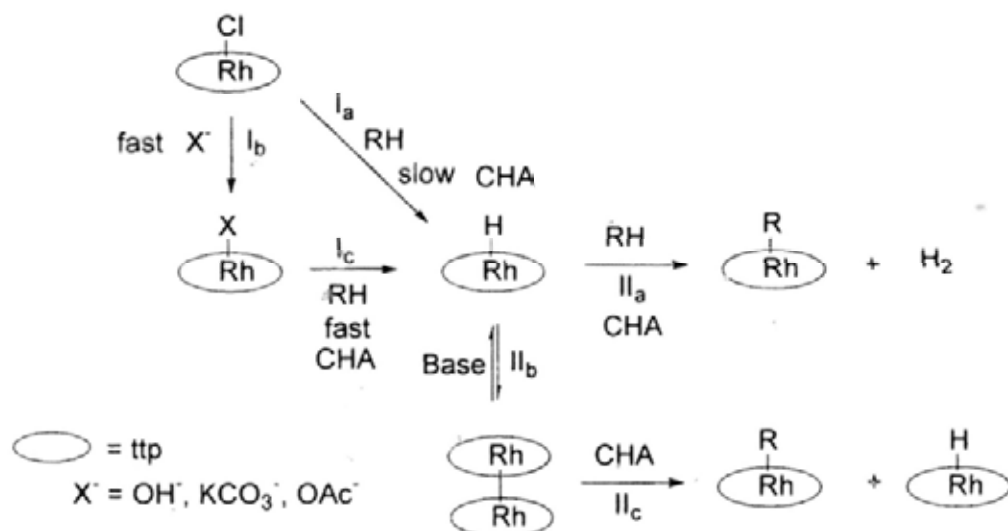


Figure 2.9b

## 2.8 Mechanistic Studies

### 2.8.1 Proposed Mechanism for CHA

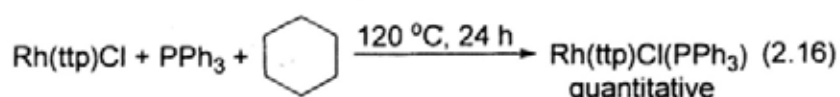
Since Rh(tpp)Cl reacted with alkane in the absence and presence of base, scheme 2.3 shows two possible pathways for the proposed mechanism of alkyl CHA with Rh(tpp)Cl **1a**.



Scheme 2.3 Proposed Mechanism of Alkyl CHA with Rh(tpp)Cl

### 2.8.2 Alkyl CHA in the Absence of Base

Pathway **I<sub>a</sub>**. In the absence of base, Rh(tpp)Cl **1a** initially undergoes heterolysis to form Rh(tpp) cation and chloride anion, most likely as an ion pair (Scheme 2.3).<sup>6-8</sup> An alkane then coordinates to the Rh metal center to form a C–H–Rh complex.<sup>21</sup> Finally, the alkyl C–H bond is cleaved to give Rh(tpp)H **1d**. The coordination of alkane to the Rh metal center is supported by the inhibition of CHA by PPh<sub>3</sub> (Table 2.2, entry 2). Upon addition of PPh<sub>3</sub>, Rh(tpp)Cl **1a** did not react with *c*-hexane at 120 °C in 24 hours to give any Rh(tpp)(*c*-hexyl) **2a** (eq 2.16).



When the reaction of Rh(tpp)Cl **1a** with *c*-hexane (50 equiv) in benzene-*d*<sub>6</sub> in a sealed NMR tube at 120 °C was traced by <sup>1</sup>H NMR spectroscopy over the course of 12 hours, no



protonation from the small amount of water present as well as forming the coproduct *c*-hexene. *c*-Hexene can also further undergo multiple CHA and E<sub>2</sub> elimination to give benzene analogous to *c*-pentene.

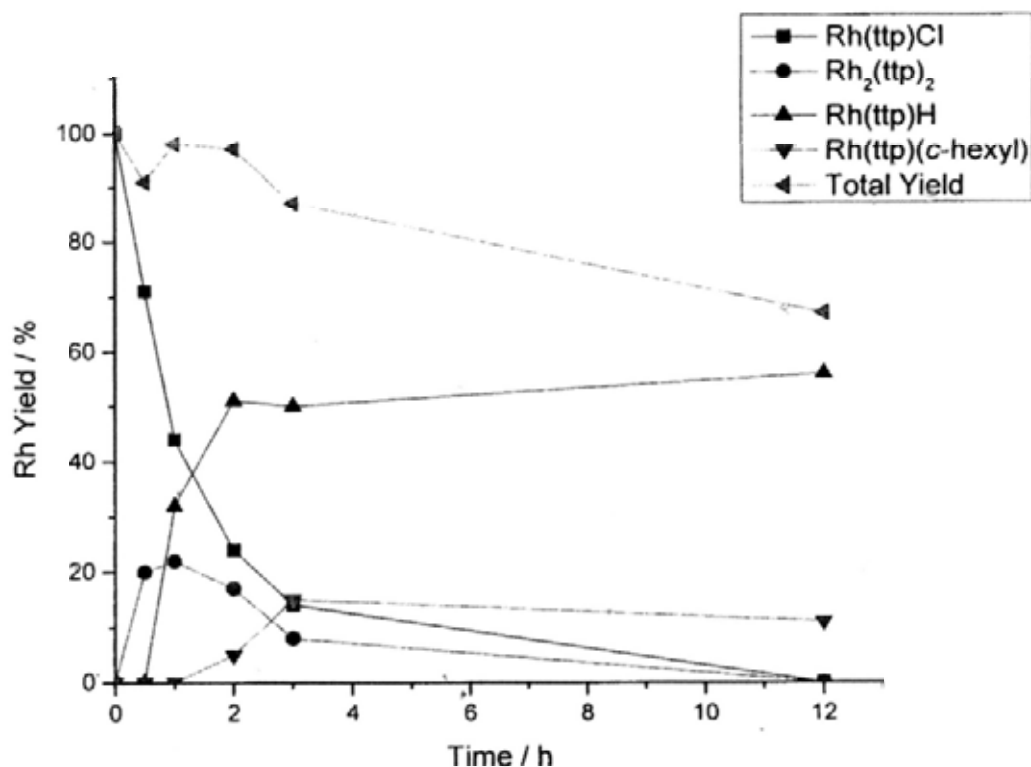
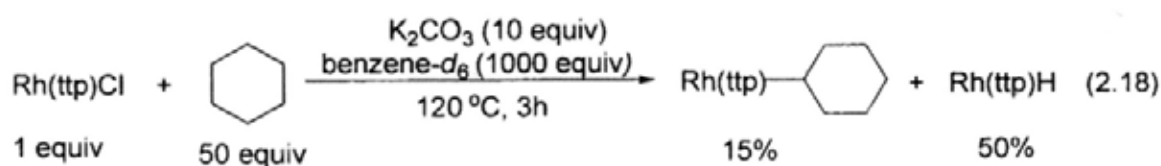
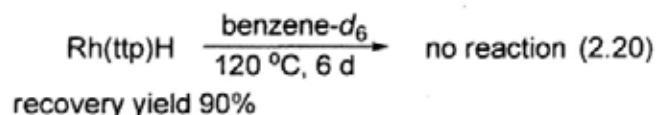
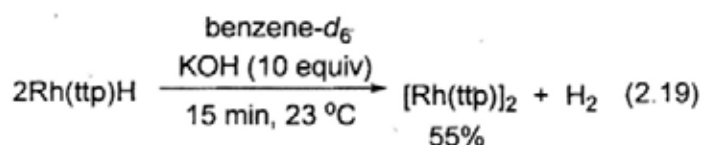


Figure 2.10 Time Profile of Reaction Rh(ttp)Cl and *c*-Hexane with K<sub>2</sub>CO<sub>3</sub>.

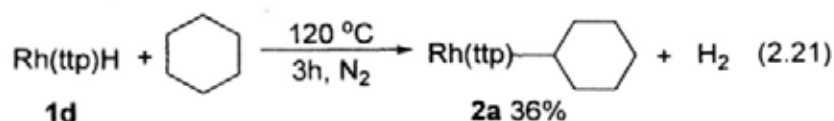
Table 2.8 Reaction Time Profile of Rh(tp)Cl and *c*-hexane with K<sub>2</sub>CO<sub>3</sub>

| Entry | Time (h) | Yield (%) |                                   |         |                          | Total |
|-------|----------|-----------|-----------------------------------|---------|--------------------------|-------|
|       |          | Rh(tp)Cl  | Rh <sub>2</sub> (tp) <sub>2</sub> | Rh(tp)H | Rh(tp)( <i>c</i> -hexyl) |       |
| 1     | 0        | 100       | 0                                 | 0       | 0                        | 100   |
| 2     | 0.5      | 71        | 20                                | 0       | 0                        | 91    |
| 3     | 1        | 44        | 22                                | 32      | 0                        | 98    |
| 4     | 2        | 24        | 17                                | 51      | 5                        | 97    |
| 5     | 3        | 14        | 8                                 | 50      | 15                       | 87    |
| 6     | 12       | 0         | 0                                 | 56      | 11                       | 67    |
| 7     | 36       | 0         | 0                                 | 53      | 8                        | 61    |
| 8     | 96       | 0         | 0                                 | 52      | 9                        | 61    |

Independent experiment showed that Rh<sub>2</sub>(tp)<sub>2</sub> **1e** and presumably H<sub>2</sub> were formed quickly over 15 minutes at room temperature from Rh(tp)H **1d** added with base (eq 2.19). However, Rh(tp)H **1d** was thermally stable in the absence of base, even upon heating at 120 °C for 6 days with 90% recovery (eq 2.20). Therefore, both Rh<sub>2</sub>(tp)<sub>2</sub> **1e** and Rh(tp)H **1d** can activate R–H to give Rh(tp)R in pathways **II<sub>a</sub>**, **II<sub>b</sub>** and **II<sub>c</sub>** (Scheme 2.3).



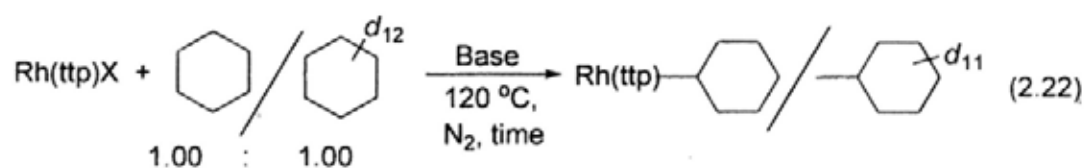
To further understand why Rh(tp)H **1d** did not react completely with slight excess *c*-hexane in benzene solvent, the thermal CHA reaction of Rh(tp)H **1d** with *c*-hexane at 120 °C in 3 hours was carried out. Indeed, Rh(tp)(*c*-hexyl) **2a** was formed in 36% yield and supported the intermediacy of Rh(tp)H **1d** (eq 2.21). The low yield of Rh(tp)(*c*-hexyl) **2a** in a slight excess of *c*-hexane is probably due to unfavorable equilibrium with limited *c*-hexane as well as the base-promoted or thermal β-H elimination of Rh(tp)(*c*-hexyl) **2a**.



#### 2.8.4 Kinetic Isotope Effect of Alkyl CHA

To gain further information about the nature of the transition state and the possible Rh species involved (pathway **I<sub>c</sub>** and **II<sub>a-c</sub>**), the kinetic isotope effects of the CHA reaction were measured by a series of competition experiments. Rh(ttp)Cl **1a** was reacted with an equimolar mixture of *c*-hexane and *c*-hexane-*d*<sub>12</sub> in the presence of 10 equivalents of K<sub>2</sub>CO<sub>3</sub> at 120 °C in 6 hours. The ratio of Rh(ttp)(*c*-hexyl) **2a** to Rh(ttp)(*c*-hexyl)-*d*<sub>11</sub> were determined to be 9.1:1.0 by <sup>1</sup>H NMR spectroscopy. The large kinetic isotope effect (KIE) supported the C–H cleavage step to give Rh(ttp)(*c*-hexyl) **2a** is involved in the rate limiting step. The observed KIE is truly a kinetic value as Rh(ttp)(*c*-hexyl) **2a** did not exchange with *c*-hexane-*d*<sub>12</sub> under the same conditions. Likewise, the KIEs of the CHA with Rh(ttp)H **1d** and Rh<sub>2</sub>(ttp)<sub>2</sub> **1e** with or without K<sub>2</sub>CO<sub>3</sub> were measured to be about 9.0. (eq 2.22, Table 2.9). Rh(ttp)H was also found to be more reactive than Rh<sub>2</sub>(ttp)<sub>2</sub> **1e**.

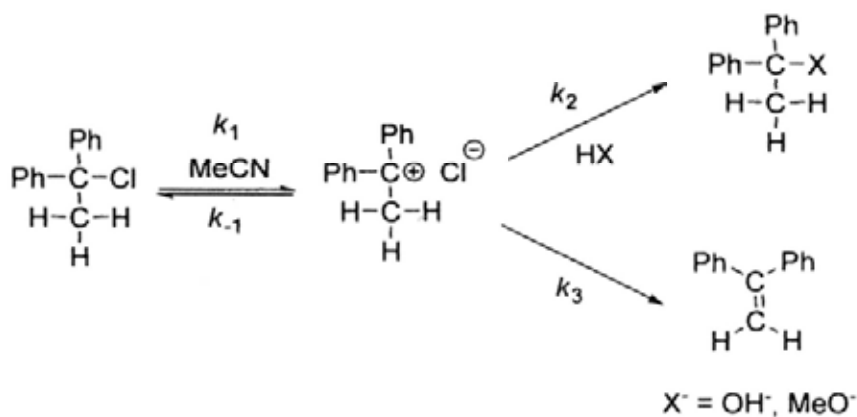
Table 2.9 KIE Values of Reactions of Rh(ttp)X with *c*-Hexane



| Entry          | Rh(ttp)X                           | Base                                      | Time (h) | KIE by <sup>1</sup> H NMR | Yield (%) |
|----------------|------------------------------------|---|----------|---------------------------|-----------|
| 1              | Rh(ttp)Cl                          | K <sub>2</sub> CO <sub>3</sub> (10 equiv) | 6        | 9.1±0.3 <sup>a</sup>      | 32        |
| 2              | Rh(ttp)H                           | Nil                                       | 3        | 8.9±0.3                   | 54        |
| 3              | Rh(ttp)H                           | K <sub>2</sub> CO <sub>3</sub> (10 equiv) | 3        | 8.5±0.4                   | 59        |
| 4              | Rh <sub>2</sub> (ttp) <sub>2</sub> | Nil                                       | 6        | 8.7±0.3                   | 38        |
| 5 <sup>6</sup> | Rh <sub>2</sub> (ttp) <sub>2</sub> | K <sub>2</sub> CO <sub>3</sub> (10 equiv) | 6        | 9.0±0.3                   | 42        |

<sup>a</sup>KIE determined by MS was 9.7(±0.2)





Scheme 2.4 Branching Reaction of Carbocation

Thibblin et. al has reported that heterolysis of C–Cl bond of 1,1-diphenylethyl chloride, which is almost rate-limiting, generates a diphenylmethylcarbocation and chloride anion (Scheme 2.4). The diphenylmethylcarbocation is a common intermediate for the subsequent branching conversion of alcohol/ether via solvolysis and olefin via elimination. The expression for the isotope effects are the following:

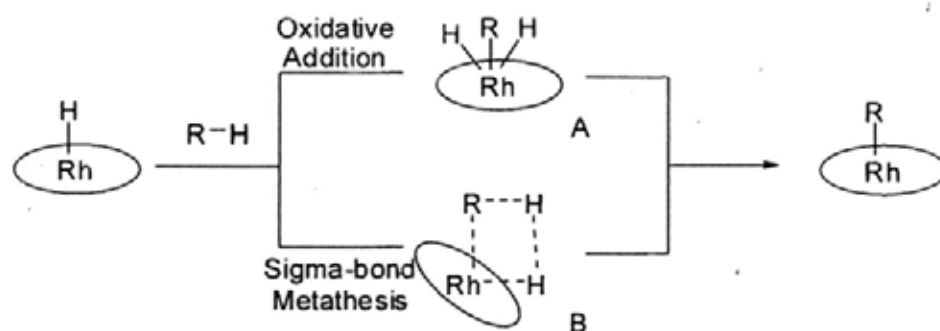
$k_s^H/k_s^D = (k_1^H/k_1^D)(k_2^H/k_2^D)(k_{-1}^D+k_2^D+k_3^D)/(k_{-1}^H+k_2^H+k_3^H)$ , where  $k_s$  is the rate of solvolysis of 1,1-diphenylethyl chloride;

$k_e^H/k_e^D = (k_1^H/k_1^D)(k_3^H/k_3^D)(k_{-1}^D+k_2^D+k_3^D)/(k_{-1}^H+k_2^H+k_3^H)$ , where  $k_e$  is the rate of elimination of 1,1-diphenylethyl chloride;

As the heterolysis does not involve a C–H cleavage, the isotope effect  $k_1^H/k_1^D$  is assumed to be a secondary isotope effect and therefore has a value of  $1.16 < k_1^H/k_1^D < 1.52$ .<sup>23c</sup> Also,  $k_2^H/k_2^D$  is a secondary isotope effect since no C–H cleavage is involved. The primary isotope effect  $k_3^H/k_3^D$  should have a substantial value. Detailed mechanistic investigation suggests that fast backward heterolysis ( $k_{-1} \gg k_2, k_3$ ) would result in enlarged kinetic isotope effect.<sup>23b</sup> This is because when ( $k_{-1} \gg k_2, k_3$ ),  $k_e^H/k_e^D$  is close to  $(k_1^H/k_1^D)(k_3^H/k_3^D)$ , where  $k_1^H/k_1^D$  is

larger than unity. In the case of alkyl CHA, the branching reaction of  $\text{Rh}_2(\text{ttp})_2$  with *c*-hexane is from the common intermediate of  $\text{Rh}(\text{ttp})\text{H}$  **1d**.

As  $\text{Rh}(\text{ttp})\text{H}$  was shown to be a viable intermediate of the CHA reaction (eq 2.21), two detailed mechanistic possibilities, oxidative addition and  $\sigma$ -bond metathesis, could exist (Scheme 2.5). For the oxidative addition, a seven-coordinated  $\text{Rh}(\text{V})$  complex (A) formed at first with three ligands R, H, and H on the same face of the porphyrin, which then undergoes reductive elimination to give  $\text{Rh}(\text{ttp})\text{R}$  and  $\text{H}_2$ . Though  $\text{Rh}(\text{V})$  organometallic complexes are uncommon, they can be stabilized by strongly  $\sigma$ -donating ligand as silyl<sup>24</sup> and hydride. The two *cis*-dihydrides e.g.  $[(\eta^5\text{-C}_5\text{Me}_5)\text{Rh}(\text{H})_2(\text{SiMe}_3)_2]$  and  $[(\eta^5\text{-C}_5\text{Me}_5)\text{Rh}(\text{H})_2(\text{SiEt}_3)_2]$ <sup>24</sup> are not sterically demanding enough to rule out the oxidative addition pathway. Alternatively, a concerted  $\sigma$ -bond metathesis or its variants like  $\sigma$ -complex (B) assisted metathesis<sup>25</sup> could be a viable pathway.

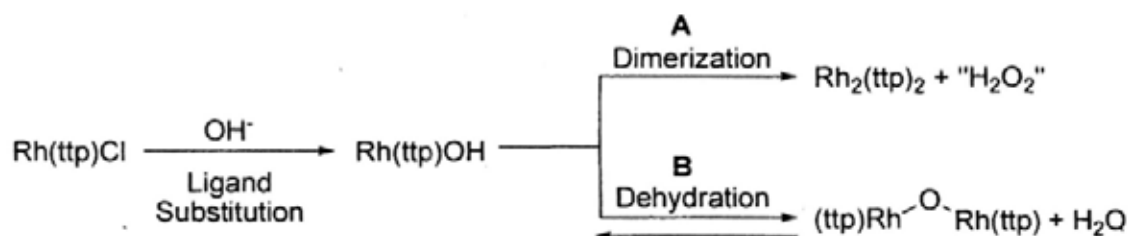


Scheme 2.5 Proposed Pathways of Alkyl CHA with  $\text{Rh}(\text{ttp})\text{H}$

The large KIE values of *c*-hexane CHA with  $\text{Rh}(\text{ttp})\text{Cl}$  (9.1) and with  $\text{Rh}(\text{ttp})\text{H}$  (8.9) are not typical of "normal"  $\sigma$ -bond metathesis process,<sup>26</sup> but they are similar to the KIE values of other CHA reactions involving methane-eliminating  $\sigma$ -bond metathetical events (8.7-9.1).<sup>27a,b</sup> As  $\text{Rh}(\text{ttp})\text{H}$  **1d** reacts with *c*-hexane to give  $\text{Rh}(\text{ttp})(c\text{-hexyl})$  **2a**, it may undergo  $\sigma$ -bond metathesis with  $\text{H}_2$ -elimination. Such  $\sigma$ -bond metathesis with  $\text{H}_2$  elimination was also proposed in the alkane metathesis catalyzed by silica-supported tantalum hydride.<sup>27c</sup>

### 2.8.6 Recent Finding in Rh(tp)OH

Recently, Mr Kwong Shing Choi in Chan's laboratory has discovered the base-promoted conversion of Rh(tp)Cl to Rh<sub>2</sub>(tp)<sub>2</sub> via the formation of Rh(tp)OH (Scheme 2.6).<sup>28</sup>



Scheme 2.6 Base-promoted reduction of Rh(tp)Cl to Rh<sub>2</sub>(tp)<sub>2</sub>

In the view of this finding, a new mechanism proposal is added for the elimination of Rh<sub>2</sub>(tp)<sub>2</sub>. Rh(tp)Cl first undergoes rapid ligand substitution with OH<sup>-</sup> to give Rh(tp)OH. The highly reactive Rh(tp)OH then dimerizes via parallel pathways A and B. In pathway A, Rh(tp)OH dimerizes to give Rh<sub>2</sub>(tp)<sub>2</sub> and H<sub>2</sub>O<sub>2</sub> which disproportionates quickly to generate water and oxygen molecule. At the same time, a  $\mu$ -oxo dirhodium complex is formed from intermolecular dehydration in pathway B. The  $\mu$ -oxo dirhodium complex probably undergoes backward reaction in the presence of H<sub>2</sub>O/OH<sup>-</sup> and eventually gives Rh<sub>2</sub>(tp)<sub>2</sub>.

### 2.9 Conclusion

Base-promoted aliphatic C<sub>H</sub>A of alkanes were achieved with rhodium(III) porphyrin complexes to give rhodium(III) porphyrin alkyls. Mechanistic investigations suggested both Rh(tp)H **1d** and Rh<sub>2</sub>(tp)<sub>2</sub> **1e** are key intermediates for the parallel C<sub>H</sub>A step. The roles of base are (i) to facilitate the formation of Rh(tp)OH; (ii) to enhance the C<sub>H</sub>A rate with alkane and generate Rh(tp)H by more reactive Rh(tp)X than Rh(tp)Cl; (iii) to provide a parallel C<sub>H</sub>A pathway by Rh<sub>2</sub>(tp)<sub>2</sub>.

## References

- (1) (a) Crabtree, R. H. *Dalton Trans.* **2001**, *17*, 2437-2450. (b) Lersch, M.; Tilset, M. *Chem. Rev.* **2005**, *105*, 2471-2526.
- (2) (a) Arndtsen, R. A.; Bergman, R. G.; Mobley, T. A.; Peterson, T. H. *Acc. Chem. Res.* **1995**, *28*, 154-162. (b) Sen, A. *Acc. Chem. Res.* **1998**, *31*, 550-557.
- (3) Zulys, A.; Dochnahl, M.; Hollmann, D.; Lohnwitz, K.; Herrmann, J. -S.; Roesky, P. W.; Blechert, S. *Angew. Chem. Int. Ed.* **2005**, *44*, 7794-7798.
- (4) (a) Ward, M. D.; Schwartz, J. *Organometallics* **1982**, *1*, 1030-1032. (b) Kitajima, N.; Schwartz, J. *J. Am. Chem. Soc.* **1984**, *106*, 2220-2222. (c) Gottker-Schnetmann, I.; Brookhart, M. *J. Am. Chem. Soc.* **2004**, *126*, 9330-9338. (d) Gottker-Schnetmann, I. White, P. S.; Brookhart, M. *Organometallics* **2004**, *23*, 1766-1776. (e) Wong-Foy, A. G.; Bhalla, G.; Liu, X. Y.; Periana, R. A. *J. Am. Chem. Soc.* **2003**, *125*, 14292-14293. (f) Bhalla, G.; Periana, R. A. *Angew. Chem. Int. Ed.* **2005**, *44*, 1540-1543. (g) Aoki, T.; Crabtree, R. H. *Organometallics* **1993**, *12*, 294-298.
- (5) (a) Gomez, M.; Robinson, D. J.; Maitlis P. M. *J. Chem. Soc., Chem. Comm.* **1983**, *15*, 825-826. (b) Monti, D.; Frachey, G.; Bassetti, M.; Haynes, A.; Sunley, G. J.; Maitlis, P. M.; Cantoni, A.; Bocelli, G. *Inorg. Chim. Acta* **1995**, *240*, 485-493. (c) Cho, J. -Y.; Tse, M. K.; Holmes, D.; Maleczka, R. E. Jr.; Smith, M. R. *Science* **2002**, *295*, 305-308.
- (6) (a) Zhou, X.; Li, Q.; Mak, T. C. W.; Chan, K. S. *Inorg. Chim. Acta* **1998**, *270*, 551-554. (b) Zhou, X.; Wang, R.-J.; Xue, F.; Mak, T. C. W.; Chan, K. S. *J. Organomet. Chem.* **1999**, *580*, 22-25. (c) Zhou, X.; Tse, M. K.; Wu, D.-D.; Mak, T. C. W.; Chan, K.S. *J. Organomet. Chem.* **2000**, *598*, 80-86.
- (7) Chan, K. S.; Lau, C. M. *Organometallics* **2006**, *25*, 260-265.

- (8) Chan, K. S.; Chiu, P. F.; Choi, K. S. *Organometallics* **2007**, *26*, 1117-1119.
- (9) (a) Wagner, R. W.; Lawrence, D. S.; Lindsey, J. S. *Tetrahedron Lett.* **1987**, *28*, 3069-3070. (b) Adler, A. D.; Longo, F. R.; Finarelli, J. D.; Goldmacher, J.; Assour, J.; Korsakoff, L. *J. Org. Chem.* **1967**, *32*, 476-477. (c) Alder, A. D.; Longo, F. R.; Shergalis, W. *J. Am. Chem. Soc.* **1964**, *86*, 3145-3149. (d) Mak, K. W.; Chan, K. S. *J. Am. Chem. Soc.* **1998**, *120*, 9686-9687. (e) Chan, K. S.; Mak, K. W.; Tse, M. K.; Yeung, S. K.; Li, B. Z.; Chan, Y. W. *J. Organomet. Chem.* **2008**, *693*, 399-407.
- (10) Mak, K. W.; Xue, F.; Mak, T. C. W.; Chan, K. S. *J. Chem. Soc., Dalton Trans.* **1999**, *19*, 3333-3334.
- (11) Buchler, J. W.; Dreher, C.; Kunzel, F. M. *In Metal Complexes with Tetrapyrrole Ligands III: Structure and Bonding, vol. 84*; Buchler, J. W.; Ed.; Springer-Verlag: Berlin Heidelberg, 1995.
- (12) Wayland, B. B.; Van Voorhees, S. L.; Wilker, C. *Inorg. Chem.* **1986**, *25*, 4039-4042.
- (13) (a) Tse, A. K.S.; Wu, B. M.; Mak, T. C. W.; Chan, K. S. *J. Organomet. Chem.* **1998**, *568*, 257-261. (b) Dolphin, D.; Halko, D. J.; Johnson, E. *Inorg. Chem.* **1981**, *20*, 4348-4351.
- (14) (a) Liang, L. C.; Lin, J. M.; Lee, W. Y. *Chem. Comm.* **2005**, *19*, 2462-2464. (b) Harkins, S. B.; Peters, J. C. *Organometallics* **2002**, *21*, 1753-1755. (c) Wang, C.; Ziller, J. W.; Flood, T. C. *J. Am. Chem. Soc.* **1995**, *117*, 1647-1648.
- (15) Mak, K. W.; Xue, F.; Mak, T. C. W.; Chan, K. S. *J. Chem. Soc., Dalton Trans.* **1999**, *19*, 3333-3334.
- (16) Nelson, A. P.; Dimagno, S. G. *J. Am. Chem. Soc.* **2000**, *122*, 8569-8570.
- (17) Sanford, M. S.; Groves, J. T. *Angew. Chem. Int. Ed.* **2004**, *43*, 588-590.

- (18) March, J. *Advanced Organic Chemistry: Reactions, Mechanisms and Structure*, 3<sup>rd</sup> Edition, Wiley: New York, **1985**.
- (19) (a) Brothers, P. J.; Collman, J. P. *Acc. Chem. Res.* **1986**, *19*, 209-215. (b) Lexa, D.; Mispelter, J.; Saveant, J. M. *J. Am. Chem. Soc.* **1981**, *103*, 6806-6812. (c) Perree-Fauvent, M.; Gaudemer, A.; Boucly, P.; Devynck, J. *J. Organomet. Chem.* **1976**, *120*, 439-451. (d) Chan, K. S.; Mak, K. W.; Tse, M. K.; Yeung, S. K.; Li, B. Z.; Chan, Y. W. *J. Organomet. Chem.* **2008**, *693*, 399-407.
- (20) Whang, D. M.; Kim, K. M. *Acta Cryst. C* **1991**, *47*, 2547-2550.
- (21) Bengali, A. A.; Schultz, H.; Moore, C. B.; Bergman, R. G. *J. Am. Chem. Soc.* **1994**, *116*, 9369-9377.
- (22) (a) Tenn, W. J.; Young, K. J. H.; Oxgaard, J.; Nielsen, R. J.; Goddard, W. A.; Periana, R. A. *Organometallics* **2006**, *25*, 5173-5175. (b) Oxgaard, J.; Tenn, W. J.; Nielson, R. J.; Periana, R. A.; Goddard, W. A. *Organometallics* **2007**, *26*, 1565-1567. (c) Fu, X. F.; Wayland, B. B. *J. Am. Chem. Soc.* **2004**, *126*, 2623-2631. (d) Feng, Y.; Lail, M.; Barakat, K. A.; Cundari, T. R.; Gunnoe, T. B.; Peterson, J. L. *J. Am. Chem. Soc.* **2005**, *127*, 14174-14175. (e) Collman, J. P.; Boulatov, R. *Inorg. Chem.* **2001**, *40*, 560-563.
- (23) (a) Wayland, B. B.; Ba, S.; Sherry, A. E. *J. Am. Chem. Soc.* **1991**, *113*, 5305-5311. (b) Thibblin, A.; Sidhu, H. *J. Am. Chem. Soc.* **1992**, *114*, 7403-7407. (c) Values of  $1.10 \pm 0.05/\beta$ -D have been reported; Westaway, K. C. *Isotopes in Organic Chemistry*; Buncl, E.; Lee, C. C., Eds.; Elsevier: Amsterdam 1987. (d) Kwart, H. *Acc. Chem. Res.* **1982**, *15*, 401-408.
- (24) Ruiz, J.; Mann, B. E.; Spencer, C. M.; Taylor, B. F.; Maitlis, P. M. *J. Chem. Soc., Dalton Trans.*, **1987**, *8*, 1963-1966.
- (25) Perutz, R. N.; Sabo-Etienne, S. *Angew. Chem. Int. Ed.* **2007**, *46*, 2578-2592.

(26) Thompson, M. E.; Baxter, S. M.; Bulls, A. R.; Burger, B. J.; Nolan, M. C.; Santarsiero, B. D.; Schaefer, W. P.; Bercaw, J. E. *J. Am. Chem. Soc.* **1987**, *109*, 203-219.

(27) (a) Zhang, S.; Piers, W. E.; Gao, X.; Parvez, M. *J. Am. Chem. Soc.* **2000**, *122*, 5499-5509. (b) Conroy, K. D.; Hayes, P. G.; Piers, W. E.; Parvez, M. *Organometallics* **2007**, *26*, 4464-4470. (c) Basset, J. M.; Coperet, C.; Lefort, L.; Maunders, B. M.; Maury, O.; Le Roux, E.; Saggio, S.; Soulivong, D.; Sunley, G. J.; Taoufik, M.; Thivolle-Cazat, J. *J. Am. Chem. Soc.* **2005**, *127*, 8604-8605.

(28) Kwong Shing Choi's unpublished results, 2010.

## Chapter 3 Metalloradical-promoted Functionalization of Cycloheptane to Rhodium Porphyrin Benzyl via C–H and C–C Bond Activation

### 3.1 Introduction

#### 3.1.1 Properties of Cycloheptane

*c*-Heptane is a colourless combustible liquid at ambient conditions. It is readily miscible with ethanol and ether but insoluble in water.<sup>1a</sup> The lowest-energy conformational isomer is a twisted chair form, which is very fluxional (fluxional energy = 8.2 kcal mol<sup>-1</sup>) (Figure 3.1).<sup>1b</sup> Some other properties concerning the reactivity of *c*-heptane are summarized in Table 3.1.

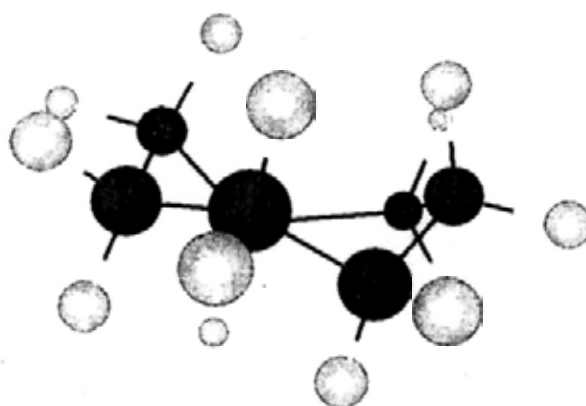


Figure 3.1 Ball and Stick Model of *c*-Heptane (twisted chair form)

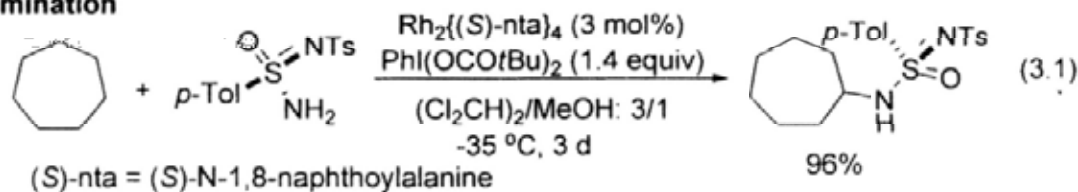
Table 3.1 Properties Concerning the Reactivity of *c*-Heptane<sup>2-4</sup>

| Properties                 | Corresponding Value  |
|----------------------------|--|
| BDE of C–H                 | 94.0 kcal mol <sup>-1</sup>                                |
| BDE of C–C                 | 86.6 kcal mol <sup>-1</sup>                                |
| Ring Strain                | 6.3 kcal mol <sup>-1</sup>                                 |
| Diamagnetic Susceptibility | -73.9 × 10 <sup>-6</sup> cm <sup>3</sup> mol <sup>-1</sup> |
| Dielectric Constant        | 2.0784 at 20.0 °C  |

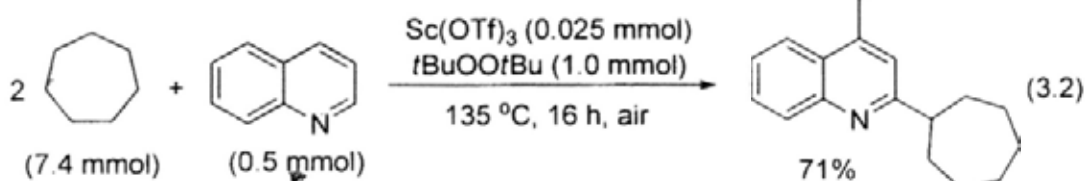
### 3.1.2 CHA of Cycloheptane

*c*-Heptane is well known to undergo transition-metal catalyzed CHA including amination,<sup>5</sup> C–C formation,<sup>6</sup> dehydrogenation<sup>7</sup> and oxidation (eqs 3.1-3.4).<sup>8</sup>

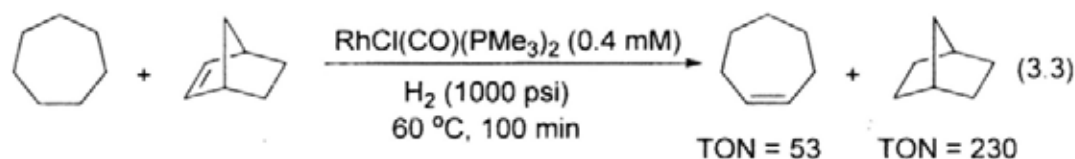
#### Amination



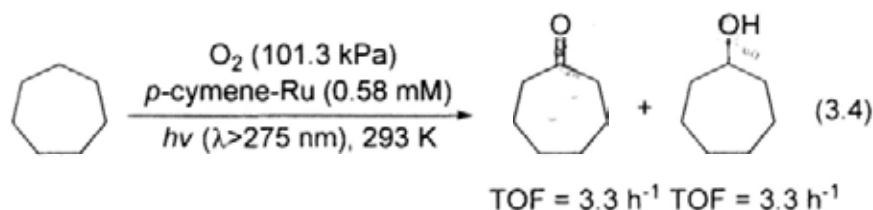
#### C-C Formation



#### Dehydrogenation



#### Oxidation



### 3.1.3 CCA of Cycloheptane

By contrast, the C–C bond of *c*-heptane is more reluctant to cleave by transition-metal complexes and consequently, there are very limited CCA examples. Aliphatic C–C bond of *c*-heptane is weaker than C–H bonds by around 8 kcal mol<sup>-1</sup>.<sup>2</sup> However, the aliphatic C–C bond is shielded by C–H bonds and this makes the transition-metal complex difficult to access the C–C bond.<sup>9</sup> Recently, Basset et al. reported the hydrogenolysis of *c*-heptane catalyzed by tantalum hydride complex supported on silica to give a mixture of acyclic alkanes and cyclic alkanes (eq 3.5).<sup>10</sup>





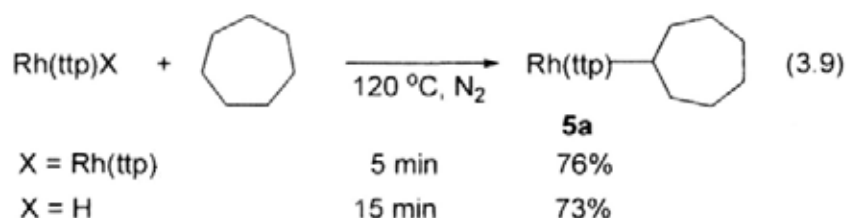
Table 3.2 Time Profile of Reaction of Rh(tp)Cl with *c*-Heptane in the Presence of K<sub>2</sub>CO<sub>3</sub>

| Time/h | Yield %            |                                     |                    |                   |   |                   | Total Rh pdt | Total Org pdt |
|--------|--------------------|-------------------------------------|--------------------|-------------------|---|-------------------|--------------|---------------|
|        | Rh(tp)Cl <b>1a</b> | Rh(tp)( <i>c</i> -heptyl) <b>5a</b> | Rh(tp)Bn <b>5b</b> | Rh(tp)H <b>1d</b> | Rh <sub>2</sub> (tp) <sub>2</sub> <b>1e</b> | <i>c</i> -heptene |              |               |
| 0      | 100                | 0                                   | 0                  | 0                 | 0   | 0                 | 100          | 0             |
| 0.5    | 72                 | 0                                   | 9                  | 16                | 3   | 0                 | 100          | 9             |
| 1      | 37                 | 0                                   | 13                 | 43                | 6   | 25                | 99           | 38            |
| 2      | 15                 | 0                                   | 13                 | 64                | 7   | 43                | 98           | 56            |
| 16     | 0                  | 18                                  | 14                 | 62                | 0   | 42                | 94           | 74            |
| 72     | 0                  | 20                                  | 14                 | 62                | 0   | 42                | 96           | 77            |
| 96     | 0                  | 23                                  | 14                 | 59                | 0   | 41                | 96           | 79            |
| 264    | 0                  | 23                                  | 15                 | 58                | 0   | 43                | 97           | 82            |

After 2 hours of reaction, only 15% yield of Rh(tp)Cl **1a** remained while Rh(tp)Bn **5b**, Rh<sub>2</sub>(tp)<sub>2</sub> **1e** and Rh(tp)H **1d** were formed in 12%, 7% and 64% yields, respectively. After 16 hours, Rh(tp)Cl **1a** and Rh<sub>2</sub>(tp)<sub>2</sub> **1e** completely reacted; the yield of Rh(tp)H **1d** still remained at 62%. At the same time, the yield of Rh(tp)Bn **5b** did not increase while Rh(tp)(*c*-heptyl) **5a** formed in 17% yield. *c*-Heptene was observed in 42% yield. Since the complete consumption of Rh<sub>2</sub>(tp)<sub>2</sub> **1e** significantly slowed down further conversion of Rh(tp)(*c*-heptyl) **5a** to Rh(tp)Bn **5b**, Rh<sub>2</sub>(tp)<sub>2</sub> **1e** likely has a promoting role in the transformation. Therefore, both Rh<sub>2</sub>(tp)<sub>2</sub> and Rh(tp)H are possible intermediates.

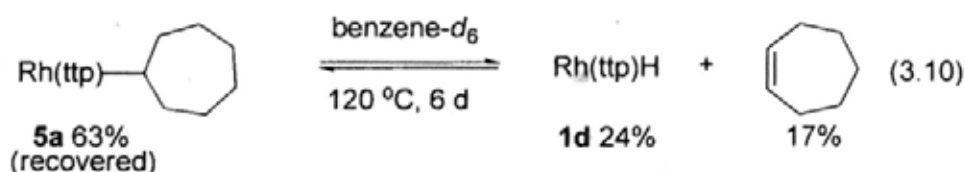
### 3.4.2 Reactivity of Rh<sub>2</sub>(ttp)<sub>2</sub> and Rh(ttp)H with *c*-Heptane

Rh<sub>2</sub>(ttp)<sub>2</sub> and Rh(ttp)H were then reacted with *c*-heptane separately. Indeed, both Rh<sub>2</sub>(ttp)<sub>2</sub> and Rh(ttp)H gave Rh(ttp)(*c*-heptyl) only in 76% and 73% yields, respectively (eq 3.9). Therefore, they are intermediates for CHA only.

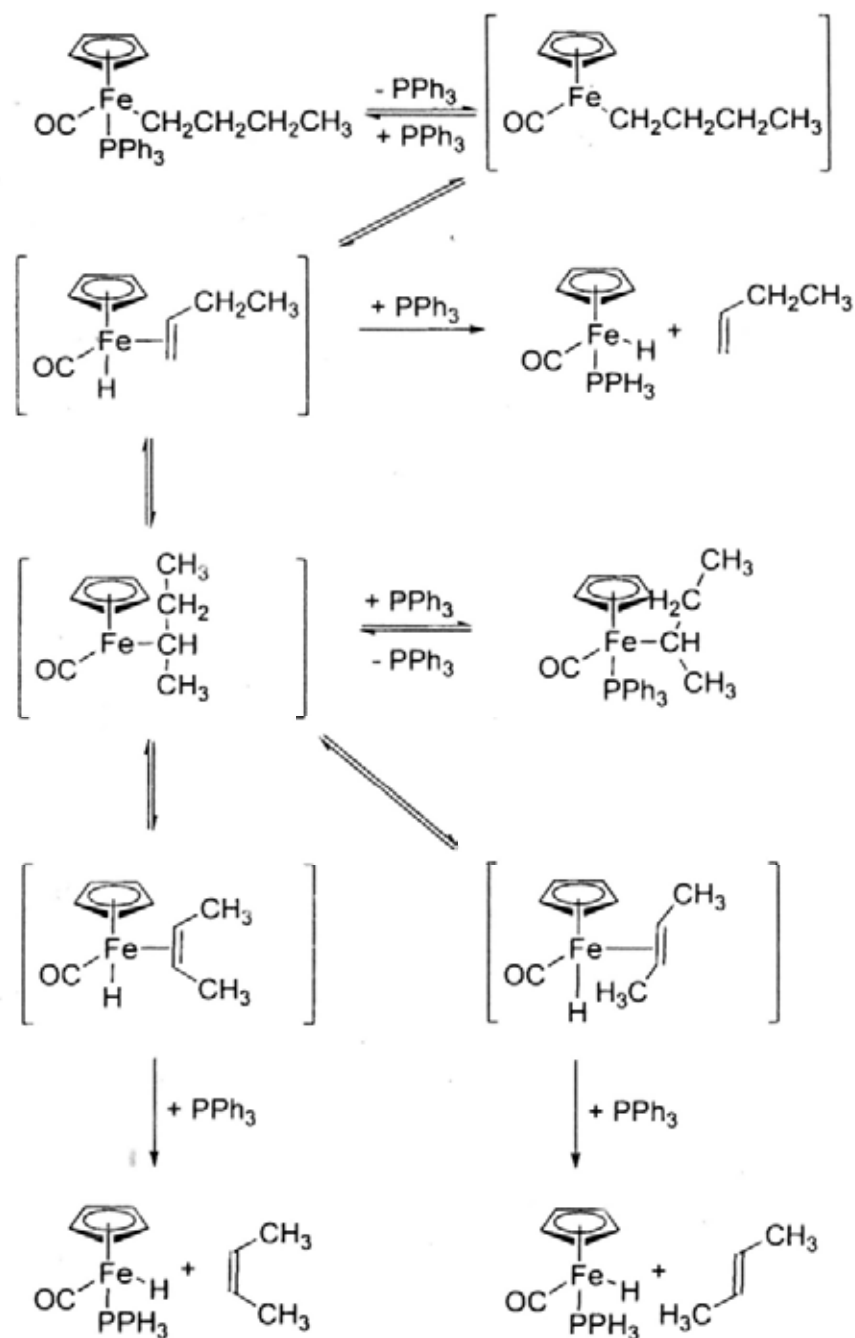


### 3.4.3 Conversion of Rh(ttp)(*c*-heptyl) to Rh(ttp)Bn

As neither Rh<sub>2</sub>(ttp)<sub>2</sub> nor Rh(ttp)H reacted with *c*-heptane to give Rh(ttp)Bn, Rh(ttp)(*c*-heptyl) likely undergoes further reaction via CCA in order to account for the formation of Rh(ttp)Bn. To find out whether the CHA product is an intermediate for CCA, Rh(ttp)(*c*-heptyl) was heated in neutral and basic conditions separately (eq 3.10 and 3.11). In neutral conditions, Rh(ttp)(*c*-heptyl) **5a** yielded only Rh(ttp)H **1d** and *c*-heptene in 24% and 17% yield, respectively after 6 days (eq 3.10, Figure 3.3, Table 3.3). Rh(ttp)H and *c*-heptene likely form from the  $\beta$ -hydride elimination of Rh(ttp)(*c*-heptyl).



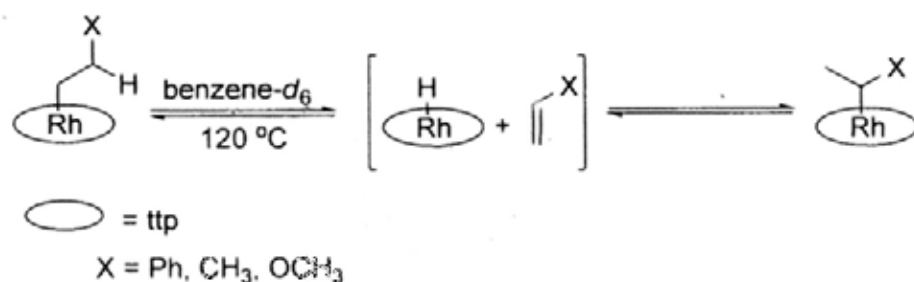
In fact, the  $\beta$ -hydride elimination of metal alkyl was well-known to give metal hydride and olefin.<sup>13</sup> Once the metal hydride and olefin forms, reverse 1,2-addition proceeds to give metal alkyl (Scheme 3.1)



Scheme 3.1  $\beta$ -Hydride Elimination of Metal Alkyl and Olefin Metal Hydride Insertion

The 1,2-rearrangement of rhodium porphyrin alkyls were reported by Chan et al.<sup>14</sup> Several  $\beta$ -substituted ethylrhodium complexes underwent 1,2-alkyl rearrangement at 120 °C in benzene-*d*<sub>6</sub>. The mechanism of the reaction is likely to proceed via a  $\beta$ -hydride elimination with an olefin formed as the intermediate (Scheme 3.2). The secondary alkylrhodium complexes yielded the primary alkylrhodium complexes. With either primary or secondary

complexes as the starting materials, similar tautomeric ratios were obtained. Therefore, the reversibility of the rearrangement was established.



Scheme 3.2 Reversible 1,2-Alkyl Rearrangement of Rhodium Porphyrin Alkyl

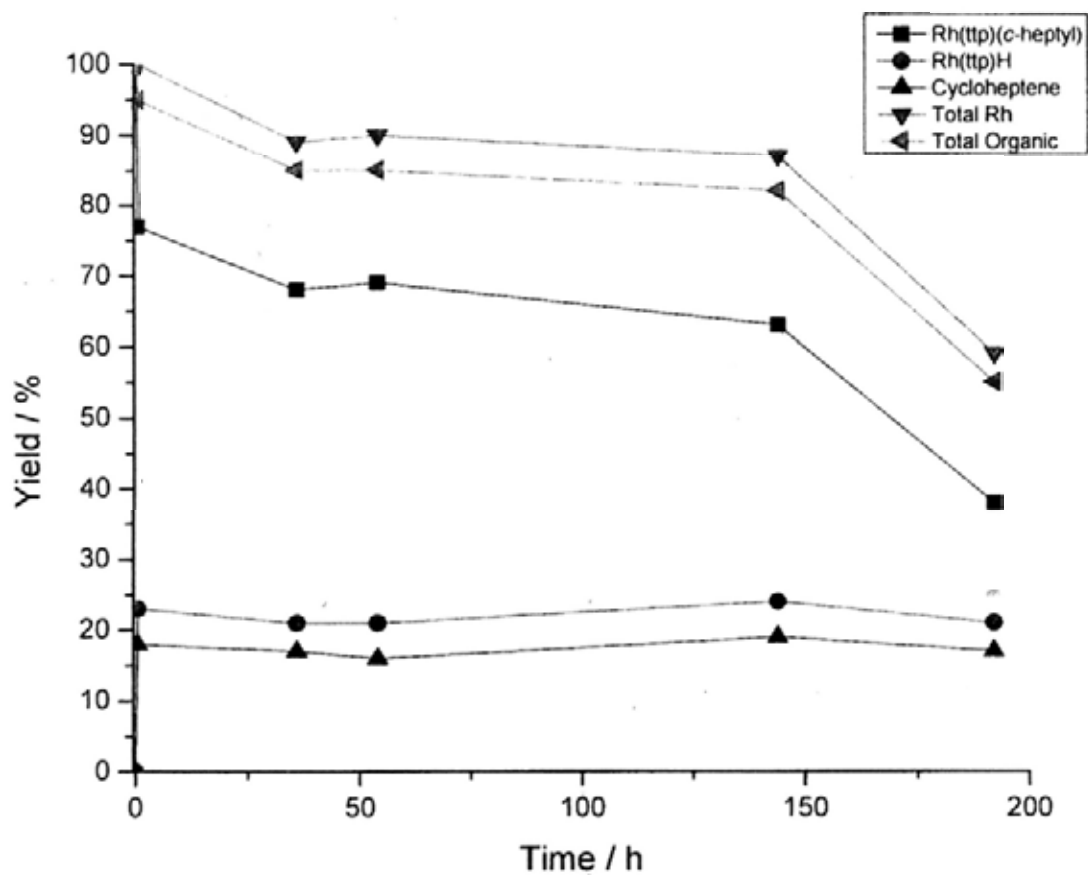
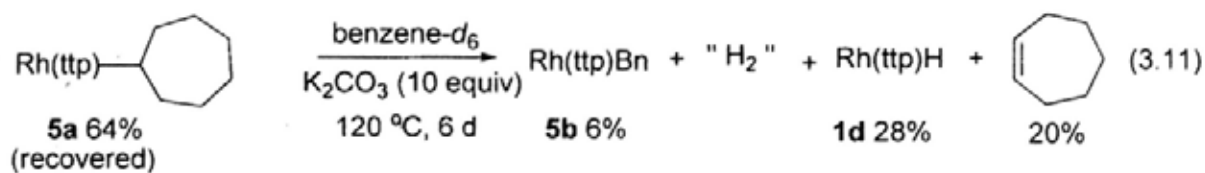


Figure 3.3 Time Profile of Thermal Reaction of Rh(ttp)(c-heptyl)

Table 3.3 Time Profile of Thermal Reaction of Rh(tp)(*c*-heptyl) **5a**

| Time/h | Yield %   |           |                   |              |               |
|--------|-----------|-----------|-------------------|--------------|---------------|
|        | <b>5a</b> | <b>1d</b> | <i>c</i> -heptene | Total Rh pdt | Total Org pdt |
| 0      | 100       | 0         | 0                 | 100          | 100           |
| 0.5    | 77        | 23        | 18                | 100          | 95            |
| 36     | 68        | 21        | 17                | 89           | 85            |
| 54     | 69        | 21        | 16                | 90           | 85            |
| 144    | 63        | 24        | 19                | 87           | 82            |
| 192    | 38        | 21        | 17                | 59           | 55            |

While in basic conditions, Rh(tp)Bn **5b** was observed in 6% yield in 6 days, together with 28% yield of Rh(tp)H and 20% yield of *c*-heptene (eq 3.11, Figure 3.4, Table 3.4).



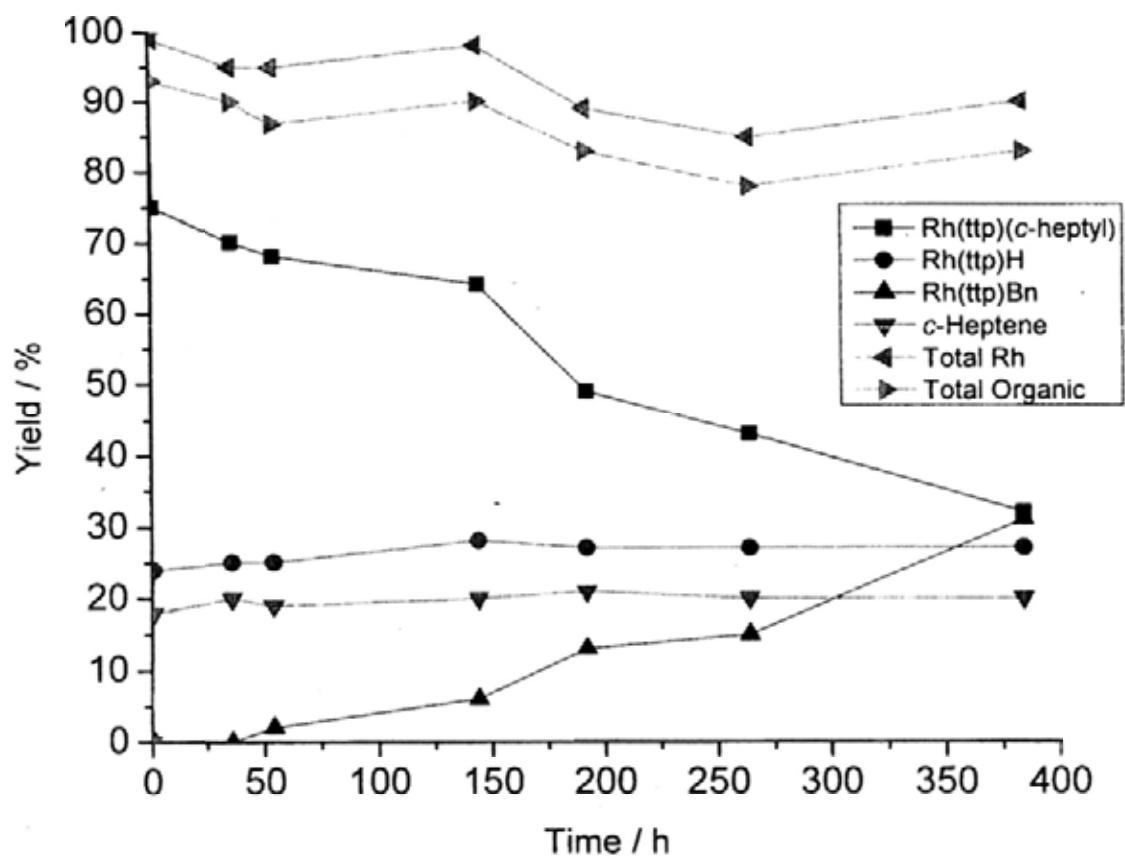


Figure 3.4 Time Profile of Thermal Reaction of Rh(tp)(c-heptyl) with  $K_2CO_3$

Table 3.4 Time Profile of Thermal Reaction of Rh(tp)(*c*-heptyl) with K<sub>2</sub>CO<sub>3</sub>

| Time/h | Yield %   |           |           |                   |              |               |
|--------|-----------|-----------|-----------|-------------------|--------------|---------------|
|        | <b>5a</b> | <b>5b</b> | <b>1d</b> | <i>c</i> -heptene | Total Rh pdt | Total Org pdt |
| 0      | 100       | 0         | 0         | 0                 | 100          | 100           |
| 1      | 75        | 24        | 0         | 18                | 99           | 93            |
| 36     | 70        | 25        | 0         | 20                | 95           | 90            |
| 54     | 68        | 25        | 2         | 19                | 95           | 87            |
| 144    | 64        | 6         | 28        | 20                | 98           | 90            |
| 192    | 49        | 13        | 27        | 21                | 89           | 83            |
| 264    | 43        | 15        | 27        | 20                | 85           | 78            |
| 384    | 32        | 31        | 27        | 20                | 90           | 83            |

The conversion of Rh(tp)(*c*-heptyl) **5a** to Rh(tp)Bn **5b** likely undergoes a  $\beta$ -hydride elimination<sup>14</sup> to give Rh(tp)H **1d** and *c*-heptene. However, a base is required for further reaction to give Rh(tp)Bn **5b**. Therefore, the CHA product is an intermediate for CCA product only in the presence of K<sub>2</sub>CO<sub>3</sub>.

As Rh<sup>II</sup>(por) dimer (por = porphyrin) can form by the thermal<sup>15</sup> or base-promoted<sup>16</sup> dehydrogenative dimerization of Rh<sup>III</sup>(por)H (eqs 3.12-3.13), the possible promoting role of Rh<sub>2</sub>(tp)<sub>2</sub> in converting Rh(tp)(*c*-heptyl) to Rh(tp)Bn was examined (eq 3.14, Figure 3.5, Table 3.5). To our delight, Rh(tp)(*c*-heptyl) added with Rh<sub>2</sub>(tp)<sub>2</sub> (1 mol%) gave Rh(tp)Bn, and the rate promoting rate effect of Rh<sub>2</sub>(tp)<sub>2</sub> (1 mol%) was about 6 times than that of K<sub>2</sub>CO<sub>3</sub> (10 equiv).

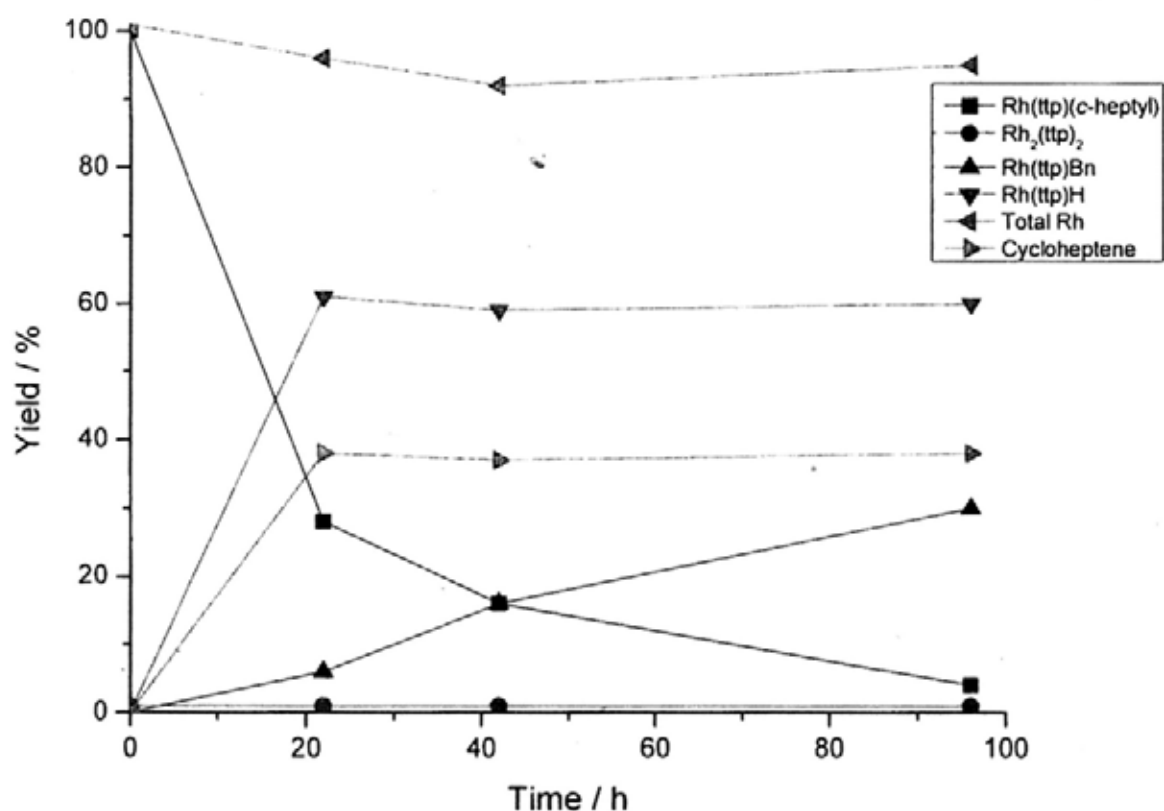
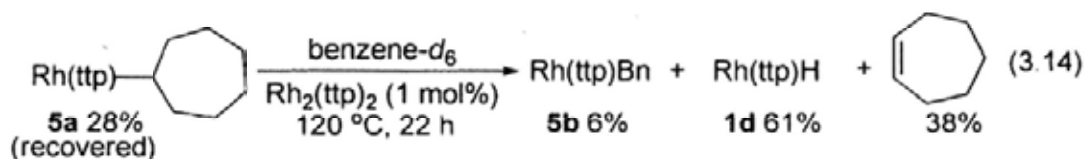
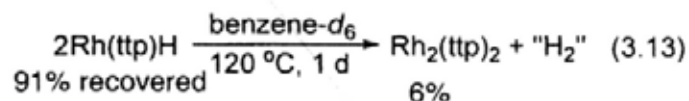
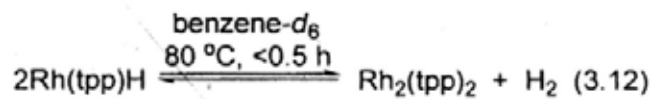


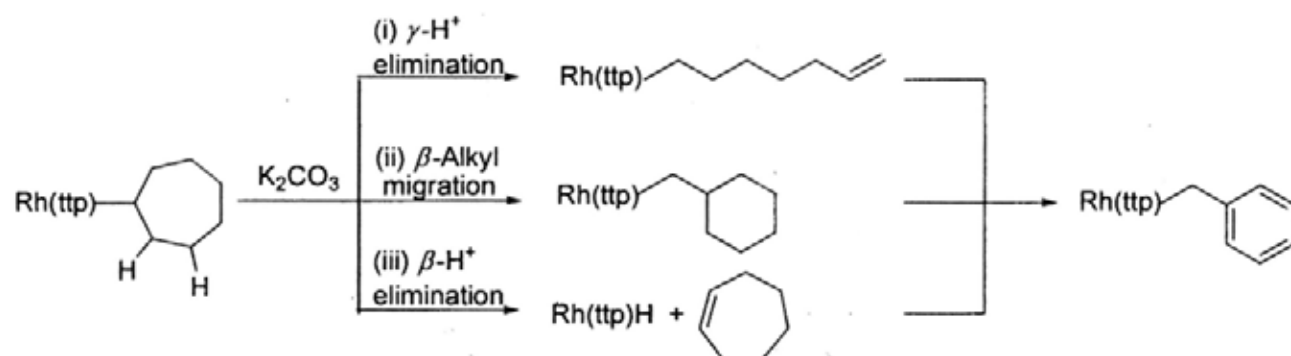
Figure 3.5 Time Profile of Conversion of Rh(tpp)(c-heptyl) to Rh(tpp)Bn with 1 mol% Rh<sub>2</sub>(tpp)<sub>2</sub>

Table 3.5 Time Profile of Conversion of Rh(tpp)(*c*-heptyl) to Rh(tpp)Bn with 1 mol% Rh<sub>2</sub>(tpp)<sub>2</sub>

| Time/h | Yield % |    |    |                   |              |               |
|--------|---------|----|----|-------------------|--------------|---------------|
|        | 5a      | 5b | 1d | <i>c</i> -heptene | Total Rh pdt | Total Org pdt |
| 0      | 100     | 0  | 0  | 0                 | 100          | 100           |
| 22     | 28      | 6  | 61 | 38                | 95           | 62            |
| 42     | 16      | 16 | 59 | 37                | 91           | 69            |
| 96     | 4       | 30 | 60 | 38                | 94           | 72            |

### 3.5 Proposed Mechanistic Pathways

As Rh(tpp)(*c*-heptyl) **5a** was converted to Rh(tpp)Bn **5b** in the presence of K<sub>2</sub>CO<sub>3</sub>, the direct transformation is very unlikely and therefore stepwise conversions are more reasonable. Scheme 3.3 shows three proposed mechanistic pathways and their corresponding key intermediates. Each one was examined to elucidate the mechanism of Rh(tpp)Bn formation.

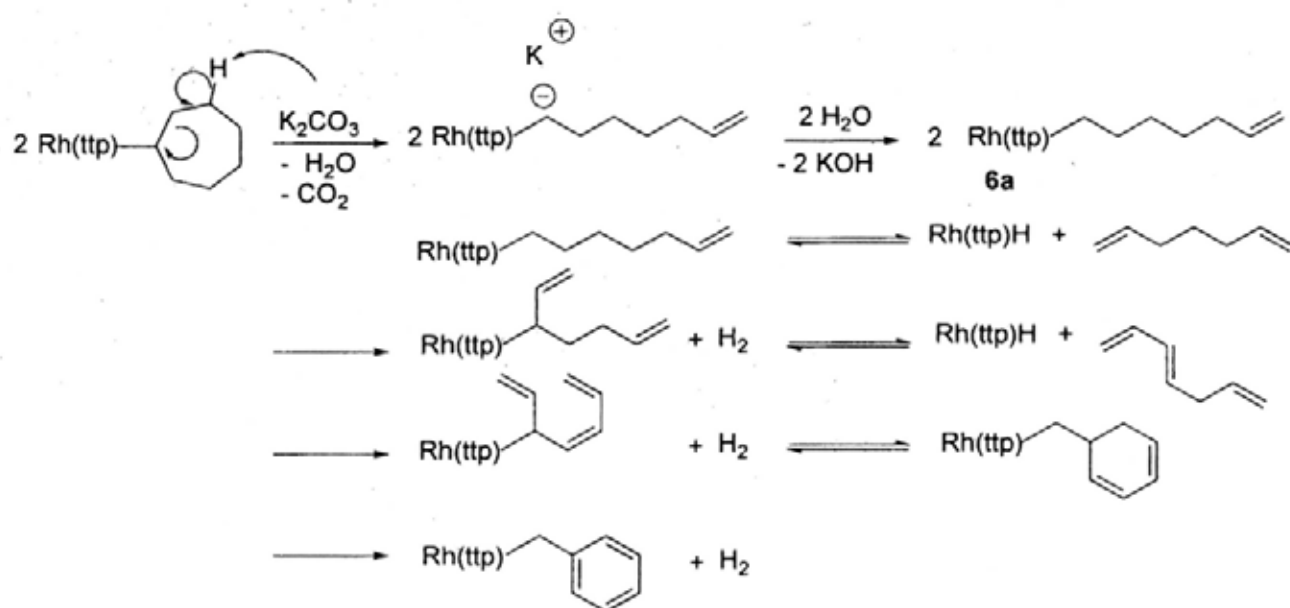


Scheme 3.3 Proposed Mechanistic Pathways for the Conversion of Rh(tpp)(*c*-heptyl) to Rh(tpp)Bn with K<sub>2</sub>CO<sub>3</sub>

#### 3.5.1 Conversion of Rh(tpp)(*c*-heptyl) to Rh(tpp)Bn via $\gamma$ -H<sup>+</sup> Elimination

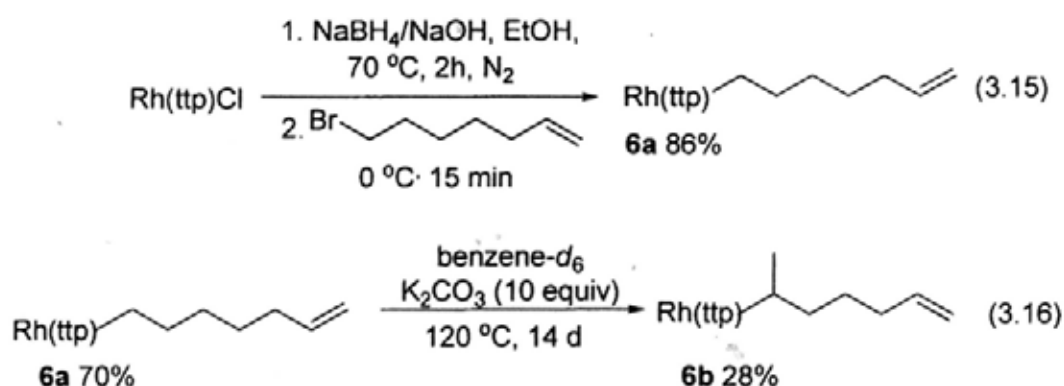
In pathway (i), Rh(tpp)(*c*-heptyl) **5a** undergoes a  $\gamma$ -H<sup>+</sup> elimination to give Rh(tpp)(CH<sub>2</sub>)<sub>5</sub>(CH=CH<sub>2</sub>) **6a** and the subsequent dehydrogenation and rearrangement lead to

the formation of Rh(ttp)Bn **5b** (Scheme 3.4). In fact, (*c*-heptyl)tantalum complex was proposed to undergo  $\gamma$ -H elimination to generate Ta(CH<sub>2</sub>)<sub>5</sub>(CH=CH<sub>2</sub>) for further reaction.<sup>17a</sup>



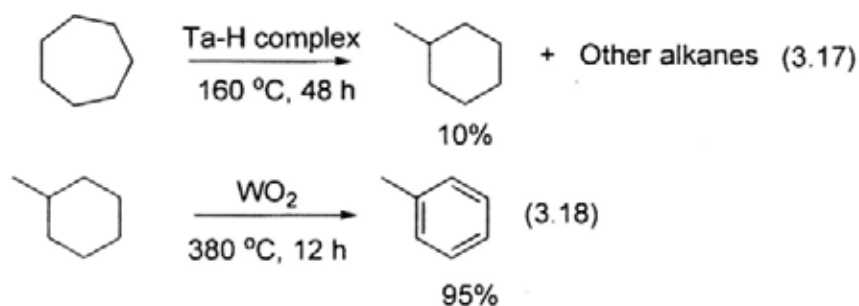
Scheme 3.4 Proposed Mechanism of  $\gamma$ -H<sup>+</sup> Elimination of Rh(ttp)(*c*-heptyl)

Rh(ttp)(CH<sub>2</sub>)<sub>5</sub>(CH=CH<sub>2</sub>) **6a** was independently synthesized by reductive alkylation (eq 3.15).<sup>18</sup> Rh(ttp)(CH<sub>2</sub>)<sub>5</sub>(CH=CH<sub>2</sub>) **6a** was then heated at 120 °C in the presence of K<sub>2</sub>CO<sub>3</sub> for 14 days and only gave 28% yield of the 1,2-rearrangement<sup>14</sup> product, Rh(ttp)(CH(CH<sub>3</sub>))CH<sub>2</sub>CH<sub>2</sub>CH<sub>2</sub>CH=CH<sub>2</sub> **6b** while 70% yield of Rh(ttp)(CH<sub>2</sub>)<sub>5</sub>(CH=CH<sub>2</sub>) **6a** was recovered (eq 3.16). No Rh(ttp)Bn **5b** was observed. Pathway (i) is ruled out.

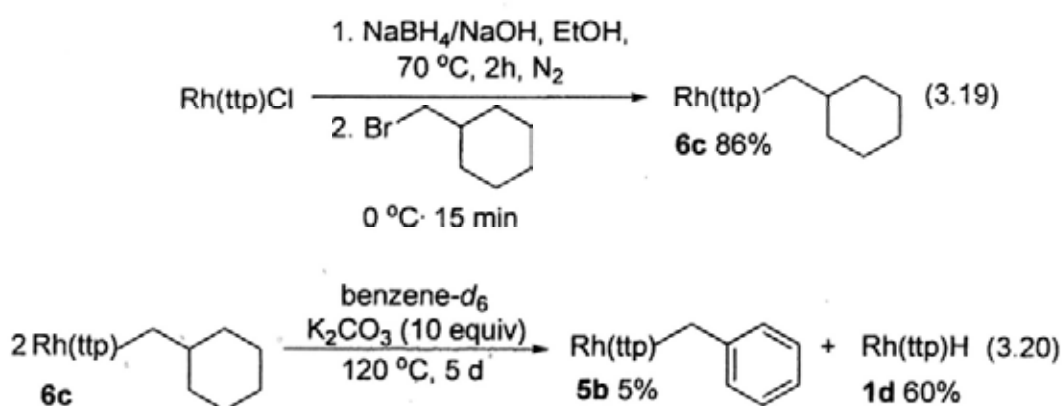


### 3.5.2 Conversion of Rh(ttp)(*c*-heptyl) to Rh(ttp)Bn via $\beta$ -Alkyl Migration

In pathway (ii), Rh(ttp)(*c*-heptyl) **5a** undergoes a  $\beta$ -alkyl migration to form ((*c*-hexyl)methyl)rhodium **6c** complex which gives Rh(ttp)Bn **5b** upon further dehydrogenation. In fact, the conversion of *c*-heptane to methylcyclohexane was achieved by a Ta-H catalyst (eq 3.17).<sup>10</sup> Besides, the WO<sub>2</sub>-catalyzed dehydrogenation of methylcyclohexane was well-documented (eq 3.18).<sup>17b</sup>



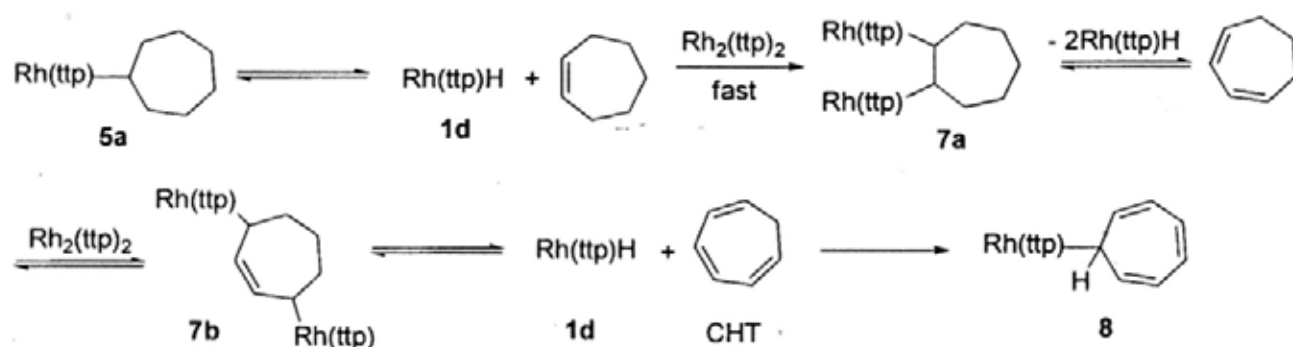
Therefore, ((*c*-hexyl)methyl)rhodium **6c** was independently synthesized by reductive alkylation (eq 3.19).<sup>18</sup> However, when ((*c*-hexyl)methyl)rhodium **6c** was heated at 120 °C for 5 days in the presence of K<sub>2</sub>CO<sub>3</sub>, only 5% yield of Rh(ttp)Bn **5b** and 60% yield of Rh(ttp)H **1d** were observed (eq 3.20). Therefore, pathway (ii) is only a minor pathway based on the yield and very slow rate.



### 3.5.3 Conversion of Rh(ttp)(*c*-heptyl) to Rh(ttp)Bn via $\beta$ -H<sup>+</sup> Elimination

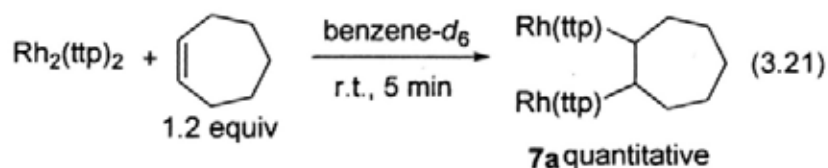
As Rh(ttp)(*c*-heptyl) **5a** gave Rh(ttp)H **1d** and *c*-heptene via  $\beta$ -H and  $\beta$ -H<sup>+</sup> elimination in the absence and presence of K<sub>2</sub>CO<sub>3</sub> (eqs 3.10 and 3.11),<sup>16</sup> *c*-heptene formed

can be dehydrogenated further to give cycloheptatriene (CHT) which can then produce Rh(tp)Bn **5b**. Scheme 3.5 illustrates the detailed proposed mechanism of the Rh<sub>2</sub>(ttp)<sub>2</sub>-catalyzed dehydrogenation of *c*-heptane to give cycloheptatriene. **5a** initially undergoes the reversible β-H elimination/addition<sup>14</sup> to give Rh(tp)H **1d** and *c*-heptene which is then rapidly trapped by Rh<sub>2</sub>(ttp)<sub>2</sub> **1e** to yield **7a**.<sup>19</sup> Successive β-H elimination and addition reactions of **7a** with Rh<sub>2</sub>(ttp)<sub>2</sub> **1e** finally gives CHT. Rh(tp)H **1d** or Rh<sub>2</sub>(ttp)<sub>2</sub> **1e** then reacts with CHT to give Rh(tp)(cycloheptatrienyl) **8**.



Scheme 3.5 Proposed Mechanism of *c*-Heptane Dehydrogenation

Supporting lines of evidence came the following experiments. Rh<sub>2</sub>(ttp)<sub>2</sub> **1e** reacted at room temperature with *c*-heptene rapidly to give the 1,2-addition product **7** quantitatively (eq 3.21).



**7a** was also found to be reactive and thermally unstable even at ambient conditions (Figure 3.6). The freshly prepared **7a** ( $t = 0$  h) gave a clean <sup>1</sup>H NMR spectrum. After standing at ambient conditions for 12 hours, **7a** decomposed to give Rh<sub>2</sub>(ttp)<sub>2</sub> **1e**, *c*-heptene and Rh(tp)(*c*-heptyl) **5a** in 5%, 2% and 42% yields, respectively, while 48% of **7a** remained (eq 3.22).

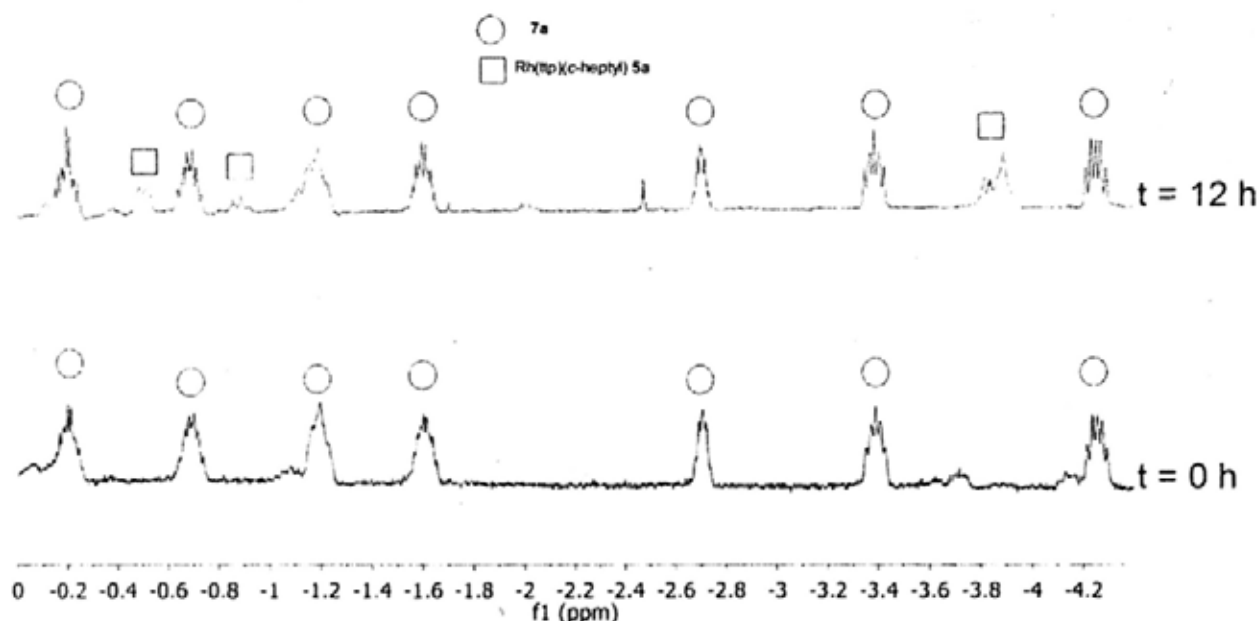
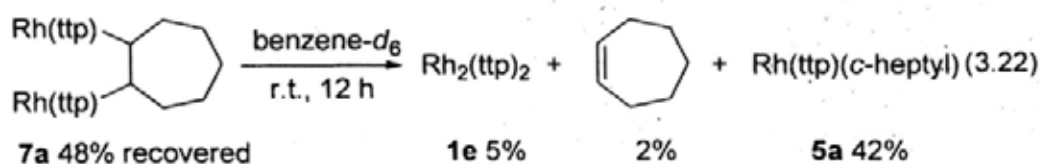
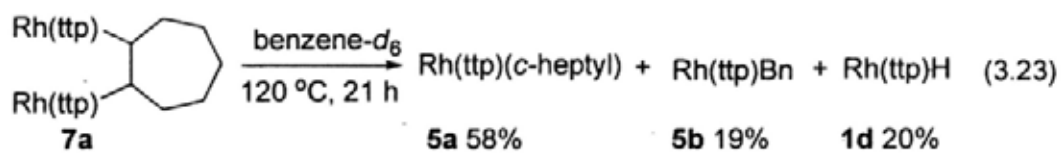


Figure 3.6  $^1\text{H}$  NMR Spectra of **7a** at 0 h and 12 h at Ambient Conditions (Upfield Region)

Thus, the freshly prepared **7a** was heated at  $120\text{ }^\circ\text{C}$  for 21 hours to give  $\text{Rh}(\text{tpp})\text{H}$  **1d**,  $\text{Rh}(\text{tpp})(\text{c-heptyl})$  **5a** and  $\text{Rh}(\text{tpp})\text{Bn}$  **5b** in 20%, 58% and 19% yields, respectively (eq 3.23, Figure 3.7, Table 3.6).<sup>20</sup> Therefore, **7a** is a viable intermediate for the formation of  $\text{Rh}(\text{tpp})\text{Bn}$ .



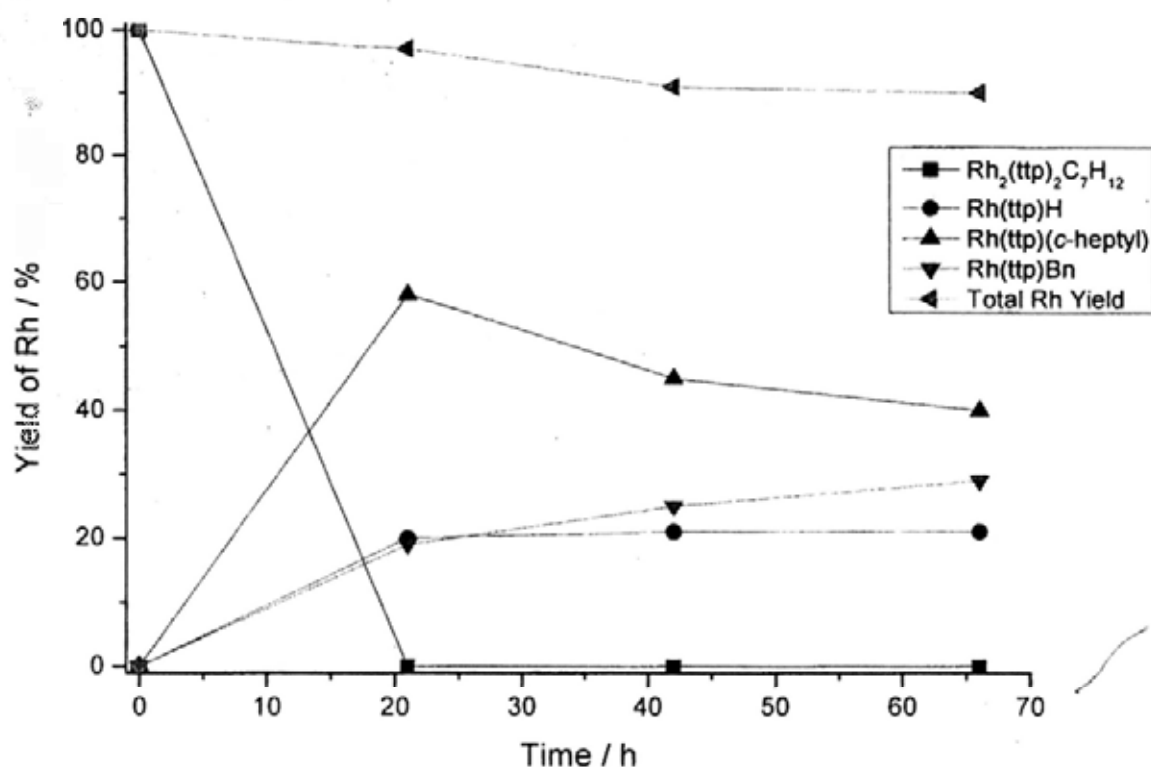


Figure 3.7 Time Profile of Conversion from 7a

Table 3.6 Time profile of conversion from 7a

| Time/h | Yield % |    |    |    | Total Rh pdt |
|--------|---------|----|----|----|--------------|
|        | 7a      | 5a | 5b | 1d |              |
| 0      | 100     | 0  | 0  | 0  | 100          |
| 21     | 0       | 58 | 19 | 20 | 97           |
| 42     | 0       | 45 | 25 | 21 | 91           |
| 66     | 0       | 40 | 29 | 21 | 90           |

As Rh(tp)(cycloheptatrienyl) **8a** is proposed to be formed from the CHA of CHT with Rh<sub>2</sub>(tp)<sub>2</sub> or Rh(tp)H (Scheme 3.6), the reactivity of Rh<sub>2</sub>(tp)<sub>2</sub> and Rh(tp)H towards CHT were examined separately. Indeed, both Rh<sub>2</sub>(tp)<sub>2</sub> and Rh(tp)H reacted with CHT

quickly at room temperature to give Rh(tpp)(cycloheptatrienyl) **8** quantitatively (eq 3.24).<sup>21</sup> The structure of Rh(tpp)(cycloheptatrienyl) **8** was elucidated by X-ray crystallography (Figure 3.8).

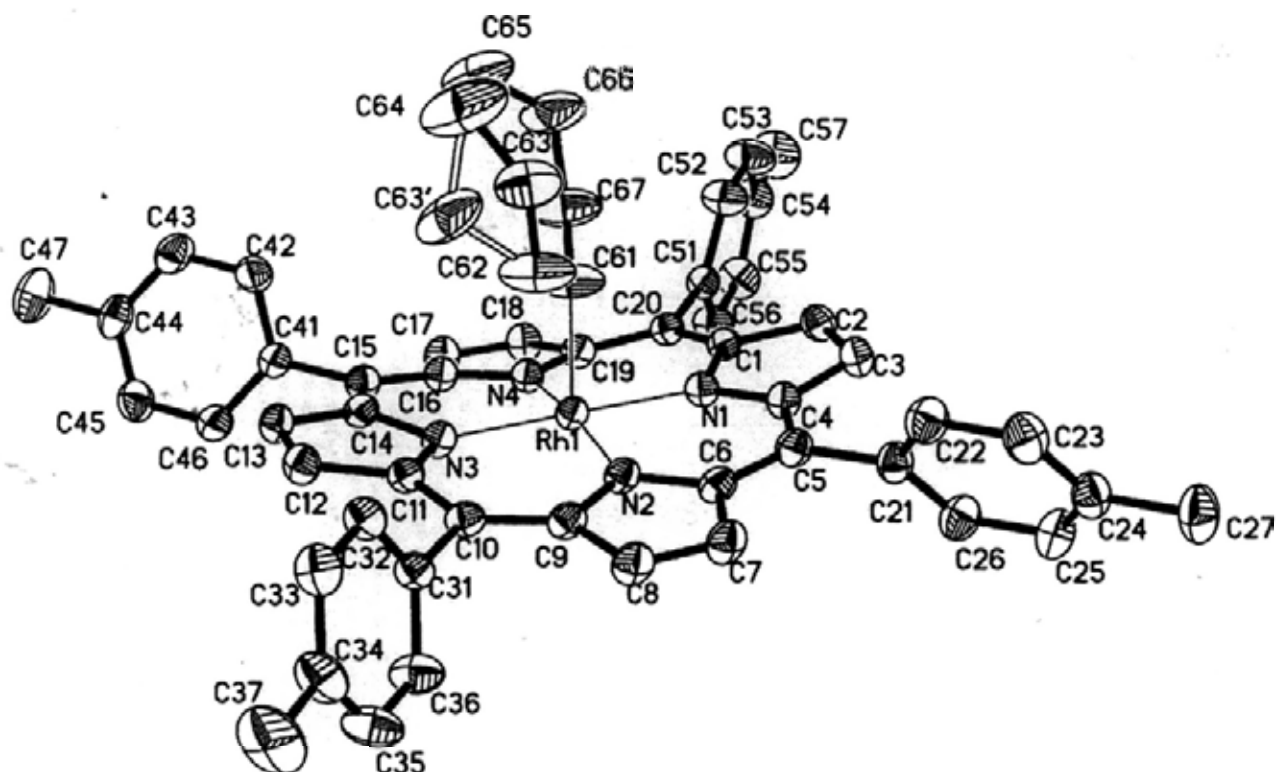
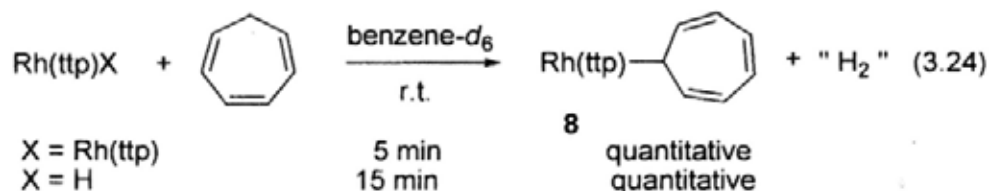
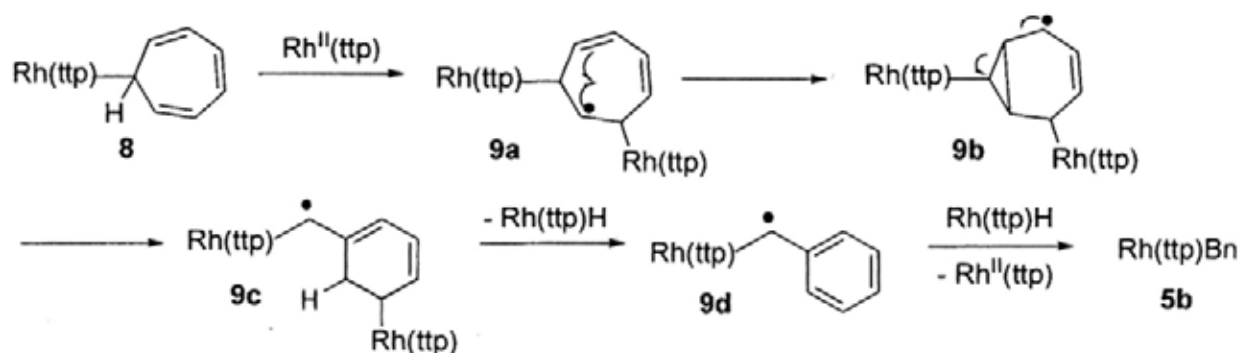


Figure 3.8 ORTEP Presentation of Rh(tpp)(cycloheptatrienyl) **8** (30% Probability Displacement Ellipsoids). Rh–C = 2.10 Å, R = 0.0364

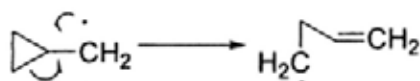
Therefore, Rh<sub>2</sub>(tp)<sub>2</sub> is shown to promote the formation of Rh(tp)(cycloheptatrienyl) **8** by rapidly trapping *c*-heptene, *c*-hepta-1,3-diene and CHT from the β-hydride elimination of **5a**, **7a** and **7b**.

To account for the formation of Rh(tp)Bn **5b**, scheme 3.6 shows the proposed mechanism of the Rh<sup>II</sup>-catalyzed transformation of **8** to **5b**. Rh<sup>II</sup>(tp), dissociated from

$\text{Rh}_2(\text{ttp})_2$  through its weak Rh–Rh bond ( $16 \text{ kcal mol}^{-1}$ ),<sup>2,15</sup> reacts with **8** to give the carbon center radical **9a** which then isomerizes to give a cyclopropylmethyl radical **9b** and subsequently upon ring opening produces **9c** (Scheme 3.7).<sup>22</sup> **9c** can undergo a  $\beta$ -H elimination to give the Rh-substituted benzyl radical **9d**. Hydrogen atom transfer from  $\text{Rh}(\text{ttp})\text{H}$  to **9d** yields  $\text{Rh}(\text{ttp})\text{Bn}$  **5b** and regenerates  $\text{Rh}^{\text{II}}(\text{ttp})$ .



Scheme 3.6 Proposed Mechanism for  $\text{Rh}^{\text{II}}$  Catalyzed CCA

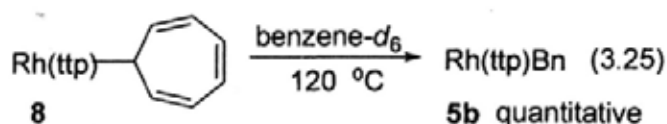


Scheme 3.7 Conversion of Cyclopropylmethyl Radical to 3-Butenyl Radical

### 3.6 Mechanistic Studies of Conversion of $\text{Rh}(\text{ttp})(\text{cycloheptatrienyl})$ to $\text{Rh}(\text{ttp})\text{Bn}$

#### 3.6.1 $^1\text{H}$ NMR Kinetics

In order to gain a deeper mechanistic understanding of the conversion of  $\text{Rh}(\text{ttp})(\text{cycloheptatrienyl})$  **8** to  $\text{Rh}(\text{ttp})\text{Bn}$  **5b**, the kinetics of the conversion of **8** to **5b** were monitored by  $^1\text{H}$  NMR spectroscopy (eq 3.25). The kinetic runs were monitored with the disappearance of  $\text{Rh}(\text{ttp})(\text{cycloheptatrienyl})$  **8** for at least three half-lives by  $^1\text{H}$  NMR spectroscopy. The NMR tube was thermostatted in a GC-oven within  $\pm 0.2$  °C.



The kinetic data taken were then fitted by first-order exponential decay with the software OriginPro 7.5.

### 3.6.2 Determination of Reaction Order and Rate Constant

The rate equation can be expressed as eq 3.26, where  $k_{\text{obs}}$  was the observed rate constant of the reaction.

$$\text{Rate} = k_{\text{obs}} [\mathbf{8}]^m \quad (3.26)$$

Firstly, the value of  $m$  was evaluated. Typical conditions were  $[\mathbf{8}]_0 = 6.95 \times 10^{-3} \text{ M}$  to  $13.90 \times 10^{-3} \text{ M}$  and  $T = 120 \text{ }^\circ\text{C}$ . The results were fitted well by a first-order exponential decay function (Figures 3.9 and 3.10). The kinetic order of  $\mathbf{8}$  is therefore one.

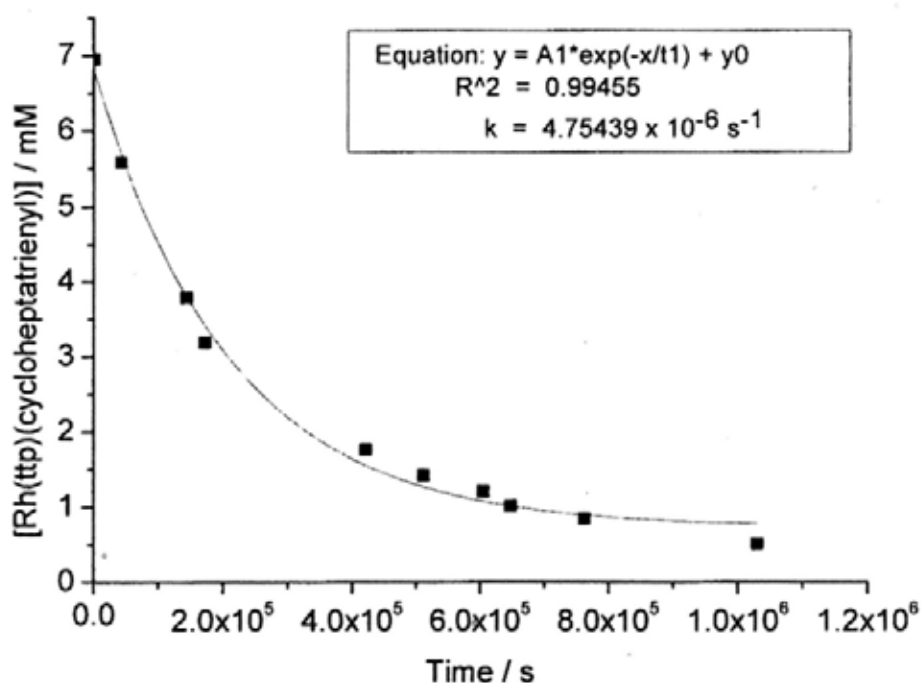


Figure 3.9 Time Profile of Rh(ttp)(cycloheptatrienyl) (6.95 mM) at 120 °C

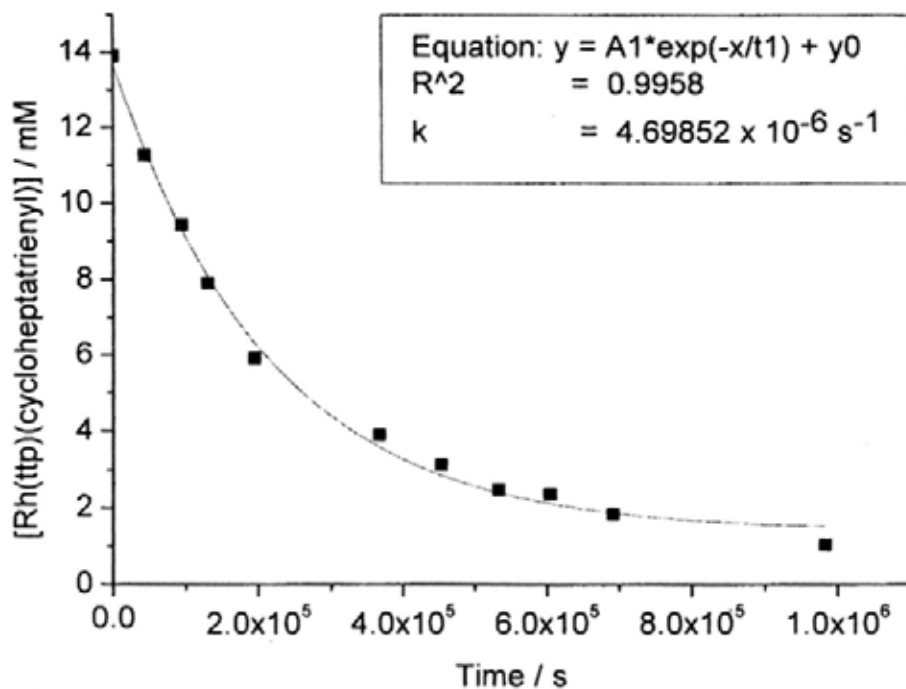


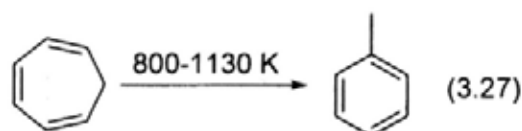
Figure 3.10 Time Profile of Rh(tp)(cycloheptatrienyl) (13.90 mM) at 120 °C

Table 3.7 (entries 1 and 2) show that  $k_{\text{obs}}$  did not change with the initial concentration of Rh(tp)(cycloheptatrienyl) **8**. The kinetic order of Rh(tp)(cycloheptatrienyl) **8** was confirmed to be one. According to the above results, the rate law can be expressed as  $\text{rate} = k[\mathbf{8}]$ , where  $k = 4.75 \times 10^{-6} \text{ s}^{-1}$  at 120 °C. The conversion of **8** to **5b** was a first order reaction.

Table 3.7  $k_{\text{obs}}$  at different conditions

| Entry | $[\mathbf{8}]_0 \times 10^3$<br>/M | Temp / °C | $1/T (\times 10^3$<br>$^3 \text{ K}^{-1})$ | $k_{\text{obs}} \times 10^6 / \text{s}^{-1}$ | Error $\times 10^7 / \text{s}^{-1}$ | $k \times 10^4 /$<br>$\text{L}^{-1} \text{ mol}^{-1}$<br>$\text{s}^{-1}$ |
|-------|------------------------------------|-----------|--|--|-------------------------------------|--|
| 1     | 6.95                               | 120       | 2.545                                      | 4.75439                                      | 3.97540                             | 6.84892  |
| 2     | 13.90                              | 120       | 2.545                                      | 4.69852                                      | 3.45935                             | 6.76046  |
| 3     | 6.95                               | 130       | 2.481                                      | 8.76127                                      | 8.45695                             | 12.6043  |
| 4     | 6.95                               | 140       | 2.421                                      | 15.4640                                      | 34.0559                             | 22.3022  |
| 5     | 6.95                               | 150       | 2.364                                      | 41.0845                                      | 57.0695                             | 59.1367  |

The thermal conversion of CHT to toluene has been reported by Gaynor et al. (eq 3.27).



According to the data obtained from literature,<sup>23</sup>  $\log (A_0/\text{s}^{-1})$  was 13.6 and  $E_\infty$  was 217.7  $\text{kJ mol}^{-1}$ . The thermal conversion rate of CHT to toluene at 120 °C is extrapolated by applying Arrhenius equation.

$$\ln k = -E_a/RT + \ln A$$

$$\text{At } 120 \text{ }^\circ\text{C}, \ln k = -217.7 \times 1000 / (8.314 \times 393) + \ln (10^{13.6})$$

$$\ln k = -35.3$$

$$k = 4.61 \times 10^{-16} \text{ s}^{-1}$$

The rate of the thermal conversion of CHT to toluene at 120 °C is evaluated to be 4.61  $\times 10^{-16} \text{ s}^{-1}$ .<sup>23</sup> Therefore, the conversion of **8** to **5b** is  $10^{10}$  faster than the organic transformation.

### 3.6.3 Activation Parameters

The rates were measured at different temperatures. Typical experimental conditions were  $[\text{Rh}(\text{ttp})(\text{cycloheptatrienyl})] = 6.95 \times 10^{-3} \text{ M}$ ,  $T = 120 \text{ }^\circ\text{C} - 150 \text{ }^\circ\text{C}$  (eq 3.28). The results are shown in Table 3.7 (entries 1, 3-5) and Figures 3.8, 3.11-3.13. These data were used in the estimation of activation parameters.

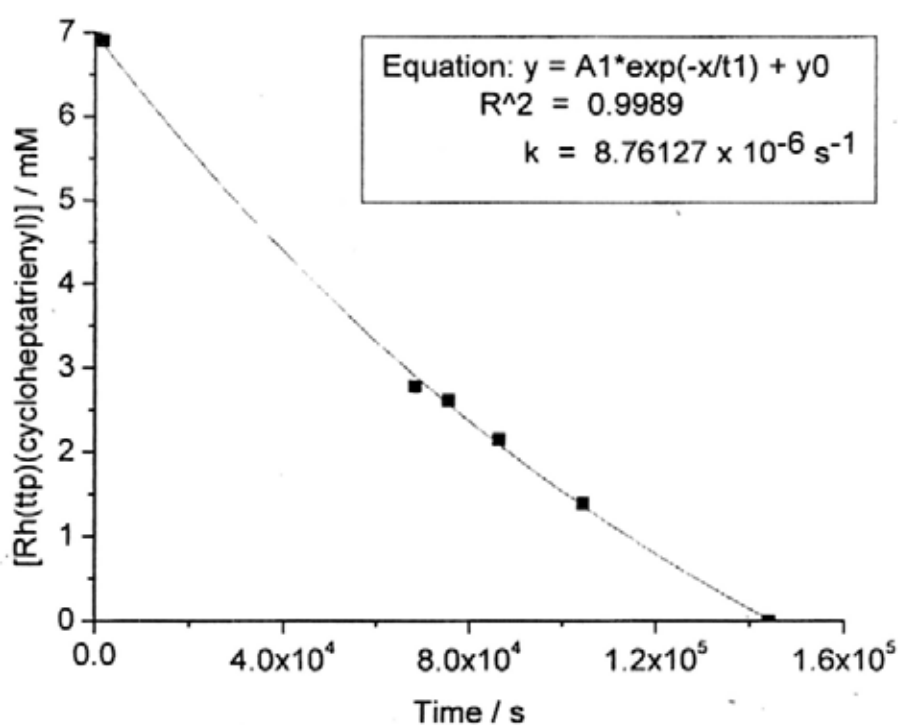
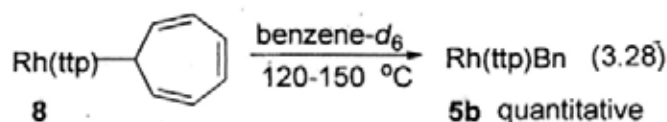


Figure 3.11 Time Profile of  $\text{Rh}(\text{ttp})(\text{cycloheptatrienyl})$  (6.95 mM) at  $130 \text{ }^\circ\text{C}$

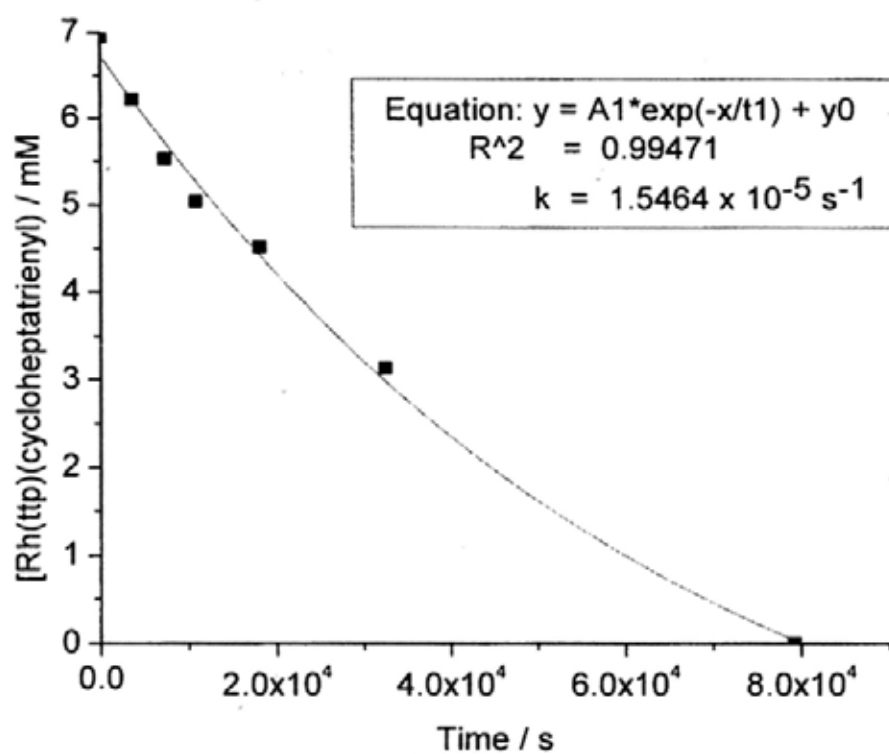


Figure 3.12 Time Profile of Rh(tp)(cycloheptatrienyl) (6.95 mM) at 140 °C

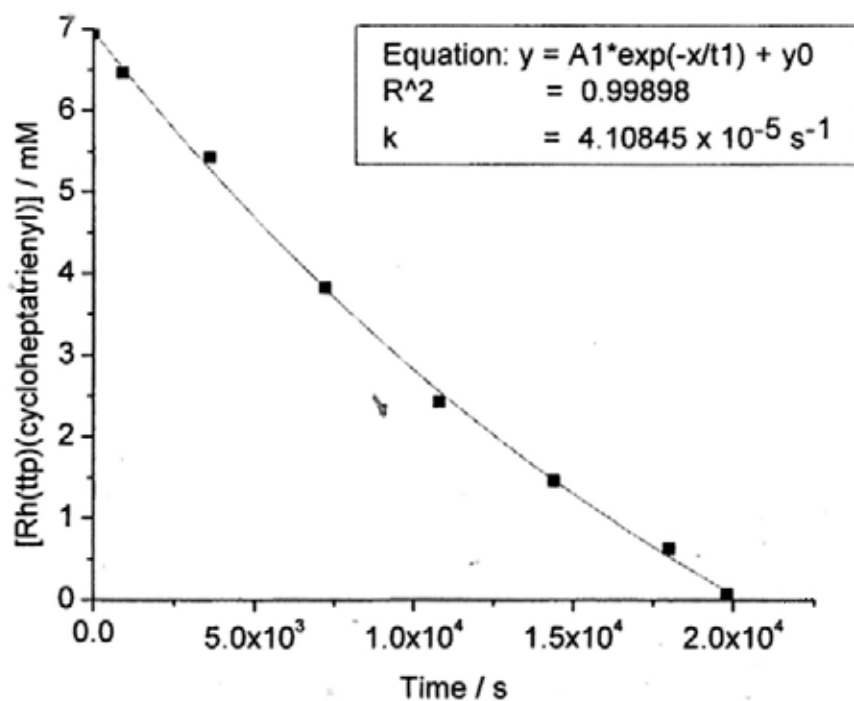


Figure 3.13 Time Profile of Rh(tp)(cycloheptatrienyl) (6.95 mM) at 150 °C

The Eyring equation describes the temperature dependence of reaction rate (eq 3.29).<sup>3a</sup>

$$\ln(k/T) = -\Delta H^\ddagger/(RT) + \ln(\kappa/h) + \Delta S^\ddagger/R \quad (3.29)$$

( $\kappa$  is the Boltzmann constant,  $R$  is the ideal gas constant and  $h$  is the Planck's constant.)

Therefore, a plot of  $\ln(k/T)$  against  $1/T$  gives a linear Eyring plot with a slope of  $-\Delta H^\ddagger/R$  and a y-intercept of  $\ln(\kappa/h) + \Delta S^\ddagger/R$  (Figure 3.13, Table 3.8).<sup>3a</sup>

Table 3.8  $\ln(k_{\text{obs}}/T)$  at different ( $1/T$ )

| Entry | Temp / °C | $1/T$ ( $\times 10^{-3} \text{ K}^{-1}$ ) | $k_{\text{obs}} \times 10^6 / \text{s}^{-1}$ | Error $\times 10^7 / \text{s}^{-1}$ | $\ln(k_{\text{obs}}/T)$ |
|-------|-----------|---|--|-------------------------------------|-------------------------|
| 1     | 120       | 2.545                                     | 4.75439                                      | 3.97540                             | -18.2303                |
| 2     | 130       | 2.481                                     | 8.76127                                      | 8.45695                             | -17.6441                |
| 3     | 140       | 2.421                                     | 15.4640                                      | 34.0559                             | -17.1004                |
| 4     | 150       | 2.364                                     | 41.0845                                      | 57.0695                             | -16.1473                |

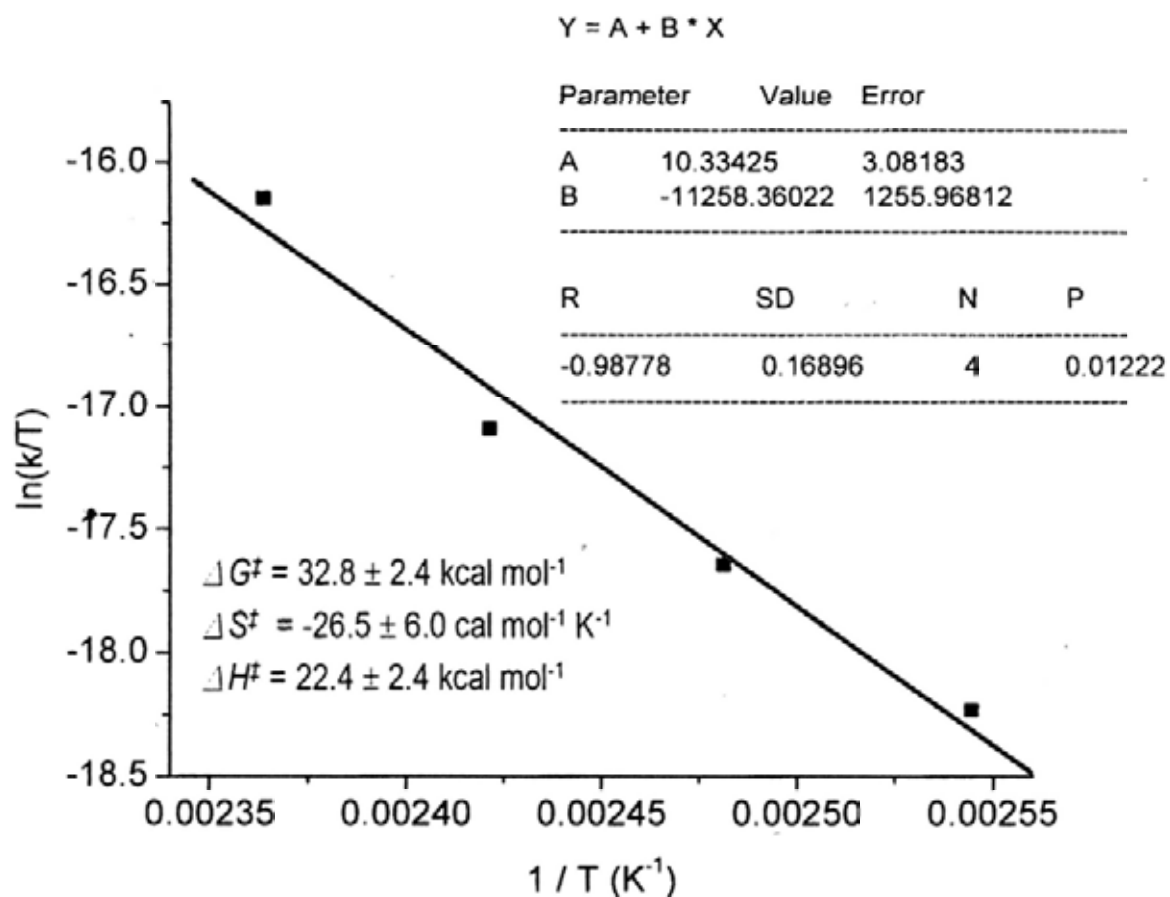


Figure 3.14 Eyring Plot of the Conversion of **8** to **5b** over the Temperature Range 120-150 °C

Since  $y\text{-intercept} = \ln(\kappa/h) + \Delta S^\ddagger/R$

$$10.39025 = \ln(1.3807 \times 10^{-23}/6.6261 \times 10^{-34}) + \Delta S^\ddagger/1.9859$$

$$\Delta S^\ddagger = -26.5 \pm 6.0 \text{ cal mol}^{-1} \text{ K}^{-1}$$

And  $\text{slope} = -\Delta H^\ddagger/R$

$$-11280 = -\Delta H^\ddagger/1.9859$$

$$\Delta H^\ddagger = 22.4 \pm 2.4 \text{ kcal mol}^{-1}$$

Then  $\Delta G^\ddagger = \Delta H^\ddagger - T \Delta S^\ddagger$

$$\Delta G^\ddagger = 32.8 \pm 2.4 \text{ kcal mol}^{-1}$$

The Eyring plot of conversion of **8** to **5b** over the temperature range 120°C – 150 °C (Figure 3.14, Table 3.8) yielded  $\Delta H^\ddagger = 22.4 \pm 2.4 \text{ kcal mol}^{-1}$ ,  $\Delta S^\ddagger = -26.5 \pm 6.0 \text{ cal mol}^{-1} \text{ K}^{-1}$ , and  $\Delta G^\ddagger = 32.8 \pm 2.4 \text{ kcal mol}^{-1}$  (Figure 3.15).

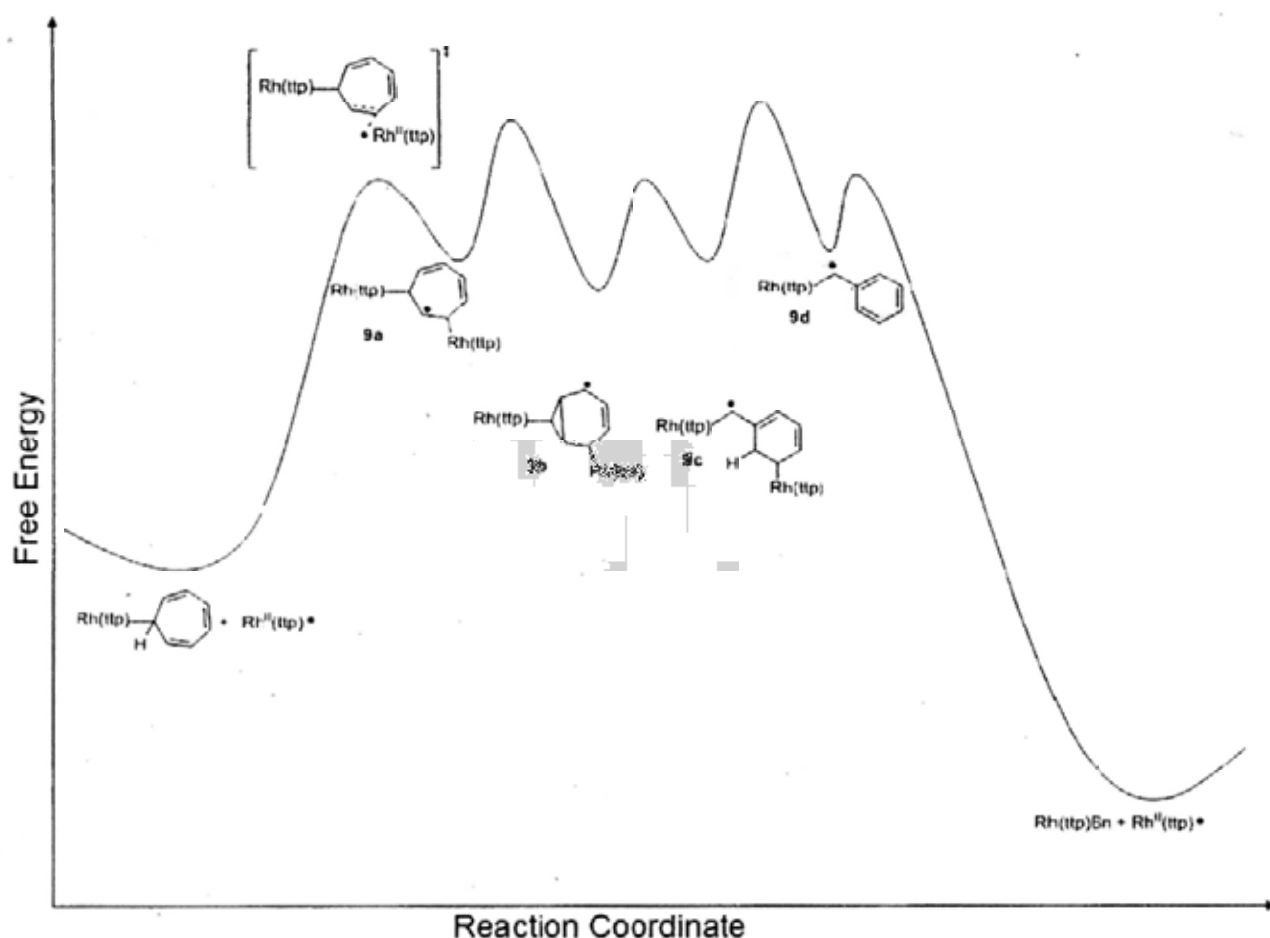
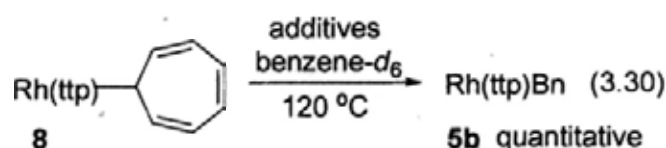


Figure 3.15 Energy Level Diagram of the Conversion of Rh(tp)(cycloheptatrienyl) to Rh(tp)Bn

### 3.6.4 Promoting Effects of Additives

Since  $\text{K}_2\text{CO}_3$  (10 equiv) promoted the reaction of Rh(tp)Cl and *c*-heptane to give Rh(tp)Bn via the promoted generation of  $\text{Rh}_2(\text{tp})_2$  from Rh(tp)H co-product (eq 3.6), the promoting effects of both  $\text{K}_2\text{CO}_3$  and  $\text{Rh}_2(\text{tp})_2$  were examined separately (eq 3.30, Figures 3.16-3.18).



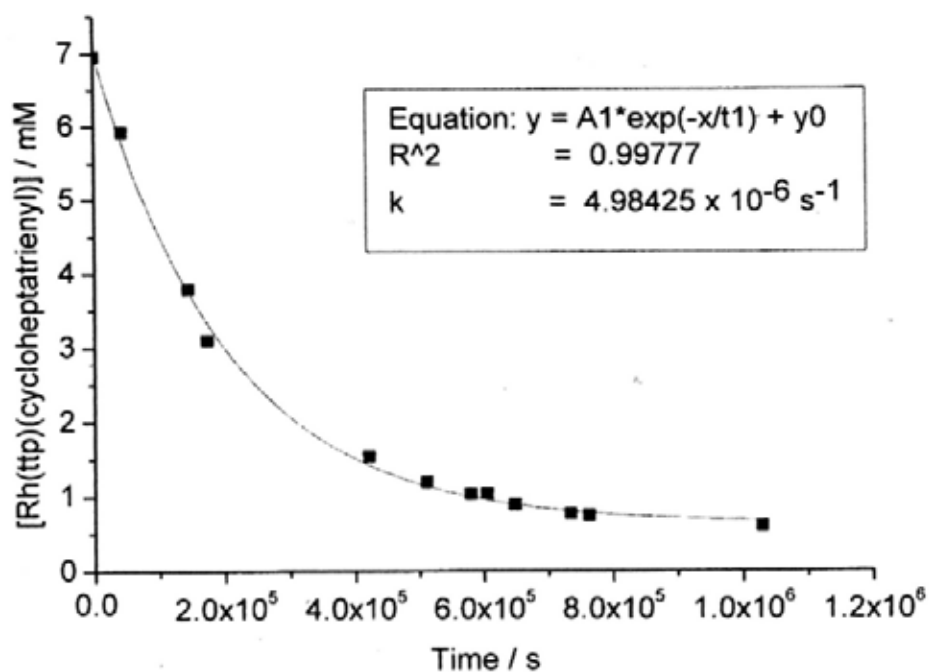


Figure 3.16 Time profile of Rh(tp)(cycloheptatrienyl) (6.95 mM) with  $\text{K}_2\text{CO}_3$  at 120 °C

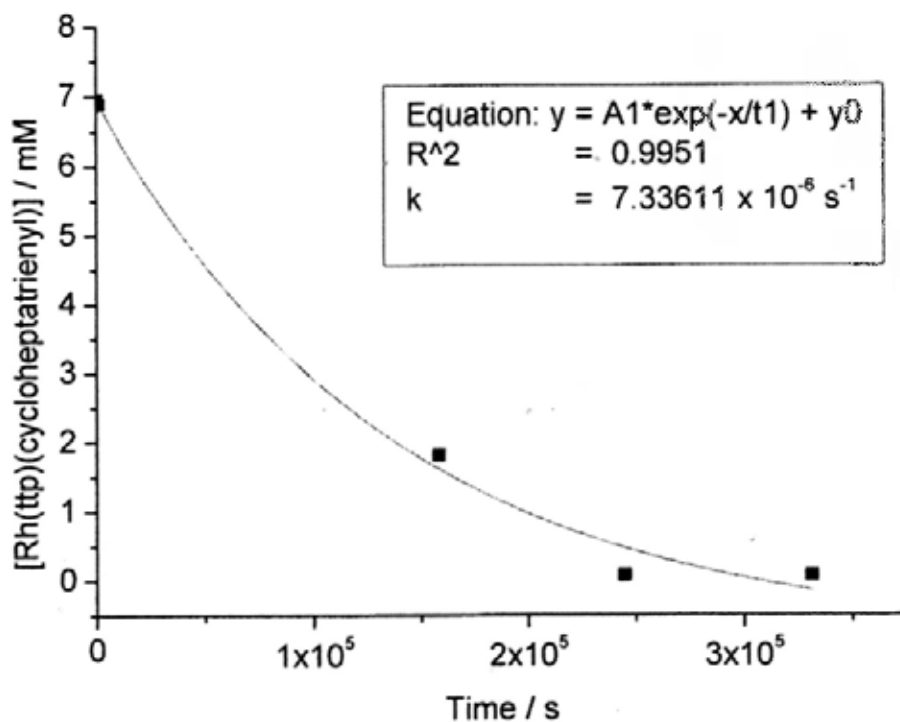


Figure 3.17 Time profile of Rh(tp)(cycloheptatrienyl) (6.95 mM) with  $\text{Rh}_2(\text{tp})_2$  ( $3.48 \times 10^{-5}$  M, 1 mol%)

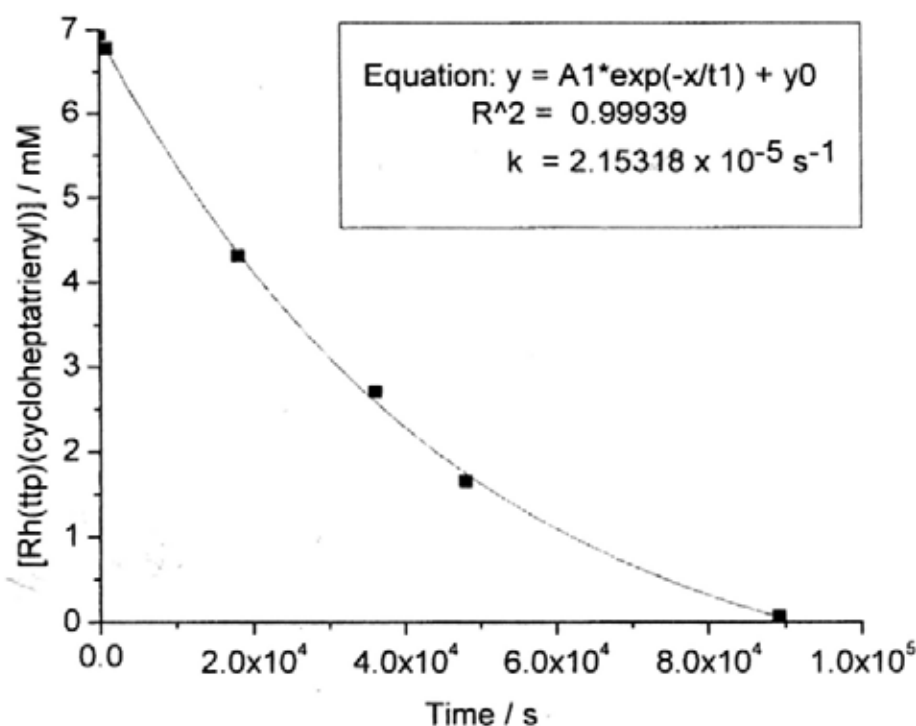


Figure 3.18 Time profile of Rh(tp)(cycloheptatrienyl) (6.95 mM) with Rh<sub>2</sub>(tp)<sub>2</sub> (3.48 x 10<sup>-4</sup> M, 10 mol%)

Table 3.9  $k_{\text{obs}}$  with different additive conditions (120 °C)

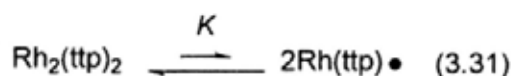
| Entry | [8] <sub>0</sub> x 10 <sup>3</sup> / M | Additive   | $k_{\text{obs}}$ x 10 <sup>6</sup> / s <sup>-1</sup> | Error x 10 <sup>7</sup> / s <sup>-1</sup> |
|-------|--|--|--|---|
| 1     | 6.95                                   | ---  | 4.75439  | 3.97540                                   |
| 2     | 6.95                                   | K <sub>2</sub> CO <sub>3</sub> (10 equiv)                                  | 4.98425  | 2.36672                                   |
| 3     | 6.95                                   | Rh <sub>2</sub> (tp) <sub>2</sub> (3.48 x 10 <sup>-5</sup> M) <sup>a</sup> | 7.33611  | 2.04693                                   |
| 4     | 6.95                                   | Rh <sub>2</sub> (tp) <sub>2</sub> (3.48 x 10 <sup>-4</sup> M) <sup>b</sup> | 21.5318  | 12.6614                                   |

<sup>a</sup> 1 mol%; <sup>b</sup> 10 mol%

With or without the addition of K<sub>2</sub>CO<sub>3</sub>, the reaction rates of the transformation of **8** to **5b** are identical within experimental errors (Table 3.9, entries 1 and 2). Therefore, the conversion of **8** to **5b** is independent of K<sub>2</sub>CO<sub>3</sub>.

On the other hand, a small amount of  $\text{Rh}_2(\text{ttp})_2$  (1 mol%,  $6.49 \times 10^{-5} \text{ M}$ ) significantly enhanced the conversion rate from  $4.75 \times 10^{-6} \text{ s}^{-1}$  to  $7.34 \times 10^{-6} \text{ s}^{-1}$  (Table 3.9, entry 3 vs 1). A further increase in the amount of  $\text{Rh}_2(\text{ttp})_2$  to 10 mol% enhanced the rate by 3 times to  $2.15 \times 10^{-5} \text{ s}^{-1}$  (Table 3.9, entry 4 vs 3).

The equilibrium concentration of  $\text{Rh}^{\text{II}}(\text{ttp})$  catalyst in solution is governed by the equilibrium constant  $K$  (eq 3.31). The equilibrium constant  $K$  is approximated according to eqs 3.32-3.33.<sup>14</sup> The bond dissociation energy of  $(\text{ttp})\text{Rh}-\text{Rh}(\text{ttp})$  bond is reported to be around  $16 \text{ kcal mol}^{-1}$ .<sup>2</sup> As two more molar of  $\text{Rh}^{\text{II}}(\text{ttp})$  radicals are generated from one molar of  $\text{Rh}_2(\text{ttp})_2$ , the estimated  $-T\Delta S_{298\text{K}}$  term is  $-10 \text{ kcal mol}^{-1}$ .<sup>3a,24</sup> Therefore, the equilibrium constant  $K$  at 298 K is  $3.95 \times 10^{-5}$ .



$$-\Delta G = RT \ln K \quad (3.32)$$

$$\Delta G = \Delta H - T\Delta S \quad (3.33)$$

Therefore,  $-(\Delta H - T\Delta S) = RT \ln K$

$$-(16 \text{ kcal mol}^{-1} - 10 \text{ kcal mol}^{-1}) = 1.9859 \times 10^{-3} \text{ kcal mol}^{-1} \text{ K}^{-1} \times 298 \text{ K} \times \ln K$$

$$K = 3.95 \times 10^{-5}$$

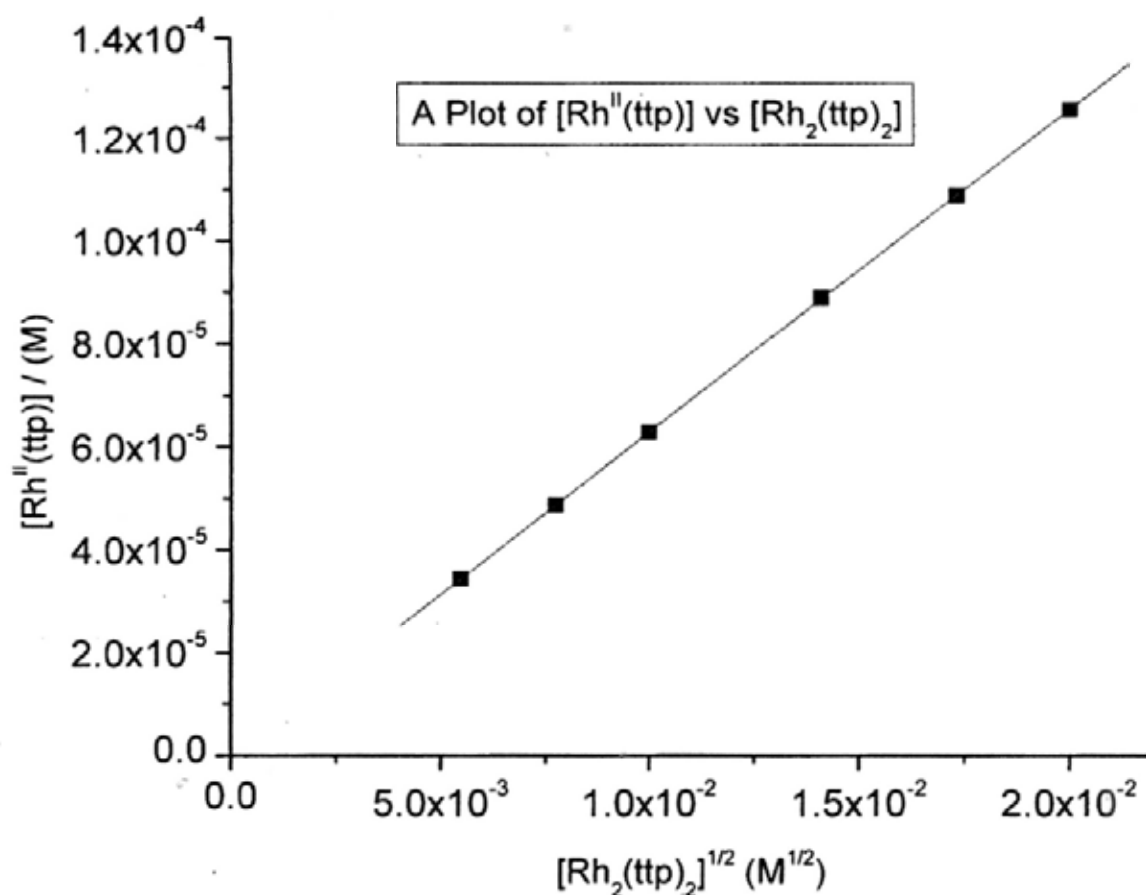


Figure 3.19 A Plot of  $[\text{Rh}^{\text{II}}(\text{ttp})]$  at Various  $[\text{Rh}_2(\text{ttp})_2]^{1/2}$

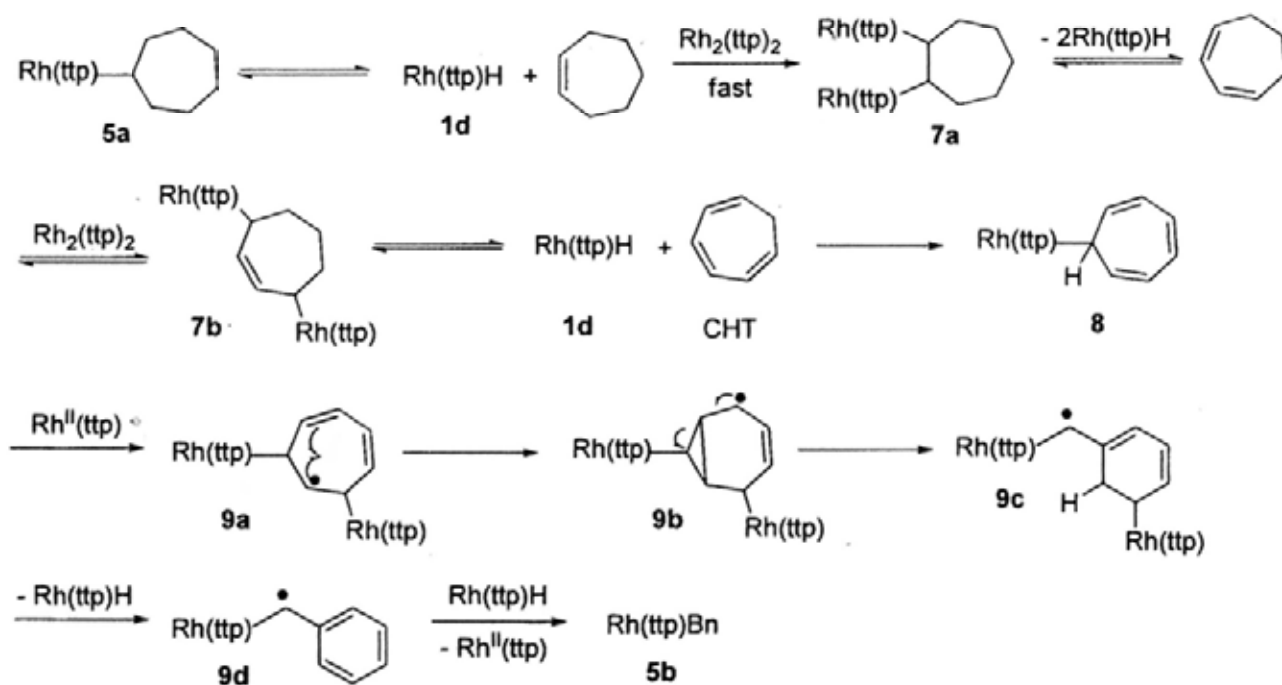
Table 3.10  $[\text{Rh}^{\text{II}}(\text{ttp})]$  at Various  $[\text{Rh}_2(\text{ttp})_2]^{1/2}$  Base on Calculation

| Entry | $[\text{Rh}_2(\text{ttp})_2] / \text{M}$ | $[\text{Rh}_2(\text{ttp})_2]^{1/2} / \text{M}^{1/2}$ | $[\text{Rh}^{\text{II}}(\text{ttp})] / \text{M}$ |
|-------|--|--|--|
| 1     | $3.0000 \times 10^{-5}$                  | $5.4772 \times 10^{-3}$                              | $3.4424 \times 10^{-5}$                          |
| 2     | $6.0000 \times 10^{-5}$                  | $7.7460 \times 10^{-3}$                              | $4.8683 \times 10^{-5}$                          |
| 3     | $1.0000 \times 10^{-4}$                  | $1.0000 \times 10^{-2}$                              | $6.2849 \times 10^{-5}$                          |
| 4     | $2.0000 \times 10^{-4}$                  | $1.4142 \times 10^{-2}$                              | $8.8882 \times 10^{-5}$                          |
| 5     | $3.0000 \times 10^{-4}$                  | $1.7321 \times 10^{-2}$                              | $1.0886 \times 10^{-4}$                          |
| 6     | $4.0000 \times 10^{-4}$                  | $2.0000 \times 10^{-2}$                              | $1.2570 \times 10^{-4}$                          |

At 298 K, the  $[\text{Rh}^{\text{II}}(\text{ttp})]$  at  $\text{Rh}_2(\text{ttp})_2$  added in 1 mol% ( $3.48 \times 10^{-5} \text{ M}$ ) and 10 mol% ( $3.48 \times 10^{-4} \text{ M}$ ) are estimated to be  $4.16 \times 10^{-5} \text{ M}$  and  $1.17 \times 10^{-4} \text{ M}$ , respectively. Therefore, even 10-fold change of  $[\text{Rh}_2(\text{ttp})_2]$  results in a 3.3-fold change of  $[\text{Rh}^{\text{II}}(\text{ttp})]$  (Table 3.10 entry 4 vs 3, Figure 3.19). The  $k_{\text{obs}}$  increased from  $7.34 \times 10^{-6} \text{ s}^{-1}$  with  $3.48 \times 10^{-5} \text{ M}$  of  $\text{Rh}_2(\text{ttp})_2$  added (entry 3) to  $2.15 \times 10^{-5} \text{ s}^{-1}$  with  $3.48 \times 10^{-4} \text{ M}$  of  $\text{Rh}_2(\text{ttp})_2$  added (entry 4). The rate equation of  $\text{Rh}^{\text{II}}(\text{ttp})$ -catalyzed conversion of **8** to **5b** is therefore 1<sup>st</sup> order in  $[\text{Rh}^{\text{II}}(\text{ttp})]$ . So,  $\text{rate} = k [\mathbf{8}][\text{Rh}^{\text{II}}(\text{ttp})]$ .

### 3.7 Overall Proposed Mechanism

Scheme 3.8 summarizes the overall proposed mechanism for the transformation of  $\text{Rh}(\text{ttp})(c\text{-heptyl})$  **5a** to  $\text{Rh}(\text{ttp})\text{Bn}$  **5b**.



Scheme 3.8 Overall Proposed Mechanism for the Conversion of **5a** to **5b**

### 3.8 Conclusion

The mild, selective conversion of *c*-heptane to rhodium porphyrin benzyl via CHA and CCA has been reported. Rh(tp)(*c*-heptyl) which formed from the base-promoted CHA of Rh(tp)Cl and *c*-heptane is the intermediate leading to the CCA product Rh(tp)Bn. Rh<sub>2</sub>(tp)<sub>2</sub> is generated from base-promoted dehydrogenative dimerization of Rh(tp)H and facilitates the functionalization as follow: i) undergoing a facile CHA process; ii) trapping the alkene intermediate formed for further dehydrogenation and iii) catalyzing the rearrangement of Rh(tp)(cycloheptatrienyl) **8** to Rh(tp)Bn **5b**.

## References

- (1) (a) Mackay, D.; Shiu, W. Y.; Ma, K. C.; Lee, S. C. *Physical-Chemical Properties and Environmental Fate for Organic Chemicals 2<sup>nd</sup> Ed, Volume. 1*, CRC Press, Boca raton, FL, 2006. (b) Bocian, D. F.; Pickett, H. M.; Rounds, T. C.; Strauss, H. L. *J. Am. Chem. Soc.* **1975**, *97*, 687-695.
- (2) Luo, Y. R. *Comprehensive Handbook of Chemical Bond Energies*, CRC Press, Boca Raton, FL, 2007.
- (3) (a) Isaacs, N. S. *Physical Organic Chemistry*; Longman: Essex, 1987. (b) The BDE of C–C bonds are calculated based on the  $\Delta H_{\text{formation}}$ , see Stull, D. R.; Westrum, E. F. Jr.; Sinke, G. C. *The Chemical Thermodynamics of Organic Compounds*; John Wiley & Sons: New York 1969.
- (4) *CRC Handbook of Chemistry & Physics 84<sup>th</sup> Ed.*, Lide, D. R. Ed. 2004.
- (5) Liang, C. G.; Collet, F.; Robert-Peillard, F.; Muller, P.; Dodd, R. H.; Dauban, P. *J. Am. Chem. Soc.* **2008**, *130*, 343-350.
- (6) Deng, G. J.; Li, C. J. *Org. Lett.* **2009**, *11*, 1171-1174.
- (7) Maguire, J. A.; Goldman, A. S. *J. Am. Chem. Soc.* **1991**, *113*, 6706-6708.
- (8) Tada, M.; Akatsuka, Y.; Yang, Y.; Sasaki, T.; Kinoshita, M.; Motokura, K.; Iwasawa, Y. *Angew. Chem. Int. Ed.* **2008**, *47*, 9252-9255.
- (9) (a) Jun, C.-H. *Chem. Soc. Rev.* **2004**, *33*, 610-618. (b) Murakami, M; Amii, H.; Ito, Y. *Nature* **1994**, *370*, 540-541.
- (10) Rataboul, F.; Chabanas, M.; de Mallmann, A.; Coperet, C.; Thivolle-Cazat, J.; Basset, J. M.; *Chem. Eur. J.* **2003**, *9*, 1426-1434.
- (11) Basset, J. M.; Coperet, C.; Lefort, L.; Maunders, B. M.; Maury, O.; Le Roux, E.; Saggio, G.; Soignier, S.; Soulivong, D.; Sunley, G. J.; Taoufik, M.; Thivolle-Cazat, J. *J. Am. Chem. Soc.* **2005**, *127*, 8604-8605.

- (12) Ruzicka, L. Seidel, C. F. *Helv. Chim. Acta* **1936**, *19*, 424-433.
- (13) (a) Reger, D. L.; Culbertson, E. C. *Inorg. Chem.* **1977**, *16*, 3104-3107. (b) Reger, D. L.; Culbertson, E. C. *J. Am. Chem. Soc.* **1976**, *98*, 2789-2794.
- (14) (a) Mak, K. W.; Chan, K. S. *J. Am. Chem. Soc.* **1998**, *120*, 9686-9687. (b) Mak, K. W.; Xue, F.; Mak, T. C. W.; Ghan, K. S. *J. Chem. Soc., Dalton Trans.* **1999**, *19*, 3333-3334.
- (15) Wayland, B. B.; van Voorhees, S. L.; Wilker, C. *Inorg. Chem.* **1986**, *25*, 4039-4042.
- (16) Chan, Y. W.; Chan, K. S. *Organometallics* **2008**, *27*, 4625-4635.
- (17) (a) Rataboul, F.; Chabanas, M.; de Mallmann, A.; Coperet, C.; Thivolle-Cazat, J.; Basset, J. M. *Chem. Eur. J.* **2003**, *9*, 1426-1434. (b) Belatel, H. Al-Kandari, H.; Al-Kharafi, F.; Garin, F.; Katrib, A. *Appl. Catal. A* **2007**, *318*, 227-233.
- (18) Chan, K. S.; Mak, K. W.; Tse, M. K.; Yeung, S. K.; Li, B. Z.; Chan, Y. W. *J. Organomet. Chem.* **2008**, *693*, 399-407.
- (19) Paonessa, R.S.; Thomas, N C.; Halpern, J. *J. Am. Chem. Soc.* **1985**, *107*, 4333-4335.
- (20) Rh(tpp)(c-heptyl) **1** is a formal monohydrogenated product from **5**. **5** likely gives Rh(tpp)(c-heptyl) radical via homolysis which then abstracts a hydrogen atom from Rh(tpp)H to give **1**.
- (21) Rh<sub>2</sub>(tpp)<sub>2</sub> reacted faster with CHT and Rh(tpp)H was formed as the intermediate co-product.
- (22) Carey, F. A.; Sundberg, R. J. *Advanced Organic Chemistry, Part A: Structure and Mechanisms*, Plenum Press, New York, 1977, 504-510.
- (23) (a) Woods, W. G. *J. Org. Chem.* **1958**, *23*, 110-112. (b) Gaynor, B. J.; Gilbert, R. G. *Int. J. Chem. Kinet.* **1976**, *8*, 695-707.
- (24) Wayland, B. B.; Ba, S; Sherry, A. E. *J. Am. Chem. Soc.* **1991**, *113*, 5305-5311.

## Chapter 4 Metalloradical-Catalyzed Aliphatic Carbon–Carbon Bond

### Activation of Cyclooctane

#### 4.1 Introduction

##### 4.1.1 Properties of Cyclooctane

*c*-Octane is a colourless combustible liquid at ambient conditions. It is readily miscible with ethanol and ether but insoluble in water.<sup>1a</sup> *c*-Octane is the conformationally most complex cycloalkane as it has so many forms of comparable energy. Computational studies suggest that the boat-chair conformation is the most stable one while the crown form is slightly less stable (fluxional energy = 7–8 kcal mol<sup>-1</sup>) (Figure 4.1).<sup>1b</sup> Some other properties concerning the reactivity of *c*-octane are summarized in Table 4.1.



Figure 4.1 Crown Form and Boat-Chair Form of *c*-Octane (Hydrogen Hidden)

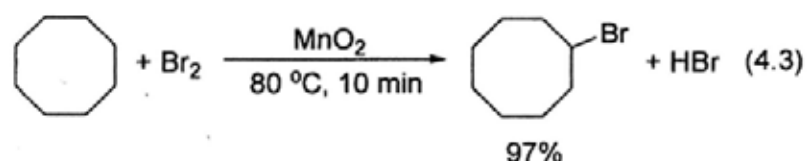
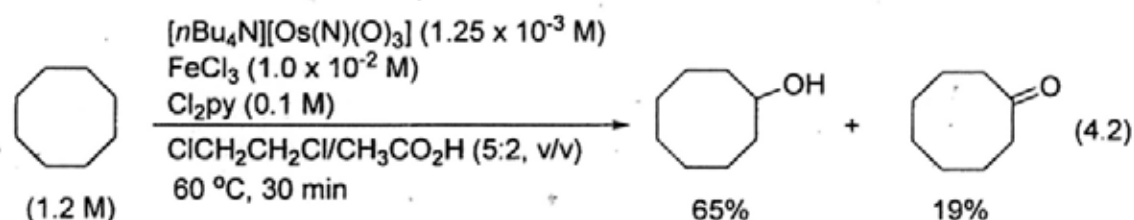
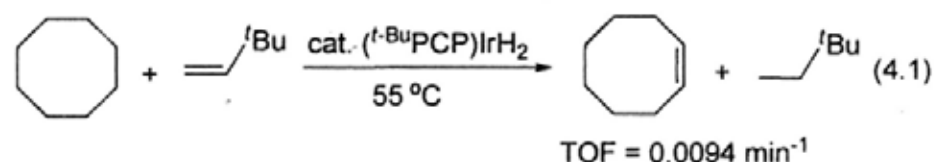
Table 4.1 Properties Concerning the Reactivity of *c*-Octane<sup>2-4</sup>

| Properties                 | Corresponding Value  |
|----------------------------|--|
| BDE of C–H                 | 95.7 kcal mol <sup>-1</sup>                                |
| BDE of C–C                 | 79.6 kcal mol <sup>-1</sup>                                |
| Ring Strain                | 9.6 kcal mol <sup>-1</sup>                                 |
| Diamagnetic Susceptibility | -85.3 × 10 <sup>-6</sup> cm <sup>3</sup> mol <sup>-1</sup> |
| Dielectric Constant        | 2.116 at 20.0 °C   |

### 4.1.2 CHA of *c*-Octane

Alkane functionalization in a homogenous medium is an important and challenging process which involves either carbon–hydrogen bond activation (CHA)<sup>5</sup> or carbon–carbon bond activation (CCA)<sup>6</sup> with organic, inorganic and organometallics reagents. Although aliphatic C–C bonds are weaker than aliphatic C–H bonds, CCA of alkanes is much less reported due to the steric hindrance of the C–C bond by the attack of a transition metal complex.<sup>7</sup>

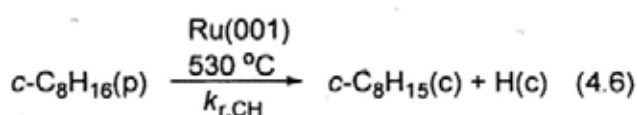
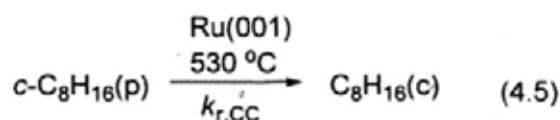
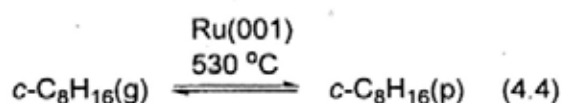
*c*-Octane is a relatively unstrained cycloalkane and therefore serves as a commonly investigated substrate in alkane functionalization, mostly involving CHA. Some examples of CHA of *c*-octane are the iridium(I) pincer dihydride-catalyzed dehydrogenation to *c*-octene (eq 4.1),<sup>8a</sup> the FeCl<sub>3</sub>-catalyzed aerobic oxidation to *c*-octanol and *c*-octanone (eq 4.2),<sup>8b</sup> as well as the MnO<sub>2</sub>-catalyzed bromination to *c*-octyl bromide (eq 4.3).<sup>8c</sup>



### 4.1.3 CCA of *c*-Octane

Examples of CCA of *c*-octane are rarely reported. A CCA of *c*-octane in a heterogenous medium requires a very high reaction temperature of 530 °C and consequently results in both CHA and CCA (eqs 4.4-4.6).<sup>7a</sup> An oxidative CCA of *c*-octane catalyzed by *N*-

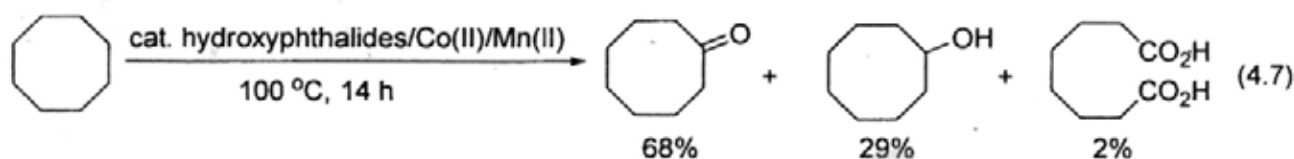
hydroxyphthalides/Co(II)/Mn(II) at 100 °C in 14 h gives  $\omega$ -dicarboxylic acids in 2% yield only (eq 4.7).<sup>7b</sup>



(g) : gaseous state;

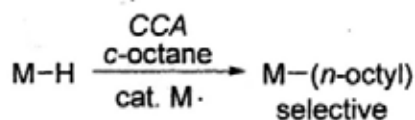
(p) : physically adsorbed state;

(c) : chemisorbed product



## 4.2 Objectives of the Work

The objectives of this work are to (i) broaden the synthetic scope; (ii) to gain further mechanistic understanding of the aliphatic CCA of *c*-octane with rhodium porphyrin complexes and (iii) identifying the unique role of Rh(II) porphyrin (Scheme 4.1).



Scheme 4.1. CCA Pathway of *c*-Octane with MH

## 4.3 Discovery of CCA of *c*-Octane

Initially, *c*-octane was found to react poorly with Rh(ttp)Cl **1a** to give Rh(ttp)(*c*-octyl) **10a** and Rh(ttp)(*n*-octyl) **10b** in 5% and 8% yields, respectively (eq 4.8, Table 4.2, entry 1). A 72% yield of Rh(ttp)Cl **1a** was recovered, and a trace amount of Rh(ttp)H **1d** was observed.

Both CHA and CCA products formed but the reaction was inefficient. The addition of KOH (10 equiv) to the reaction mixture, Rh(tp)(*c*-octyl), Rh(tp)(*n*-octyl) and Rh(tp)H were obtained in 6%, 25% and 62% yields, respectively in 7.5 h (Table 4.2, entry 2). When K<sub>2</sub>CO<sub>3</sub> (10 equiv) was added,<sup>9</sup> Rh(tp)Cl was consumed in 7.5 h and Rh(tp)(*n*-octyl) **10b** and Rh(tp)H **1d** were obtained in 33% and 58% yields, respectively (Table 4.2, entry 3). The CCA product **10b** is the formal 1,2-addition product of Rh(tp)H **1d** into *c*-octane. The substrate *c*-octane was found to be free of *n*-octane and 1-octene by GC-MS analysis (Appendix). Therefore, Rh(tp)(*n*-octyl) was indeed the CCA product of *c*-octane. The structures of **10a** and **10b** were confirmed by independent syntheses (eq 4.9).<sup>10</sup> **10b** was further characterized by X-ray crystallography (Figure 4.2).

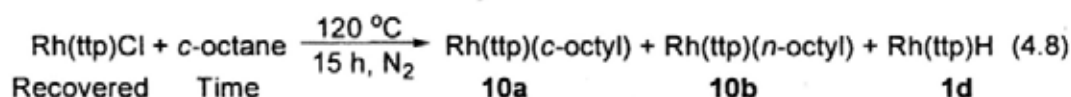
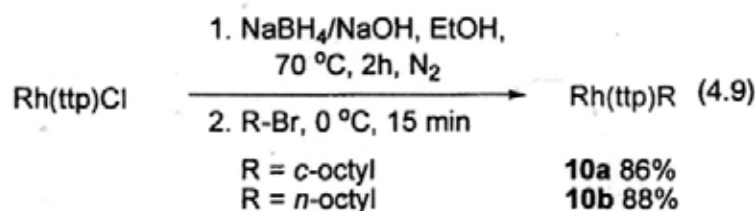


Table 4.2 Reaction of *c*-Octane with Rh(tp)Cl in the Absence and Presence of Base

| Entry | Additive <sup>a</sup>          | Time  | Yield (%)          |                          |                          |         | Total |
|-------|--------------------------------|-------|--------------------|--------------------------|--------------------------|---------|-------|
|       |                                |       | Rh(tp)Cl recovered | Rh(tp)( <i>c</i> -octyl) | Rh(tp)( <i>n</i> -octyl) | Rh(tp)H |       |
| 1     | -----                          | 2 d   | 72                 | 5                        | 8                        | 0       | 85    |
| 2     | KOH                            | 7.5 h | 0                  | 6                        | 25                       | 62      | 93    |
| 3     | K <sub>2</sub> CO <sub>3</sub> | 7.5 h | 0                  | 0                        | 33                       | 58      | 91    |

<sup>a</sup> 10 equiv



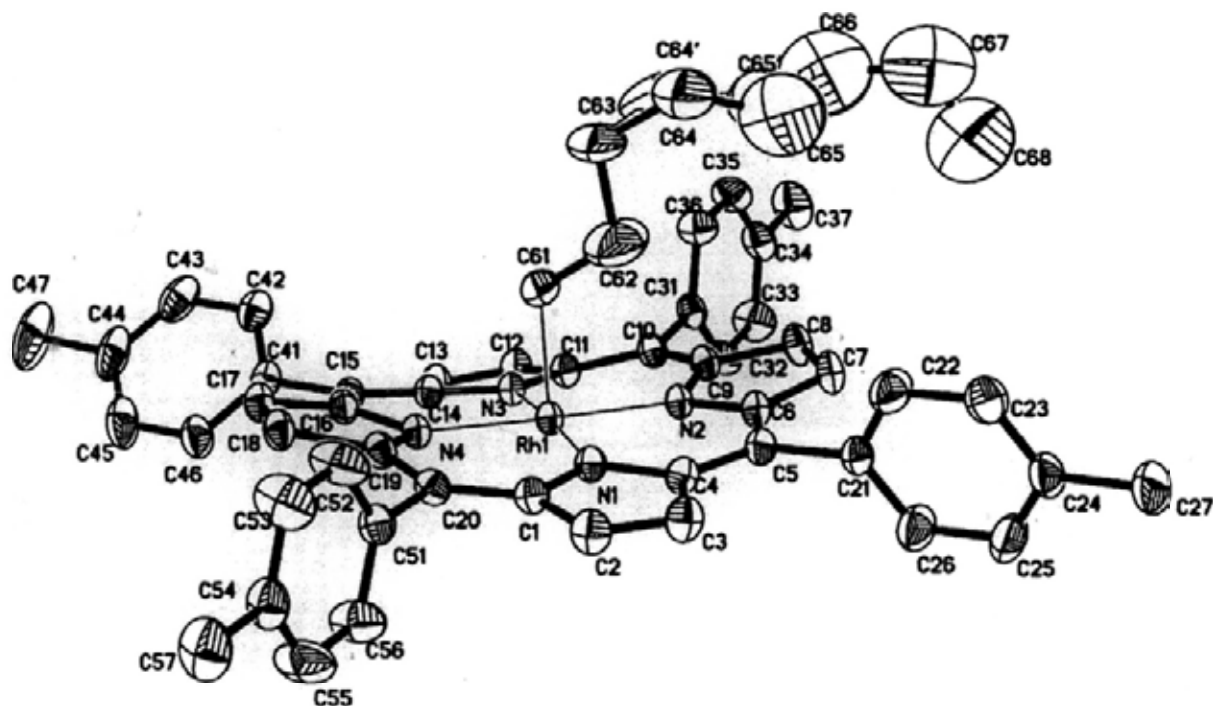
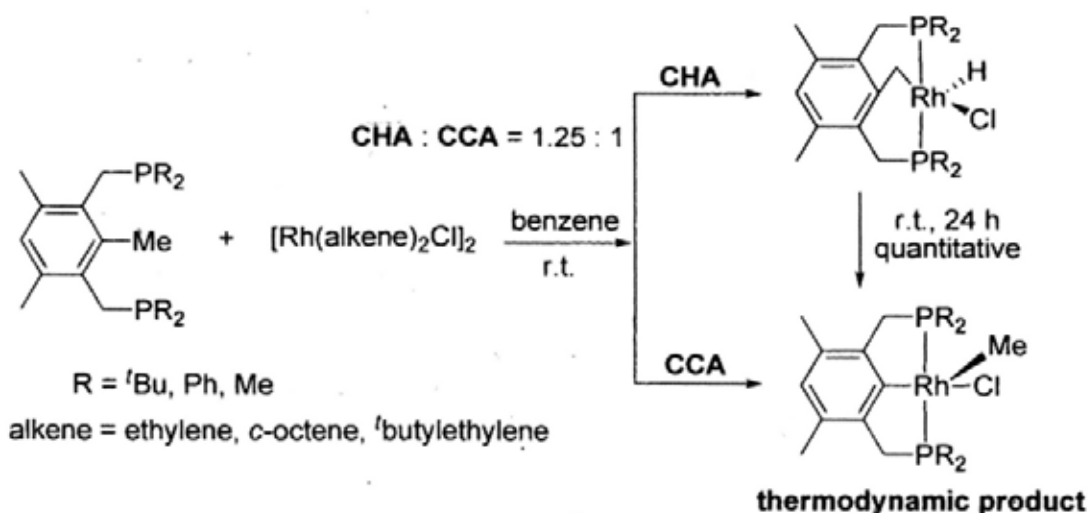


Figure 4.2 ORTEP Presentation of Rh(tp)(*n*-octyl) **10b** (30% Probability Displacement Ellipsoids). Rh-C = 2.03 Å, R = 0.0522

#### 4.4 Mechanistic Investigation

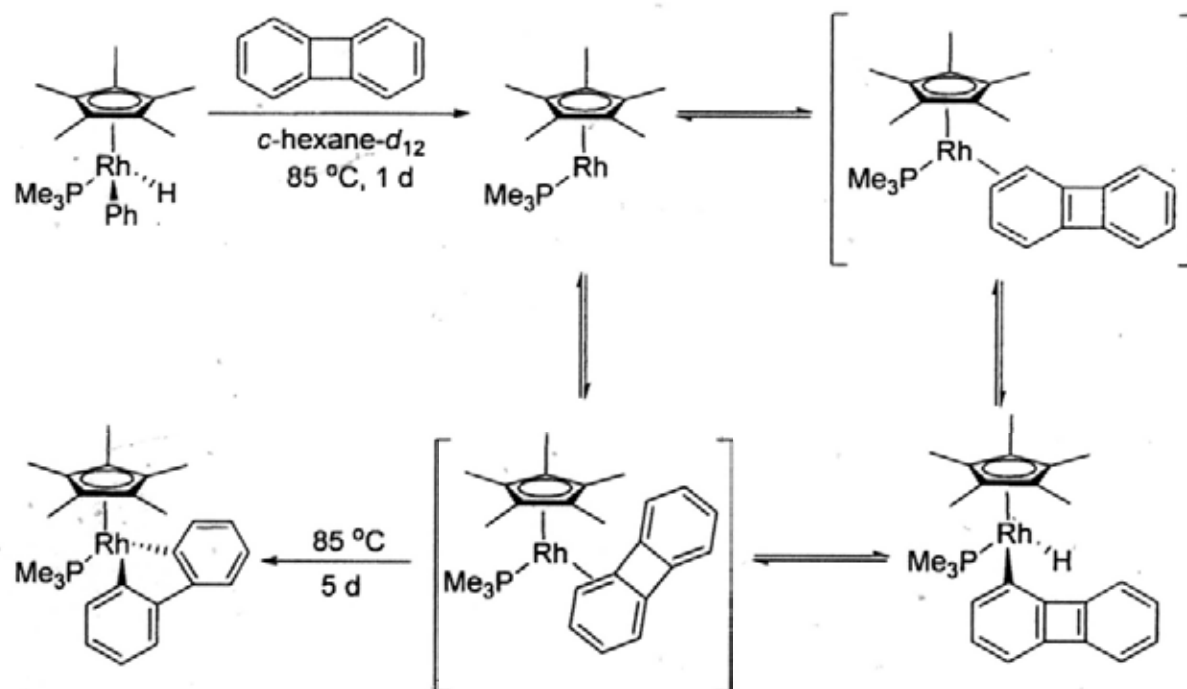
##### 4.4.1 Conversion of CHA Product Rh(tp)(*c*-octyl) to CCA Product Rh(tp)(*n*-octyl)

In some CCA of hydrocarbons, transition metal complexes reacted with hydrocarbons to give CHA and CCA products in parallel and consecutive pathways.<sup>11</sup> Milstein et al. discovered that diphosphine 1,3-bis[(di-*tert*-butylphosphino)methyl]-2,4,6-trimethylbenzene reacted with [Rh(alkene)Cl]<sub>2</sub> with parallel CHA and CCA pathways (Scheme 4.2).<sup>11a</sup> The CHA product was eventually converted to the thermodynamically favorable CCA product in prolonged reaction.



Scheme 4.2 Proposed Mechanism of Parallel CHA and CCA in PCP System

Jones and co-workers discovered that  $\text{Cp}^*\text{Rh}(\text{PMe}_3)(\text{Ph})(\text{H})$  activated the aromatic C–H bond of biphenylene to give Rh–aryl complex.<sup>11b</sup> The Rh–aryl complex was found to be an intermediate to the final CCA product (Scheme 4.3).



Scheme 4.3 Proposed Mechanism of the CCA of Biphenylene with  $\text{Cp}^*\text{Rh}(\text{PMe}_3)(\text{Ph})(\text{H})$  via CHA Intermediate

To investigate whether the CHA product is an intermediate for CCA,<sup>11</sup> Rh(tp)(*c*-octyl) **10a** was heated in benzene-*d*<sub>6</sub> in both neutral and basic conditions separately. Without K<sub>2</sub>CO<sub>3</sub>, Rh(tp)(*c*-octyl) **10a** gave Rh(tp)(*n*-octyl) **10b**, Rh(tp)H **1d** and *c*-octene in 10%, 76%, and 36% yields, respectively after 21 h (eq 4.10, Figure 4.3, Table 4.3).

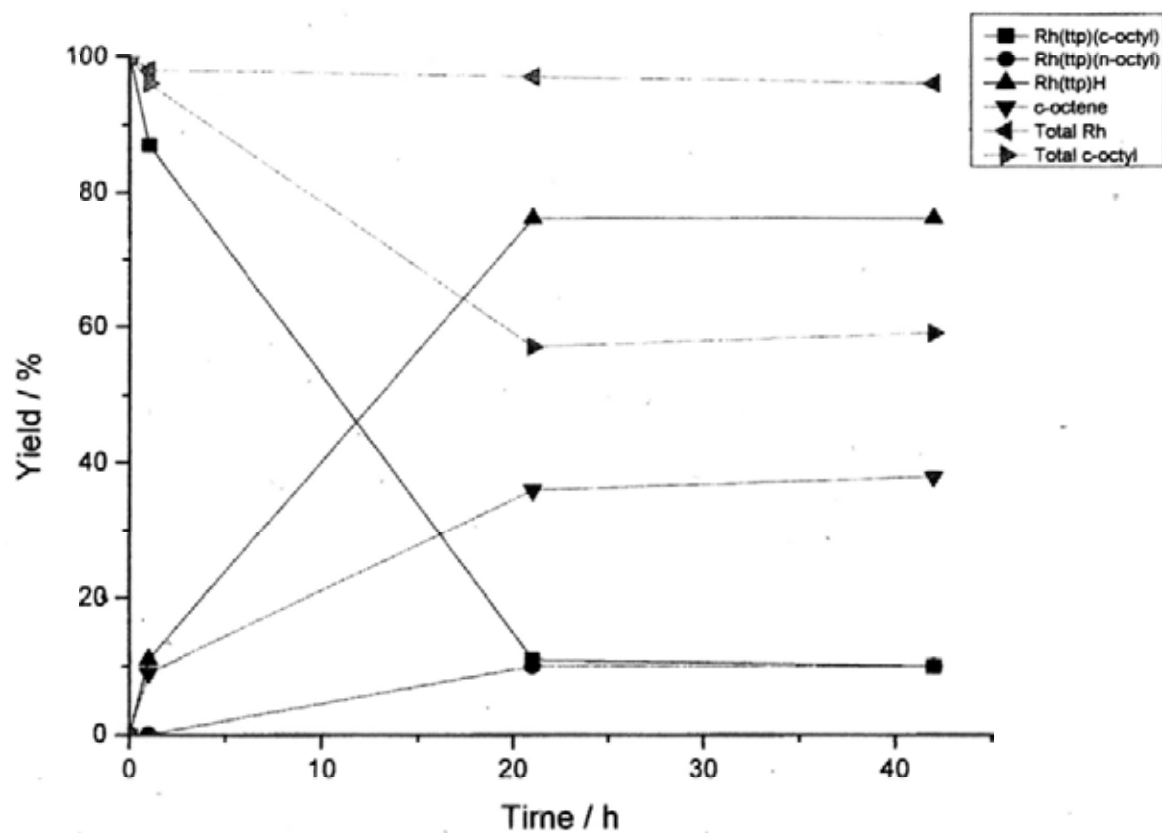
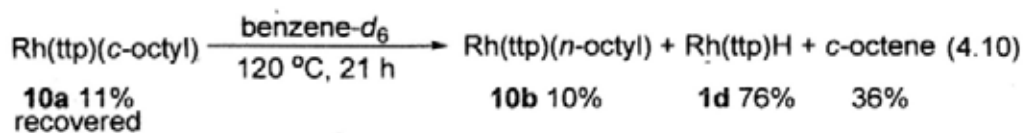
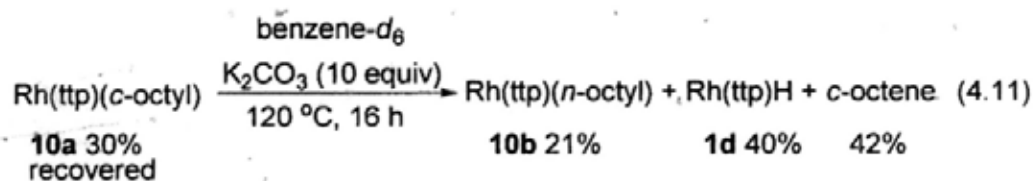


Figure 4.3 Time Profile of Thermal Reaction of Rh(tp)(*c*-octyl) **10a**

Table 4.3 Time Profile of Thermal Reaction of Rh(tp)(*c*-octyl) **10a**

| Time/h | Yield %                      |                              |         |                  |  | Total Rh<br>pdt | Total Org<br>pdt |
|--------|------------------------------|------------------------------|---------|------------------|--|-----------------|------------------|
|        | Rh(tp)( <i>c</i> -<br>octyl) | Rh(tp)( <i>n</i> -<br>octyl) | Rh(tp)H | <i>c</i> -octene |  |                 |                  |
| 0      | 100                          | 0                            | 0       | 0                |  | 100             | 0                |
| 1      | 87                           | 0                            | 11      | 9                |  | 98              | 96               |
| 21     | 11                           | 10                           | 76      | 36               |  | 97              | 57               |
| 42     | 10                           | 10                           | 76      | 38               |  | 96              | 59               |

In the presence of K<sub>2</sub>CO<sub>3</sub> (10 equiv), Rh(tp)(*n*-octyl) **10b** was isolated in a higher yield of 21% in 16 h (eq 4.11, Figure 4.4, Table 4.4). However, both reactions were low yielding and incomplete. Therefore, the CHA product is not a major intermediate leading to the CCA product.



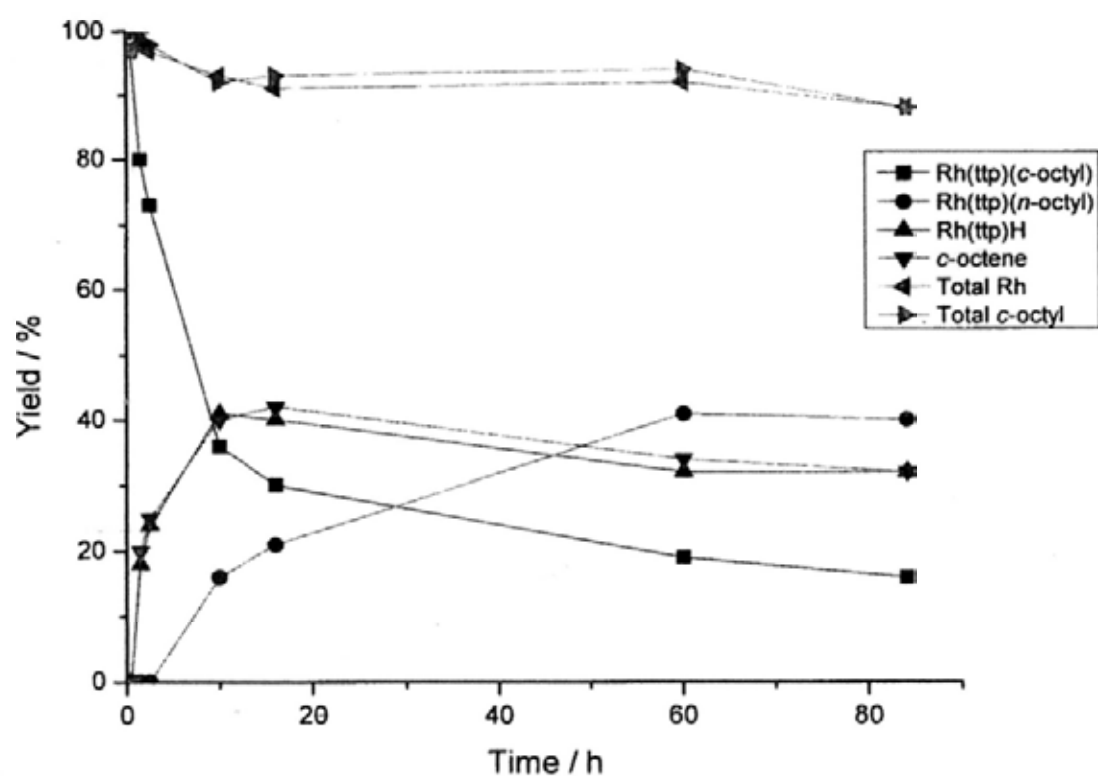


Figure 4.4 Time Profile of Basic Reaction of Rh(tp)(c-octyl) 10a

Table 4.4 Time Profile of Basic Reaction of Rh(tp)(c-octyl) 10a

| Time/h | Yield %             |                     |         |          |  | Total Rh<br>pdt | Total Org<br>pdt |
|--------|---------------------|---------------------|---------|----------|--|-----------------|------------------|
|        | Rh(tp)(c-<br>octyl) | Rh(tp)(n-<br>octyl) | Rh(tp)H | c-octene |  |                 |                  |
| 0      | 100                 | 0                   | 0       | 0        |  | 100             | 100              |
| 0.5    | 97                  | 00                  | 0       | 0        |  | 97              | 97               |
| 1.5    | 80                  | 100                 | 18      | 20       |  | 98              | 100              |
| 2.5    | 73                  | 100                 | 24      | 25       |  | 97              | 98               |
| 10     | 36                  | 16                  | 41      | 40       |  | 93              | 92               |
| 16     | 30                  | 21                  | 40      | 42       |  | 91              | 93               |
| 60     | 19                  | 41                  | 32      | 34       |  | 92              | 94               |
| 84     | 16                  | 40                  | 32      | 32       |  | 88              | 88               |

#### 4.4.2 Reaction Time Profile

To enhance the CCA reaction of Rh(tp)Cl **1a** with *c*-octane based on mechanistic understandings, the reaction was monitored by  $^1\text{H}$  NMR spectroscopy in a sealed NMR tube (eq 4.12, Figure 4.5, Table 4.5).

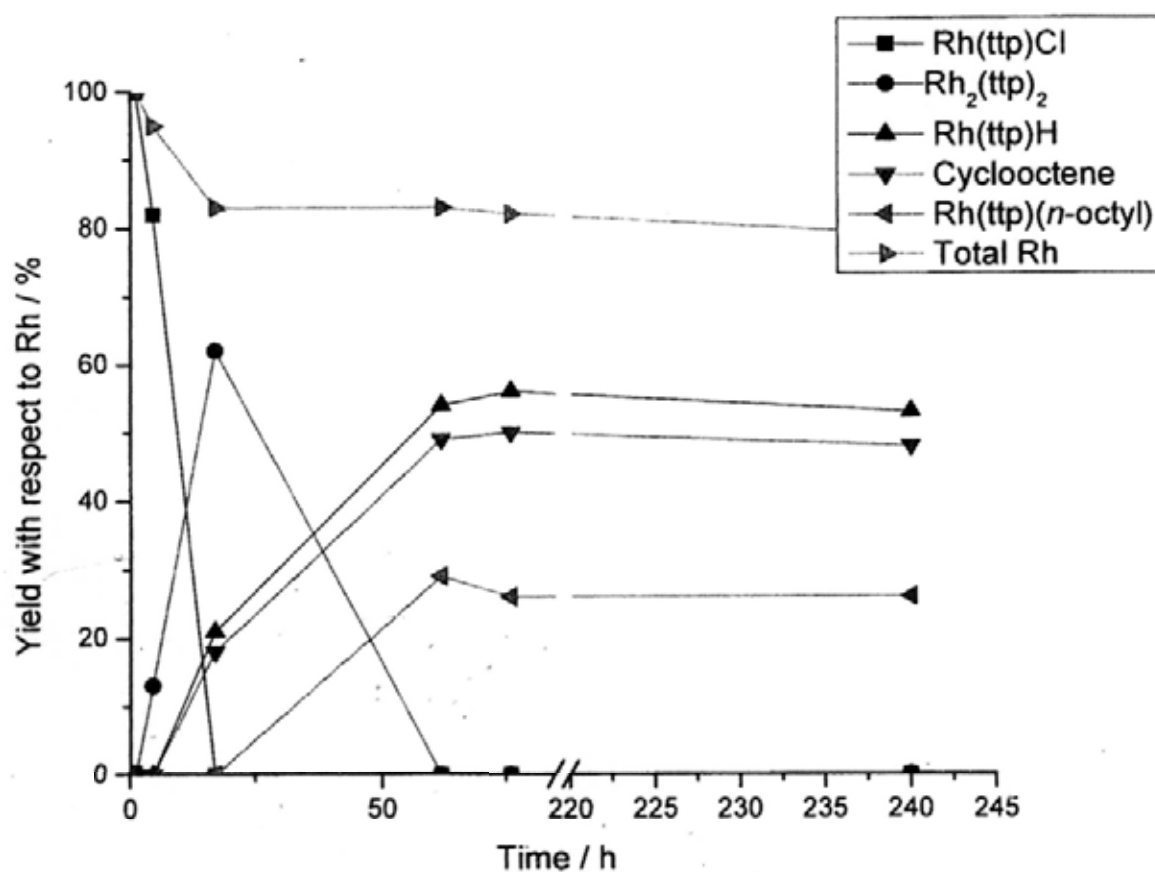
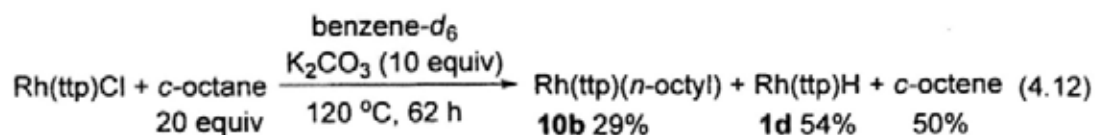


Figure 4.5 Time Profile of Reaction of Rh(tp)Cl with *c*-Octane in the Presence of Potassium Carbonate

Table 4.5 Time Profile of Reaction of Rh(tp)Cl with *c*-Octane in the Presence of Potassium Carbonate

| Time/h | Yield %  |                          |         |                  |                                   |     | Total Rh | Total Org |
|--------|----------|--------------------------|---------|------------------|-----------------------------------|-----|----------|-----------|
|        | Rh(tp)Cl | Rh(tp)( <i>n</i> -octyl) | Rh(tp)H | <i>c</i> -octene | Rh <sub>2</sub> (tp) <sub>2</sub> |     |          |           |
| 0      | 100      | 0                        | 0       | 0                | 0                                 | 100 | 0        |           |
| 0.5    | 100      | 0                        | 0       | 0                | 0                                 | 100 | 0        |           |
| 1      | 100      | 0                        | 0       | 0                | 0                                 | 100 | 0        |           |
| 4.5    | 82       | 0                        | 0       | 0                | 13                                | 95  | 0        |           |
| 17     | 0        | 0                        | 21      | 18               | 62                                | 83  | 18       |           |
| 62     | 0        | 29                       | 54      | 50               | 0                                 | 83  | 79       |           |
| 76     | 0        | 26                       | 56      | 52               | 0                                 | 82  | 78       |           |
| 240    | 0        | 26                       | 53      | 48               | 0                                 | 79  | 74       |           |

Initially, Rh(tp)Cl was first converted to Rh<sub>2</sub>(tp)<sub>2</sub> **1e** in the presence of K<sub>2</sub>CO<sub>3</sub>.<sup>12</sup> At 4.5 h, 82% yield of Rh(tp)Cl remained while Rh<sub>2</sub>(tp)<sub>2</sub> **1e** was formed in 13% yield. After 17 h, Rh(tp)Cl completely reacted. Rh<sub>2</sub>(tp)<sub>2</sub> **1e**, Rh(tp)H **1d** and *c*-octene were formed in 62%, 21% and 18% yields, respectively. After 62 h, Rh<sub>2</sub>(tp)<sub>2</sub> **1e** completely reacted. The yields of Rh(tp)H **1d** and *c*-octene increased to 54% and 50%, respectively and only 29% yield of Rh(tp)(*n*-octyl) **10b**, the CCA product, was obtained. Finally, Rh(tp)(*n*-octyl) was generated in prolonged heating and still, Rh(tp)H was consumed slowly and mostly remained unreacted even after 10 days. Therefore, both Rh<sub>2</sub>(tp)<sub>2</sub> and Rh(tp)H are possible intermediates. The observed <sup>1</sup>H NMR upfield signals at δ = -5 to 1 ppm (Figure 4.6) were assigned to Rh(tp)-incorporated *c*-octene oligomers (about 15% NMR yield), which indicate the occurrence of Rh<sup>II</sup>(tp)-initiated oligomerization of *c*-octene.<sup>13</sup>

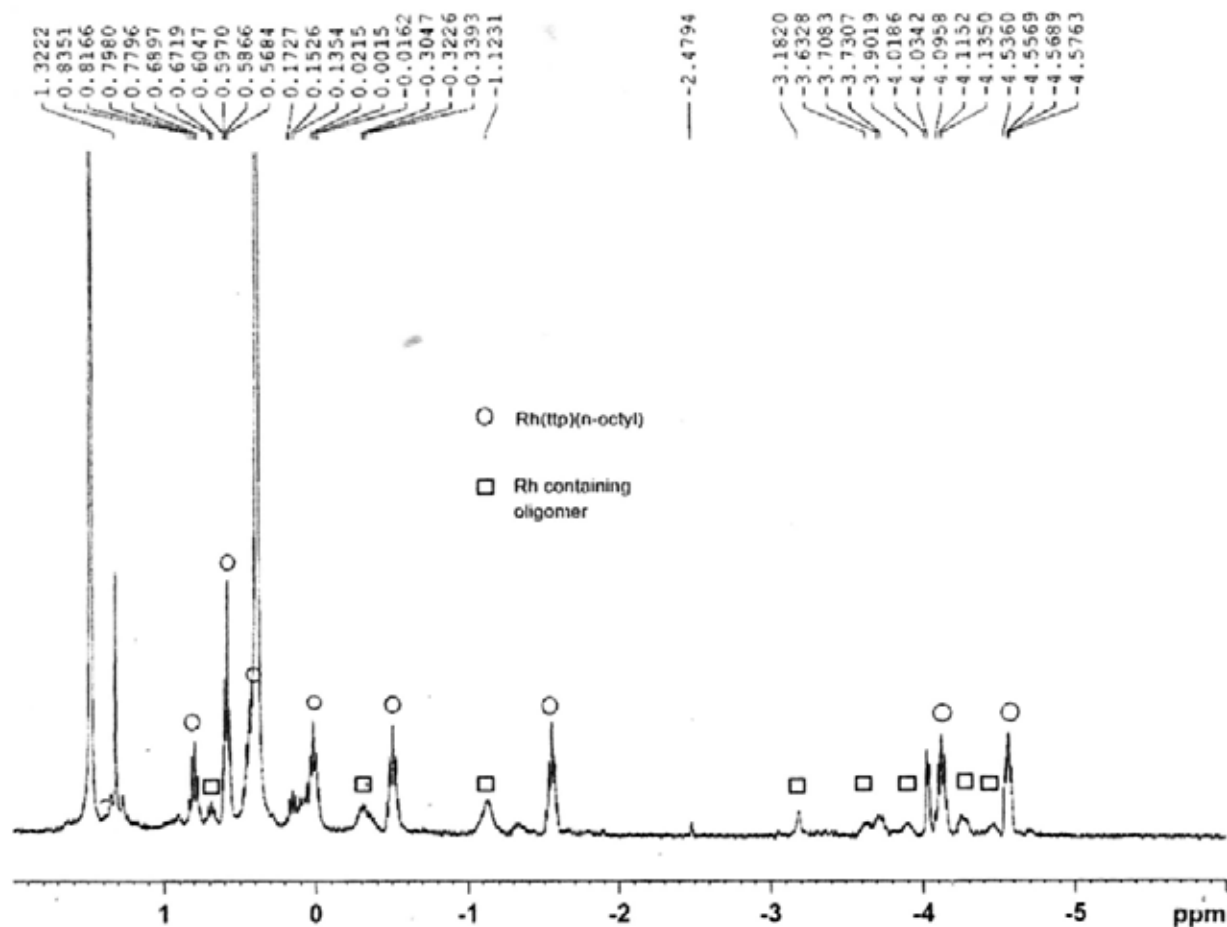
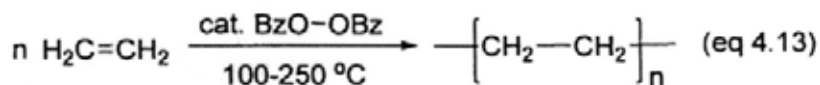


Figure 4.6  $^1\text{H}$  NMR Spectrum of  $\text{Rh}(\text{tp})(n\text{-octyl})$  and Suspected Oligomer in  $\text{Benzene-}d_6$

Olefin is well known to undergo polymerization.<sup>13</sup> For example, ethene polymerized readily in the presence of  $\text{BzO-OBz}$ , which produces  $\text{BzO}\cdot$  radical by homolysis (eq 4.13, scheme 4.4).<sup>13c</sup> *c*-Octene underwent polymerization to produce a vinyl polymer in the presence of appropriate transition metal catalyst (eq 4.14).<sup>13d</sup>



### Free Radical Chain Mechanism

#### Initiation



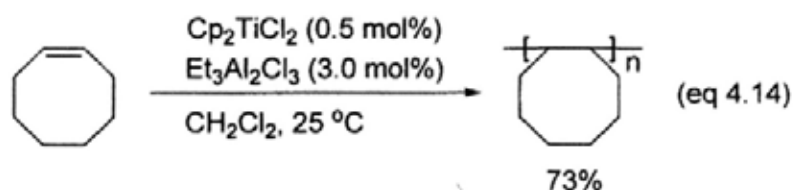
#### Propagation



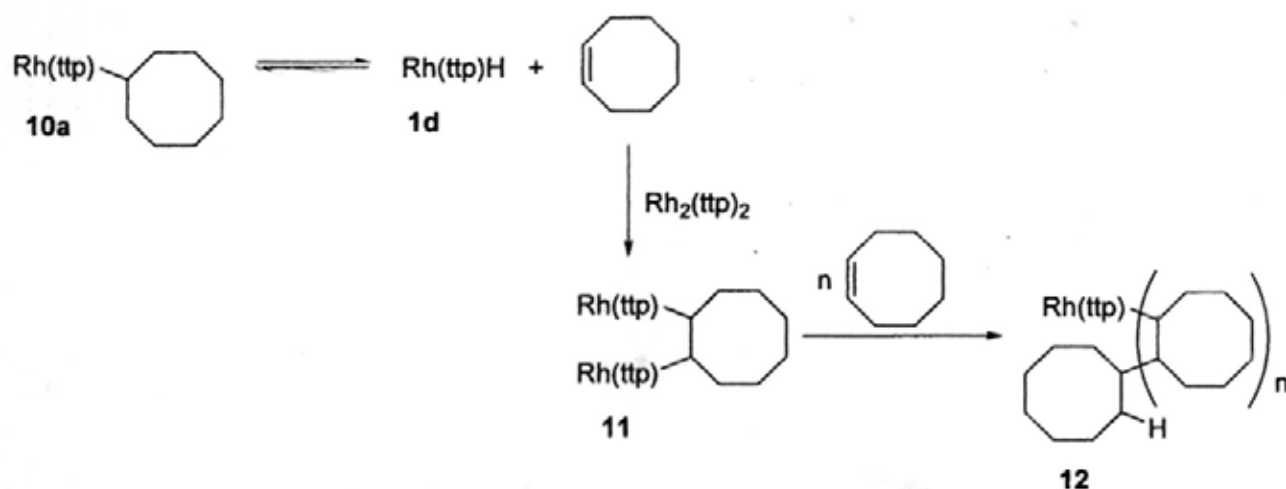
#### Termination



Scheme 4.4 Free Radical Chain Mechanism of Ethylene



The formation of *c*-octene, which forms from the  $\beta$ -H elimination of Rh(tpp)(*c*-octyl) **10a**, indicated the CHA of *c*-octane. When *c*-octene accumulates, it serves as a trap for Rh<sub>2</sub>(tpp)<sub>2</sub> and therefore stops the CCA (Scheme 4.5).



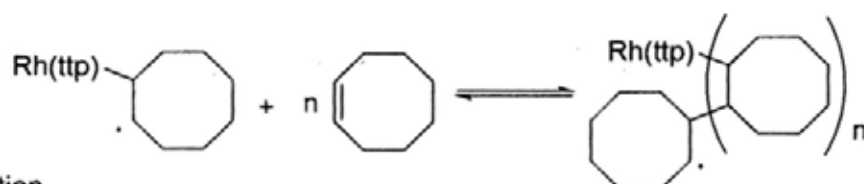
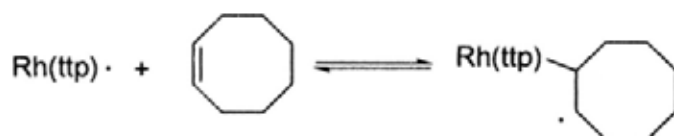
Scheme 4.5 Formation of *c*-Octene and Trap for Rh<sub>2</sub>(tpp)<sub>2</sub>

In fact, in the reaction of eq 4.12, a small piece of gum-like substance was observed in the red reaction mixture which was more viscous than *c*-octane solution. Rh<sup>II</sup>(ttp) radical likely polymerizes the *c*-octene formed in the reaction mixture as shown in scheme 4.6.

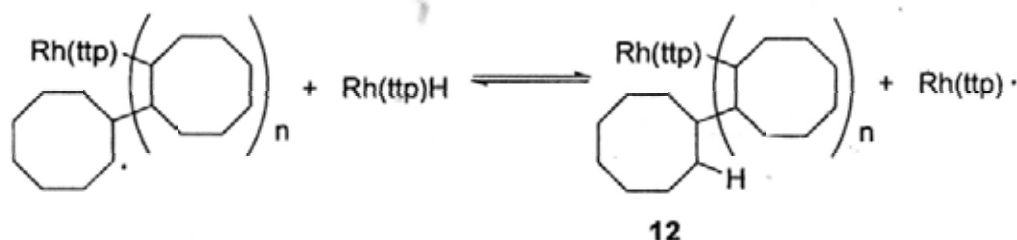
Chain initiation



Chain propagation

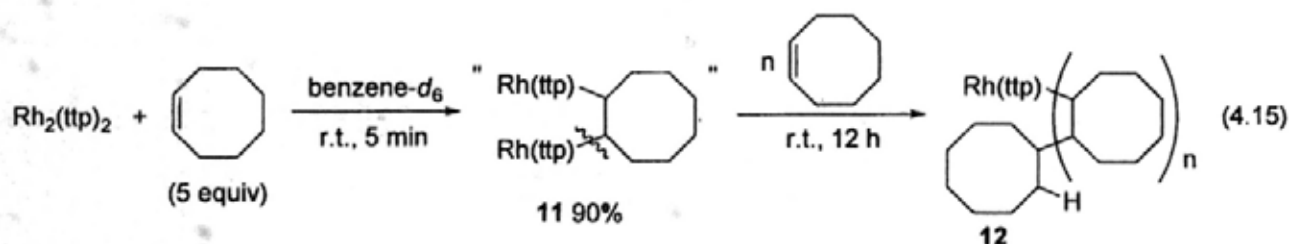


Chain termination

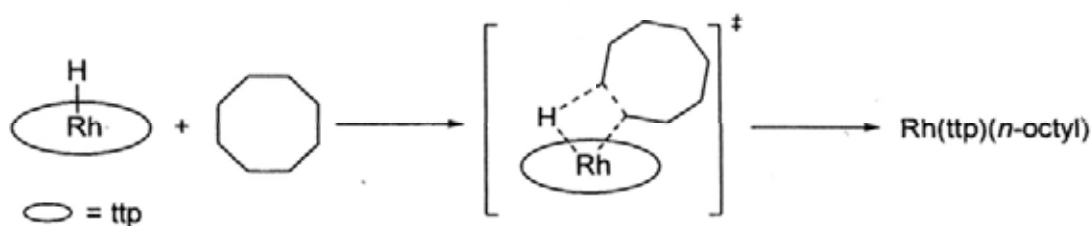


Scheme 4:6 Rh<sup>II</sup>(ttp)-Initiated Oligomerization of *c*-Octene

Indeed, Rh<sub>2</sub>(ttp)<sub>2</sub> reacted with *c*-octene to give a suspected di-rhodium alkyl **11** ( $\delta = 4.70$  ppm) (eq 4.15). However, **11** was thermally unstable even at room temperature and decomposed possibly via Rh-C homolysis.<sup>14</sup> The Rh-alkyl radical then reacts with excess *c*-octene to give **12**.

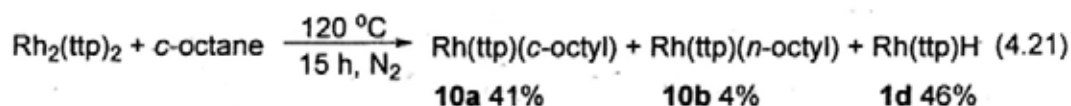






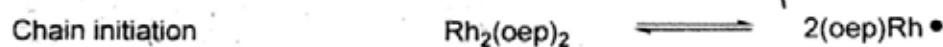
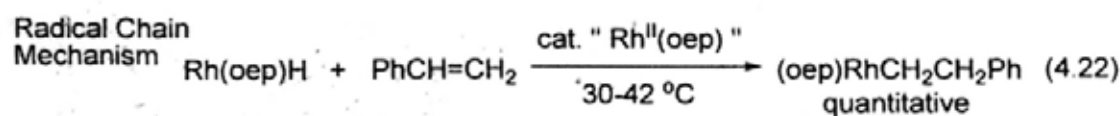
Scheme 4.7 4-Centered Transition State via  $\sigma$ -Bond Metathesis

The other possible intermediate  $\text{Rh}_2(\text{ttp})_2$  **1e** was also reacted with *c*-octane.  $\text{Rh}(\text{ttp})(c\text{-octyl})$  **10a**,  $\text{Rh}(\text{ttp})(n\text{-octyl})$  **10b** and  $\text{Rh}(\text{ttp})\text{H}$  **1d** were formed in 41%, 4% and 46% yields, respectively (eq 4.21) with a very low yield of CCA product.<sup>18</sup> Therefore, both  $\text{Rh}(\text{ttp})\text{H}$  **1d** and  $\text{Rh}_2(\text{ttp})_2$  **1e** gave low yielding reactions and are likely only minor reaction intermediates by themselves.



#### 4.5 Proposed Mechanism of $\text{Rh}^{\text{II}}(\text{ttp})$ -Catalyzed CCA of *c*-Octane

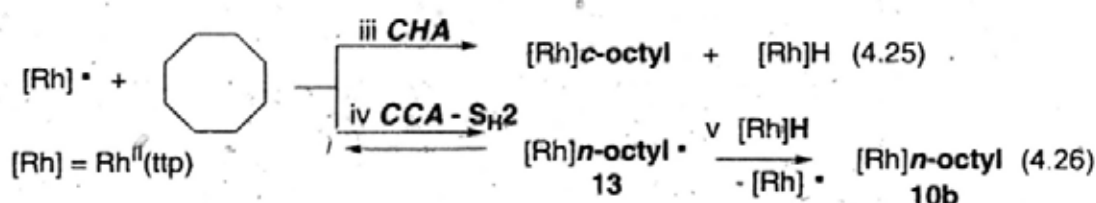
Even though both  $\text{Rh}(\text{ttp})\text{H}$  and  $\text{Rh}_2(\text{ttp})_2$  are intermediates, independent experiments showed that they separately reacted with *c*-octane to give poor CCA yields. Therefore,  $\text{Rh}^{\text{II}}(\text{ttp})/\text{Rh}_2(\text{ttp})_2$  may act as a catalyst to facilitate the 1,2-addition of *c*-octane with  $\text{Rh}(\text{ttp})\text{H}$ . Indeed, a  $\text{Rh}^{\text{II}}(\text{oep})$ -catalyzed ( $\text{oep}$  = octylethylporphyrin dianion) 1,2-addition of styrene was reported by Hapler et al.<sup>16</sup> Styrene underwent facile 1,2-addition reaction with  $\text{Rh}(\text{oep})\text{H}$  to give  $\text{Rh}(\text{oep})\text{CH}_2\text{CH}_2\text{Ph}$  (eq 4.22).<sup>16</sup>  $\text{Rh}^{\text{II}}(\text{oep})$ , which forms from homolysis of  $\text{Rh}_2(\text{oep})_2$ , inserts into the C=C bond to give a Rh-alkyl radical (Scheme 4.8). The Rh-alkyl radical formed then abstracts a hydrogen atom from  $\text{Rh}(\text{oep})\text{H}$  to yield the 1,2-addition product  $\text{Rh}(\text{oep})\text{CH}_2\text{CH}_2\text{Ph}$  and regenerates  $\text{Rh}^{\text{II}}(\text{oep})$ .



Scheme 4.8 Proposed Radical Chain Mechanism of  $\text{Rh}^{\text{II}}(\text{oep})$ -catalyzed 1,2-addition of Styrene with  $\text{Rh}(\text{oep})\text{H}$

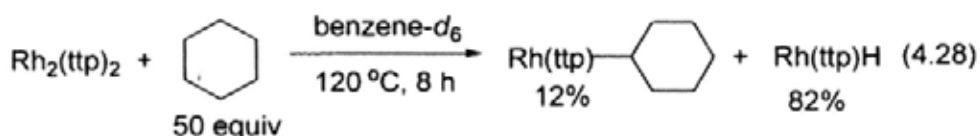
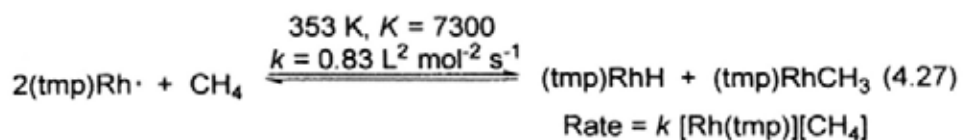
Based on the mechanism of the  $\text{Rh}^{\text{II}}$ -catalyzed insertion of  $\text{Rh}(\text{oep})\text{H}$  into styrene reported by Halpern et al.,<sup>16</sup> the CCA of *c*-octane, being a 1,2-addition reaction, is proposed to be catalyzed by  $\text{Rh}^{\text{II}}$  (Scheme 4.9).

**CCA catalyzed by  $[\text{Rh}^{\text{II}}]$**



Scheme 4.9 Proposed Mechanism of  $\text{Rh}^{\text{II}}$ -Catalyzed 1,2-Addition of *c*-Octane with  $\text{RhH}$

$\text{Rh}_2(\text{ttp})_2$  **1e** formed from thermolysis of  $\text{Rh}(\text{ttp})\text{H}$ , initially undergoes homolysis to give  $\text{Rh}^{\text{II}}(\text{ttp})$  (eqs 4.23 and 4.24).<sup>15</sup>  $\text{Rh}^{\text{II}}(\text{ttp})$  then reacts with *c*-octane in parallel CHA (pathway iii, eq 4.25) and CCA (pathway iv, eq 4.26).  $\text{Rh}^{\text{II}}(\text{por})$  has been shown to undergo CHA with alkane to give  $\text{Rh}(\text{por})\text{R}$  and  $\text{Rh}(\text{por})\text{H}$  with a termolecular rate law (eqs 4.27-4.28).<sup>12,19</sup>



For the CCA pathway,  $\text{Rh}^{\text{II}}(\text{ttp})$  can cleave the C–C bond of *c*-octane to generate the alkyl radical **13** (pathway iv, eq 4.26) which can also reverse back rapidly (Figure 4.7).<sup>20</sup> **13** can then abstract a hydrogen atom from the weak (ttp)Rh–H bond ( $\sim 60 \text{ kcal mol}^{-1}$ )<sup>21a</sup> to form a strong alkyl C–H bond,<sup>21b</sup> providing the driving force of the reaction (pathway v).

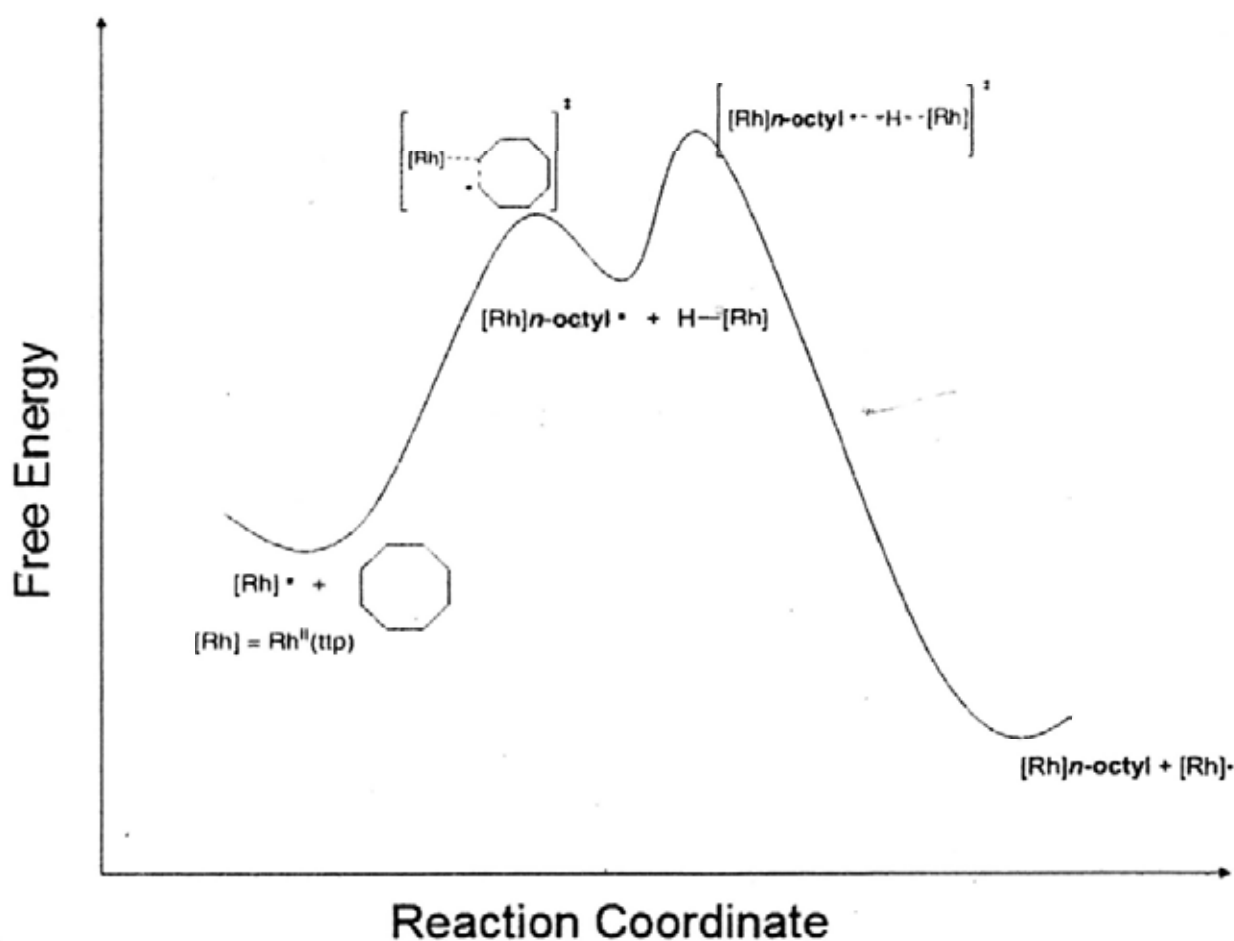
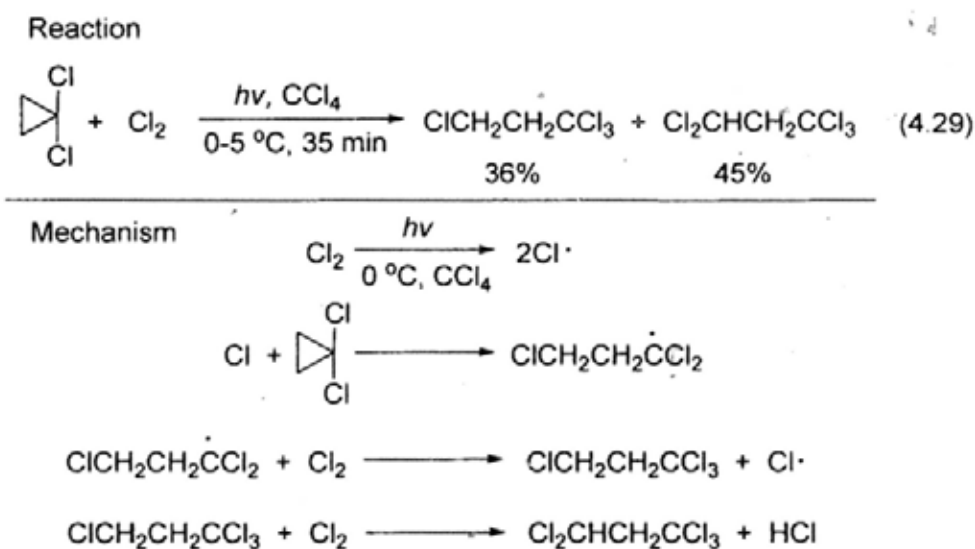


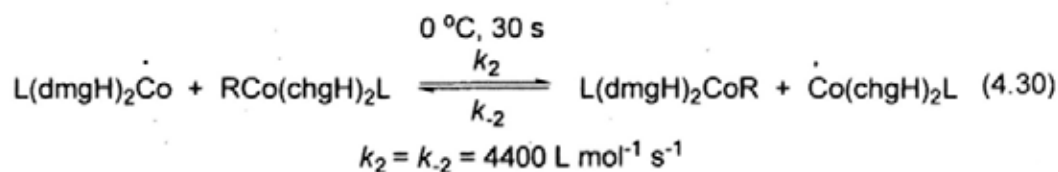
Figure 4.7 Energy Profile of  $\text{Rh}^{\text{II}}(\text{ttp})$ -Catalyzed 1,2-Addition of  $\text{Rh}(\text{ttp})\text{H}$  with *c*-octane (eq 4.26)

Indeed, the cleavage of C–C bond via bimolecular homolytic substitution ( $S_{H2}$ ) has been reported (eq 4.29).<sup>20a</sup> Scheme 4.10 shows a ring opening reaction of cyclopropane via  $S_{H2}$ . The Cl atom formed from photolysis of  $Cl_2$  attacks the  $\alpha$ -carbon to give an alkyl radical. Finally, the chlorine-substituted alkyl radical abstracts a Cl atom from  $Cl_2$  to yield the product.



Scheme 4.10 CCA of Cyclopropane with Chlorine Radical via  $S_{H2}$

Furthermore,  $Co^{II}$  radical was reported to attack an  $sp^3$  carbon to give Co–alkyl complex via  $S_{H2}$  (eq 4.30).<sup>20b</sup> Therefore, the C–C bond of *c*-octane is proposed to be cleaved by  $Rh^{II}(ttp)$  radical via  $S_{H2}$ .



R = Me; L = py; dmgH = dimethylglyoximato ligand  
 chgH = conjugate base of cyclohexanedione dioxime

#### 4.5.1 Synergetic Effect of Rh(tpp)H/Rh<sub>2</sub>(tpp)<sub>2</sub> in CCA of *c*-Octane

Therefore, the proposed mechanism can be validated qualitatively by increasing the ratio of Rh(tpp)H/Rh<sub>2</sub>(tpp)<sub>2</sub> for more efficient trapping of **11** to **10b** (eq 4.31, Table 4.6).

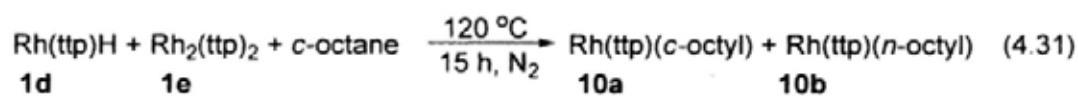


Table 4.6 Rh<sup>II</sup>(tpp)-Catalyzed CCA of *c*-Octane with Rh(tpp)H

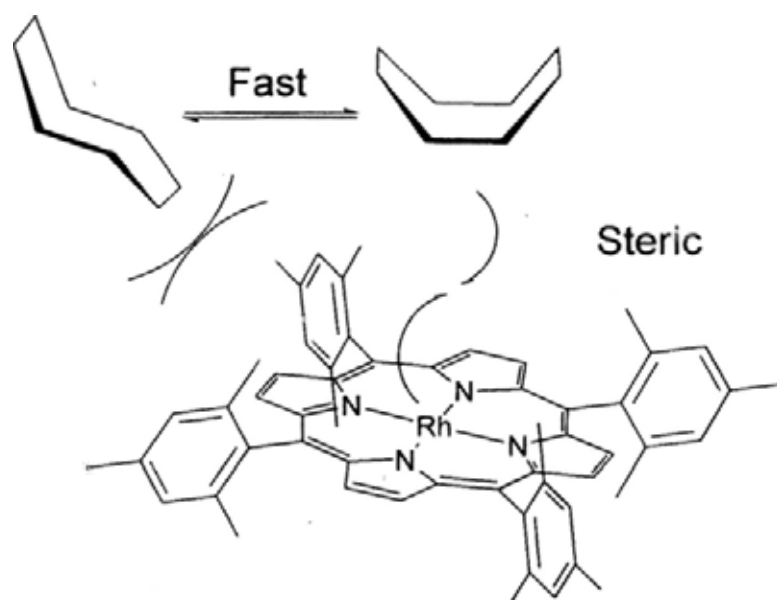
| Entry <sup>a</sup> | Rh(tpp)H:Rh <sub>2</sub> (tpp) <sub>2</sub> | Yield <b>10a</b> (%) | Yield <b>10b</b> (%) | Total yield (%) |
|--------------------|---|----------------------|----------------------|-----------------|
| 1 <sup>b</sup>     | 1:0   | 0                    | 21                   | 21              |
| 2                  | 2:1   | 60                   | 18                   | 78              |
| 3                  | 5:1   | 53                   | 26                   | 79              |
| 4                  | 10:1  | 0                    | 73                   | 73              |

<sup>a</sup> The results are the average of at least duplicate. <sup>b</sup> 73% Rh(tpp)H recovered

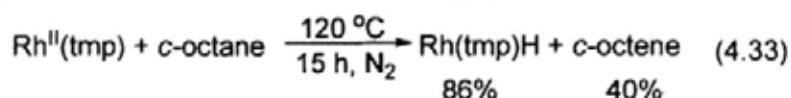
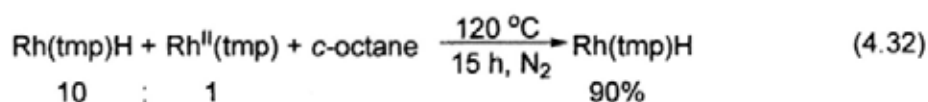
Indeed, mixtures of Rh(tpp)H and Rh<sub>2</sub>(tpp)<sub>2</sub> were more efficient reagents and enhanced the total yields up to 79% (Table 4.6, entries 2-4 vs 1). The selectivity towards CCA was further enhanced by an increase of the Rh(tpp)H:Rh<sub>2</sub>(tpp)<sub>2</sub> ratio. The CCA of *c*-octane with the mixture of Rh(tpp)H:Rh<sub>2</sub>(tpp)<sub>2</sub> in 2:1 ratio gave Rh(tpp)(*c*-octyl) and Rh(tpp)(*n*-octyl) in 60% and 18% yields, respectively (Table 4.6, entry 2). When the Rh(tpp)H/Rh<sub>2</sub>(tpp)<sub>2</sub> ratio increased to 5:1, the yield of Rh(tpp)(*n*-octyl) increased to 26% yield but that of Rh(tpp)(*c*-octyl) decreased to 53% yield (entry 3). Rh(tpp)(*n*-octyl) was selectively obtained in 73% yield from the reaction with the 10:1 ratio of Rh(tpp)H:Rh<sub>2</sub>(tpp)<sub>2</sub> (entry 4). The aliphatic CCA of *c*-octane was thus achieved successfully with the Rh<sup>II</sup>-catalyzed 1,2-addition of Rh(tpp)H.

## 4.5.2 Steric of Porphyrin

The sterically more hindered Rh(tmp) was not effective for CCA (tmp = 5,10,15,20-tetramesitylporphyrinato dianion) (Scheme 4.11). When the mixture of Rh(tmp)H **14a** and Rh<sup>II</sup>(tmp) **14b** (10:1) was reacted with *c*-octane at 120 °C for 15 h, no reaction occurred and 90% yield of Rh(tmp)H **14a** was recovered (eq 4.32). Rh<sup>II</sup>(tmp) **14b** only underwent CHA with *c*-octane to give Rh(tmp)H **14a** and *c*-octene in 86% and 40% yields, respectively (eq 4.33).



Scheme 4.11 Sterically Hindered Transition State for Rh<sup>II</sup>(tmp)



The formation of *c*-octene likely results from the CHA product Rh(tmp)(*c*-octyl) **14c** which rapidly undergoes facile  $\beta$ -hydride elimination to give *c*-octene and Rh(tmp)H (Scheme 4.12). Indeed, the attempted synthesis of Rh(tmp)(*c*-octyl) **14c** by reductive alkylation (NaBH<sub>4</sub>/*c*-octyl bromide) gave Rh(tmp)H **14a** and *c*-octene in 89 and 77% yields, respectively.



## References

- (1) (a) Mackay, D.; Shiu, W. Y.; Ma, K. C.; Lee, S. C. *Physical-Chemical Properties and Environmental Fate for Organic Chemicals 2<sup>nd</sup> Ed, Volume. 1*, CRC Press, Boca raton, FL, 2006. (b) Pakes, P. W.; Rounds, T. C.; Strauss, H. L. *J. Phys. Chem.* **1981**, *85*, 2469-2475.
- (2) Luo, Y. R. *Comprehensive Handbook of Chemical Bond Energies*, CRC Press, Boca Raton, FL, 2007.
- (3) (a) Isaacs, N. S. *Physical Organic Chemistry*; Longman: Essex, 1987. (b) The BDE of C–C bonds are calculated based on the  $\Delta H_{\text{formation}}$ , see Stull, D. R.; Westrum, E. F. Jr.; Sinke, G. C. *The Chemical Thermodynamics of Organic Compounds*; John Wiley & Sons: New York 1969.
- (4) *CRC Handbook of Chemistry & Physics 84<sup>th</sup> Ed.*, Lide, D. R. Ed. 2004.
- (5) (a) Shilov, A. E.; Shul'pin, G. B. *Chem. Rev.* **1997**, *97*, 2879-2932. (b) Crabtree, R. H. *Chem. Rev.* **1985**, *85*, 245-269.
- (6) (a) Jun, C. H. *Chem. Soc. Rev.* **2004**, *33*, 610-618. (b) Murakami, M; Amii, H.; Ito, Y. *Nature* **1994**, *370*, 540-541. (c) van der Boom, M. E.; Milstein, D. *Chem. Rev.* **2003**, *103*, 1759-1792. (d) Goldman, A. S. *Nature* **2010**, *463*, 435-436.
- (7) (a) For a heterogeneous medium: see Hagedom, C. J.; Weiss, M. J.; Kim, T. W.; Weinberg, W. H. *J. Am. Chem. Soc.* **2001**, *123*, 929-940. (b) Sawatari, N.; Yokota, T.; Sakaguchi, S.; Ishii, Y. *J. Org. Chem.* **2001**, *66*, 7889-7891.
- (8) (a) For a leading reference: see Renkema, K. B.; Kissin, Y. V.; Goldman, A. S. *J. Am. Chem. Soc.* **2003**, *125*, 7770-7771. (b) Yiu, S. M.; Wu, Z. B.; Lau, T. C. *J. Am. Chem. Soc.* **2004**, *126*, 14921-14929. (c) Jiang, X. F.; Shen, M. H.; Tang, Y.; Li, C. Z. *Tetrahedron Lett.* **2005**, *46*, 487-489.

- (9) Rh(ttp)Cl reacted with alkane in basic medium to give Rh<sub>2</sub>(ttp)<sub>2</sub> and Rh(ttp)H as intermediates. See ref 12.
- (10) **10a** and **10b** were fully characterized. The chemical shifts of <sup>13</sup>C NMR of Rh–C of **10a** and **10b** were  $\delta = 40.62$  (d,  $^1J_{\text{Rh-C}} = 26.4$  Hz) and  $15.69$  (d,  $^1J_{\text{Rh-C}} = 26.8$  Hz), respectively.
- (11) (a) Rybtchinski, B.; Vigalok, A.; Ben-David, Y.; Milstein, D. *J. Am. Chem. Soc.* **1996**, *118*, 12406-12415. (b) Perthuisot, C.; Jones, W. D. *J. Am. Chem. Soc.* **1994**, *116*, 3647-3648.
- (12) Chan, Y. W.; Chan, K. S. *Organometallics* **2008**, *27*, 4625-4635.
- (13) (a) Cho, I. *Prog. Polym. Sci.* **2000**, *25*, 1043-1087. (b) Stohandl, J.; Vozka, P.; Varekova, I.; Karafiat, M.; Ondr J, J.; Mejzlik, J.; Balcar, H.; Stepanek, K.; Heller, G.; Lederer, J. U.S. Patent 5 455 318, 1995. (c) Motherwell, W. B.; Crich, D. *Free Radical Chain Reaction in Organic Synthesis*, Academic Press, London, 1992. (d) Dragutan, V.; Streck, R. *Catalytic Polymerization of Cycloolefins: Ionic, Ziegler-Natta and Ring-Opening Metathesis Polymerization 1<sup>st</sup> Ed.*, Elsevier, Amsterdam, 2000
- (14) Homolytic cleavage Rh–C of di-rhodium alkyl complex likely occurs. A similar case of **7a** was reported in Chapter 3, see eq 3.20 and reference 20 of Chapter 3.
- (15) Wayland, B. B.; van Voorhees, S. L.; Wilker, C. *Inorg. Chem.* **1986**, *25*, 4039-4042.
- (16) Paonessa, R.S.; Thomas, N C.; Halpern, J. *J. Am. Chem. Soc.* **1985**, *107*, 4333-4335.
- (17) For 4 centered transition state, see (a) Mak, K. W.; Chan, K. S. *J. Am. Chem. Soc.* **1998**, *120*, 9686-9687. (b) Mak, K. W.; Xue, F.; Mak, T. C. W.; Chan, K. S. *J. Chem. Soc., Dalton Trans.* **1999**, *19*, 3333-3334.
- (18) Wayland, B. B.; Ba, S.; Sherry, A. E. *J. Am. Chem. Soc.* **1991**, *113*, 5305-5311.

- (19) (a) Davies, A. G.; Roberts, B. P. *Acc. Chem. Res.* **1972**, *5*, 387-392. (b) Johnson, M. D. *Acc. Chem. Res.* **1983**, *16*, 343-349. (c) Incremona, J. H.; Upton, C. J. *J. Am. Chem. Soc.* **1972**, *94*, 301-303.
- (20) (a) The estimated bond dissociation energy (BDE) of (ttp)Rh-H is  $\sim 60$  kcal mol<sup>-1</sup>, See ref 19. (b) The BDE of *n*-octyl-H is  $\sim 100$  kcal mol<sup>-1</sup>, see Luo, Y. R. *Handbook of Bond Dissociation Energies in Organic Compounds*, CRC Press, Boca Raton, FL, 2003.

## Chapter 5 Comparison of CHA and CCA of Various Cycloalkanes

The reactivity patterns of cycloalkanes with rhodium porphyrin complexes are analyzed by the C–H and C–C bond strengths as well as the ring closing rate of cycloalkanes. The previous findings in Chapters 2, 3 and 4 show that *c*-pentane and *c*-hexane reacted with rhodium porphyrin complexes via CHA to yield only the corresponding CHA products while *c*-heptane and *c*-octane gave the corresponding CHA and CCA products. *c*-Octane underwent the Rh<sup>II</sup>(ttp)-catalyzed 1,2-addition with Rh(ttp)H to give Rh(ttp)(*n*-octyl) selectively. To account for the different reactivity of cycloalkanes with rhodium porphyrin complexes, the C–H and C–C bond dissociation energies, ring strains and ring closure rates of various cycloalkanes listed in Table 5.1 are used as the physical base.

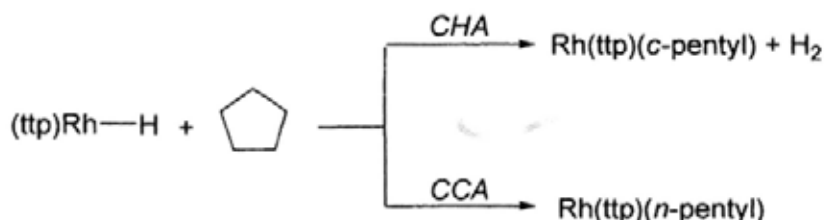
Table 5.1 Bond Dissociation Energies and Ring Strains of Various Cycloalkanes<sup>1-2</sup>

| Alkane            | BDE                              |                                  |  | Ring Strain<br>(kcal mol <sup>-1</sup> ) |
|-------------------|----------------------------------|----------------------------------|--|--|
|                   | C–H<br>(kcal mol <sup>-1</sup> ) | C–C<br>(kcal mol <sup>-1</sup> ) | ΔBDE <sup>a</sup><br>(kcal mol <sup>-1</sup> ) |  |
| <i>n</i> -pentane | 100.2                            | 88.8                             | 11.4   | Not Applicable                           |
| <i>n</i> -hexane  | 99.0                             | 88.1                             | 10.9   | Not Applicable                           |
| <i>n</i> -heptane | 98.0                             | 88.0                             | 10.0   | Not Applicable                           |
| <i>c</i> -pentane | 95.6                             | 86.9 <sup>2d</sup>               | 12.7   | 6.5                                      |
| <i>c</i> -hexane  | 99.5                             | 87.3                             | 16.8   | 0  |
| <i>c</i> -heptane | 94.0                             | 86.6                             | 7.4  | 6.3                                      |
| <i>c</i> -octane  | 95.7                             | 79.6                             | 16.1   | 9.6                                      |

<sup>a</sup> ΔBDE is the BDE difference of C–H and C–C.

## 5.1 Thermodynamics Consideration of CHA and CCA of Cycloalkanes

The estimation of the thermodynamics of CHA and CCA with Rh(tp)H allows the quantitative understandings of these processes. Scheme 5.1 outlines the computation of the thermodynamics of CHA and CCA of *c*-pentane as a general example.



Scheme 5.1 CHA and CCA of *c*-Pentane with Rh(tp)H

The BDEs of Rh-H, Rh-C and H-H are taken to be 60 kcal mol<sup>-1</sup>, 48 kcal mol<sup>-1</sup> and 105 kcal mol<sup>-1</sup>, respectively.<sup>1</sup>

For CHA,

$$\begin{aligned}
 \Delta H_{(CHA, 298)} &= \text{BDE of (Rh-H + C-H of } c\text{-pentane)} - \text{BDE of (Rh-C + H-H)} \\
 &= (60 + 95.6) - (48 + 105) \text{ kcal mol}^{-1} \\
 &= 2.6 \text{ kcal mol}^{-1}
 \end{aligned}$$

Assuming the molar entropies of Rh(tp)H ~ Rh(tp)(*c*-pentyl), the molar entropy of H<sub>2</sub> and *c*-pentane at 298 K are 31.0 and 48.9 cal mol<sup>-1</sup> K<sup>-1</sup>, respectively.<sup>2a,2c</sup>

$$\begin{aligned}
 \Delta S_{(CHA, 298)} &= -(48.9) + (31.0) \text{ cal mol}^{-1} \text{ K}^{-1} \\
 &= -17.9 \text{ cal mol}^{-1} \text{ K}^{-1}
 \end{aligned}$$

$$\begin{aligned}
 \Delta G_{(CHA, 298)} &= \Delta H_{(CHA, 298)} - T\Delta S_{(CHA, 298)} \\
 &= (2.6) - 298(-17.9/1000) \text{ kcal mol}^{-1} \\
 &= 2.6 + 5.3 \text{ cal mol}^{-1} \text{ K}^{-1} \\
 &= 7.9 \text{ kcal mol}^{-1}
 \end{aligned}$$

For CCA,

$$\begin{aligned}\Delta H_{(CCA, 298)} &= \text{BDE of (Rh-H + C-C of } c\text{-pentane)} - \text{BDE of (Rh-C + C-H of } n\text{-pentyl)} \\ &\quad - \text{ring strain} \\ &= (60 + 86.9) - (48 + 100) - (6.5) \text{ kcal mol}^{-1} \\ &= -7.6 \text{ kcal mol}^{-1}\end{aligned}$$

The molar entropies of Rh(tp)H is assumed to be similar to that of Rh(tp)(*n*-pentyl). The molar entropy of H<sub>2</sub> and *c*-pentane at 298 K are 31.0 and 48.9 cal mol<sup>-1</sup> K<sup>-1</sup>, respectively.<sup>2a,2c</sup>

$$\begin{aligned}\Delta S_{(CCA, 298)} &= -48.88 \text{ cal mol}^{-1} \text{ K}^{-1} \\ \Delta G_{(CCA, 298)} &= \Delta H_{(CHA, 298)} - T\Delta S_{(CHA, 298)} \\ &= (-7.6) - 298(-48.88/1000) \text{ kcal mol}^{-1} \\ &= (-7.6) - (-14.56) \text{ kcal mol}^{-1} \\ &= 7.0 \text{ kcal mol}^{-1}\end{aligned}$$

The estimated  $\Delta H$ ,  $\Delta S$  and  $\Delta G$  of CHA and CCA of various cycloalkanes and Rh(tp)H are listed (Table 5.2).

Table 5.2  $\Delta H$ ,  $\Delta S$  and  $\Delta G$  of CHA and CCA of Various Cycloalkanes and Rh(tp)H

|                   | kcal mol <sup>-1</sup> |                         |                        |                        |                         |                        |
|-------------------|------------------------|-------------------------|------------------------|------------------------|-------------------------|------------------------|
|                   | $\Delta H_{(CHA,298)}$ | $T\Delta S_{(CHA,298)}$ | $\Delta G_{(CHA,298)}$ | $\Delta H_{(CCA,298)}$ | $T\Delta S_{(CCA,298)}$ | $\Delta G_{(CCA,298)}$ |
| <i>c</i> -pentane | 2.6                    | -5.3                    | 7.9                    | -7.6                   | -14.6                   | 7.0                    |
| <i>c</i> -hexane  | 6.5                    | -5.3                    | 11.8                   | -4.3                   | -14.6                   | 10.3                   |
| <i>c</i> -heptane | 1.0                    | -5.3                    | 6.3                    | -5.7                   | -14.6                   | 5.9                    |
| <i>c</i> -octane  | 2.7                    | -5.3                    | 8.0                    | -16.0                  | -14.6                   | -1.4                   |

Based on the above estimation, the CHA of *c*-pentane, *c*-hexane, *c*-heptane and *c*-octane with Rh(ttp)H are slightly unfavorable at 298 K (Table 5.2). However, at 393 K (120 °C), the formation of co-product, gaseous hydrogen ( $\Delta S_{393} = 33.1978 \text{ cal mol}^{-1} \text{ K}^{-1}$ ),<sup>3</sup> provides the extra driving force to make the CHA spontaneous (Table 5.3).

Table 5.3 Entropy of H<sub>2</sub> in Different Temperature<sup>a</sup>

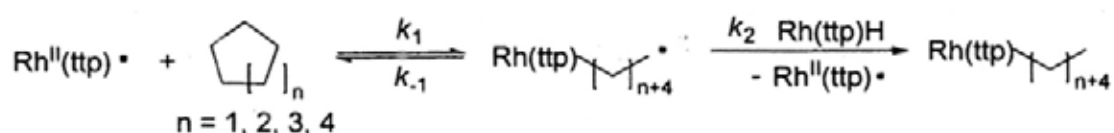
| Temp<br>(K) | $\Delta S$<br>(cal mol <sup>-1</sup> K <sup>-1</sup> ) | T $\Delta S$<br>(kcal mol <sup>-1</sup> ) |
|-------------|--|---|
| 298         | 31.2679  | 9.3178                                    |
| 393         | 33.1938  | 13.0452                                   |
| 433         | 33.8780  | 14.6692                                   |
| 453         | 34.1962  | 15.4909                                   |

<sup>a</sup> $\Delta S(T_2, G) = \Delta S(298 \text{ K}, G) + (C_{pm})(\ln(T_2/298))$ , where  $T_2$  is the temperature interested,  $C_{pm}(\text{H}_2)$  at 298 K is 6.88038 cal mol<sup>-1</sup> K<sup>-1</sup>,  $S_{(298)}$  of H<sub>2</sub> is 31.2679 cal mol<sup>-1</sup> K<sup>-1</sup>. See ref 3.

The CCA of *c*-pentane, *c*-hexane, *c*-heptane and *c*-octane with Rh(ttp)H are thermodynamically more favorable than the CHA (Table 5.2). The CCA of *c*-octane is thermodynamically favorable ( $\Delta G < 0$ ) while *c*-pentane, *c*-hexane and *c*-heptane are slightly unfavorable ( $\Delta G > 0$ ). Therefore, the ring opening product was only observed in *c*-octane case. As  $\Delta H_{(CCA)}$  is negative and  $-T\Delta S_{(CCA)}$  is positive, the CCA of cycloalkane is more probable at lower temperature.

## 5.2 Kinetic Consideration of CHA and CCA of Cycloalkanes

As the CCA of *c*-octane is shown to be Rh<sup>II</sup>-catalyzed, the kinetics of the key Rh<sup>II</sup>(ttp)-catalyzed 1,2-addition of cycloalkane with Rh(ttp)H is considered (Scheme 5.2).



Scheme 5.2 Mechanistic Scheme of Rh<sup>II</sup>(ttp)-Catalyzed 1,2-Addition of Cycloalkane with Rh(ttp)H

$$\text{Rate of CCA} = k_1[\text{Rh}^{\text{II}}(\text{ttp})][\text{cycloalkane}]$$

$$\text{Rate of Backward CCA} = k_{-1}[\text{Rh}(\text{ttp})\text{alkyl}\cdot]$$

$$\text{Rate of H Abstraction} = k_2[\text{Rh}(\text{ttp})\text{alkyl}\cdot][\text{Rh}(\text{ttp})\text{H}]$$

At steady state,  $d[\text{Rh}(\text{ttp})\text{alkyl}\cdot]/dt = 0$ ,

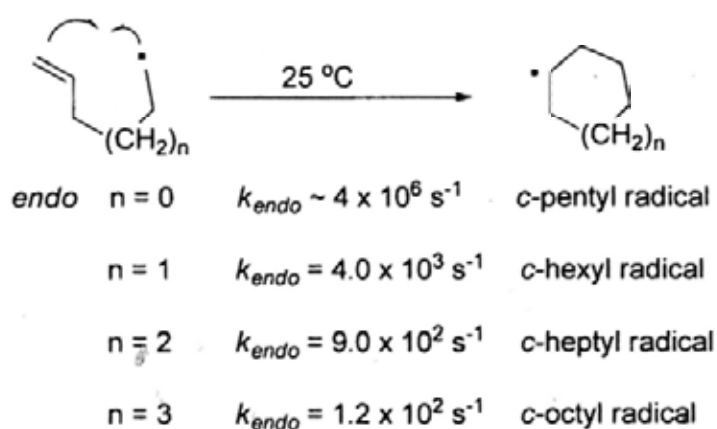
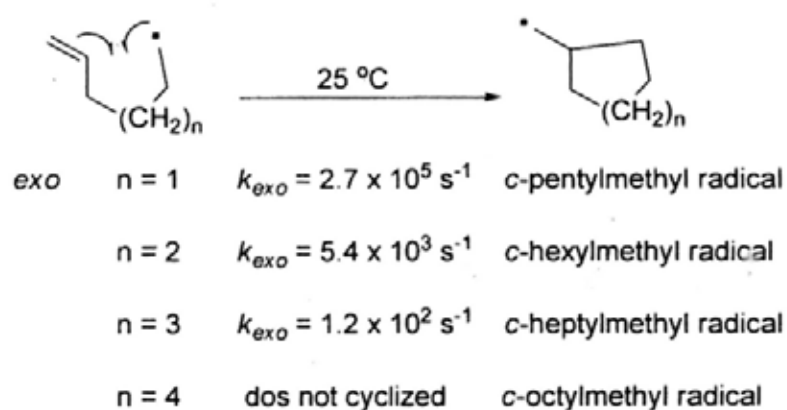
$$k_1[\text{Rh}^{\text{II}}(\text{ttp})][\text{cycloalkane}] = k_{-1}[\text{Rh}(\text{ttp})\text{alkyl}\cdot] + k_2[\text{Rh}(\text{ttp})\text{alkyl}\cdot][\text{Rh}(\text{ttp})\text{H}]$$

In order to achieve a successful CCA, the ring closure rate of cycloalkane should be slow enough so that the Rh-alkyl radical has sufficient time to abstract the H atom from Rh(ttp)H ( $k_{-1}$  is comparable to  $k_2[\text{Rh}(\text{ttp})\text{H}]$ ). Since the ring closure rates of bi-alkyl radical are not reported, the ring closure rate of olefin radical cyclization (Scheme 5.3)<sup>4a-c</sup> and anionic cyclization of ( $\omega$ -brom-oalkyl)malonates (Scheme 5.4)<sup>4d</sup> are listed for reference (Table 5.4).

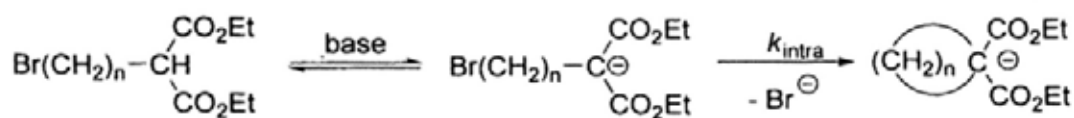
Table 5.4 Ring Closing Rates of Various Cycloalkane<sup>4</sup>

| Ring Size | Olefin Radical Cyclization <sup>a</sup> |                                     | Anionic Cyclization <sup>b</sup> |
|-----------|---|-------------------------------------|----------------------------------|
|           | <i>exo</i> rate (s <sup>-1</sup> )      | <i>endo</i> rate (s <sup>-1</sup> ) | Rate (s <sup>-1</sup> )          |
| 5         | 2.7 x 10 <sup>5</sup>                   | ~4 x 10 <sup>6</sup>                | 6.0 x 10 <sup>2</sup>            |
| 6         | 5.4 x 10 <sup>3</sup>                   | 4.0 x 10 <sup>3</sup>               | 7.2 x 10 <sup>-1</sup>           |
| 7         | 1.2 x 10 <sup>2</sup>                   | 9.0 x 10 <sup>2</sup>               | 6.3 x 10 <sup>-3</sup>           |
| 8         | 0                                       | 1.2 x 10 <sup>2</sup>               | 1.1 x 10 <sup>-4</sup>           |

<sup>a</sup> at 25 °C, see ref 4a-c. <sup>b</sup> at 25 °C, see ref 4d



Scheme 5.3 Olefin Radical Cyclization



3 Scheme 5.4 Cyclization of ( $\omega$ -brom-alkyl)malonates

The rate closure rates of various cycloalkanes follow the order:



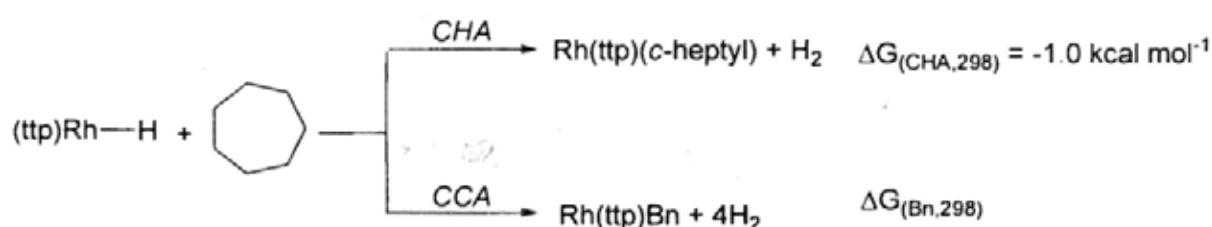
As *c*-octane has the slowest ring closure rate among the four cycloalkanes, the CCA product Rh(tp)(*n*-octyl) was obtained. Furthermore, the higher ring strain of *c*-octane (9.6 kcal mol<sup>-1</sup>) favors the ring opening and disfavors the ring closure.<sup>2a</sup> The ring closure rate of *c*-pentane, *c*-hexane and *c*-heptane are much faster and their ring strains are smaller. So, no corresponding Rh(tp)(*n*-alkyl) was obtained. Therefore, the ring opening CCA of *c*-octane is favored by both thermodynamic and kinetic factors.

On the other side, the rate closure rates of *c*-pentane and *c*-hexane are very fast. So even the corresponding Rh-alkyl radicals form, the lifetimes of the Rh-alkyl radicals are too short to abstract H atom from Rh(tp)H due to rapid ring closure. Therefore, the CCA of *c*-pentane, *c*-hexane and *c*-heptane with Rh(tp)H are both thermodynamically and kinetically less unfavorable.

### 5.3 Consideration of Rh(tpp)Bn Formation

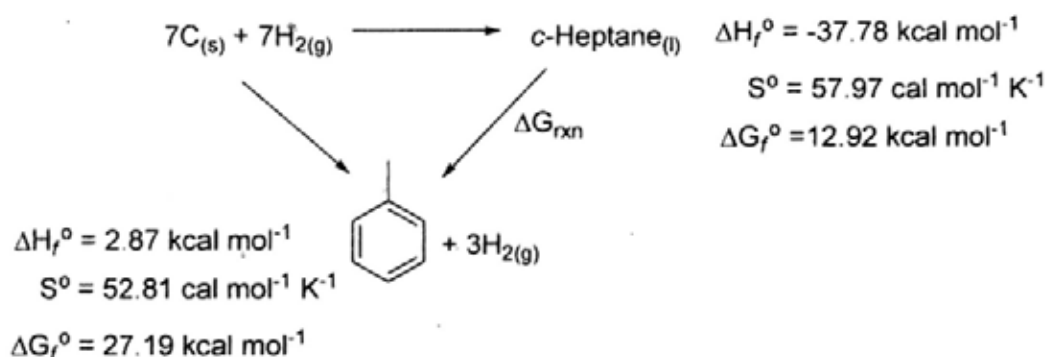
For *c*-heptane, the formation of Rh(tpp)Bn is a consequence of Rh<sup>II</sup>-catalyzed successive dehydrogenation of *c*-heptane, *c*-heptene and *c*-hepta-1,3-diene which then gives cycloheptatriene. Cycloheptatriene further reacted with Rh(tpp)H/Rh<sub>2</sub>(tpp)<sub>2</sub> to generate Rh(tpp)(cycloheptatrienyl) and eventually form Rh(tpp)Bn via Rh<sup>II</sup>-catalyzed CCA.

Therefore, the thermodynamic of Rh(tpp)Bn formation is considered below (Scheme 5.5).



Scheme 5.5 CHA and CCA of *c*-Heptane with Rh(tpp)H

The difference of  $\Delta G_f^\circ$  of *c*-heptane and toluene is estimated to be the same as the difference of  $\Delta G_{(\text{CHA},298)}$  and  $\Delta G_{(\text{Bn},298)}$  (Scheme 5.6).



Scheme 5.6 Conversion of *c*-Heptane to Toluene<sup>5</sup>

$$\begin{aligned} \Delta G_{\text{rxn}} &= (27.19 - 12.92) \text{ kcal mol}^{-1} \\ &= 14.27 \text{ kcal mol}^{-1} \end{aligned}$$

Therefore,  $\Delta G_{(Bn,298)}$  is estimated to be 13.3 kcal mol<sup>-1</sup>. Since 3 moles of H<sub>2</sub> are generated from the conversion of Rh(tp)(*c*-heptyl) to Rh(tp)Bn, they are likely to provide the driving force of the reaction at 120 °C. The  $\Delta G_{(Bn,393)}$  is estimated as below.

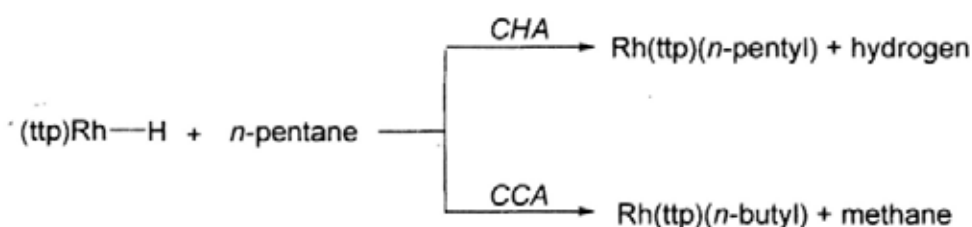
$$\begin{aligned}\Delta G_{(Bn,393)} &= \Delta G_{(Bn,298)} - T(\Delta\Delta S) \\ \Delta\Delta S &= \Delta S_{393} - \Delta S_{298} \\ &= 3 \times (1.3875 \times 10^2 - 1.3070 \times 10^2) \\ &= 24.15 \text{ J mol}^{-1} \text{ K}^{-1} \text{ or } 5.78 \text{ cal mol}^{-1} \text{ K}^{-1}\end{aligned}$$

So,

$$\begin{aligned}\Delta G_{(Bn,393)} &= \Delta G_{(Bn,298)} - T\Delta\Delta S \\ &= 13.3 - 393(5.78/1000) \text{ kcal mol}^{-1} \\ &= 11.0 \text{ kcal mol}^{-1}\end{aligned}$$

#### 5.4 Thermodynamic Consideration of CHA and CCA of *n*-Alkanes

The extension of the above analysis raises an interesting question whether a straight chain alkane can undergo CCA. The thermodynamics of CHA and CCA of *n*-pentane are estimated as an example (Scheme 5.7).



Scheme 5.7 CHA and CCA of *n*-Pentane with Rh(tp)H

For CHA,

$$\begin{aligned}\Delta H_{(\text{CHA}, 298)} &= \text{BDE of (Rh-H + C-H of } n\text{-pentane)} - \text{BDE of (Rh-C + H-H)} \\ &= (60 + 100.2) - (50 + 105) \text{ kcal mol}^{-1} \\ &= 5.2 \text{ kcal mol}^{-1}\end{aligned}$$

Assuming the molar entropies of  $\text{Rh}(\text{ttp})\text{H} \sim \text{Rh}(\text{ttp})(n\text{-pentyl})$ , the molar entropies of  $\text{H}_2$ ,  $\text{CH}_4$  and  $n\text{-pentane}$  at 298 K are  $31.0 \text{ cal mol}^{-1} \text{ K}^{-1}$ ,  $44.5 \text{ cal mol}^{-1} \text{ K}^{-1}$  and  $62.5 \text{ cal mol}^{-1} \text{ K}^{-1}$ , respectively.<sup>2a,2c</sup>

$$\begin{aligned}\Delta S_{(\text{CHA}, 298)} &= -(\text{S of } n\text{-pentane}) + (\text{S of } \text{H}_2) \\ &= -(62.5) + (31.0) \text{ cal mol}^{-1} \text{ K}^{-1} \\ &= -31.5 \text{ cal mol}^{-1} \text{ K}^{-1}\end{aligned}$$

$$\begin{aligned}\Delta G_{(\text{CHA}, 298)} &= \Delta H_{(\text{CHA}, 298)} - T\Delta S_{(\text{CHA}, 298)} \\ &= (5.2) - 298(-31.5/1000) \text{ kcal mol}^{-1} \\ &= (5.2) + (9.4) \text{ kcal mol}^{-1} \\ &= 14.6 \text{ kcal mol}^{-1}\end{aligned}$$

For CCA,

$$\begin{aligned}\Delta H_{(\text{CCA}, 298)} &= \text{BDE of } (\text{Rh-H} + \text{C-C of } n\text{-pentane}) - \text{BDE of } (\text{Rh-C} + \text{C-H of methane}) \\ &= (60 + 88.8) - (50 + 105) \text{ kcal mol}^{-1} \\ &= -6.2 \text{ kcal mol}^{-1}\end{aligned}$$

$$\begin{aligned}\Delta S_{(\text{CCA}, 298)} &= -(\text{Molar entropy of } n\text{-pentane}) + (\text{Molar entropy of methane}) \\ &= -(62.5) + (44.5) \text{ cal mol}^{-1} \text{ K}^{-1} \\ &= -18.0 \text{ cal mol}^{-1} \text{ K}^{-1}\end{aligned}$$

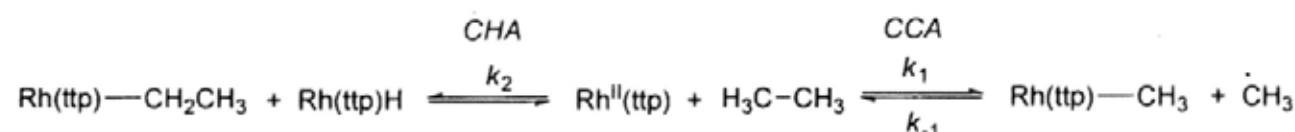
$$\begin{aligned}\Delta G_{(\text{CCA}, 298)} &= \Delta H_{(\text{CCA}, 298)} - T\Delta S_{(\text{CCA}, 298)} \\ &= (-6.2) - 298(-18.0/1000) \text{ kcal mol}^{-1} \\ &= (-6.2) - (-5.4) \text{ kcal mol}^{-1} \\ &= -0.8 \text{ kcal mol}^{-1}\end{aligned}$$

The above analysis show that the CCA of  $n\text{-pentane}$  with  $\text{Rh}(\text{ttp})\text{H}$  is thermodynamically more favorable than the CHA. However,  $n\text{-pentane}$  only undergoes CHA.

The kinetic barrier of a  $\text{Rh}^{\text{II}}(\text{por})$  attack at the carbon center is sterically more hindered to allow this reaction channel. Moreover, the C–H bonds of *n*-pentane are kinetically more accessible than C–C bonds.<sup>6</sup>

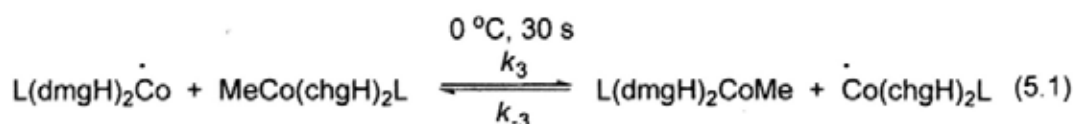
### 5.5 Kinetic Consideration of CHA and CCA of *n*-Alkanes

Since ethane is the simplest molecule with only one C–C bond, the kinetics of CHA and CCA consideration of ethane are estimated as well (Scheme 5.8).  $\text{Rh}^{\text{II}}(\text{ttp})$  may either react with ethane to give  $\text{Rh}(\text{ttp})\text{Me}$  and a methyl radical via CHA or generate  $\text{Rh}(\text{ttp})\text{Et}$  and  $\text{Rh}(\text{ttp})\text{H}$  via CHA.



Scheme 5.8 Proposed Mechanistic Scheme of  $\text{Rh}^{\text{II}}(\text{ttp})$ -Catalyzed CCA of *n*-Alkane with  $\text{Rh}(\text{ttp})\text{H}$

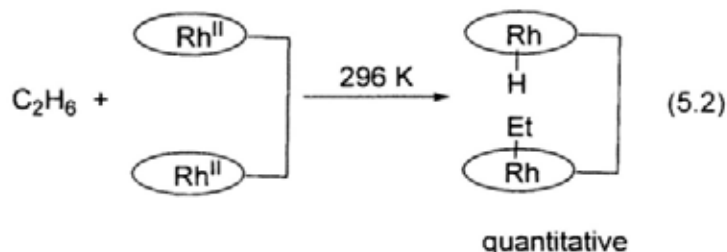
For the CCA,  $\text{Rh}^{\text{II}}(\text{ttp})$  likely cleaves the C–C bond of ethane via  $\text{S}_{\text{H}}2$ .<sup>6</sup> However, as shown in scheme 5.8, the methyl radical can undergo reverse reaction with  $\text{Rh}(\text{ttp})\text{Me}$  to regenerate the  $\text{Rh}^{\text{II}}(\text{ttp})$  and  $\text{C}_2\text{H}_6$ . Neither the forward reaction rate ( $k_1$ ) nor the backward reaction rate ( $k_{-1}$ ) are reported. Therefore, the rate of  $\text{S}_{\text{H}}2$  can only be estimated from other  $\text{S}_{\text{H}}2$  examples. The rate of alkyl exchange of  $(\text{chgH})_2\text{Co}-\text{Me}$  to  $(\text{dmgH})_2\text{Co}-\text{Me}$  via  $\text{S}_{\text{H}}2$  was reported to be  $4400 \text{ M}^{-1} \text{ s}^{-1}$  (eq 5.1).<sup>6</sup>



$$k_2 = k_{-2} = 4400 \text{ L mol}^{-1} \text{ s}^{-1}$$

L = py; dmgH = dimethylglyoximato ligand  
chgH = conjugate base of cyclohexanedione dioxime

For the CHA channel,  $\text{Rh}^{\text{II}}(\text{ttp})$  reacts with ethane to give  $\text{Rh}(\text{ttp})\text{Et}$  and  $\text{Rh}(\text{ttp})\text{H}$ . In fact, Wayland et al. reported that  $\text{Rh}_2(\text{DPB})$  ( $\text{DPB} = 1,8\text{-bis}[5\text{-(2,8,13,17-tetraethyl-3,7,12,18-tetramethylporphyrinyl)}]\text{biphenylene}$ ) reacted with ethane to give the CHA product exclusively (eq 5.2).<sup>7a</sup>



Even the CCA is thermodynamically more favorable than the CHA by  $10 \text{ kcal mol}^{-1}$ , no CCA occurs. Therefore, Wayland et al. proposed that the absence of observed C–C cleavage is kinetic in origin. The interaction of  $\text{Rh}^{\text{II}}$  center with the C–H unit is kinetically more favorable for the near concerted cleavage than the C–C bond (Figures 5.1a and 5.1b). The rate of reaction follows:  $\text{rate} = k [\text{Rh}^{\text{II}}(\text{tmp})]^2 [\text{C}_2\text{H}_6]$ . Indeed, Wayland reported that the CHA of methane with  $\text{Rh}^{\text{II}}(\text{tmp})$  with  $\text{rate} = k [\text{Rh}^{\text{II}}(\text{tmp})]^2 [\text{CH}_4]$ , where  $k_{(296 \text{ K})} = 0.132 \text{ M}^{-2} \text{ s}^{-1}$

2.7b

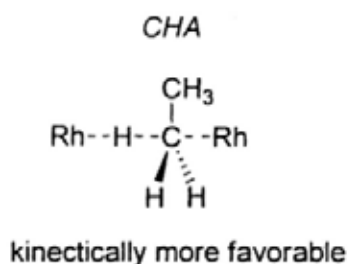


Figure 5.1a 4-Centered Transition State of CHA

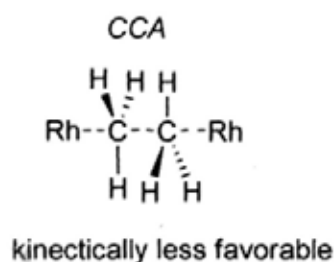


Figure 5.1b 4-Centered Transition State of CCA

$$\text{Rate of CCA} = k_1[\text{Rh}^{\text{II}}(\text{ttp})][\text{C}_2\text{H}_6]$$

$$\text{Rate of backward CCA} = k_{-1}[\text{Rh}^{\text{II}}(\text{ttp})\text{Me}][\cdot\text{CH}_3]$$

$$\text{Rate of CHA} = k_2[\text{Rh}^{\text{II}}(\text{ttp})]^2[\text{C}_2\text{H}_6]$$

So, the CCA of ethane is possible when  $k_1[\text{Rh}^{\text{II}}(\text{ttp})][\text{C}_2\text{H}_6] > k_{-1}[\text{Rh}^{\text{II}}(\text{ttp})\text{Me}][\cdot\text{CH}_3]$  and  $k_2[\text{Rh}^{\text{II}}(\text{ttp})]^2[\text{C}_2\text{H}_6]$  (Scheme 5.8).

## 5.6 Conclusion

The thermodynamics and kinetics of the CHA and CCA of alkanes with  $\text{Rh}(\text{ttp})\text{H}$  were considered. The CHA of cycloalkane is usually thermodynamically less favorable but kinetically more favorable while the CCA is thermodynamically more favorable but kinetically less favorable. The CCA of *c*-octane is spontaneous ( $\Delta G_{(\text{CCA}, 298)} < 0$ ). The ring opening CCA of *c*-octane is accounted by the relatively slow ring closure rate. The CCA of *n*-alkane with  $\text{Rh}(\text{ttp})\text{H}$  is spontaneous, but is not observed, possibly due to kinetic reasons.

## References

- (1) Luo, Y. R. *Comprehensive Handbook of Chemical Bond Energies*, CRC Press, Boca Raton, FL, 2007.
- (2) (a) Isaacs, N. S. *Physical Organic Chemistry*; Longman: Essex, 1987. (b) The BDE of C–C bonds are calculated based on the  $\Delta H_{\text{formation}}$ , see Stull, D. R.; Westrum, E. F. Jr.; Sinke, G. C. *The Chemical Thermodynamics of Organic Compounds*; John Wiley & Sons: New York 1969. (c) *CRC Handbook of Chemistry & Physics 84<sup>th</sup> Ed.*, Lide, D. R. Ed. 2004. (d) The C–C BDE of *c*-hexane is calculated to be 82.7 kcal mol<sup>-1</sup> and the literature reported value is 87.3 kcal mol<sup>-1</sup>. The C–C BDE of *c*-pentane is calculated to be 82.9 kcal mol<sup>-1</sup>. So, the C–C BDE of *c*-pentane is corrected by 4 kcal mol<sup>-1</sup> to 86.9 kcal mol<sup>-1</sup>.
- (3) Yaws, C. L. *Chemical Properties Handbook: Physical, Thermodynamic, Environmental, Transport, Safety, and Health Related Properties for Organic and Inorganic Chemicals*; McGraw-Hill: New York, 1999.
- (4) For exo- and endo-cyclization, see (a) Li, A.; Shtarev, A. B.; Smart, B. E.; Yang, Z. Y.; Luszyk, J. Ingold, K. U.; Bravo, A.; Dolbier, W. R. Jr. *J. Org. Chem.* **1999**, *64*, 5993-5999. For exo-cyclization, see (b) Newcomb, M. *Tetrahedron* **1993**, *49*, 1151-1176. (c) Walton, J. C. *Topics in Current Chemistry: Radicals in Synthesis II, Chapter Unusual Radical Cyclisations*; Springer Berlin: Heidelberg 2006. For anionic cyclization, see (d) Casadei, M. A.; Galli, C.; Mandolini, L. *J. Am. Chem. Soc.* **1984**, *106*, 1051-1056.
- (5) Stull, D. R.; Westrum, E. F. Jr.; Sinke, G. C. *The Chemical Thermodynamics of Organic Compounds*; John Wiley & Sons: New York 1969.
- (6) Johnson, M. D. *Acc. Chem. Res.* **1983**, *16*, 343-349.
- (7) (a) Zhang, X. X.; Wayland, B. B. *J. Am. Chem. Soc.* **1994**, *116*, 7897-7898. (b) Wayland, B. B.; Ba, S.; Sherry, A. E. *J. Am. Chem. Soc.* **1991**, *113*, 5305-5311.

## Chapter 6 Experimental Section

### 6.1 General Procedure

All materials were obtained from commercial suppliers and used without further purification unless otherwise specified. Benzene was distilled from sodium. Benzene- $d_6$  was vacuum distilled from sodium, degassed thrice by freeze-thaw-pump cycle and store in a Teflon scrawhead stoppered flask. Hexanes for chromatography were distilled from anhydrous calcium chloride. *N,N*-Dimethylformamide (DMF) was distilled from magnesium sulfate under reduced pressure. Tetrahydrofuran (THF) was distilled from sodium benzophenone ketyl prior to use. Ethers were distilled from sodium. Benzonitrile was distilled from anhydrous  $P_2O_5$ . Thin layer chromatography was performed on Merck pre-coated silica gel 60 F<sub>254</sub> plates. Silica gel (Merck, 70-230 and 230-400 mesh) was used for column chromatography.

### 6.2 Experimental Instrumentation

$^1H$  NMR spectra were recorded on a Bruker DPX 300 (300 MHz) spectrometer and a Bruker AvanceIII 400 (400 MHz). Spectra were referenced internally to the residual proton resonance in  $C_6D_6$  ( $\delta$  7.15 ppm) or  $CDCl_3$  ( $\delta$  7.26 ppm) or with tetramethylsilane (TMS,  $\delta$  0.00 ppm) as the internal standard. Chemical shifts ( $\delta$ ) are reported in parts per million (ppm).  $^{13}C$  NMR spectra were recorded on a Bruker DPX 300 (75 MHz) and a Bruker AvanceIII 400 (100 MHz) spectrometer and referenced to  $CDCl_3$  ( $\delta$  77.10 ppm) spectra. Coupling constants ( $J$ ) are reported in hertz (Hz). Mass spectra (HRMS) were performed on a Thermofinnigan MAT 95 XL instrument (FABMS).

GC-MS analysis was conducted on a GCMS-QP2010 Plus system using a Rtx-5MS column (30 m x 0.25 mm). The details of GC program are as follow:

The column oven temperature and injection temperature are 50.0 and 250.0 °C. Helium is used as carrier gas. Flow control mode is chosen as linear velocity (36.3 cm s<sup>-1</sup>) with pressure 53.5 kPa. The total flow, column flow and purge flow are 24.0, 1.0 and 3.0 mL min<sup>-1</sup>, respectively. Split mode injection with split ratio 20.0 is applied. After injection, the column oven temperature is kept at 50 °C for 5 minutes and then temperature is elevated at a rate of 20 °C min<sup>-1</sup> for 10 minutes until 250 °C. The temperature of 250 °C is kept for 5 minutes.

### 6.3 Experimental Procedure

#### Chapter 2

**Preparation of 5,10,15,20-Tetratolylporphyrin [H<sub>2</sub>ttp]<sup>1,2</sup>** Pyrrole (24 mL, 340 mmol) was added dropwise to a refluxing solution of tolylaldehyde (35 mL, 340 mmol) in propionic acid (1.25 L). The resulting mixture was refluxed in air for 30 minutes. The resulting black solution was cooled to room temperature, and MeOH (1.5 L) was added to obtain the solid purple porphyrin. The mixture was filtered and washed with MeOH. Purple powder (10.3 g, 15 mmol, 18 %) were obtained.  $R_f = 0.87$  (CH<sub>2</sub>Cl<sub>2</sub>). <sup>1</sup>H NMR (CDCl<sub>3</sub>, 300 MHz) δ -2.78 (s, 2 H), 2.71 (s, 12 H), 7.54 (d, 8 H,  $J = 8.0$  Hz), 8.08 (d, 8 H,  $J = 8.0$  Hz), 8.85 (s, 8 H).

**Preparation of 5,10,15,20-Tetraphenylporphyrin [H<sub>2</sub>tpp]<sup>1,2</sup>** Pyrrole (24 mL, 340 mmol) was added dropwise to a refluxing solution of benzaldehyde (35 mL, 344 mmol) in propionic acid (1.25 L). The resulting mixture was refluxed in air for 30 minutes. The resulting black solution was cooled to room temperature, and MeOH (1.5 L) was added to obtain the solid purple porphyrin. The mixture was filtered and washed with MeOH. Purple powder (8.3 g, 14 mmol, 16 %) were obtained.  $R_f = 0.87$  (CH<sub>2</sub>Cl<sub>2</sub>). <sup>1</sup>H NMR (CDCl<sub>3</sub>, 400 MHz) δ -2.77 (s, 2 H), 7.74 (d, 12 H,  $J = 8.0$  Hz), 8.23 (d, 8 H,  $J = 8.0$  Hz), 8.85 (s, 8 H).

**Preparation of 5,10,15,20-Tetra(4-*tert*-butylphenyl)porphyrin [H<sub>2</sub>(btpp)]<sup>2</sup>** Pyrrole (24 mL, 340 mmol) was added dropwise to a refluxing solution of 4-*tert*-benzaldehyde (55 g, 340

mmol) in propionic acid (1.25 L). The resulting mixture was refluxed in air for 30 minutes. The resulting black solution was cooled to room temperature, and MeOH (1.5 L) was added to obtain the solid purple porphyrin. The mixture was filtered and washed with MeOH. Purple powder (9.6 g, 11 mmol, 13 %) were obtained.  $R_f = 0.71$  (hexane/ $\text{CH}_2\text{Cl}_2 = 1:1$ ).  $^1\text{H}$  NMR ( $\text{CDCl}_3$ , 300 MHz)  $\delta$  -2.76 (s, 2 H), 1.60 (s, 36 H), 7.75 (d, 8 H,  $J = 8.2$  Hz), 8.14 (d, 8 H,  $J = 8.2$  Hz), 8.86 (s, 8 H).

**Preparation of 2,3,7,8,12,13,17,18-Octachloro-5,10,15,20-tetrakis-(*p*-tert-butylphenyl)porphyrin [ $\text{H}_2\text{bocp}$ ] $^2$**  A suspension of  $\text{H}_2(\text{btp})$  (2.00 g, 2.39 mmol) and  $\text{Ni}(\text{OAc})_2 \cdot 4\text{H}_2\text{O}$  (2.41 g, 4.80 mmol) in DMF (200 mL) was refluxed for 1.5 h. The color of the suspension changed from purple to reddish purple. The reaction mixture was cooled to room temperature and was worked up by extraction with  $\text{CHCl}_3/\text{H}_2\text{O}$ . The combined organic extract was rotary evaporated and the reddish purple residue obtained was purified by recrystallization with  $\text{CHCl}_3/\text{MeOH}$  to give reddish purple crystalline solids of 5,10,15,20-tetrakis(*p*-tert-butylphenyl)porphyrinato nickel(II)  $\text{Ni}(\text{btp})$  (1.91 g, 2.11 mmol, 89 %).

$\text{Ni}(\text{btp})$  (1.91 g, 2.11 mmol) and NCS (2.88 g, 21.6 mmol) were dissolved in *o*-dichlorobenzene (200 mL) and the mixture was heated at 140 °C for 3 h to give a red mixture. The solvent was then removed under high vacuum. The dark red residue was purified by flash column chromatography over neutral alumina using  $\text{CHCl}_3$  as the eluent. The second major red band was collected.  $\text{Ni}(\text{bocp})$  (1.96 g, 1.68 mmol, 80 %) was obtained after removal of solvent by rotary evaporation.

Concentrated sulfuric acid (200 mL) was then added to a solution of  $\text{Ni}(\text{bocp})$  (1.96 g, 1.68 mmol) in  $\text{CH}_2\text{Cl}_2$  (300 mL). The mixture was stirred at room temperature for 30 min. The resulting green suspension was then poured onto ice cubes and the mixture was extracted with  $\text{CH}_2\text{Cl}_2/\text{H}_2\text{O}$ . The combined green organic extract was neutralized with  $\text{Na}_2\text{CO}_3$ , washed with saturated NaCl solution, dried with  $\text{MgSO}_4$ , and filtered. The solvent was then removed

by rotary evaporation. The greenish blue crude product obtained was purified by column chromatography over silica gel using a solvent mixture of hexane/CH<sub>2</sub>Cl<sub>2</sub> (2:1) as the eluent. The fast moving brown fraction was discarded. The column was then eluted with CH<sub>2</sub>Cl<sub>2</sub> and the major green band was collected. After removal of solvent by rotary evaporation, greenish blue solids (1.02 g, 0.94 mmol, 56 %) were obtained.  $R_f = 0.26$  (hexane/CH<sub>2</sub>Cl<sub>2</sub> = 2:1). <sup>1</sup>H NMR (CDCl<sub>3</sub>, 300 MHz)  $\delta$  1.52 (s, 36 H), 7.74 (d, 8 H,  $J = 7.8$  Hz), 8.06 (d, 8 H,  $J = 7.8$  Hz).

**Preparation of 5,10,15,20-Tetratolylporphyrinatorhodium(III) Chloride, Rh(ttp)Cl.<sup>2</sup>**

H<sub>2</sub>ttp (350 mg, 0.51 mmol) and RhCl<sub>3</sub>·xH<sub>2</sub>O (206 mg, 1.00 mmol) were refluxed in PhCN (30 mL) in air for 3 h. The solvent was then removed under high vacuum and the crude product was purified by column chromatography over silica gel (70-230 mesh) eluting with a solvent mixture of hexane/CH<sub>2</sub>Cl<sub>2</sub> (1:1) then by pure CH<sub>2</sub>Cl<sub>2</sub>. The major red band was collected. After removal of solvent by rotary evaporation, red solids (373 mg, 0.39 mmol, 72 %) were obtained and were further purified by recrystallization from CH<sub>2</sub>Cl<sub>2</sub>/CH<sub>3</sub>OH.  $R_f = 0.30$  (CH<sub>2</sub>Cl<sub>2</sub>). <sup>1</sup>H NMR (CDCl<sub>3</sub>, 300 MHz)  $\delta$  2.70 (s, 12 H), 7.50-7.56 (m, 8 H), 8.07 (d, 4 H,  $J = 7.5$  Hz), 8.20 (d, 4 H,  $J = 7.5$  Hz) 8.94 (s, 8 H).

**Preparation of 5,10,15,20-Tetraphenylporphyrinatorhodium(III) Chloride, Rh(tpp)Cl.<sup>2</sup>**

H<sub>2</sub>tpp (350 mg, 0.51 mmol) and RhCl<sub>3</sub>·xH<sub>2</sub>O (206 mg, 1.00 mmol) were refluxed in PhCN (30 mL) in air for 3 h. The solvent was then removed under high vacuum and the crude product was purified by column chromatography over silica gel (70-230 mesh) eluting with a solvent mixture of hexane/CH<sub>2</sub>Cl<sub>2</sub> (1:1) then by pure CH<sub>2</sub>Cl<sub>2</sub>. The major red band was collected. After removal of solvent by rotary evaporation, red solids (373 mg, 0.39 mmol, 72 %) were obtained and were further purified by recrystallization from CH<sub>2</sub>Cl<sub>2</sub>/CH<sub>3</sub>OH.  $R_f = 0.30$  (CH<sub>2</sub>Cl<sub>2</sub>). <sup>1</sup>H NMR (CDCl<sub>3</sub>, 300 MHz)  $\delta$  7.75 (m, 12 H), 8.22 (d, 4 H,  $J = 7.5$  Hz), 8.28 (d, 4 H,  $J = 7.5$  Hz) 8.94 (s, 8 H).

**Preparation of 2,3,7,8,12,13,17,18-Octachloro-5,10,15,20-tetrakis-(*p*-tert-butylphenyl)porphyrinato](benzonitrile) rhodium(III) Chloride [Rh(bocp)Cl].<sup>2</sup>**

Rh(bocp)Cl was synthesized from H<sub>2</sub>bocp (500 mg, 0.45 mmol) and RhCl<sub>3</sub>·xH<sub>2</sub>O (142 mg, 0.54 mmol) by the same procedure as described for **1a**. The crude product was purified by column chromatography over silica gel using a solvent mixture of hexane/CH<sub>2</sub>Cl<sub>2</sub> (2:3) as the eluent. The fast moving green fraction was discarded and the major red fraction that eluted off with CH<sub>2</sub>Cl<sub>2</sub> was collected. After rotary evaporated to dryness, reddish brown solids (460 mg, 0.37 mmol, 82 %) were obtained.  $R_f = 0.62$  (hexane/CH<sub>2</sub>Cl<sub>2</sub> = 2:3); <sup>1</sup>H NMR (CDCl<sub>3</sub>, 300 MHz)  $\delta$  1.55 (s, 36 H), 5.69 (d, 2 H,  $J = 7.7$  Hz), 6.77 - 6.83 (m, 2 H), 7.12 (t, 1 H,  $J = 7.3$  Hz), 7.61 - 7.76 (m, 8 H), 8.01 (m, 8 H).

**Preparation of 5, 10, 15, 20-Tetratolylporphyrinatorhodium(III) Hydride [Rh(ttp)H] (**1d**).<sup>3,4</sup>** A suspension of Rh(ttp)Cl **3a** (100 mg, 0.11 mmol) in MeOH (50 mL) and a solution of NaBH<sub>4</sub> (17 mg, 0.45 mmol) in aq. NaOH (0.1 M, 2 mL) were purged with N<sub>2</sub> for 15 min separately. The solution of NaBH<sub>4</sub> was added slowly to the suspension of Rh(ttp)Cl via a cannula. The mixture was heated at 50 °C under N<sub>2</sub> for 1 h to give a brown solution. The solution was then cooled to 0 °C under N<sub>2</sub> and degassed 0.1 M HCl (40 mL) was added via a cannula. A brick red suspension was formed. After stirred at room temperature for another 15 min under N<sub>2</sub>, the brick red precipitate was collected after filtration and washing with water (2 x 10 mL) under N<sub>2</sub>. The brick red residues (80 mg, 0.10 mmol, 92 %) were obtained after vacuum dried. <sup>1</sup>H NMR (C<sub>6</sub>D<sub>6</sub>, 300 MHz)  $\delta$  -40.12 (d, 1 H,  $J_{\text{Rh-H}} = 43.5$  Hz), 2.42 (s, 12 H), 7.16 (d, 4 H,  $J = 8.2$  Hz), 7.35 (d, 4 H,  $J = 8.2$  Hz), 7.95 (d, 4 H,  $J = 8.1$  Hz), 8.22 (d, 4 H,  $J = 8.1$  Hz), 9.03 (s, 8 H).

**Preparation of Rh<sub>2</sub>(ttp)<sub>2</sub>**<sup>4</sup> Rh(ttp)H (10.0 mg, 0.013 mmol) was dissolved in degassed benzene (4.0 mL). The reaction mixture was then degassed by three freeze-pump-thaw method and refilled with N<sub>2</sub>. The solution was irradiated under a 400 W Hg-lamp at 6-11 °C

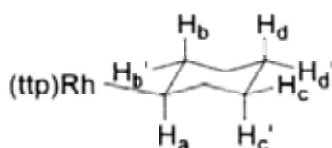
until all the starting material was consumed as indicated by TLC analysis (~10 h) to give  $\text{Rh}_2(\text{ttp})_2$  in quantitative yield.

**Preparation of  $\text{Rh}(\text{ttp})\text{Na}^+$**   $\text{Rh}(\text{ttp})\text{Ca}$  (10.0 mg, 0.013 mmol) was dissolved in degassed benzene (4.0 mL). The reaction mixture was then degassed by three freeze-pump-thaw method and refilled with  $\text{N}_2$ . Na/Hg was added into the reaction mixture. The reaction mixture was stirred at room temperature for 15 min. The resultant deep reddish brown solution was transferred via cannular under nitrogen atmosphere for subsequent reaction.  $\text{Rh}(\text{ttp})\text{Na}^+$  was formed quantitatively.

#### **Reaction of Alkanes with $\text{Rh}(\text{ttp})\text{Cl}$ (1a).**

##### **(5, 10, 15, 20-Tetratolylporphyrinato)(cyclohexyl) rhodium(III), $[\text{Rh}(\text{ttp})(c\text{-hexyl})]$ (2a).**

$\text{Rh}(\text{ttp})\text{Cl}$  (1a) (20.1 mg, 0.025 mmol) was added into *c*-hexane (3.0 mL). The red suspension was degassed for three freeze-thaw-pump cycles and was then heated at 120 °C under  $\text{N}_2$  in the dark for 24 hours. After 24 hours, the mixture turned into dark red. Excess *c*-hexane was removed by vacuum distillation. The dark red residue was then purified by column chromatography on silica gel eluting with a solvent mixture of hexane/ $\text{CH}_2\text{Cl}_2$  (4:1) to give  $\text{Rh}(\text{ttp})(c\text{-hexyl})$  (2a) as a red solid (6.6 mg, 0.007 mmol, 31%) which was further recrystallized from  $\text{CH}_2\text{Cl}_2/\text{MeOH}$ .  $R_f = 0.84$  (hexane/ $\text{CH}_2\text{Cl}_2 = 1:1$ ).  $^1\text{H}$  NMR ( $\text{CDCl}_3$ , 300 MHz)  $\delta$  -4.25 (m, 5 H,  $\text{H}_a$ ,  $\text{H}_b$  and  $\text{H}_b'$ ), -1.23 (q, 2 H,  $J = 12.3$  Hz,  $\text{H}_c'$ ), -0.95 (tq, 1 H,  $J = 3.3, 12.9$  Hz,  $\text{H}_d$ ), -0.58 (d, 2 H,  $J = 12.6$  Hz,  $\text{H}_c$ ), -0.08 (d, 1 H,  $J = 12.6$  Hz,  $\text{H}_d'$ ), 2.69 (s, 12 H, *p*-methyl), 7.52 (d, 8 H,  $J = 7.5$  Hz, *m*-phenyl), 8.01 (d, 4 H,  $J = 8.4$  Hz, *o'*-phenyl), 8.06 (d, 4 H,  $J = 7.8$  Hz, *o*-phenyl), 8.68 (s, 8 H, pyrrole).  $^{13}\text{C}$  NMR ( $\text{CDCl}_3$ , 75 MHz)  $\delta$  21.69, 25.17, 26.95, 33.36, 39.37 (d,  $^1J_{\text{Rh-C}} = 27.6$  Hz), 122.81, 127.40, 127.55, 130.88, 131.52, 131.71, 134.25, 137.23, 139.53, 143.40. Calcd. for  $(\text{C}_{54}\text{H}_{46}\text{N}_4\text{Rh})^+$ :  $m/z$  854.2850. Found:  $m/z$  854.2859. Anal. Calcd. for  $\text{C}_{54}\text{H}_{46}\text{N}_4\text{Rh}$ : C, 75.87; H, 5.54; N, 6.55. Found C, 75.41; H, 5.57; N, 6.50. Single crystal for X-ray diffraction analysis was grown from  $\text{CH}_2\text{Cl}_2/\text{methanol}$ .



**Reaction of Rh(ttp)Cl with *c*-Hexane at 80 °C.** Rh(ttp)Cl (**1a**) (20.2 mg, 0.025 mmol) was added into *c*-hexane (3.0 mL). The red suspension was degassed for three freeze-thaw-pump cycles and was then heated at 80 °C under N<sub>2</sub> in the dark for 24 hours. After 24 hours, the mixture turned into dark red. Excess *c*-hexane was removed by vacuum distillation. The dark red residue was then purified by column chromatography on silica gel eluting with a solvent mixture of hexane/CH<sub>2</sub>Cl<sub>2</sub> (4:1) to give Rh(ttp)(*c*-hexyl) (**2a**) as a red solid (0.2 mg, 0.00023 mmol, 1%).

**Reaction of Rh(ttp)Cl with *c*-Hexane at 100 °C.** Rh(ttp)Cl (**1a**) (19.9 mg, 0.025 mmol) was added into *c*-hexane (3.0 mL). The red suspension was degassed for three freeze-thaw-pump cycles and was then heated at 100 °C under N<sub>2</sub> in the dark for 24 hours. After 24 hours, the mixture turned into dark red. Excess *c*-hexane was removed by vacuum distillation. The dark red residue was then purified by column chromatography on silica gel eluting with a solvent mixture of hexane/CH<sub>2</sub>Cl<sub>2</sub> (4:1) to give Rh(ttp)(*c*-hexyl) (**2a**) as a red solid (0.6 mg, 0.00070 mmol, 3%).

**Reaction of Rh(ttp)Cl with *c*-Hexane at 150 °C.** Rh(ttp)Cl (**1a**) (20.0 mg, 0.025 mmol) was added into *c*-hexane (3.0 mL). The red suspension was degassed for three freeze-thaw-pump cycles and was then heated at 150 °C under N<sub>2</sub> in the dark for 24 hours. After 24 hours, the mixture turned into dark red. Excess *c*-hexane was removed by vacuum distillation. The dark red residue was then purified by column chromatography on silica gel eluting with a solvent mixture of hexane/CH<sub>2</sub>Cl<sub>2</sub> (4:1) to give Rh(ttp)(*c*-hexyl) (**2a**) as a red solid (3.4 mg, 0.0040 mmol, 16%).

**Reaction of Rh(ttp)Cl with *c*-Hexane at 200 °C.** Rh(ttp)Cl (**1a**) (20.0 mg, 0.025 mmol) was added into *c*-hexane (3.0 mL). The red suspension was degassed for three freeze-thaw-pump

cycles and was then heated at 200 °C under N<sub>2</sub> in the dark for 24 hours. After 24 hours, the mixture turned into dark red. Excess *c*-hexane was removed by vacuum distillation. The dark red residue was then purified by column chromatography on silica gel eluting with a solvent mixture of hexane/CH<sub>2</sub>Cl<sub>2</sub> (4:1) to give Rh(ttp)(*c*-hexyl) (**2a**) as a red solid (3.8 mg, 0.0045 mmol, 18%).

**Thermal Stability of Rh(ttp)(*c*-hexyl) (**2a**) at 120 °C.** Rh(ttp)(*c*-hexyl) (**2a**) (10.9 mg, 0.013 mmol) was added in *c*-hexane (3.0 mL). The red solution was degassed for three freeze-thaw-pump cycles and was heated at 120 °C under N<sub>2</sub> in the dark for 24 hours. Excess *c*-hexane was removed by vacuum distillation. The dark red residue was purified by column chromatography on silica gel with solvent mixture of hexane/CH<sub>2</sub>Cl<sub>2</sub> (4:1). Rh(ttp)(*c*-hexyl) (**2a**) as a red solid (8.7 mg, 0.010 mmol, 80%).

**Thermal Stability of Rh(ttp)(*c*-hexyl) (**2a**) at 150 °C.** Rh(ttp)(*c*-hexyl) (**2a**) (10.4 mg, 0.012 mmol) was added in *c*-hexane (3.0 mL). The red solution was degassed for three freeze-thaw-pump cycles and was heated at 150 °C under N<sub>2</sub> in the dark for 24 hours. Excess *c*-hexane was removed by vacuum distillation. The dark red residue was purified by column chromatography on silica gel with solvent mixture of hexane/CH<sub>2</sub>Cl<sub>2</sub> (4:1). Rh(ttp)(*c*-hexyl) (**2a**) as a red solid (4.3 mg, 0.005 mmol, 41%).

**Reaction of Rh(ttp)Cl and *c*-Hexane with K<sub>2</sub>CO<sub>3</sub>.** Rh(ttp)Cl (**1a**) (20.4 mg, 0.025 mmol) and anhydrous potassium carbonate (34.9 mg, 0.252 mmol) were added in *c*-hexane (3.0 mL). The red reaction mixture was degassed for three freeze-thaw-pump cycles and was heated at 120 °C under N<sub>2</sub> for 6 hours. Excess *c*-hexane was removed by vacuum distillation, the dark red crude product was extracted with CH<sub>2</sub>Cl<sub>2</sub>/H<sub>2</sub>O. The organic layer was collected, dried and evaporated to dryness and the residue was purified by column chromatography on silica gel eluting with a solvent mixture of hexane/CH<sub>2</sub>Cl<sub>2</sub> (4:1). Red solid, Rh(ttp)(*c*-hexyl) (**2a**) (12.7 mg, 0.015 mmol, 59%) was collected.

The *c*-hexane fraction removed by vacuum distillation was extracted with water (3.0 mL). The colourless organic layer was diluted by dichloromethane (3.0 mL) and then was injected for GC-MS analysis.

**Reaction of Rh(*ttp*)Cl and *c*-Hexane with NaOH.** Rh(*ttp*)Cl (**1a**) (20.4 mg, 0.025 mmol) and sodium hydroxide (10.1 mg, 0.252 mmol) were added in *c*-hexane (3.0 mL). The red reaction mixture was degassed for three freeze-thaw-pump cycles and was heated at 120 °C under N<sub>2</sub> for 6 hours. Excess *c*-hexane was removed by vacuum distillation, the dark red crude product was extracted with CH<sub>2</sub>Cl<sub>2</sub>/H<sub>2</sub>O. The organic layer was collected, dried and evaporated to dryness and the residue was purified by column chromatography on silica gel eluting with a solvent mixture of hexane/CH<sub>2</sub>Cl<sub>2</sub> (4:1). Red solid, Rh(*ttp*)(*c*-hexyl) (**2a**) was collected as the only product (10.2 mg, 0.012 mmol, 47%). The *c*-hexane fraction removed by vacuum distillation was extracted with water (3.0 mL). The colourless organic layer was diluted by dichloromethane (3.0 mL) and then was injected for GC-MS analysis.

**Reaction of Rh(*ttp*)Cl and *c*-Hexane with NaOAc.** Rh(*ttp*)Cl (**1a**) (20.1 mg, 0.025 mmol) and sodium acetate (20.4 mg, 0.249 mmol) were added in *c*-hexane (3.0 mL). The red reaction mixture was degassed for three freeze-thaw-pump cycles and was heated at 120 °C under N<sub>2</sub> for 6 hours. Excess *c*-hexane was removed by vacuum distillation, the dark red crude product was extracted with CH<sub>2</sub>Cl<sub>2</sub>/H<sub>2</sub>O. The organic layer was collected, dried and evaporated to dryness and the residue was purified by column chromatography on silica gel eluting with a solvent mixture of hexane/CH<sub>2</sub>Cl<sub>2</sub> (4:1) to give the red solid Rh(*ttp*)(*c*-hexyl) (**2a**) (10.9 mg, 0.013 mmol, 51%).

**Reaction of Rh(*ttp*)Cl and *c*-Hexane with 2,2'-Bipyridine.** Rh(*ttp*)Cl (**1a**) (20.6 mg, 0.026 mmol) and 2,2'-bipyridine (39.9 mg, 0.255 mmol) were added in *c*-hexane (3.0 mL). The red reaction mixture was degassed for three freeze-thaw-pump cycles and was heated at 120 °C under N<sub>2</sub> for 48 hours. Excess *c*-hexane was removed by vacuum distillation, the residue was

purified by column chromatography on silica gel eluting with a solvent mixture of hexane/CH<sub>2</sub>Cl<sub>2</sub> (4:1) to give the red solid, Rh(ttp)(*c*-hexyl) (**2a**) (11.0 mg, 0.013 mmol, 50%).

**Reaction of Rh(ttp)Cl and *c*-Hexane with 2,6-Diphenylpyridine.** Rh(ttp)Cl (**1a**) (19.8 mg, 0.025 mmol) and 2,6-diphenylpyridine (57.2 mg, 0.245 mmol) were added in *c*-hexane (3.0 mL). The red reaction mixture was degassed for three freeze-thaw-pump cycles and was heated at 120 °C under N<sub>2</sub> for 24 hours. Excess *c*-hexane was removed by vacuum distillation, the residue was purified by column chromatography on silica gel eluting with a solvent mixture of hexane/CH<sub>2</sub>Cl<sub>2</sub> (4:1) to give the red solid, Rh(ttp)(*c*-hexyl) (**2a**) (12.2 mg, 0.014 mmol, 58%).

**Reaction of Rh(ttp)Cl and *c*-Hexane with 2,6-di-*tert*-Butylpyridine.** Rh(ttp)Cl (**1a**) (19.7 mg, 0.024 mmol) and 2,6-di-*tert*-butylpyridine (46.4 mg, 54.5 μL, 0.243 mmol) were added in *c*-hexane (3.0 mL). The red reaction mixture was degassed for three freeze-thaw-pump cycles and was heated at 120 °C under N<sub>2</sub> for 24 hours after excess *c*-hexane was removed by vacuum distillation, the residue was then purified by column chromatography on silica gel eluting with a solvent mixture of hexane/CH<sub>2</sub>Cl<sub>2</sub> (4:1) to give the red solid, Rh(ttp)(*c*-hexyl) (**2a**) (10.3 mg, 0.012 mmol, 50%).

**Reaction of Rh(ttp)Cl and *c*-Hexane with K<sub>2</sub>CO<sub>3</sub> for 24 h.** Rh(ttp)Cl (**1a**) (20.1 mg, 0.025 mmol) and anhydrous potassium carbonate (34.7 mg, 0.252 mmol) were added in *c*-hexane (3.0 mL). The red reaction mixture was degassed for three freeze-thaw-pump cycles and was heated at 120 °C under N<sub>2</sub> for 24 hours. Excess *c*-hexane was removed by vacuum distillation, the dark red crude product was extracted with CH<sub>2</sub>Cl<sub>2</sub>/H<sub>2</sub>O. The organic layer was collected, dried and evaporated to dryness and the residue was purified by column chromatography on silica gel eluting with a solvent mixture of hexane/CH<sub>2</sub>Cl<sub>2</sub> (4:1). Red solid, Rh(ttp)(*c*-hexyl) (**2a**) (8.6 mg, 0.010 mmol, 40%) was collected

**Reaction of Rh(ttp)Cl and *c*-Hexane with 2,6-di-*tert*-Butylpyridine for 6 h.** Rh(ttp)Cl (**1a**) (20.3 mg, 0.025 mmol) and 2,6-diphenylpyridine (57.0 mg, 0.245 mmol) were added in *c*-hexane (3.0 mL). The red reaction mixture was degassed for three freeze-thaw-pump cycles and was heated at 120 °C under N<sub>2</sub> for 6 hours. Excess *c*-hexane was removed by vacuum distillation, the residue was purified by column chromatography on silica gel eluting with a solvent mixture of hexane/CH<sub>2</sub>Cl<sub>2</sub> (4:1) to give the red solid, Rh(ttp)(*c*-hexyl) (**2a**) (4.9 mg, 0.0057 mmol, 23%).

**Chloro(5, 10, 15, 20-Tetratolylporphyrinato)(triphenylphosphine)rhodium(III), [Rh(ttp)Cl(PPh<sub>3</sub>)] (**2f**).** Rh(ttp)Cl (**1a**) (19.9 mg, 0.025 mmol) and triphenylphosphine (64.7 mg, 0.247 mmol) were added in *c*-hexane (3.0 mL). The red reaction mixture was degassed for three freeze-thaw-pump cycles and was heated at 120 °C under N<sub>2</sub> for 24 hours. Excess *c*-hexane was removed by vacuum distillation, the residue was purified by column chromatography on silica gel eluting with ethyl acetate to give Rh(ttp)Cl(PPh<sub>3</sub>) (**2f**) (21.9 mg, 0.021 mmol, 83%). *R<sub>f</sub>* = 0.65 (ethyl acetate). <sup>1</sup>H NMR (CDCl<sub>3</sub>, 300 MHz) δ 2.68 (s, 12 H, *p*-methyl), 3.84 (dd, 6 H, *J* = 7.6, 10.7 Hz, *m*-phenyl of PPh<sub>3</sub>), 6.51 (td, 6 H, *J* = 2.2, 7.8 Hz, *o*-phenyl of PPh<sub>3</sub>), 6.90 (td, 3 H, *J* = 5.3, 11.2 Hz, *p*-phenyl of PPh<sub>3</sub>), 7.49 (d, 8 H, *J* = 8.0 Hz, *m*-phenyl), 7.66 (d, 4 H, *J* = 7.6 Hz, *o*'-phenyl), 8.04 (d, 4 H, *J* = 7.49 Hz, *o*-phenyl), 8.72 (s, 8 H, pyrrole). <sup>13</sup>C NMR (CDCl<sub>3</sub>, 75 MHz) δ 21.63, 121.63, 126.79, 126.92, 127.00, 127.66, 129.36, 131.02, 131.14, 132.15, 132.65, 134.16, 135.05, 137.05, 139.31, 142.75. Calcd. for (C<sub>66</sub>H<sub>51</sub>N<sub>4</sub>PRh)<sup>+</sup>: *m/z* 1033.2901. Found: *m/z* 1033.2885.

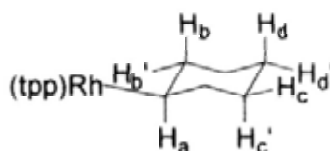
**Investigation of Base Loading in CHA of *c*-Hexane (5 equiv of K<sub>2</sub>CO<sub>3</sub>).** Rh(ttp)Cl (**1a**) (20.3 mg, 0.025 mmol) and anhydrous potassium carbonate (34.9 mg, 0.126 mmol) were added in *c*-hexane (3.0 mL). The red reaction mixture was degassed for three freeze-thaw-pump cycles and was heated at 120 °C under N<sub>2</sub> for 24 hours. Excess *c*-hexane was removed by vacuum distillation, the dark red crude product was extracted with CH<sub>2</sub>Cl<sub>2</sub>/H<sub>2</sub>O. The

organic layer was collected, dried and evaporated to dryness and the residue was purified by column chromatography on silica gel eluting with a solvent mixture of hexane/CH<sub>2</sub>Cl<sub>2</sub> (4:1). Red solid, Rh(tp)(*c*-hexyl) (**2a**) (7.5 mg, 0.0088 mmol, 35%) was collected.

**Investigation of Base Loading in CHA of *c*-Hexane (20 equiv of K<sub>2</sub>CO<sub>3</sub>).** Rh(tp)Cl (**1a**) (20.1 mg, 0.025 mmol) and anhydrous potassium carbonate (68.8 mg, 0.498 mmol) were added in *c*-hexane (3.0 mL). The red reaction mixture was degassed for three freeze-thaw-pump cycles and was heated at 120 °C under N<sub>2</sub> for 6 hours. Excess *c*-hexane was removed by vacuum distillation, the dark red crude product was extracted with CH<sub>2</sub>Cl<sub>2</sub>/H<sub>2</sub>O. The organic layer was collected, dried and evaporated to dryness and the residue was purified by column chromatography on silica gel eluting with a solvent mixture of hexane/CH<sub>2</sub>Cl<sub>2</sub> (4:1). Red solid, Rh(tp)(*c*-hexyl) (**2a**) (11.9 mg, 0.014 mmol, 56%) was collected.

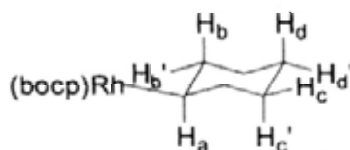
**(5, 10, 15, 20-Tetraphenylporphyrinato)(cyclohexyl)rhodium(III), [Rh(tp)(*c*-hexyl)] (**4a**).** Rh(tp)Cl (**1b**)<sup>25,26</sup> (20.2 mg, 0.027 mmol) and anhydrous potassium carbonate (37.2 mg, 0.269 mmol) were added in *c*-hexane (3.0 mL) and formed a bright red reaction mixture. The bright red reaction mixture was degassed for three freeze-thaw-pump cycles and was heated at 120 °C under N<sub>2</sub> in the dark for 5 hours. After 5 hours, the mixture turned into dark red. Excess *c*-hexane was removed by vacuum distillation. The dark red residue was extracted with CH<sub>2</sub>Cl<sub>2</sub>/H<sub>2</sub>O. The organic layer was collected, dried and evaporated to dryness and then purified by column chromatography on silica gel eluting with a solvent mixture of hexane/CH<sub>2</sub>Cl<sub>2</sub> (4:1). Rh(tp)(*c*-hexyl) (**4a**) was collected as a red solid was collected (11.2 mg, 0.014 mmol, 52%), *R<sub>f</sub>* = 0.83 (hexane/CH<sub>2</sub>Cl<sub>2</sub> = 1:1). <sup>1</sup>H NMR (CDCl<sub>3</sub>, 300 MHz) δ -4.26 (m, 5 H, H<sub>a</sub>, H<sub>b</sub> and H<sub>b</sub>'), -1.21 (q, 2 H, *J* = 12.3 Hz, H<sub>c</sub>'), -0.94 (tq, 1 H, *J* = 3.3, 12.9 Hz, H<sub>d</sub>), -0.56 (d, 2 H, *J* = 11.4 Hz, H<sub>c</sub>), -0.07 (d, 1 H, *J* = 12.9 Hz, H<sub>d</sub>'), 7.50 (m, 8 H, *m*-phenyl), 8.13 (d, 4 H, *J* = 4.5 Hz, *o*'-phenyl), 8.19 (d, 4 H, *J* = 6.6 Hz, *o*-phenyl), 8.67 (s, 8 H, pyrrole). <sup>13</sup>C NMR (CDCl<sub>3</sub>, 75 MHz) δ 25.14, 26.95, 33.39, 39.65 (d, <sup>1</sup>*J*<sub>Rh-C</sub> = 29.5 Hz),

122.87, 126.70, 126.84, 127.69, 131.61, 133.78, 134.34, 142.39, 143.30. Calcd. for  $(C_{50}H_{39}N_4Rh)^+$ :  $m/z$  798.2224 Found:  $m/z$  798.2171. Anal. Calcd. for  $C_{50}H_{39}N_4Rh$ : C, 75.18; H, 4.92; N, 7.01; Found C, 74.68; H, 4.89; N, 6.70.



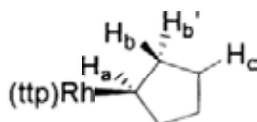
**[2,3,7,8,12,13,17,18-Octachloro-5,10,15,20-tetrakis(*p*-tert-butylphenyl)porphyrinato]**

**(cyclohexyl)rhodium(III), Rh(bocp)(*c*-hexyl) (4b).** Rh(bocp)Cl (**1c**)<sup>25,26</sup> (21.7 mg, 0.017 mmol) and anhydrous potassium carbonate (24.0 mg, 0.174 mmol) were added in *c*-hexane (3.0 mL) and formed a bright red reaction mixture. The bright red reaction mixture was degassed for three freeze-thaw-pump cycles and was heated at 120 °C under N<sub>2</sub> in the dark for 1 hour. After 1 hour, the mixture turned into dark red. Excess *c*-hexane was removed by vacuum distillation. The dark red residue was extracted with CH<sub>2</sub>Cl<sub>2</sub>/H<sub>2</sub>O. The organic layer was collected, dried and evaporated to dryness and then purified by column chromatography on silica gel eluting with a solvent mixture of hexane/CH<sub>2</sub>Cl<sub>2</sub> (4:1) to give the red solid, Rh(bocp)(*c*-hexyl) (**4b**) (13.8 mg, 0.011 mmol, 61%).  $R_f = 0.86$  (hexane/CH<sub>2</sub>Cl<sub>2</sub> = 1:1). <sup>1</sup>H NMR (CDCl<sub>3</sub>, 300 MHz)  $\delta$  -3.63 (q, 2 H,  $J = 9.6$  Hz, H<sub>b</sub>), -3.46 (q, 2 H,  $J = 9.3$  Hz, H<sub>b'</sub>), -3.17 (td, 1 H,  $J = 3.0, 9.0$  Hz, H<sub>a</sub>), -0.85 (q, 2 H,  $J = 12.3$  Hz, H<sub>c'</sub>), -0.71 (t, 1 H,  $J = 12.9$  Hz, H<sub>d</sub>), -0.25 (d, 2 H,  $J = 12.0$  Hz, H<sub>c</sub>), 1.36 (d, 1 H,  $J = 12.0$  Hz, H<sub>d'</sub>), 1.55 (s, 36 H, <sup>t</sup>Bu), 7.70 (d, 8 H,  $J = 8.7$  Hz, *m*-phenyl), 8.54 (d, 4 H,  $J = 7.2$  Hz, *o'*-phenyl), 7.95 (d, 4 H,  $J = 7.2$  Hz, *o*-phenyl). <sup>13</sup>C NMR (CDCl<sub>3</sub>, 75 MHz)  $\delta$  25.18, 27.61, 29.86, 31.85, 35.11, 35.78, 122.56, 124.71, 133.02, 134.05, 134.73, 138.11, 152.76. Calcd. for  $(C_{66}H_{63}N_4Cl_8Rh)^+$ :  $m/z$  1298.1551 Found:  $m/z$  1298.1519. Anal. Calcd. for  $C_{66}H_{63}N_4Cl_8Rh$ : C, 61.04; H, 4.89; N, 4.31; Found C, 61.11; H, 5.05; N, 4.19.



**(5, 10, 15, 20-Tetratolylporphyrinato)(cyclopentyl)rhodium(III), [Rh(ttp)(c-pentyl)] (2b).**

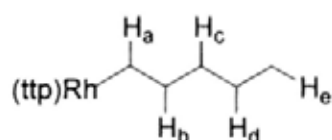
Rh(ttp)Cl (**1a**) (20.0 mg, 0.025 mmol) and anhydrous potassium carbonate (34.2 mg, 0.248 mmol) were added in *c*-pentane (3.0 mL). The red reaction mixture was degassed for three freeze-thaw-pump cycles and was heated at 120 °C under N<sub>2</sub> in the dark for 6 hours. Excess *c*-pentane was removed by vacuum distillation. The dark red crude product was extracted with CH<sub>2</sub>Cl<sub>2</sub>/H<sub>2</sub>O. The organic layer was collected, dried and evaporated to dryness and then residue was purified by column chromatography on silica gel eluting with a solvent mixture of hexane/CH<sub>2</sub>Cl<sub>2</sub> (4:1). The red solid of Rh(ttp)(*c*-pentyl) (**2b**) was collected (16.0 mg, 0.017 mmol, 75%). *R<sub>f</sub>* = 0.85 (hexane/CH<sub>2</sub>Cl<sub>2</sub> = 1:1). <sup>1</sup>H NMR (CDCl<sub>3</sub>, 300 MHz) δ -4.90 (m, 2 H, H<sub>b</sub>), -4.37 (m, 1 H, H<sub>a</sub>), -3.46 (m, 2 H, H<sub>b'</sub>), -1.03 (m, 4 H, H<sub>c</sub>), 2.69 (s, 12 H, *p*-methyl), 7.52 (t, 8 H, *J* = 6.2 Hz, *m*-phenyl), 8.00 (d, 4 H, *J* = 8.5 Hz, *o'*-phenyl), 8.09 (d, 4 H, *J* = 8.6 Hz, *o*-phenyl), 8.69 (s, 8 H, pyrrole). <sup>13</sup>C NMR (CDCl<sub>3</sub>, 75 MHz) δ 18.87, 22.14, 29.52, 34.53, 123.20, 127.86, 127.92, 131.91, 134.19, 134.61, 137.69, 139.94, 143.93. Calcd. for (C<sub>53</sub>H<sub>45</sub>N<sub>4</sub>Rh)<sup>+</sup>: *m/z* 840.2694. Found: *m/z* 840.2694. Anal. Calcd. for C<sub>53</sub>H<sub>45</sub>N<sub>4</sub>Rh: C, 75.71; H, 5.39; N, 6.66. Found C, 75.29; H, 5.37; N, 6.53. Single crystal for X-ray diffraction analysis was grown from CH<sub>2</sub>Cl<sub>2</sub>/ethanol.



**(5, 10, 15, 20-Tetratolylporphyrinato)(*n*-pentyl)rhodium(III), [Rh(ttp)(*n*-pentyl)] (2c).**

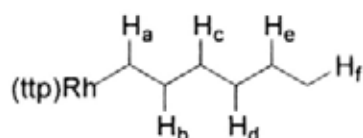
Rh(ttp)Cl (**1a**) (20.4 mg, 0.025 mmol) and anhydrous potassium carbonate (34.9 mg, 0.252 mmol) were added in *n*-pentane (3.0 mL) and formed a bright red reaction mixture. The bright red reaction mixture was degassed for three freeze-thaw-pump cycles and was heated

at 120 °C under N<sub>2</sub> in the dark for 24 hours. After 24 hours, the mixture turned into dark red. Excess *n*-pentane was removed by vacuum distillation. The dark red residue was extracted with CH<sub>2</sub>Cl<sub>2</sub>/H<sub>2</sub>O. The organic layer was collected, dried and evaporated to dryness and then purified by column chromatography on silica gel eluting with a solvent mixture of hexane/CH<sub>2</sub>Cl<sub>2</sub> (4:1). Rh(ttp)(*n*-pentyl) (**2c**) was collected as the major product. Red solid, Rh(ttp)(*n*-pentyl) (**2c**), was collected (6.5 mg, 0.008 mmol, 31%). *R<sub>f</sub>* = 0.78 (hexane/CH<sub>2</sub>Cl<sub>2</sub> = 1:1). <sup>1</sup>H NMR (CDCl<sub>3</sub>, 300 MHz) δ -4.97 (td, 2 H, *J* = 2.4, 7.5 Hz, H<sub>a</sub>), -4.50 (qu, 2 H, *J* = 7.2 Hz, H<sub>b</sub>), -1.59 (qu, 2 H, *J* = 2.1 Hz, H<sub>c</sub>), -0.49 (q, 2 H, *J* = 6.9 Hz, H<sub>d</sub>), -0.25 (t, 3 H, *J* = 7.2 Hz, H<sub>e</sub>), 2.69 (s, 12 H, *p*-methyl), 7.53 (t, 8 H, *J* = 6.0 Hz, *m*-phenyl), 7.98 (d, 4 H, *J* = 8.6 Hz, *o*-phenyl), 8.08 (d, 4 H, *J* = 8.3 Hz, *o*-phenyl), 8.70 (s, 8 H, pyrrole) <sup>13</sup>C NMR (CDCl<sub>3</sub>, 75 MHz) δ 12.81, 15.66 (d, <sup>1</sup>*J*<sub>Rh-C</sub> = 27.2 Hz), 20.72, 21.69, 26.86, 28.50, 122.51, 127.47, 127.52, 131.49, 133.81, 134.10, 137.25, 139.50, 143.37 Calcd. for (C<sub>53</sub>H<sub>47</sub>N<sub>4</sub>Rh)<sup>+</sup>: *m/z* 840.2694. Found: *m/z* 840.2682. Anal. Calcd. for C<sub>53</sub>H<sub>47</sub>N<sub>4</sub>Rh: C, 75.52; H, 5.62; N, 6.64; Found C, 75.43; H, 5.67; N, 6.36. (qu = quintet)



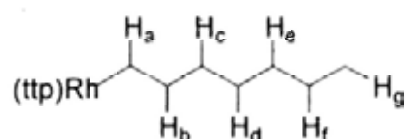
**(5, 10, 15, 20-Tetratolylporphyrinato)(*n*-hexyl)rhodium(III), [Rh(ttp)(*n*-hexyl)] (**2d**).** Rh(ttp)Cl (**1a**) (20.6 mg, 0.026 mmol) and anhydrous potassium carbonate (35.3 mg, 0.255 mmol) were added in *n*-hexane (3.0 mL) and formed a bright red reaction mixture. The bright red reaction mixture was degassed for three freeze-thaw-pump cycles and was heated at 120 °C under N<sub>2</sub> in the dark for 24 hours. After 24 hours, the mixture turned into dark red. Excess *n*-hexane was removed by vacuum distillation. The dark red residue was extracted with CH<sub>2</sub>Cl<sub>2</sub>/H<sub>2</sub>O. The organic layer was collected, dried and evaporated to dryness and then purified by column chromatography on silica gel with a solvent mixture of hexane/CH<sub>2</sub>Cl<sub>2</sub>

(4:1). Rh(ttp)(*n*-hexyl) (**2d**) was collected as the major product. The red solid of Rh(ttp)(*n*-hexyl) (**2d**), was collected (10.6 mg, 0.012 mmol, 49%).  $R_f = 0.84$  (hexane/CH<sub>2</sub>Cl<sub>2</sub> = 1:1). <sup>1</sup>H NMR (CDCl<sub>3</sub>, 300 MHz) δ -4.96 (td, 2 H,  $J = 3.0, 9.0$  Hz, H<sub>a</sub>), -4.51 (qu, 2 H,  $J = 7.8$  Hz, H<sub>b</sub>), -1.58 (qu, 2 H,  $J = 7.5$  Hz, H<sub>c</sub>), -0.57 (qu, 2 H,  $J = 7.5$  Hz, H<sub>d</sub>), 0.10 (m, 2 H, H<sub>e</sub>), 0.17 (t, 3 H,  $J = 7.2$  Hz, H<sub>f</sub>), 2.68 (s, 12 H, *p*-methyl), 7.52 (d, 4 H,  $J = 5.7$  Hz, *m'*-phenyl), 7.54 (d, 4 H,  $J = 5.7$  Hz, *m*-phenyl), 7.97 (d, 4 H,  $J = 7.2$  Hz, *o'*-phenyl), 8.06 (d, 4 H,  $J = 8.3$  Hz, *o*-phenyl), 8.69 (s, 8 H, pyrrole) <sup>13</sup>C NMR (CDCl<sub>3</sub>, 75 MHz) δ 13.53, 15.69 (d,  $^1J_{\text{Rh-C}} = 27.2$  Hz), 21.40, 21.69, 26.06, 27.13, 29.84, 122.53, 127.47, 130.89, 131.51, 131.85, 133.83, 134.11, 137.25, 139.52, 143.39 Calcd. for (C<sub>54</sub>H<sub>49</sub>N<sub>4</sub>Rh)<sup>+</sup>:  $m/z$  856.3007. Found:  $m/z$  856.3017. Anal. Calcd. for C<sub>54</sub>H<sub>49</sub>N<sub>4</sub>Rh: C, 75.69; H, 5.76; N, 6.54; Found C, 75.61; H, 5.72; N, 6.53.



(5, 10, 15, 20-Tetratolyporphyrinato)(*n*-heptyl)rhodium(III), [Rh(ttp)(*n*-heptyl)] (**2e**). Rh(ttp)Cl (**1a**) (20.9 mg, 0.026 mmol) and anhydrous potassium carbonate (35.3 mg, 0.255 mmol) were added in *n*-heptane (3.0 mL) and formed a bright red reaction mixture. The bright red reaction mixture was degassed for three freeze-thaw-pump cycles and was heated at 120 °C under N<sub>2</sub> in the dark for 24 hours. After 24 hours, the mixture turned into dark red. Excess *n*-heptane was removed by vacuum distillation. The dark red residue was extracted with CH<sub>2</sub>Cl<sub>2</sub>/H<sub>2</sub>O. The organic layer was collected, dried and evaporated to dryness and then purified by column chromatography on silica gel with a solvent mixture of hexane/CH<sub>2</sub>Cl<sub>2</sub> (4:1). Rh(ttp)(*n*-heptyl) (**2e**) was collected as the major product. Red solid, Rh(ttp)(*n*-heptyl) (**2e**), was collected (13.2 mg, 0.015 mmol, 59%).  $R_f = 0.83$  (hexane/CH<sub>2</sub>Cl<sub>2</sub> = 1:1). <sup>1</sup>H NMR (CDCl<sub>3</sub>, 300 MHz) δ -4.97 (td, 2 H,  $J = 3.0, 8.7$  Hz, H<sub>a</sub>), -4.53 (qu, 2 H,  $J = 7.2$  Hz, H<sub>b</sub>), -1.63

(qu, 2 H,  $J = 7.2$  Hz,  $H_c$ ), -0.55 (qu, 2 H,  $J = 7.2$  Hz,  $H_d$ ), -0.04 (d, 2 H,  $J = 9.0$  Hz,  $H_e$ ), 0.45 (q, 3 H,  $J = 6.0$  Hz,  $H_g$ ), 0.52 (qu, 2 H,  $J = 7.2$  Hz,  $H_f$ ), 2.69 (s, 12 H, *p*-methyl), 7.51 (d, 4 H,  $J = 6.6$  Hz, *m*'-phenyl), 7.53 (d, 4 H,  $J = 6.3$  Hz, *m*-phenyl), 7.98 (d, 4 H,  $J = 6.9$  Hz, *o*'-phenyl), 8.08 (d, 4 H,  $J = 7.2$  Hz, *o*-phenyl), 8.70 (s, 8 H, pyrrole)  $^{13}\text{C}$  NMR ( $\text{CDCl}_3$ , 75 MHz)  $\delta$  13.89, 15.71 (d,  $^1J_{\text{Rh-C}} = 27.5$  Hz), 21.69, 22.10, 26.25, 27.06, 27.24, 30.57, 122.52, 126.22, 127.45, 127.52, 131.49, 133.80, 134.11, 137.23, 139.51, 143.38 Calcd. for  $(\text{C}_{55}\text{H}_{51}\text{N}_4\text{Rh})^+$ :  $m/z$  870.3163 Found:  $m/z$  870.3167. Anal. Calcd. for  $\text{C}_{55}\text{H}_{51}\text{N}_4\text{Rh}$ : C, 75.85; H, 5.90; N, 6.43; Found C, 75.77; H, 5.96; N, 6.31. Single crystal for X-ray diffraction analysis was grown from  $\text{CH}_2\text{Cl}_2/\text{methanol}$ .



**Decomposition of Rh(*ttp*)(*c*-pentyl) (2b) with  $\text{K}_2\text{CO}_3$  in Benzene- $d_6$ .** Rh(*ttp*)(*c*-pentyl) (6.7 mg, 0.0080 mmol) and potassium carbonate (11.0 mg, 0.080 mmol) were added into benzene- $d_6$  (520  $\mu\text{L}$ ) in a NMR tube. The red reaction mixture was degassed for three freeze-thaw-pump cycles and the NMR tube was sealed under vacuum. It was heated to 120  $^\circ\text{C}$  and the reaction mixture was monitored with  $^1\text{H}$  NMR spectroscopy and NMR yields were taken.

For the observation of Rh(*ttp*)H, dilute HCl solution was added into the NMR tube with shaking. It was brought to take a  $^1\text{H}$  NMR spectrum immediately after the addition of dilute HCl.

**Decomposition of Rh(*ttp*)(*c*-hexyl) (2a) with  $\text{K}_2\text{CO}_3$  in Benzene- $d_6$ .** Rh(*ttp*)(*c*-hexyl) (6.9 mg, 0.0081 mmol) and potassium carbonate (11.0 mg, 0.080 mmol) were added into benzene- $d_6$  (520  $\mu\text{L}$ ) in a NMR tube. The red reaction mixture was degassed for three freeze-thaw-pump cycles and the NMR tube was sealed under vacuum. It was heated to 120  $^\circ\text{C}$  and the reaction mixture was monitored with  $^1\text{H}$  NMR spectroscopy and NMR yields were taken.

**Decomposition of Rh(tp)(*n*-hexyl) (2d) with K<sub>2</sub>CO<sub>3</sub> in Benzene-*d*<sub>6</sub>.** Rh(tp)(*n*-hexyl) (6.9 mg, 0.0081 mmol) and potassium carbonate (11.0 mg, 0.080 mmol) were added into benzene-*d*<sub>6</sub> (520 μL) in a NMR tube. The red reaction mixture was degassed for three freeze-thaw-pump cycles and the NMR tube was sealed under vacuum. It was heated to 120 °C and the reaction mixture was monitored with <sup>1</sup>H NMR spectroscopy and NMR yields were taken.

**Sealed NMR Tube Experiment of Rh(tp)Cl and *c*-hexane in Benzene-*d*<sub>6</sub>.** Rh(tp)Cl (1a) (5.1 mg, 0.0066 mmol) and *c*-hexane (34 μL, 0.316 mmol) were added into benzene-*d*<sub>6</sub> (520 μL) in a NMR tube. The red mixture was degassed for three freeze-thaw-pump cycles and the NMR tube was sealed under vacuum. It was heated at 120 °C in the dark. It was monitored with <sup>1</sup>H NMR spectroscopy at particular time intervals and the NMR yields were taken.

**Sealed NMR Tube Experiment of Rh(tp)Cl and *c*-hexane with K<sub>2</sub>CO<sub>3</sub> in Benzene-*d*<sub>6</sub>.** Rh(tp)Cl (1a) (5.1 mg, 0.0066 mmol), *c*-hexane (34 μL, 0.316 mmol) and K<sub>2</sub>CO<sub>3</sub> (8.7 mg, 0.063 mmol) were added into benzene-*d*<sub>6</sub> (520 μL) in a NMR tube. The red mixture was degassed for three freeze-thaw-pump cycles and the NMR tube was sealed under vacuum. It was heated at 120 °C in the dark. It was monitored with <sup>1</sup>H NMR spectroscopy at particular time intervals and the NMR yields were taken.

**Reaction of Rh(tp)H with KOH.** Rh(tp)H (1d) (8.0 mg, 0.010 mmol) and potassium hydroxide (14.3 mg, 0.104 mmol) were added into degassed benzene-*d*<sub>6</sub> (520 μL) in NMR tube. The reaction mixture was degassed for three freeze-thaw-pump cycles and the NMR tube was sealed under vacuum. The reaction mixture was then warmed to 23 °C in a water bath for 15 minutes. It was brought to <sup>1</sup>H NMR spectroscopy. Rh<sub>2</sub>(tp)<sub>2</sub> was obtained (55% NMR yield).

**Thermal Stability of Rh(tp)H.** Rh(tp)H (1d) (7.9 mg, 0.010 mmol) and was added into degassed benzene-*d*<sub>6</sub> (520 μL) in NMR tube. The reaction mixture was degassed for three freeze-thaw-pump cycles and the NMR tube was sealed under vacuum. The reaction mixture

was then heated to 120 °C for 6 days. It was brought to <sup>1</sup>H NMR spectroscopy. The NMR yield of Rh(tp)H was found to be 90%.

**Reaction of Alkanes with Rh(tp)H (1d).** Rh(tp)H (1d) (10.0 mg, 0.013 mmol) was added into *c*-hexane (3.0 mL). The red suspension was degassed for three freeze-thaw-pump cycles and was then heated at 120 °C under N<sub>2</sub> in the dark for 3 hours. After 3 hours, the mixture turned into red. Excess *c*-hexane was removed by vacuum distillation. The dark red residue was then purified by column chromatography on silica gel eluting with a solvent mixture of hexane/CH<sub>2</sub>Cl<sub>2</sub> (4:1) to give Rh(tp)(*c*-hexyl) (2a) as a red solid (4.0 mg, 0.0047 mmol, 36%).

**Competition Reaction of *c*-hexane and *c*-hexane-*d*<sub>12</sub> with Rh(tp)Cl (1a) with K<sub>2</sub>CO<sub>3</sub>.** Rh(tp)Cl (1a) (19.6 mg, 0.021 mmol) and potassium carbonate (33.6 mg, 0.243 mmol) were added into mixture of *c*-hexane (1.50 ml, 14.000 mmol) and *c*-hexane-*d*<sub>12</sub> (1.49 ml, 14.000 mmol). The red mixture was degassed for three freeze-thaw-pump cycles and was heated at 120 °C under N<sub>2</sub> in the dark for 6 hours. Then excess *c*-hexane/*c*-hexane-*d*<sub>12</sub> mixture was removed by vacuum distillation. Part of the red residue (0.2 mg) was taken to the mass spectroscopy to obtain the ratio of the two products. The remaining crude product was brought to <sup>1</sup>H NMR spectroscopy for product ratio. It was then extracted with CH<sub>2</sub>Cl<sub>2</sub>/H<sub>2</sub>O and purified by column chromatography on silica gel eluting with a solvent mixture of hexane/CH<sub>2</sub>Cl<sub>2</sub> (4:1). The red fraction was collected. After rotary evaporation, product mixture of Rh(tp)(*c*-hexyl) (2a) and Rh(tp)(*c*-hexyl)-*d*<sub>11</sub> was obtained as a red solid (6.7 mg, 0.0078 mmol, 32%).

The product ratio was calculated as follow:

(i) <sup>1</sup>H NMR

Integration of alkyl proton of Rh(tp)(*c*-hexyl) at  $\delta = -4.26$  (observed = 5.193) and integration of alkyl proton of the Rh(tp)(*c*-hexyl)/Rh(tp)(*c*-hexyl)-*d*<sub>11</sub>  $\delta = -4.26$  (observed = 4.680) were

used to calculate the ratio with the integration of pyrrole signal of **2a** ( $\delta = 8.63$ ) was taken as 8. Let the integration of that alkyl deuterium be  $Y$ .  $Y$  is equal to the integration of that alkyl proton without deuterium incorporation (5.193) minus the observed integration of that alkyl proton with deuterium incorporation (4.680).  $k_H/k_D$  is equal to the integration of alkyl proton (4.680) over the integration of alkyl deuterium (5.193-4.680). The calculated  $k_H/k_D$  is 9.1( $\pm 0.3$ ).

(ii) MS method:

The product ratio is calculated to be the molecular peak intensity of Rh(tpp)(*c*-hexyl) (observed to be 60.0) over the molecular peak intensity of Rh(tpp)(*c*-hexyl)- $d_{11}$  (observed to be 6.1). The product ratio is calculated to be 9.7( $\pm 0.2$ ).

**Alkyl exchange of Rh(tpp)(*c*-hexyl) (**2a**) with *c*-hexane- $d_{12}$  at 120 °C.** Rh(tpp)(*c*-hexyl) (**2a**) (5.4 mg, 0.0063 mmol) was added with cyclohexane- $d_{12}$  (0.5 mL) in a Teflon screw capped NMR tube. The red solution was degassed for three freeze-thaw-pump cycles. The NMR tube was sealed under vacuum. It was heated at 120 °C in the dark and the reaction was monitored by  $^1\text{H}$  NMR. The product ratio was calculated as follows:

For the case of 3 hours, the integration of alkyl proton at  $\delta = -4.171$  (observed = 5.370) was used to calculate the ratio with the integration of pyrrole signal of **2a** ( $\delta = 8.63$ ) was taken as 8. Let the integration of that alkyl deuterium be  $Y$ .  $Y$  is equal to the integration of that alkyl proton without deuterium incorporation (5.370) minus the observed integration of that alkyl proton with deuterium incorporation (5.144).  $k_H/k_D$  is equal to the integration of alkyl proton over the integration of alkyl deuterium.  $k_H/k_D$  is calculated to be 22.8.

For the case of 42 hours,  $k_H/k_D$  is equal to the integration of alkyl proton (5.191) over the integration of alkyl deuterium (5.370-5.191). The calculated  $k_H/k_D$  is 22.9.

**Competition Reaction of *c*-hexane and *c*-hexane- $d_{12}$  with Rh(tpp)H (**1d**).** Rh(tpp)H (**1d**) (10.1 mg, 0.013 mmol) was added into mixture of *c*-hexane (1.50 mL, 14.000 mmol) and *c*-

hexane- $d_{12}$  (1.49 ml, 14.000 mmol). The red mixture was degassed for three freeze-thaw-pump cycles and was heated at 120 °C under  $N_2$  in the dark for 3 hours. Then excess  $c$ -hexane/ $c$ -hexane- $d_{12}$  mixture was removed by vacuum distillation. Dark red residue was brought to  $^1H$  NMR spectroscopy. It was then purified by column chromatography on silica gel eluting with a solvent mixture of hexane/ $CH_2Cl_2$  (4:1). The red fraction was collected. After rotary evaporation, product mixture of  $Rh(ttp)(c\text{-hexyl})$  (**2a**) and  $Rh(ttp)(c\text{-hexyl})\text{-}d_{11}$  was obtained as a red solid (6.0 mg, 0.0070 mmol, 54%). Integration of alkyl proton of the  $Rh(ttp)(c\text{-hexyl})/Rh(ttp)(c\text{-hexyl})\text{-}d_{11}$   $\delta = -4.26$  was found to be 4.668. The calculated  $k_H/k_D$  was 8.9( $\pm 0.3$ ).

**Competition Reaction of  $c$ -hexane and  $c$ -hexane- $d_{12}$  with  $Rh(ttp)H$  (**1d**) with  $K_2CO_3$ .**

$Rh(ttp)H$  (**1d**) (10.0 mg, 0.013 mmol) and potassium carbonate (17.9 mg, 0.130 mmol) were added into mixture of  $c$ -hexane (1.50 ml, 14.000 mmol) and  $c$ -hexane- $d_{12}$  (1.49 ml, 14.000 mmol). The red mixture was degassed for three freeze-thaw-pump cycles and was heated at 120 °C under  $N_2$  in the dark for 3 hours. Then excess  $c$ -hexane/ $c$ -hexane- $d_{12}$  mixture was removed by vacuum distillation. Dark red residue was brought to  $^1H$  NMR spectroscopy for product ratio. It was then extracted with  $CH_2Cl_2/H_2O$  and purified by column chromatography on silica gel eluting with a solvent mixture of hexane/ $CH_2Cl_2$  (4:1). The red fraction was collected. After rotary evaporation, product mixture of  $Rh(ttp)(c\text{-hexyl})$  (**2a**) and  $Rh(ttp)(c\text{-hexyl})\text{-}d_{11}$  was obtained as a red solid (6.2 mg, 0.0073 mmol, 56%). Integration of alkyl proton of the  $Rh(ttp)(c\text{-hexyl})/Rh(ttp)(c\text{-hexyl})\text{-}d_{11}$   $\delta = -4.26$  was found to be 4.647. The calculated  $k_H/k_D$  was 8.5( $\pm 0.4$ ).

**Competition Reaction of  $c$ -hexane and  $c$ -hexane- $d_{12}$  with  $Rh_2(ttp)_2$  (**1e**).**

$Rh_2(ttp)_2$  (**1e**) (10.3 mg, 0.0067 mmol) was added into mixture of  $c$ -hexane (1.50 ml, 14.000 mmol) and  $c$ -hexane- $d_{12}$  (1.49 ml, 14.000 mmol). The red mixture was degassed for three freeze-thaw-pump cycles and was heated at 120 °C under  $N_2$  in the dark for 6 hours. Then excess  $c$ -

hexane/*c*-hexane-*d*<sub>12</sub> mixture was removed by vacuum distillation. Dark red residue was brought to <sup>1</sup>H NMR spectroscopy. It was then purified by column chromatography on silica gel eluting with a solvent mixture of hexane/CH<sub>2</sub>Cl<sub>2</sub> (4:1). The red fraction was collected. After rotary evaporation, product mixture of Rh(*ttp*)(*c*-hexyl) (**2a**) and Rh(*ttp*)(*c*-hexyl)-*d*<sub>11</sub> was obtained as a red solid (4.3 mg, 0.0050 mmol, 38%). Integration of alkyl proton of the Rh(*ttp*)(*c*-hexyl)/Rh(*ttp*)(*c*-hexyl)-*d*<sub>11</sub>  $\delta = -4.26$  was found to be 4.659. The calculated  $k_H/k_D$  was 8.7( $\pm 0.3$ ).

**Competition Reaction of *c*-hexane and *c*-hexane-*d*<sub>12</sub> with Rh<sub>2</sub>(*ttp*)<sub>2</sub> (**1e**) with K<sub>2</sub>CO<sub>3</sub>.**

Rh<sub>2</sub>(*ttp*)<sub>2</sub> (**1e**) (10.1 mg, 0.0065 mmol) and potassium carbonate (9.0 mg, 0.065 mmol) were added into mixture of *c*-hexane (1.50 ml, 14.000 mmol) and *c*-hexane-*d*<sub>12</sub> (1.49 ml, 14.000 mmol). The red mixture was degassed for three freeze-thaw-pump cycles and was heated at 120 °C under N<sub>2</sub> in the dark for 6 hours. Then excess *c*-hexane/*c*-hexane-*d*<sub>12</sub> mixture was removed by vacuum distillation. Dark red residue was brought to <sup>1</sup>H NMR spectroscopy. It was then purified by column chromatography on silica gel eluting with a solvent mixture of hexane/CH<sub>2</sub>Cl<sub>2</sub> (4:1). The red fraction was collected. After rotary evaporation, product mixture of Rh(*ttp*)(*c*-hexyl) (**2a**) and Rh(*ttp*)(*c*-hexyl)-*d*<sub>11</sub> was obtained as a red solid (4.7 mg, 0.0055 mmol, 42%). Integration of alkyl proton of the Rh(*ttp*)(*c*-hexyl)/Rh(*ttp*)(*c*-hexyl)-*d*<sub>11</sub>  $\delta = -4.26$  was found to be 4.673. The calculated  $k_H/k_D$  was 9.0( $\pm 0.3$ ).

**Scaled NMR Tube Experiment of Rh<sub>2</sub>(*ttp*)<sub>2</sub> (**1e**) and *c*-hexane in Benzene-*d*<sub>6</sub>.**

Rh<sub>2</sub>(*ttp*)<sub>2</sub> (**1e**) (5.1 mg, 0.0033 mmol) and *c*-hexane (34  $\mu$ L, 0.316 mmol) were added into benzene-*d*<sub>6</sub> (520  $\mu$ L) in a NMR tube. The red mixture was degassed for three freeze-thaw-pump cycles and the NMR tube was sealed under vacuum. It was heated at 120 °C in the dark. It was monitored with <sup>1</sup>H NMR spectroscopy at particular time intervals and the NMR yields were taken.

**$\beta$ -Hydride Elimination of Rh(tp)(*c*-hexyl) (2a).** Rh(tp)(*c*-hexyl) (6.8 mg, 0.0081 mmol) was added into benzene-*d*<sub>6</sub> (520  $\mu$ L) in a NMR tube. The red reaction mixture was degassed for three freeze-thaw-pump cycles and the NMR tube was sealed under vacuum. It was heated to 120 °C and the reaction mixture was monitored with <sup>1</sup>H NMR spectroscopy and NMR yields were taken.

### Chapter 3

#### Reaction of Cycloheptane with Rh(tp)Cl.

**(5, 10, 15, 20-Tetratolylporphyrinato)(cycloheptyl) rhodium(III), [Rh(tp)(*c*-heptyl)] (5a).** Rh(tp)Cl<sup>1</sup> (20.4 mg, 0.025 mmol) was added in *c*-heptane (3.0 mL). The red reaction mixture was degassed for three freeze-thaw-pump cycles, purged with N<sub>2</sub> and heated at 120 °C under N<sub>2</sub> for 24 hours. Excess *c*-heptane was removed by vacuum distillation. The residue was purified by column chromatography on silica gel eluting with a solvent mixture of hexane/CH<sub>2</sub>Cl<sub>2</sub> (1:1). Red solid, Rh(tp)(*c*-heptyl) (5a) (4.0 mg, 0.0046 mmol, 18%) was collected and was further recrystallized from CH<sub>2</sub>Cl<sub>2</sub>/MeOH. *R<sub>f</sub>* = 0.84 (hexane/CH<sub>2</sub>Cl<sub>2</sub> = 1:1). <sup>1</sup>H NMR (CDCl<sub>3</sub>, 300 MHz)  $\delta$  -4.53 (m, 2), -4.05 (m, 3 H), -1.26 (m, 4 H), -0.22 (m, 2 H), -0.06 (m, 2 H), 2.69 (s, 12 H, *p*-methyl), 7.54 (d, 8 H, *J* = 5.4 Hz, *m*-phenyl), 8.00 (d, 4 H, *J* = 7.5 Hz, *o*'-phenyl), 8.08 (d, 4 H, *J* = 7.8 Hz, *o*-phenyl), 8.69 (s, 8 H, pyrrole). <sup>13</sup>C NMR (CDCl<sub>3</sub>, 75 MHz)  $\delta$  21.69, 22.09, 27.85, 33.24, 39.37 (d, <sup>1</sup>*J*<sub>Rh-C</sub> = 27.6 Hz), 122.87, 127.42, 127.55, 131.52, 133.63, 134.25, 137.23, 137.23, 139.53, 143.50. Calcd. for (C<sub>55</sub>H<sub>49</sub>N<sub>4</sub>Rh)<sup>+</sup>: *m/z* 868.3007. Found: *m/z* 868.3016. Single crystal for X-ray diffraction analysis was grown from CH<sub>2</sub>Cl<sub>2</sub>/methanol.

**Reaction of Cycloheptane and Rh(tp)Cl with Potassium Carbonate.** Rh(tp)Cl (20.4 mg, 0.025 mmol) and anhydrous potassium carbonate (34.9 mg, 0.252 mmol) was added in *c*-heptane (3.0 mL). The red reaction mixture was degassed for three freeze-thaw-pump cycles,

purged with N<sub>2</sub> and heated at 120 °C under N<sub>2</sub> for 6 hours. Excess *c*-heptane was removed by vacuum distillation. The dark red crude product was extracted with CH<sub>2</sub>Cl<sub>2</sub>/H<sub>2</sub>O. The organic layer was collected, dried and evaporated to dryness and the residue was purified by column chromatography on silica gel eluting with a solvent mixture of hexane/CH<sub>2</sub>Cl<sub>2</sub> (1:1). Red solids, Rh(tp)(*c*-heptyl) (**5a**) (6.6 mg, 0.0076 mmol, 30%) and Rh(tp)Bn (**5b**) (5.5 mg, 0.0064 mmol, 25%) were collected.

**Sealed NMR Tube Experiment of Rh(tp)Cl and Cycloheptane with Potassium Carbonate in Benzene-*d*<sub>6</sub>.** Rh(tp)Cl (3.5 mg, 0.0043 mmol), cycloheptane (11 μL, 0.091 mmol) and potassium carbonate (5.9 mg, 0.0427 mmol) were added into benzene-*d*<sub>6</sub> (500 μL) in a NMR tube. The red mixture was degassed for three freeze-thaw-pump cycles and the NMR tube was flame-sealed under vacuum. It was heated at 120 °C in the dark. It was monitored with <sup>1</sup>H NMR spectroscopy at particular time intervals and the NMR yields were taken.

**Reaction of Cycloheptane with Rh<sub>2</sub>(tp)<sub>2</sub>.** Rh<sub>2</sub>(tp)<sub>2</sub> (9.5 mg, 0.0062 mmol) was added in *c*-heptane (1.5 mL). The red reaction mixture was degassed for three freeze-thaw-pump cycles, purged with N<sub>2</sub> and heated at 120 °C under N<sub>2</sub> for 5 minutes. Excess *c*-heptane was removed by vacuum distillation. The residue was purified by column chromatography on silica gel eluting with a solvent mixture of hexane/CH<sub>2</sub>Cl<sub>2</sub> (1:1). Red solid, Rh(tp)(*c*-heptyl) (**1**) (8.2 mg, 0.0093 mmol, 76%) was collected and was further recrystallized from CH<sub>2</sub>Cl<sub>2</sub>/MeOH.

**Reaction of Cycloheptane with Rh(tp)H.** Rh(tp)H (9.5 mg, 0.012 mmol) was added in *c*-heptane (1.5 mL). The red reaction mixture was degassed for three freeze-thaw-pump cycles, purged with N<sub>2</sub> and heated at 120 °C under N<sub>2</sub> for 15 minutes. Excess *c*-heptane was removed by vacuum distillation. The residue was purified by column chromatography on silica gel eluting with a solvent mixture of hexane/CH<sub>2</sub>Cl<sub>2</sub> (1:1). Red solid, Rh(tp)(*c*-heptyl) (**5a**) (7.8 mg, 0.090 mmol, 73%) was collected and was further recrystallized from CH<sub>2</sub>Cl<sub>2</sub>/MeOH.

**Sealed NMR Tube Experiment of Rh(tp)(c-heptyl) in Benzene- $d_6$ .** Rh(tp)(c-heptyl) (**5a**) (3.8 mg, 0.0044 mmol) was added into benzene- $d_6$  (500  $\mu$ L) in a NMR tube. The red solution was degassed for three freeze-thaw-pump cycles and the NMR tube was flame-sealed under vacuum. It was heated at 120  $^{\circ}$ C in the dark. It was monitored with  $^1$ H NMR spectroscopy at particular time intervals and the NMR yields were taken.

**Sealed NMR Tube Experiment of Rh(tp)(c-heptyl) with Potassium Carbonate in Benzene- $d_6$ .** Rh(tp)(c-heptyl) (**5a**) (3.8 mg, 0.0044 mmol) and potassium carbonate (6.0 mg, 0.044 mmol) were added into benzene- $d_6$  (500  $\mu$ L) in a NMR tube. The red solution was degassed for three freeze-thaw-pump cycles and the NMR tube was flame-sealed under vacuum. It was heated at 120  $^{\circ}$ C in the dark. It was monitored with  $^1$ H NMR spectroscopy at particular time intervals and the NMR yields were taken.

**Sealed NMR Tube Experiment of Rh(tp)(c-heptyl) with 1 mol% of Rh $_2$ (tp) $_2$  in Benzene- $d_6$ .** Rh(tp)(c-heptyl) (**5a**) (3.8 mg, 0.0044 mmol) and 1 mol% of Rh $_2$ (tp) $_2$  (0.034 mg,  $4.4 \times 10^{-5}$  mmol) which was previously dissolved in 500  $\mu$ L degassed benzene- $d_6$  were added together in a NMR tube. The red solution was degassed for three freeze-thaw-pump cycles and the NMR tube was flame-sealed under vacuum. It was heated at 120  $^{\circ}$ C in the dark. It was monitored with  $^1$ H NMR spectroscopy at particular time intervals and the NMR yields were taken.

**Independent Synthesis of Rh(tp)(n-heptyl).**<sup>6</sup> A suspension of Rh(tp)Cl (100 mg, 0.11 mmol) in EtOH (50 mL) and a solution of NaBH $_4$  (17 mg, 0.45 mmol) in aq. NaOH (0.1 M, 2 mL) were purged with N $_2$  for 15 minutes separately. The solution of NaBH $_4$  was added slowly to the suspension of Rh(tp)Cl via a cannula. The mixture was heated at 50  $^{\circ}$ C under N $_2$  for 1 hour. The solution was then cooled to 30  $^{\circ}$ C under N $_2$  and 7-heptenyl bromide (23 mg, 1.20 mmol) was added. A reddish orange suspension was formed. After stirred at room temperature for another 15 minutes under N $_2$ , the reaction mixture was worked up by

extraction with  $\text{CH}_2\text{Cl}_2/\text{H}_2\text{O}$ . The combined organic extract was dried ( $\text{MgSO}_4$ ), filtered and rotatory evaporated. The reddish orange residue was purified by column chromatography over silica gel (250 - 400 mesh) using a solvent mixture of hexane/ $\text{CH}_2\text{Cl}_2$  (1:1) as the eluent. The major orange fraction was collected and gave a reddish orange solid of  $\text{Rh}(\text{ttp})(\text{CH}_2)_5(\text{CH}=\text{CH}_2)$  **6a** (96.0 mg, 0.11 mmol, 86%) as the product after rotary evaporation.

**Sealed NMR Tube Experiment of  $\text{Rh}(\text{ttp})(\text{CH}_2)_5(\text{CH}=\text{CH}_2)$  **6a** with Potassium Carbonate in Benzene- $d_6$ .**  $\text{Rh}(\text{ttp})(\text{CH}_2)_5(\text{CH}=\text{CH}_2)$  **6a** (3.8 mg, 0.0044 mmol) and potassium carbonate (6.0 mg, 0.044 mmol) were added into benzene- $d_6$  (500  $\mu\text{L}$ ) in a NMR tube. The red solution was degassed for three freeze-thaw-pump cycles and the NMR tube was flame-sealed under vacuum. It was heated at 120  $^\circ\text{C}$  in the dark. It was monitored with  $^1\text{H}$  NMR spectroscopy at particular time intervals and the NMR yields were taken.

**Independent Synthesis of  $\text{Rh}(\text{ttp})(\text{cyclohexylmethyl})$ .**<sup>6</sup> A suspension of  $\text{Rh}(\text{ttp})\text{Cl}$  (100 mg, 0.11 mmol) in EtOH (50 mL) and a solution of  $\text{NaBH}_4$  (17 mg, 0.45 mmol) in aq. NaOH (0.1 M, 2 mL) were purged with  $\text{N}_2$  for 15 minutes separately. The solution of  $\text{NaBH}_4$  was added slowly to the suspension of  $\text{Rh}(\text{ttp})\text{Cl}$  via a cannula. The mixture was heated at 50  $^\circ\text{C}$  under  $\text{N}_2$  for 1 hour. The solution was then cooled to 30  $^\circ\text{C}$  under  $\text{N}_2$  and *c*-hexylmethyl bromide (23 mg, 1.20 mmol) was added. A reddish orange suspension was formed. After stirred at room temperature for another 15 minutes under  $\text{N}_2$ , the reaction mixture was worked up by extraction with  $\text{CH}_2\text{Cl}_2/\text{H}_2\text{O}$ . The combined organic extract was dried ( $\text{MgSO}_4$ ), filtered and rotatory evaporated. The reddish orange residue was purified by column chromatography over silica gel (250 - 400 mesh) using a solvent mixture of hexane/ $\text{CH}_2\text{Cl}_2$  (1:1) as the eluent. The major orange fraction was collected and gave a reddish orange solid of  $\text{Rh}(\text{ttp})\text{CH}_2(\text{c-C}_6\text{H}_{11})$  **6c** (92.5 mg, 0.11 mmol, 86%) as the product after rotary evaporation.

**Scaled NMR Tube Experiment of Rh(ttp)CH<sub>2</sub>(*c*-C<sub>6</sub>H<sub>11</sub>) 6c with Potassium Carbonate in Benzene-*d*<sub>6</sub>.** Rh(ttp)CH<sub>2</sub>(*c*-C<sub>6</sub>H<sub>11</sub>) **6c** (3.8 mg, 0.0044 mmol) and potassium carbonate (6.0 mg, 0.044 mmol) were added into benzene-*d*<sub>6</sub> (500 μL) in a NMR tube. The red solution was degassed for three freeze-thaw-pump cycles and the NMR tube was flame-sealed under vacuum. It was heated at 120 °C in the dark. It was monitored with <sup>1</sup>H NMR spectroscopy at particular time intervals and the NMR yields were taken.

**Scaled NMR Tube Experiment of Rh<sub>2</sub>(ttp)<sub>2</sub> and Cycloheptene in Benzene-*d*<sub>6</sub>.** *c*-Heptene (2 μL, 0.021 mmol) was added into a solution of Rh<sub>2</sub>(ttp)<sub>2</sub> (3.4 mg, 0.0022 mmol) in 500 μL degassed benzene in a NMR tube. The solvent was removed by vacuum distillation after 5 minutes. 500 μL degassed benzene-*d*<sub>6</sub> was then added. The red solution was degassed for three freeze-thaw-pump cycles and the NMR tube was flame-sealed under vacuum. It was brought to <sup>1</sup>H NMR analysis after sealed. The <sup>1</sup>H NMR signal of Rh<sub>2</sub>(ttp)<sub>2</sub> was not observed. Instead, a clean NMR spectrum was obtained. The newly formed Rh(ttp) compound was proposed to be the 1,2-addition product **5**. <sup>1</sup>H NMR (C<sub>6</sub>D<sub>6</sub>, 400 MHz) δ -4.24 (m, 1), -3.39 (m, 1 H), -2.70 (m, 1 H), -1.60 (m, 1 H), -1.20 (m, 1 H), -0.68 (m, 1 H), -0.18 (m, 1 H), 0.13 (m, 2 H), 2.41 (s, 24 H, *p*-methyl), 4.01 (m, 2 H), 7.30 (d, 8 H, *J* = 6.4 Hz, *m*-phenyl), 7.33 (d, 8 H, *J* = 8.0 Hz, *m'*-phenyl), 8.13 (d, 8 H, *J* = 7.6 Hz, *o'*-phenyl), 8.19 (d, 8 H, *J* = 7.5 Hz, *o*-phenyl), 8.97 (s, 16 H, pyrrole).

**Scaled NMR Tube Experiment of Rh<sub>2</sub>(ttp)<sub>2</sub> and Cycloheptene Benzene-*d*<sub>6</sub> at 120 °C.** *c*-Heptene (2 μL, 0.021 mmol) was added into a solution of Rh<sub>2</sub>(ttp)<sub>2</sub> (3.4 mg, 0.0022 mmol) in 500 μL degassed benzene in a NMR tube. The solvent was removed by vacuum distillation after 5 minutes. 500 μL degassed benzene-*d*<sub>6</sub> was then added. The red solution was degassed for three freeze-thaw-pump cycles and the NMR tube was flame-sealed under vacuum. It was brought to <sup>1</sup>H NMR analysis after sealed. The <sup>1</sup>H NMR signal of Rh<sub>2</sub>(ttp)<sub>2</sub> was not observed. Instead, a clean NMR spectrum was obtained. The newly formed Rh(ttp) compound was

proposed to be the 1,2-addition product **5**. The reaction tube was heated to 120 °C. It was monitored with <sup>1</sup>H NMR spectroscopy at particular time intervals and the NMR yields were taken.

**Sealed NMR Tube Experiment of Rh<sub>2</sub>(ttp)<sub>2</sub> and Cycloheptatriene in Benzene-*d*<sub>6</sub>.**

Rh<sub>2</sub>(ttp)<sub>2</sub> (3.6 mg, 0.0047 mmol), cycloheptatriene (5 μL) and degassed benzene-*d*<sub>6</sub> (500 μL) were added in a NMR tube. The red solution was degassed for three freeze-thaw-pump cycles and the NMR tube was flame-sealed under vacuum. It was kept at room temperature, monitored with <sup>1</sup>H NMR spectroscopy at particular time intervals and the NMR yields were taken. **8** was obtained quantitatively. <sup>1</sup>H NMR (C<sub>6</sub>D<sub>6</sub>, 400 MHz) δ 2.44 (s, 19), 7.32 (d, 8 H, *J* = 7.4 Hz, *m*-phenyl), 7.35 (d, 4 H, *J* = 7.8 Hz, *o*-phenyl), 8.13 (d, 4 H, *J* = 5.4 Hz, *m*'-phenyl), 8.14 (d, 4 H, *J* = 5.4 Hz, *o*'-phenyl), 8.93 (s, 8 H, pyrrole). <sup>13</sup>C NMR (C<sub>6</sub>D<sub>6</sub>, 100 MHz) δ 21.50, 123.47, 131.82, 132.80, 134.22, 134.28, 134.92, 137.11, 140.43, 144.24. Calcd. for (C<sub>55</sub>H<sub>43</sub>N<sub>4</sub>Rh)<sup>+</sup>: *m/z* 862.2537. Found: *m/z* 862.2549.

**Sealed NMR Tube Experiment of Rh(ttp)H and Cycloheptatriene in Benzene-*d*<sub>6</sub>.**

Rh(ttp)H (3.6 mg, 0.0047 mmol), cycloheptatriene (5 μL) and degassed benzene-*d*<sub>6</sub> (500 μL) were added in a NMR tube. The red solution was degassed for three freeze-thaw-pump cycles and the NMR tube was flame-sealed under vacuum. It was kept at room temperature, monitored with <sup>1</sup>H NMR spectroscopy at particular time intervals and the NMR yields were taken.

**Synthesis of Rh(ttp)(cycloheptatrienyl) **8**.** Rh(ttp)H (3.6 mg, 0.0047 mmol) and cycloheptatriene (5 μL) were added into degassed benzene (500 μL). The red solution was degassed for three freeze-thaw-pump cycles, purged with N<sub>2</sub> and put into a water bath at 25 °C for 15 minutes. Excess solvent was removed by vacuum distillation. 500 μL degassed benzene-*d*<sub>6</sub> was then added. The product was found to be air-sensitive and decomposed

during column chromatography. As the  $^1\text{H}$  NMR spectrum was clean, no further purification step was required.

**Rearrangement reaction of Rh(ttp)(cycloheptatrienyl) at 6.95 mM.**

Rh(ttp)(cycloheptatrienyl) (3.0 mg, 0.0035 mmol) was added into degassed benzene- $d_6$  (500  $\mu\text{L}$ ) in a NMR tube. The red solution was degassed for three freeze-thaw-pump cycles and the NMR tube was flame-sealed under vacuum. It was heated at 120  $^\circ\text{C}$  in the dark. It was monitored with  $^1\text{H}$  NMR spectroscopy at particular time intervals and the NMR yields were taken. For this and the following reactions, the collected kinetic data were fitted by first-order exponential decay using OriginPro 7.5 software.

**Rearrangement reaction of Rh(ttp)(cycloheptatrienyl) at 13.90 mM.**

Rh(ttp)(cycloheptatrienyl) (6.0 mg, 0.0070 mmol) was added into degassed benzene- $d_6$  (500  $\mu\text{L}$ ) in a NMR tube. The red solution was degassed for three freeze-thaw-pump cycles and the NMR tube was flame-sealed under vacuum. It was heated at 120  $^\circ\text{C}$  in the dark. It was monitored with  $^1\text{H}$  NMR spectroscopy at particular time intervals and the NMR yields were taken.

**Rearrangement reaction of Rh(ttp)(cycloheptatrienyl) at 6.95 mM at 130  $^\circ\text{C}$ .**

Rh(ttp)(cycloheptatrienyl) (3.0 mg, 0.0035 mmol) was added into degassed benzene- $d_6$  (500  $\mu\text{L}$ ) in a NMR tube. The red solution was degassed for three freeze-thaw-pump cycles and the NMR tube was flame-sealed under vacuum. It was heated at 130  $^\circ\text{C}$  in the dark. It was monitored with  $^1\text{H}$  NMR spectroscopy at particular time intervals and the NMR yields were taken.

**Rearrangement reaction of Rh(ttp)(cycloheptatrienyl) at 6.95 mM at 140  $^\circ\text{C}$ .**

Rh(ttp)(cycloheptatrienyl) (3.0 mg, 0.0035 mmol) was added into degassed benzene- $d_6$  (500  $\mu\text{L}$ ) in a NMR tube. The red solution was degassed for three freeze-thaw-pump cycles and the NMR tube was flame-sealed under vacuum. It was heated at 140  $^\circ\text{C}$  in the dark. It was

monitored with  $^1\text{H}$  NMR spectroscopy at particular time intervals and the NMR yields were taken.

**Rearrangement reaction of Rh(ttp)(cycloheptatrienyl) at 6.95 mM at 150 °C.**

Rh(ttp)(cycloheptatrienyl) (3.0 mg, 0.0035 mmol) was added into degassed benzene- $d_6$  (500  $\mu\text{L}$ ) in a NMR tube. The red solution was degassed for three freeze-thaw-pump cycles and the NMR tube was flame-sealed under vacuum. It was heated at 150 °C in the dark. It was monitored with  $^1\text{H}$  NMR spectroscopy at particular time intervals and the NMR yields were taken.

**Rate extrapolation of CHT to toluene at 120 °C.** According to the data obtained from literature,<sup>5</sup>  $\log(\underline{A}/\text{s}^{-1})$  was 13.6 and  $\underline{E}_a$  was 217.7  $\text{kJmol}^{-1}$ . By Arrhenius equation,

$$\ln k = -E_a/RT + \ln A$$

$$\text{At } 120\text{ °C, } \ln k = -217.7 \times 1000 / (8.314 \times 393) + \ln(10^{13.6})$$

$$\ln k = -35.3$$

$$k = 4.61 \times 10^{-16} \text{ s}^{-1}$$

**Rearrangement reaction of Rh(ttp)(cycloheptatrienyl) at 6.95 mM with Potassium**

**Carbonate.** Rh(ttp)(cycloheptatrienyl) (3.0 mg, 0.0035 mmol) and potassium carbonate (4.8 mg, 0.035 mmol) were added into degassed benzene- $d_6$  (500  $\mu\text{L}$ ) in a NMR tube. The red reaction mixture was degassed for three freeze-thaw-pump cycles and the NMR tube was flame-sealed under vacuum. It was heated at 120 °C in the dark. It was monitored with  $^1\text{H}$  NMR spectroscopy at particular time intervals and the NMR yields were taken.

**Rearrangement reaction of Rh(ttp)(cycloheptatrienyl) at 6.95 mM with 1 mol%**

**Rh<sub>2</sub>(ttp)<sub>2</sub>.** Rh(ttp)(cycloheptatrienyl) (3.0 mg, 0.0035 mmol) and 1 mol% Rh<sub>2</sub>(ttp)<sub>2</sub> (0.027 mg,  $1.7 \times 10^{-5}$  mmol) were added into degassed benzene- $d_6$  (500  $\mu\text{L}$ ) in a NMR tube. The red reaction mixture was degassed for three freeze-thaw-pump cycles and the NMR tube was

flame-sealed under vacuum. It was heated at 120 °C in the dark. It was monitored with  $^1\text{H}$  NMR spectroscopy at particular time intervals and the NMR yields were taken.

**Rearrangement reaction of Rh(ttp)(cycloheptatrienyl) at 6.95 mM with 10 mol% Rh<sub>2</sub>(ttp)<sub>2</sub>.** Rh(ttp)(cycloheptatrienyl) (3.0 mg, 0.0035 mmol) and 10 mol% Rh<sub>2</sub>(ttp)<sub>2</sub> (0.27 mg,  $1.7 \times 10^{-4}$  mmol) were added into degassed benzene-*d*<sub>6</sub> (500  $\mu\text{L}$ ) in a NMR tube. The red reaction mixture was degassed for three freeze-thaw-pump cycles and the NMR tube was flame-sealed under vacuum. It was heated at 120 °C in the dark. It was monitored with  $^1\text{H}$  NMR spectroscopy at particular time intervals and the NMR yields were taken.

#### Chapter 4

**Reaction of *c*-octane with Rh(ttp)Cl.** Rh(ttp)Cl (20.6 mg, 0.026 mmol) was added in *c*-octane (3.0 mL). The red reaction mixture was degassed for three freeze-thaw-pump cycles, purged with N<sub>2</sub> and heated at 120 °C under N<sub>2</sub> for 48 hours. Excess *c*-octane was removed by vacuum distillation. The residue was purified by column chromatography on silica gel eluting with a solvent mixture of hexane/CH<sub>2</sub>Cl<sub>2</sub> (1:1). Red solid, Rh(ttp)(*c*-octyl) **10a** (1.0 mg, 0.0011 mmol, 5%) and Rh(ttp)(*n*-octyl) **10b** (1.9 mg, 0.0021 mmol, 8%) were collected, and further recrystallized from CH<sub>2</sub>Cl<sub>2</sub>/MeOH. The product ratio was calculated by  $^1\text{H}$  NMR integration. Rh(ttp)Cl was recovered (14.8 mg) after column chromatography. Characterization of Rh(ttp)(*c*-octyl) **1**:  $R_f = 0.84$  (hexane/CH<sub>2</sub>Cl<sub>2</sub> = 1:1).  $^1\text{H}$  NMR (C<sub>6</sub>D<sub>6</sub>, 400 MHz)  $\delta$  -4.25 (m, 2), -3.66 (m, 3 H), -1.13 (m, 4 H), -0.32 (m, 2 H), 0.90 (m, 4 H), 2.41 (s, 12 H, *p*-methyl), 7.30 (d, 4 H,  $J = 7.3$  Hz, *m*-phenyl), 7.33 (d, 4 H,  $J = 7.2$  Hz, *m'*-phenyl), 8.18 (d, 4 H,  $J = 7.7$  Hz, *o'*-phenyl), 8.97 (s, 8 H, pyrrole).  $^{13}\text{C}$  NMR (CDCl<sub>3</sub>, 75 MHz)  $\delta$  21.70, 22.54, 25.23, 25.85, 30.40, 40.62 (d,  $^1J_{\text{Rh-C}} = 26.4$  Hz), 122.86, 127.42, 127.54, 131.48, 133.62, 134.25, 137.22, 139.52, 143.52. HRMS: calcd. for (C<sub>56</sub>H<sub>51</sub>N<sub>4</sub>Rh+H)<sup>+</sup>:  $m/z$  883.3242. Found:  $m/z$  883.3214. Characterization of Rh(ttp)(*n*-octyl) **2**:  $R_f = 0.84$  (hexane/CH<sub>2</sub>Cl<sub>2</sub> =

1:1).  $^1\text{H}$  NMR ( $\text{C}_6\text{D}_6$ , 400 MHz)  $\delta$  -4.55 (td, 2 H,  $J = 2.8, 8.7$  Hz), -4.11 (qu, 2 H,  $J = 8.2$  Hz), -1.55 (qu, 2 H,  $J = 7.8$  Hz), -0.50 (qu, 2 H,  $J = 8.0$  Hz), 0.02 (qu, 2 H,  $J = 7.5$  Hz), 0.44 (qu, 2 H,  $J = 7.4$  Hz), 0.59 (t, 3 H,  $J = 7.2$  Hz), 0.80 (qu, 2 H,  $J = 7.6$  Hz), 2.41 (s, 12 H, *p*-methyl), 7.27 (d, 4 H,  $J = 8.1$  Hz, *m*-phenyl), 7.35 (d, 4 H,  $J = 6.4$  Hz, *m'*-phenyl), 8.12 (dd, 4 H,  $J = 1.7, 7.6$  Hz, *o*-phenyl), 8.22 (dd, 4 H,  $J = 1.6, 7.6$  Hz, *o'*-phenyl), 8.99 (s, 8 H, pyrrole).  $^{13}\text{C}$  NMR ( $\text{CDCl}_3$ , 100 MHz)  $\delta$  14.00, 15.69 (d,  $^1J_{\text{Rh-C}} = 26.8$  Hz), 21.68, 22.41, 26.28, 27.04, 27.52, 27.96, 31.31, 122.49, 127.43, 127.51, 131.47, 133.78, 134.09, 137.23, 139.48, 143.35. HRMS: calcd. for  $(\text{C}_{56}\text{H}_{53}\text{N}_4\text{Rh})^+$ :  $m/z$  884.3320. Found:  $m/z$  884.3336. Single crystal for X-ray diffraction analysis was grown from  $\text{CH}_2\text{Cl}_2/\text{CH}_3\text{OH}$ .

**Reaction of *c*-Octane and Rh(*ttp*)Cl with Potassium Hydroxide.** Rh(*ttp*)Cl (20.4 mg, 0.025 mmol) and potassium hydroxide (14.2 mg, 0.254 mmol) was added in *c*-octane (3.0 mL). The red reaction mixture was degassed for three freeze-thaw-pump cycles, purged with  $\text{N}_2$  and heated at 120  $^\circ\text{C}$  under  $\text{N}_2$  for 7.5 hours. Excess *c*-octane was removed by vacuum distillation. The red residue was added with benzene- $d_6$  (500  $\mu\text{L}$ ) under  $\text{N}_2$  for  $^1\text{H}$  NMR spectroscopy and the NMR yield of Rh(*ttp*)H (62%) was estimated. The crude mixture was then extracted with  $\text{CH}_2\text{Cl}_2/\text{H}_2\text{O}$ . The organic layer was collected, dried and evaporated to dryness and the residue was purified by column chromatography on silica gel eluting with a solvent mixture of hexane/ $\text{CH}_2\text{Cl}_2$  (1:1). Red solids, Rh(*ttp*)(*c*-octyl) **10a** (1.3 mg, 0.0015 mmol, 6%) and Rh(*ttp*)(*n*-octyl) **10b** (5.6 mg, 0.0063 mmol, 25%) were collected.

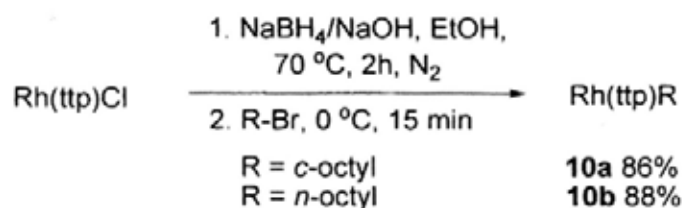
**Reaction of *c*-Octane and Rh(*ttp*)Cl with Potassium Carbonate.** Rh(*ttp*)Cl (20.4 mg, 0.025 mmol) and anhydrous potassium carbonate (34.9 mg, 0.252 mmol) was added in *c*-octane (3.0 mL). The red reaction mixture was degassed for three freeze-thaw-pump cycles, purged with  $\text{N}_2$  and heated at 120  $^\circ\text{C}$  under  $\text{N}_2$  for 7.5 hours. Excess *c*-octane was removed by

vacuum distillation. The red residue was added with benzene- $d_6$  (500  $\mu$ L) under  $N_2$  for  $^1H$  NMR spectroscopy and the NMR yield of Rh(tp)H (58%) was estimated. The crude mixture was then extracted with  $CH_2Cl_2/H_2O$ . The organic layer was collected, dried and evaporated to dryness and the residue was purified by column chromatography on silica gel eluting with a solvent mixture of hexane/ $CH_2Cl_2$  (1:1). Red solids, Rh(tp)(*n*-octyl) **10b** (7.5 mg, 0.0085 mmol, 33%) were collected.

**Independent Synthesis of Rh(tp)(*c*-octyl).**<sup>6</sup> A suspension of Rh(tp)Cl (100 mg, 0.11 mmol) in EtOH (50 mL) and a solution of  $NaBH_4$  (17 mg, 0.45 mmol) in aq. NaOH (0.1 M, 2 mL) were purged with  $N_2$  for 15 minutes separately. The solution of  $NaBH_4$  was added slowly to the suspension of Rh(tp)Cl via a cannula. The mixture was heated at 50  $^\circ C$  under  $N_2$  for 1 hour. The solution was then cooled to 30  $^\circ C$  under  $N_2$  and *c*-octyl bromide (23 mg, 1.20 mmol) was added. A reddish orange suspension was formed. After stirred at room temperature for another 15 minutes under  $N_2$ , the reaction mixture was worked up by extraction with  $CH_2Cl_2/H_2O$ . The combined organic extract was dried ( $MgSO_4$ ), filtered and rotatory evaporated. The reddish orange residue was purified by column chromatography over silica gel (250 - 400 mesh) using a solvent mixture of hexane/ $CH_2Cl_2$  (1:1) as the eluent. The major orange fraction was collected and gave a reddish orange solid of Rh(tp)(*c*-octyl) **10a** (94.1 mg, 0.11 mmol, 86%) as the product after rotary evaporation.

**Independent Synthesis of Rh(tp)(*n*-octyl).**<sup>6</sup> A suspension of Rh(tp)Cl (100 mg, 0.11 mmol) in EtOH (50 mL) and a solution of  $NaBH_4$  (17 mg, 0.45 mmol) in aq. NaOH (0.1 M, 2 mL) were purged with  $N_2$  for 15 minutes separately. The solution of  $NaBH_4$  was added slowly to the suspension of Rh(tp)Cl via a cannula. The mixture was heated at 50  $^\circ C$  under  $N_2$  for 1 hour. The solution was then cooled to 30  $^\circ C$  under  $N_2$  and *n*-octyl bromide (23 mg, 1.20 mmol) was added. A reddish orange suspension was formed. After stirred at room temperature for another 15 minutes under  $N_2$ , the reaction mixture was worked up by

extraction with CH<sub>2</sub>Cl<sub>2</sub>/H<sub>2</sub>O. The combined organic extract was dried (MgSO<sub>4</sub>), filtered and rotatory evaporated. The reddish orange residue was purified by column chromatography over silica gel (250 - 400 mesh) using a solvent mixture of hexane/CH<sub>2</sub>Cl<sub>2</sub> (1:1) as the eluent. The major orange fraction was collected and gave a reddish orange solid of Rh(tp)(*n*-octyl) **10b** (96.5 mg, 0.11 mmol, 88%) as the product after rotary evaporation.



**Thermal Stability of Rh(tp)(*c*-octyl) in Benzene-*d*<sub>6</sub>.** Rh(tp)(*c*-octyl) **10a** (3.9 mg, 0.0044 mmol) was added into benzene-*d*<sub>6</sub> (500 μL) in a NMR tube. The red solution was degassed for three freeze-thaw-pump cycles and the NMR tube was flame-sealed under vacuum. It was heated at 120 °C in the dark. It was monitored with <sup>1</sup>H NMR spectroscopy at particular time intervals and the NMR yields were taken.

**Stability of Rh(tp)(*c*-octyl) with Potassium Carbonate in Benzene-*d*<sub>6</sub>.** Rh(tp)(*c*-octyl) **10a** (3.9 mg, 0.0044 mmol) and potassium carbonate (6.0 mg, 0.044 mmol) were added into benzene-*d*<sub>6</sub> (500 μL) in a NMR tube. The red solution was degassed for three freeze-thaw-pump cycles and the NMR tube was flame-sealed under vacuum. It was heated at 120 °C in the dark. It was monitored with <sup>1</sup>H NMR spectroscopy at particular time intervals and the NMR yields were taken.

**Reaction of Rh(tp)Cl and *c*-Octane with Potassium Carbonate in Benzene-*d*<sub>6</sub>.** Rh(tp)Cl (3.5 mg, 0.0043 mmol), *c*-octane (11 μL, 0.087 mmol) and potassium carbonate (5.9 mg, 0.0427 mmol) were added into benzene-*d*<sub>6</sub> (500 μL) in a NMR tube. The red mixture was degassed for three freeze-thaw-pump cycles and the NMR tube was flame-sealed under vacuum. It was heated at 120 °C in the dark. It was monitored with <sup>1</sup>H NMR spectroscopy at particular time intervals and the NMR yields were taken.

**Sealed NMR Tube Experiment of Rh<sub>2</sub>(ttp)<sub>2</sub> and Cyclooctene Benzene-*d*<sub>6</sub> at Room Temperature.** *c*-Octene (2 μL, 0.021 mmol) was added into a solution of Rh<sub>2</sub>(ttp)<sub>2</sub> (3.4 mg, 0.0022 mmol) in 500 μL degassed benzene in a NMR tube. The solvent was removed by vacuum distillation after 5 minutes. 500 μL degassed benzene-*d*<sub>6</sub> was then added. The red solution was degassed for three freeze-thaw-pump cycles and the NMR tube was flame-sealed under vacuum. It was brought to <sup>1</sup>H NMR analysis after sealed. The <sup>1</sup>H NMR signal of Rh<sub>2</sub>(ttp)<sub>2</sub> was not observed. Instead, a clean NMR spectrum was obtained. The newly formed Rh(tp) compound was proposed to be the 1,2-addition product. The reaction tube was kept at room temperature. It was monitored with <sup>1</sup>H NMR spectroscopy at particular time intervals and the NMR yields were taken.

**Reaction of *c*-Octane with Rh(tp)H.** Rh(tp)H (9.6 mg, 0.012 mmol) was added in *c*-octane (1.5 mL). The red reaction mixture was degassed for three freeze-thaw-pump cycles, purged with N<sub>2</sub> and heated at 120 °C under N<sub>2</sub> for 15 hours. Excess *c*-octane was removed by vacuum distillation. The residue was added with benzene-*d*<sub>6</sub> (500 μL) under N<sub>2</sub> protection for <sup>1</sup>H NMR spectroscopy and the recovered yield of Rh(tp)H (73%) was estimated. The residue was purified by column chromatography on silica gel eluting with a solvent mixture of hexane/CH<sub>2</sub>Cl<sub>2</sub> (1:1). Red solid, Rh(tp)(*n*-octyl) **10b** (2.3 mg, 0.0026 mmol, 21%) was collected and was further recrystallized from CH<sub>2</sub>Cl<sub>2</sub>/MeOH.

**Reaction of *c*-Octane with Rh(tp)H and PPh<sub>3</sub>.** Rh(tp)H (9.6 mg, 0.012 mmol) and PPh<sub>3</sub> (3.2 mg, 0.012 mmol) were added in *c*-octane (1.5 mL). The red reaction mixture was degassed for three freeze-thaw-pump cycles, purged with N<sub>2</sub> and heated at 120 °C under N<sub>2</sub> for 15 hours. Excess *c*-octane was removed by vacuum distillation. The residue was added with benzene-*d*<sub>6</sub> (500 μL) under N<sub>2</sub> protection for <sup>1</sup>H NMR spectroscopy. Rh(tp)H(PPh<sub>3</sub>) was obtained in quantitative NMR yield. <sup>1</sup>H NMR (C<sub>6</sub>D<sub>6</sub>, 400 MHz) δ -33.42 (b, 1 H), 2.39

(s, 12 H, *p*-methyl); 4.16 (t, 2 H,  $J = 9.2$  Hz), 6.28 (td, 2 H,  $J = 2.4, 7.6$  Hz, *m*-phenyl), 6.52 (t, 1 H,  $J = 6.8$  Hz), 7.35 (d, 4 H,  $J = 7.2$  Hz, *m'*-phenyl), 7.84 (d, 4 H,  $J = 7.6$  Hz, *o*-phenyl), 7.89 (d, 4 H,  $J = 7.6$  Hz, *o'*-phenyl), 8.98 (s, 8 H, pyrrole).

**Thermal Dehydrogenative Dimerization of Rh(tp)H.** Rh(tp)H (3.2 mg, 0.0041 mmol) was added in benzene- $d_6$  (500  $\mu$ L). The red reaction mixture was degassed for three freeze-thaw-pump cycles, and the NMR tube was flame-sealed under vacuum. It was heated at 120  $^{\circ}$ C in the dark. It was monitored with  $^1$ H NMR spectroscopy at particular time intervals and the NMR yields were taken.

**Reaction of *c*-Octane with Rh<sub>2</sub>(tp)<sub>2</sub>.** Rh<sub>2</sub>(tp)<sub>2</sub> (9.6 mg, 0.012 mmol) was added in *c*-octane (1.5 mL). The red reaction mixture was degassed for three freeze-thaw-pump cycles, purged with N<sub>2</sub> and heated at 120  $^{\circ}$ C under N<sub>2</sub> for 15 hours. Excess *c*-octane was removed by vacuum distillation. The red residue was added with benzene- $d_6$  (500  $\mu$ L) under N<sub>2</sub> protection for  $^1$ H NMR spectroscopy and the yield of Rh(tp)H (46%) was estimated. The residue was purified by column chromatography on silica gel eluting with a solvent mixture of hexane/CH<sub>2</sub>Cl<sub>2</sub> (1:1). Red solids, Rh(tp)(*c*-octyl) **10a** (4.5 mg, 0.0051 mmol, 41%) and Rh(tp)(*n*-octyl) **10b** (0.4 mg, 0.00045 mmol, 4%) were collected and the product ratio was calculated by  $^1$ H NMR integration.

**Reaction of *c*-Octane with 2:1 Mixture of Rh(tp)H and Rh<sub>2</sub>(tp)<sub>2</sub>.** Rh(tp)H (9.6 mg, 0.012 mmol) and Rh<sub>2</sub>(tp)<sub>2</sub> (4.8 mg, 0.0031 mmol) were added in *c*-octane (1.5 mL). The red reaction mixture was degassed for three freeze-thaw-pump cycles, purged with N<sub>2</sub> and heated at 120  $^{\circ}$ C under N<sub>2</sub> for 15 hours. Excess *c*-octane was removed by vacuum distillation. The residue was purified by column chromatography on silica gel eluting with a solvent mixture of hexane/CH<sub>2</sub>Cl<sub>2</sub> (1:1). Red solid, Rh(tp)(*c*-octyl) **10a** (9.8 mg, 0.011 mmol, 60%) and Rh(tp)(*n*-octyl) **10b** (3.0 mg, 0.0034 mmol, 18%) were collected and the product ratio was calculated by  $^1$ H NMR integration.

**Reaction of *c*-Octane with 5:1 Mixture of Rh(*ttp*)H and Rh<sub>2</sub>(*ttp*)<sub>2</sub>.** Rh(*ttp*)H (9.6 mg, 0.012 mmol) and Rh<sub>2</sub>(*ttp*)<sub>2</sub> (1.9 mg, 0.0012 mmol) were added in *c*-octane (1.5 mL). The red reaction mixture was degassed for three freeze-thaw-pump cycles, purged with N<sub>2</sub> and heated at 120 °C under N<sub>2</sub> for 15 hours. Excess *c*-octane was removed by vacuum distillation. The residue was purified by column chromatography on silica gel eluting with a solvent mixture of hexane/CH<sub>2</sub>Cl<sub>2</sub> (1:1). Red solid, Rh(*ttp*)(*c*-octyl) **10a** (6.9 mg, 0.0078 mmol, 53%) and Rh(*ttp*)(*n*-octyl) **10b** (3.4 mg, 0.0038 mmol, 26%) were collected and the product ratio was calculated by <sup>1</sup>H NMR integration.

**Reaction of *c*-Octane with 10:1 Mixture of Rh(*ttp*)H and Rh<sub>2</sub>(*ttp*)<sub>2</sub>.** Rh(*ttp*)H (9.6 mg, 0.012 mmol) and Rh<sub>2</sub>(*ttp*)<sub>2</sub> (1.0 mg, 0.00065 mmol) were added in *c*-octane (1.5 mL). The red reaction mixture was degassed for three freeze-thaw-pump cycles, purged with N<sub>2</sub> and heated at 120 °C under N<sub>2</sub> for 15 hours. Excess *c*-octane was removed by vacuum distillation. The residue was purified by column chromatography on silica gel eluting with a solvent mixture of hexane/CH<sub>2</sub>Cl<sub>2</sub> (1:1). Red solid Rh(*ttp*)(*n*-octyl) **10b** (8.9 mg, 0.010 mmol, 73%) was collected and was further recrystallized from CH<sub>2</sub>Cl<sub>2</sub>/MeOH.

**Reaction of *c*-Octane with 10:1 Mixture of Rh(*tmp*)H and Rh<sup>II</sup>(*tmp*).** Rh(*tmp*)H<sup>7</sup> (10.6 mg, 0.012 mmol) and Rh<sup>II</sup>(*tmp*)<sup>8</sup> (1.1 mg, 0.0012 mmol) were added in *c*-octane (1.5 mL). The red reaction mixture was degassed for three freeze-thaw-pump cycles, purged with N<sub>2</sub> and heated at 120 °C under N<sub>2</sub> for 24 hours. Excess *c*-octane was removed by vacuum distillation. The colourless organic distillate was added with benzene-*d*<sub>6</sub> for <sup>1</sup>H NMR spectroscopy and *c*-octene was not observed. Degassed benzene-*d*<sub>6</sub> was added N<sub>2</sub> for <sup>1</sup>H NMR spectroscopy. Red solution of Rh(*tmp*)H (90% yield, estimated by <sup>1</sup>H NMR spectroscopy) was obtained.

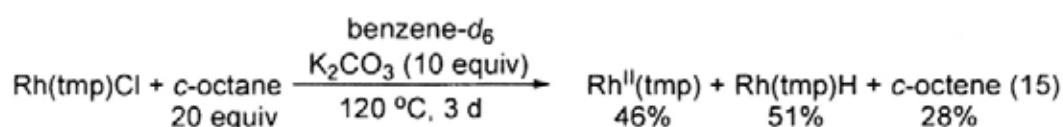
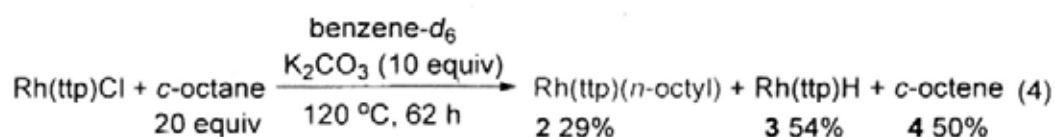
**Reaction of *c*-octane with Rh<sup>II</sup>(*tmp*).** Rh<sup>II</sup>(*tmp*) (10.6 mg, 0.0012 mmol) were added in *c*-octane (1.5 mL). The red reaction mixture was degassed for three freeze-thaw-pump cycles,



The sterically less hindered Rh(tp)Cl gave 86% yield of Rh(tp)(*c*-octyl) via reductive alkylation while more hindered Rh(tmp)Cl resulted in 89% yield of Rh(tmp)H but not Rh(tmp)(*c*-octyl).

**Reaction of Rh(tmp)Cl and *c*-Octane with Potassium Carbonate in Benzene-*d*<sub>6</sub>.**

Rh(tmp)Cl<sup>9</sup> (4.0 mg, 0.0043 mmol), *c*-octane (11 μL, 0.087 mmol) and potassium carbonate (5.8 mg, 0.0420 mmol) were added into benzene-*d*<sub>6</sub> (500 μL) in a NMR tube. The red mixture was degassed for three freeze-thaw-pump cycles and the NMR tube was flame-sealed under vacuum. It was heated at 120 °C in the dark. It was monitored with <sup>1</sup>H NMR spectroscopy at particular time intervals and the NMR yields were taken.



Rh(tmp)Cl reacted with *c*-octane in benzene-*d*<sub>6</sub> in the presence of K<sub>2</sub>CO<sub>3</sub> and gave Rh<sup>II</sup>(tmp), Rh(tmp)H and *c*-octene in 46%, 51% and 50% yields, respectively at 120 °C in 3 days. Compared to Rh(tp)Cl, Rh(tmp)Cl is likely too bulky to react with the C-C bond of *c*-octane to give Rh(tmp)(*n*-octyl).

## References

1. (a) Adler, A. D.; Longo, F. R.; Finarelli, J. D.; Goldmacher, J.; Assour, J.; Korsakoff, L. *J. Org. Chem.* **1967**, *32*, 476. (b) Alder, A. D.; Longo, F. R.; Shergalis, W. *J. Am. Chem. Soc.* **1964**, *86*, 3145-3149.
2. (a) Mak, K. W. *PhD. Thesis*, The Chinese University of Hong Kong, 1998. (b) Mak, K. W.; Chan, K. S. *J. Am. Chem. Soc.* **1998**, *120*, 9686-9687.
3. Mak, K. W.; Xue, F.; Mak, T. C. W.; Chan, K. S. *J. Chem. Soc., Dalton Trans.* **1999**, *19*, 3333-3334.
4. (a) Wayland, B. B.; Van Voorhees, S. L. Wilker, C. *Inorg. Chem.* **1986**, *25*, 4039-4042. (b) Ogoshi, H.; Setsune, J.; Omura, T.; Yoshida, Z. *J. Am. Chem. Soc.* **1975**, *97*, 6461-6466.
5. (a) Tse, A. K.S.; Wu, B. M.; Mak, T. C. W.; Chan, K. S. *J. Organomet. Chem.* **1998**, *568*, 257-261. (b) Dolphin, D.; Halko, D. J.; Johnson, E. *Inorg. Chem.* **1981**, *20*, 4348-4351.
6. (a) Ogoshi, H.; Setsune, J.; Omura, T.; Yoshida, Z. *J. Am. Chem. Soc.* **1975**, *97*, 6461-6466. (b) Chan, K. S.; Mak, K. W.; Tse, M. K.; Yeung, S. K.; Li, B. Z.; Chan, Y. W. *J. Organomet. Chem.* **2008**, *693*, 399-407.
7. Wayland, B. B.; Ba, S.; Sherry, A. E. *J. Am. Chem. Soc.* **1991**, *113*, 5305-5311.
8. (a) Wayland, B. B.; Sherry, A. E.; Poszmik, G.; Bunn, A. G. *J. Am. Chem. Soc.* **1992**, *114*, 1673-1681. (b) Li, G.; Zhang, F. F.; Pi, N.; Chen, H. L.; Zhang, S. Y.; Chan, K. S. *Chem. Lett.* **2001**, 284-285.

## Appendix

## X-ray Data

Table 1. Crystal Data and Structure Refinement Parameters for 2a, 2b, 2c, 2e, 5a and 10b

|  | Rh(tp)(c-hexyl)<br>2a  | Rh(tp)(c-pentyl)<br>2b  | Rh(tp)(n-heptyl)<br>2e                            | Rh(tp)(c-heptyl)<br>5a   | Rh(tp)(cyclohep<br>tatrienyl) 8                   | Rh(tp)(n-octyl) 10b                               |
|--|--|---|---|--|---|---|
| Color, shape                           | Purple Prism   | Purple Prism  | Purple Prism                                      | Purple Prism   | Purple Prism                                      | Purple Prism                                      |
| empirical formula                      | C <sub>54</sub> H <sub>47</sub> N <sub>4</sub> Rh·CH <sub>2</sub><br>Cl <sub>2</sub> | C <sub>53</sub> H <sub>45</sub> N <sub>4</sub> Rh·CH <sub>3</sub><br>CH <sub>2</sub> OH | C <sub>56</sub> H <sub>51</sub> N <sub>4</sub> Rh | C <sub>55</sub> H <sub>48</sub> N <sub>4</sub> Rh·CH <sub>2</sub><br>Cl <sub>2</sub> | C <sub>55</sub> H <sub>42</sub> N <sub>4</sub> Rh | C <sub>56</sub> H <sub>53</sub> N <sub>4</sub> Rh |
| formula wt                             | 939.79   | 886.91  | 882.92  | 952.81   | 861.84  | 884.93  |
| Temp (K)                               | 293 (2)  | 293 (2)   | 293 (2)   | 293 (2)  | 296(2)  | 293 (2)   |
| wavelength(Å)                          | 0.71073  | 0.71073   | 0.71073   | 0.71073  | 0.71073   | 0.71073   |
| cryst syst                             | monoclinic   | monoclinic  | triclinic   | monoclinic   | monoclinic  | triclinic   |
| Space group                            | P2 <sub>1</sub> /n   | P2 <sub>1</sub> /n  | P1  | P2 <sub>1</sub> /n   | P2 <sub>1</sub> /n                                | P-1   |
| unit cell dimens                       |  |   |   |  |   |   |
| a (Å)                                  | 15.509 (2)   | 15.579 (2)  | 10.578 (2)  | 15.510 (4)   | 15.486 (1)  | 10.578 (2)  |
| b (Å)                                  | 18.651 (2)   | 18.482 (2)  | 14.575 (3)  | 18.697 (5)   | 18.711 (1)  | 14.574 (3)  |
| c (Å)                                  | 16.266 (2)   | 16.155 (2)  | 16.226 (4)  | 16.441 (4)   | 16.421 (1)  | 16.226 (4)  |
| α (deg)                                | 90   | 90  | 65.745 (4)  | 90   | 90  | 65.745 (4)  |
| β (deg)                                | 106.993 (2)  | 107.516 (2)   | 77.764 (4)  | 106.569 (2)  | 106.763 (1)                                       | 77.764 (4)  |
| γ (deg)                                | 90   | 90  | 82.348 (4)  | 90   | 90  | 82.348 (4)  |
| Volume (Å <sup>3</sup> )               | 4499.6 (9)   | 4436.1 (10)   | 2225.8 (9)  | 4570 (2)   | 4555.9 (2)  | 2225.8 (9)  |
| Z                                      | 4  | 4   | 2   | 4  | 4   | 2   |
| Calcd density (g<br>cm <sup>-3</sup> ) | 1.387  | 1.328   | 1.317   | 1.385  | 1.256   | 1.320   |
| abs coeff (mm <sup>-1</sup> )          | 0.541  | 0.430   | 0.426   | 0.534  | 0.415   | 0.426   |
| F(000)                                 | 1944   | 1848  | 920   | 1972   | 1780  | 924   |

|   |  |  |  |  |  |  |
|---|--|--|--|--|--|--|
| cryst size (mm)                             | 0.40 x 0.30 x<br>0.20                          | 0.50 x 0.30 x<br>0.20                          | 0.50 x 0.40 x<br>0.30                          | 0.40 x 0.30 x<br>0.20                              | 0.50 x 0.40 x<br>0.30                              | 0.50 x 0.40 x 0.30                                 |
| $\theta$ range for data<br>collection (deg) | 1.60 to 28.04                                  | 1.72 to 25.00                                  | 1.53 to 28.08                                  | 1.59 to 25.00                                      | 1.59 to 25.25                                      | 1.53 to 25.00                                      |
| Limiting indices                            | -20 = h = 18<br>-24 = k = 24<br>-21 = l = 20   | -18 = h = 18<br>-21 = k = 19<br>-19 = l = 19   | -13 = h = 13<br>-19 = k = 18<br>-21 = l = 12   | -17 <= h <= 18<br>-22 <= k <= 15<br>-19 <= l <= 19 | -18 <= h <= 16<br>-22 <= h <= 22<br>-19 <= h <= 19 | -12 <= h <= 12<br>-17 <= k <= 16<br>-19 <= l <= 11 |
| no. of rflns<br>collected/ unique           | 30232/10856 [(R<br>(int) = 0.0414)             | 23310/7800 [R<br>(int) = 0.0479]               | 15187/10539<br>[R (int) =<br>0.0239]           | 24091/8037 [(R<br>(int) = 0.0679)                  | 42092/8244<br>[R(int) = 0.0468]                    | 12098/7803 [(R (int) =<br>0.0230)                  |
| Completeness to<br>$\theta = 28$            | 99.6   | 99.8   | 97.3   | 99.7   | 100.0  | 99.5   |
| Absorp corr                                 | SADABS   | SADABS   | SADABS   | SADABS   | Multi-scan   | SADABS   |
| max. and min.<br>transm                     | 1.0000 and<br>0.836682                         | 1.0000 and<br>0.660829                         | 1.0000 and<br>0.616130                         | 1.0000 and<br>0.351677                             | 0.7456 and<br>0.6264                               | 1.0000 and 0.616130                                |
| Refinement<br>method                        | Full-matrix least<br>squares on F <sup>2</sup>     | Full-matrix least<br>squares on F <sup>2</sup>     | Full-matrix least<br>squares on F <sup>2</sup>     |
| no. of data/<br>restraints /<br>params      | 10856 / 2 / 559                                | 7800 / 14 / 550                                | 10539 / 10 / 568                               | 8037 / 20 / 568                                    | 8244 / 17 / 550                                    | 7803 / 40 / 568                                    |
| GOF   | 1.025  | 1.069  | 1.036  | 1.058  | 1.061  | 1.054  |
| final R indices<br>[ $I > 2\sigma(I)$ ]     | R <sub>1</sub> = 0.0572                        | R <sub>1</sub> = 0.0677                        | R <sub>1</sub> = 0.0449                        | R <sub>1</sub> = 0.0920                            | R <sub>1</sub> = 0.0364                            | R <sub>1</sub> = 0.0424                            |
|   | $wR_2 = 0.1511$                                | $wR_2 = 0.1861$                                | $wR_2 = 0.1124$                                | $wR_2 = 0.2530$                                    | $wR_2 = 0.1030$                                    | $wR_2 = 0.1119$                                    |

|  |                                      |                                      |                                      |                                      |                                      |                                      |
|--|--------------------------------------|--------------------------------------|--------------------------------------|--------------------------------------|--------------------------------------|--------------------------------------|
| R indices (all data)                           | $R_1 = 0.0945$<br>${}_wR_2 = 0.1784$ | $R_1 = 0.1032$<br>${}_wR_2 = 0.2249$ | $R_1 = 0.0616$<br>${}_wR_2 = 0.1245$ | $R_1 = 0.1513$<br>${}_wR_2 = 0.3138$ | $R_1 = 0.0435$<br>${}_wR_2 = 0.1081$ | $R_1 = 0.0522$<br>${}_wR_2 = 0.1208$ |
| Largest diff peak and hole (e Å <sup>3</sup> ) | 1.597 and -1.788                     | 2.976 and -0.711                     | 0.774 and -0.421                     | 1.509 and -1.136                     | 0.750 and -0.336                     | 0.868 and -0.536                     |

$${}^a R_1 = \frac{\sum (|F_o| - |F_c|)}{\sum |F_o|}, {}^b R_2 = \left\{ \frac{\sum [{}_w(F_o^2 - F_c^2)^2]}{\sum [{}_w(F_o^2)]} \right\}^{1/2}. {}^c \text{Weighting scheme } w^{-1} = \sigma^2(F_o^2) + (w_1 P)^2 + w_2 P \text{ where } P = (F_o^2 + 2F_c^2)/3.$$

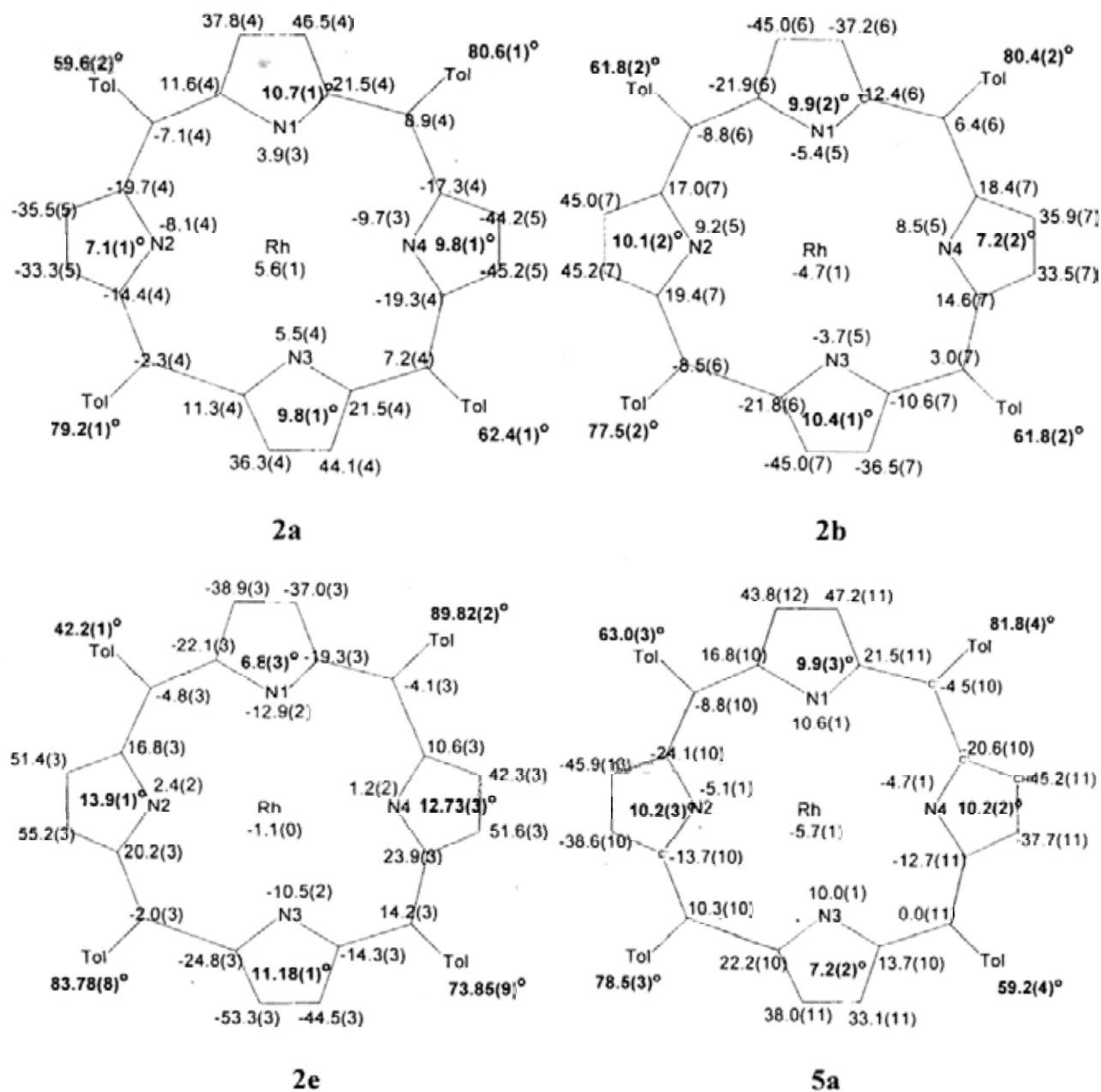


Figure 1. The conformations of porphyrins showing the displacement of the core atoms and of Rh from the 24-atom least squares plane of porphyrin core (in pm; negative values correspond to displacement towards the alkyl group). Absolute values of the angles between pyrrole rings and the least-squares plane, and angles between pyrrole rings and the least-squares plane, and angles between phenyl substituents and the least-squares plane, are shown in bold.

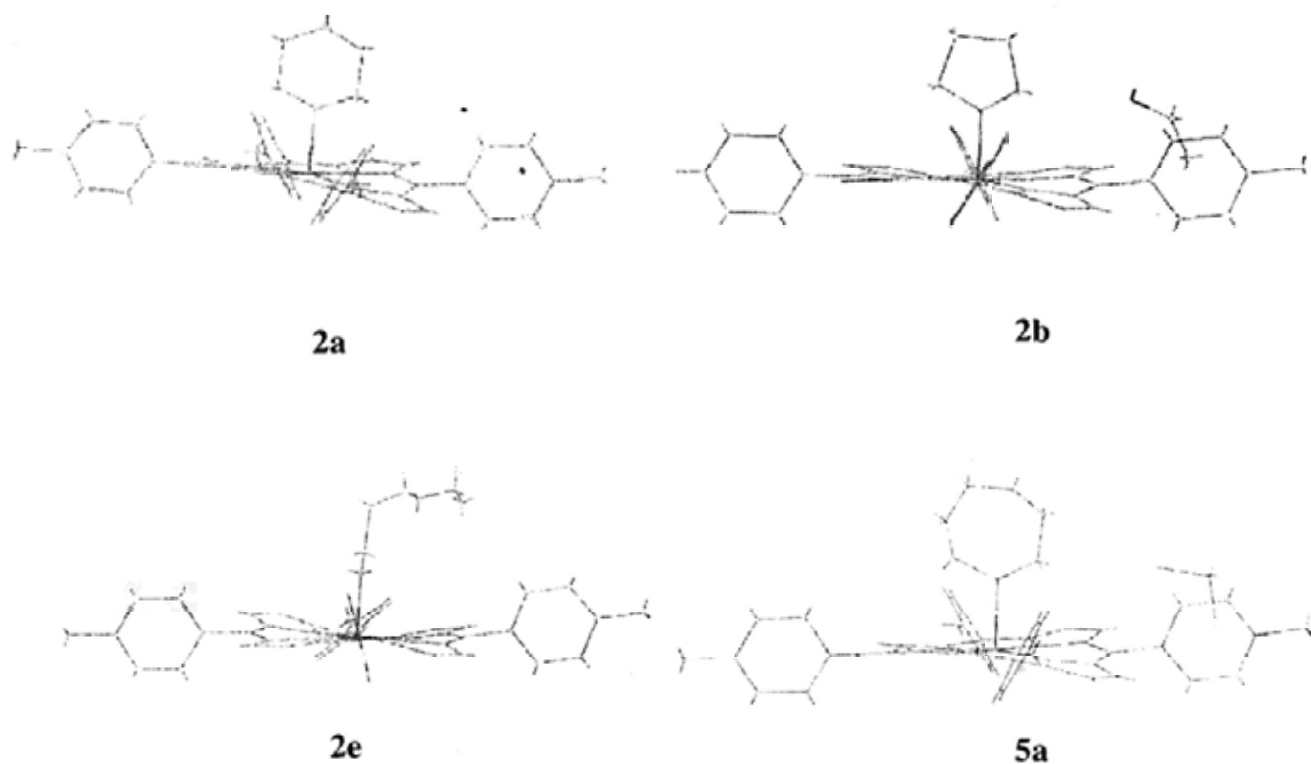


Figure 2. Wireframe presentation of the molecular structures for **2a**, **2b**, **2e** and **5a**, respectively.

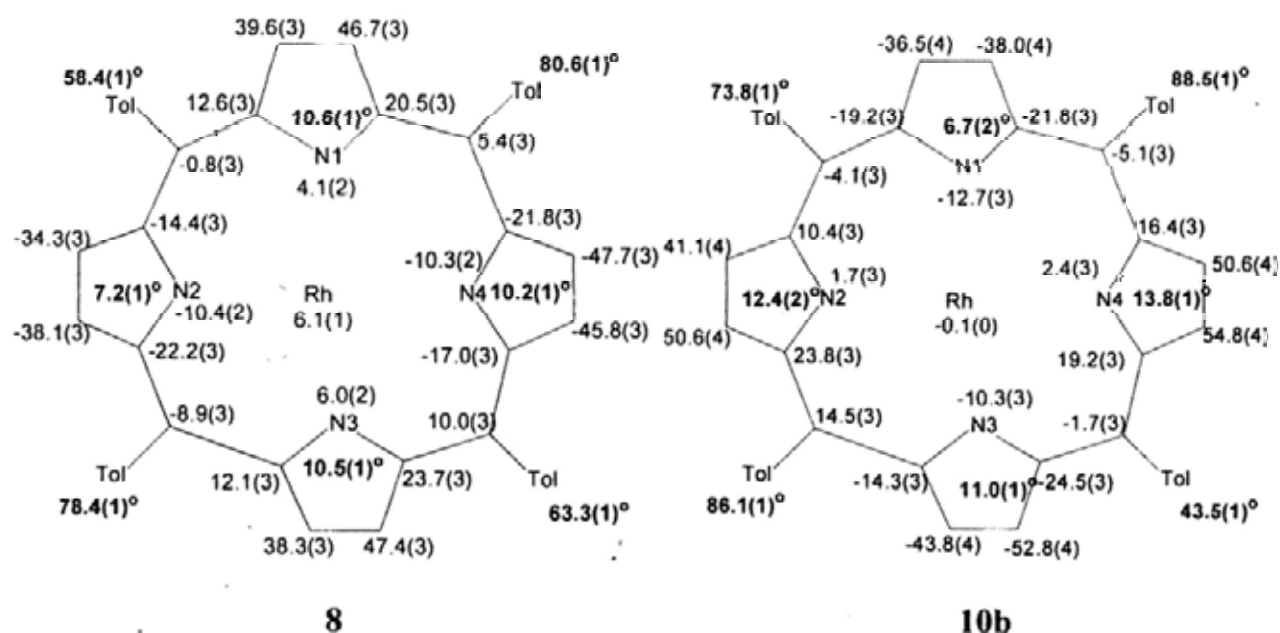


Figure 3. The conformations of porphyrins in **10b** showing the displacement of the core atoms and of Rh from the 24-atom least squares plane of porphyrin core (in pm; positive values correspond to displacement towards the alkyl group). Absolute values of the angles

between pyrrole rings and the least-squares plane, and angles between pyrrole rings and the least-squares plane, and angles between phenyl substituents and the least-squares plane, are shown in bold.

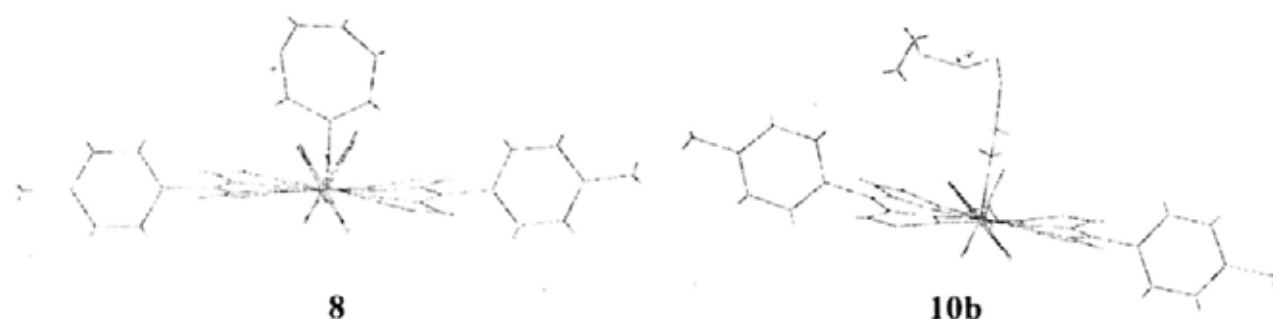


Figure 4. Wireframe presentation of the molecular structures for **8** and **10b**.

Table 2. Bond lengths [Å] and angles [deg] for Rh(ttp)(*c*-hexyl) **2a**.

|             |          |             |          |
|-------------|----------|-------------|----------|
| Rh(1)-N(2)  | 2.012(3) | C(12)-C(13) | 1.345(7) |
| Rh(1)-N(4)  | 2.016(3) | C(13)-C(14) | 1.442(6) |
| Rh(1)-N(1)  | 2.021(3) | C(14)-C(15) | 1.390(6) |
| Rh(1)-N(3)  | 2.026(3) | C(15)-C(16) | 1.393(6) |
| Rh(1)-C(61) | 2.093(5) | C(15)-C(41) | 1.506(6) |
| N(1)-C(1)   | 1.376(5) | C(16)-C(17) | 1.431(6) |
| N(1)-C(4)   | 1.381(5) | C(17)-C(18) | 1.346(6) |
| N(2)-C(6)   | 1.380(5) | C(18)-C(19) | 1.434(6) |
| N(2)-C(9)   | 1.383(5) | C(19)-C(20) | 1.401(6) |
| N(3)-C(11)  | 1.377(5) | C(20)-C(51) | 1.493(6) |
| N(3)-C(14)  | 1.378(5) | C(21)-C(22) | 1.376(6) |
| N(4)-C(19)  | 1.371(5) | C(21)-C(26) | 1.381(7) |
| N(4)-C(16)  | 1.388(5) | C(22)-C(23) | 1.387(7) |
| C(1)-C(20)  | 1.404(6) | C(23)-C(24) | 1.368(8) |
| C(1)-C(2)   | 1.433(6) | C(24)-C(25) | 1.370(9) |
| C(2)-C(3)   | 1.336(6) | C(24)-C(27) | 1.523(7) |
| C(3)-C(4)   | 1.436(6) | C(25)-C(26) | 1.387(7) |
| C(4)-C(5)   | 1.395(6) | C(31)-C(36) | 1.379(7) |
| C(5)-C(6)   | 1.390(6) | C(31)-C(32) | 1.389(7) |
| C(5)-C(21)  | 1.496(6) | C(32)-C(33) | 1.382(7) |
| C(6)-C(7)   | 1.445(6) | C(33)-C(34) | 1.371(8) |
| C(7)-C(8)   | 1.333(7) | C(34)-C(35) | 1.381(8) |
| C(8)-C(9)   | 1.445(6) | C(34)-C(37) | 1.520(7) |
| C(9)-C(10)  | 1.389(6) | C(35)-C(36) | 1.377(7) |
| C(10)-C(11) | 1.392(6) | C(41)-C(42) | 1.365(6) |
| C(10)-C(31) | 1.507(6) | C(41)-C(46) | 1.381(6) |
| C(11)-C(12) | 1.447(6) | C(42)-C(43) | 1.383(6) |

|                  |            |                   |          |
|------------------|------------|-------------------|----------|
| C(43)-C(44)      | 1.363(7)   | C(6)-C(5)-C(4)    | 124.2(4) |
| C(44)-C(45)      | 1.390(8)   | C(6)-C(5)-C(21)   | 117.5(4) |
| C(44)-C(47)      | 1.509(7)   | C(4)-C(5)-C(21)   | 118.3(4) |
| C(45)-C(46)      | 1.384(7)   | N(2)-C(6)-C(5)    | 125.9(4) |
| C(51)-C(56)      | 1.371(6)   | N(2)-C(6)-C(7)    | 109.2(4) |
| C(51)-C(52)      | 1.385(6)   | C(5)-C(6)-C(7)    | 124.7(4) |
| C(52)-C(53)      | 1.378(6)   | C(8)-C(7)-C(6)    | 107.3(4) |
| C(53)-C(54)      | 1.382(7)   | C(7)-C(8)-C(9)    | 108.3(4) |
| C(54)-C(55)      | 1.371(8)   | N(2)-C(9)-C(10)   | 125.9(4) |
| C(54)-C(57)      | 1.515(7)   | N(2)-C(9)-C(8)    | 108.5(4) |
| C(55)-C(56)      | 1.406(7)   | C(10)-C(9)-C(8)   | 125.6(4) |
| C(61)-C(62)      | 1.466(7)   | C(9)-C(10)-C(11)  | 124.8(4) |
| C(61)-C(66)      | 1.479(8)   | C(9)-C(10)-C(31)  | 117.3(4) |
| C(62)-C(63)      | 1.528(8)   | C(11)-C(10)-C(31) | 117.9(4) |
| C(63)-C(64)      | 1.489(9)   | N(3)-C(11)-C(10)  | 125.7(4) |
| C(64)-C(65)      | 1.462(10)  | N(3)-C(11)-C(12)  | 109.0(4) |
| C(65)-C(66)      | 1.531(8)   | C(10)-C(11)-C(12) | 125.3(4) |
| Cl(1)-C(71)      | 1.776(8)   | C(13)-C(12)-C(11) | 107.2(4) |
| Cl(2)-C(71)      | 1.713(9)   | C(12)-C(13)-C(14) | 107.8(4) |
|                  |            | N(3)-C(14)-C(15)  | 125.1(4) |
| N(2)-Rh(1)-N(4)  | 171.59(14) | N(3)-C(14)-C(13)  | 108.8(4) |
| N(2)-Rh(1)-N(1)  | 89.93(14)  | C(15)-C(14)-C(13) | 125.8(4) |
| N(4)-Rh(1)-N(1)  | 90.00(14)  | C(14)-C(15)-C(16) | 125.0(4) |
| N(2)-Rh(1)-N(3)  | 90.33(14)  | C(14)-C(15)-C(41) | 117.4(4) |
| N(4)-Rh(1)-N(3)  | 89.64(14)  | C(16)-C(15)-C(41) | 117.5(4) |
| N(1)-Rh(1)-N(3)  | 179.25(14) | N(4)-C(16)-C(15)  | 124.3(4) |
| N(2)-Rh(1)-C(61) | 91.63(18)  | N(4)-C(16)-C(17)  | 108.9(4) |
| N(4)-Rh(1)-C(61) | 96.77(18)  | C(15)-C(16)-C(17) | 126.5(4) |
| N(1)-Rh(1)-C(61) | 92.14(17)  | C(18)-C(17)-C(16) | 107.5(4) |
| N(3)-Rh(1)-C(61) | 88.56(18)  | C(17)-C(18)-C(19) | 107.6(4) |
| C(1)-N(1)-C(4)   | 106.5(3)   | N(4)-C(19)-C(20)  | 125.5(4) |
| C(1)-N(1)-Rh(1)  | 126.0(3)   | N(4)-C(19)-C(18)  | 109.3(4) |
| C(4)-N(1)-Rh(1)  | 126.3(3)   | C(20)-C(19)-C(18) | 125.0(4) |
| C(6)-N(2)-C(9)   | 106.7(4)   | C(19)-C(20)-C(1)  | 124.0(4) |
| C(6)-N(2)-Rh(1)  | 126.8(3)   | C(19)-C(20)-C(51) | 118.4(4) |
| C(9)-N(2)-Rh(1)  | 126.5(3)   | C(1)-C(20)-C(51)  | 117.6(4) |
| C(11)-N(3)-C(14) | 107.0(3)   | C(22)-C(21)-C(26) | 117.9(4) |
| C(11)-N(3)-Rh(1) | 126.1(3)   | C(22)-C(21)-C(5)  | 121.5(4) |
| C(14)-N(3)-Rh(1) | 126.1(3)   | C(26)-C(21)-C(5)  | 120.5(4) |
| C(19)-N(4)-C(16) | 106.4(3)   | C(21)-C(22)-C(23) | 121.0(5) |
| C(19)-N(4)-Rh(1) | 126.5(3)   | C(24)-C(23)-C(22) | 121.2(5) |
| C(16)-N(4)-Rh(1) | 127.0(3)   | C(23)-C(24)-C(25) | 117.9(5) |
| N(1)-C(1)-C(20)  | 125.0(4)   | C(23)-C(24)-C(27) | 121.0(6) |
| N(1)-C(1)-C(2)   | 109.3(4)   | C(25)-C(24)-C(27) | 121.1(6) |
| C(20)-C(1)-C(2)  | 125.6(4)   | C(24)-C(25)-C(26) | 121.6(6) |
| C(3)-C(2)-C(1)   | 107.5(4)   | C(21)-C(26)-C(25) | 120.4(5) |
| C(2)-C(3)-C(4)   | 107.9(4)   | C(36)-C(31)-C(32) | 117.5(5) |
| N(1)-C(4)-C(5)   | 125.4(4)   | C(36)-C(31)-C(10) | 121.4(4) |
| N(1)-C(4)-C(3)   | 108.7(4)   | C(32)-C(31)-C(10) | 121.0(4) |
| C(5)-C(4)-C(3)   | 125.8(4)   | C(33)-C(32)-C(31) | 120.7(5) |

|                   |          |                   |          |
|-------------------|----------|-------------------|----------|
| C(34)-C(33)-C(32) | 121.7(5) | C(52)-C(51)-C(20) | 120.1(4) |
| C(33)-C(34)-C(35) | 117.5(5) | C(53)-C(52)-C(51) | 120.8(5) |
| C(33)-C(34)-C(37) | 122.1(5) | C(52)-C(53)-C(54) | 121.5(5) |
| C(35)-C(34)-C(37) | 120.4(5) | C(55)-C(54)-C(53) | 117.5(5) |
| C(36)-C(35)-C(34) | 121.4(5) | C(55)-C(54)-C(57) | 121.1(5) |
| C(35)-C(36)-C(31) | 121.1(5) | C(53)-C(54)-C(57) | 121.4(5) |
| C(42)-C(41)-C(46) | 117.5(4) | C(54)-C(55)-C(56) | 121.6(5) |
| C(42)-C(41)-C(15) | 121.9(4) | C(51)-C(56)-C(55) | 120.0(5) |
| C(46)-C(41)-C(15) | 120.5(4) | C(62)-C(61)-C(66) | 114.6(5) |
| C(41)-C(42)-C(43) | 121.3(5) | C(62)-C(61)-Rh(1) | 114.5(4) |
| C(44)-C(43)-C(42) | 121.7(5) | C(66)-C(61)-Rh(1) | 114.5(4) |
| C(43)-C(44)-C(45) | 117.2(4) | C(61)-C(62)-C(63) | 113.3(5) |
| C(43)-C(44)-C(47) | 121.7(5) | C(64)-C(63)-C(62) | 114.2(5) |
| C(45)-C(44)-C(47) | 121.1(5) | C(65)-C(64)-C(63) | 112.1(6) |
| C(46)-C(45)-C(44) | 120.9(5) | C(64)-C(65)-C(66) | 114.3(6) |
| C(41)-C(46)-C(45) | 121.0(5) | C(61)-C(66)-C(65) | 112.5(5) |
| C(56)-C(51)-C(52) | 118.5(4) | Cl(2)-C(71)-Cl(1) | 114.9(6) |
| C(56)-C(51)-C(20) | 121.4(4) |                   |          |

Table 3. Bond lengths [Å] and angles [deg] for Rh(ttp)(*c*-pentyl) **2b**.

|             |           |             |           |
|-------------|-----------|-------------|-----------|
| Rh(1)-N(4)  | 2.014(6)  | C(9)-C(10)  | 1.395(9)  |
| Rh(1)-N(1)  | 2.015(5)  | C(10)-C(11) | 1.393(9)  |
| Rh(1)-N(3)  | 2.018(5)  | C(10)-C(31) | 1.502(9)  |
| Rh(1)-N(2)  | 2.019(5)  | C(11)-C(12) | 1.442(9)  |
| Rh(1)-C(61) | 2.073(7)  | C(12)-C(13) | 1.325(10) |
| N(1)-C(1)   | 1.388(8)  | C(13)-C(14) | 1.446(10) |
| N(1)-C(4)   | 1.394(8)  | C(14)-C(15) | 1.401(10) |
| N(2)-C(6)   | 1.364(8)  | C(15)-C(16) | 1.392(10) |
| N(2)-C(9)   | 1.376(8)  | C(15)-C(41) | 1.503(10) |
| N(3)-C(11)  | 1.375(8)  | C(16)-C(17) | 1.453(10) |
| N(3)-C(14)  | 1.384(8)  | C(17)-C(18) | 1.347(11) |
| N(4)-C(16)  | 1.366(9)  | C(18)-C(19) | 1.426(10) |
| N(4)-C(19)  | 1.380(9)  | C(19)-C(20) | 1.402(10) |
| C(1)-C(20)  | 1.386(9)  | C(20)-C(51) | 1.491(9)  |
| C(1)-C(2)   | 1.438(9)  | C(21)-C(22) | 1.372(10) |
| C(2)-C(3)   | 1.351(10) | C(21)-C(26) | 1.397(10) |
| C(3)-C(4)   | 1.435(9)  | C(22)-C(23) | 1.397(11) |
| C(4)-C(5)   | 1.385(9)  | C(23)-C(24) | 1.394(12) |
| C(5)-C(6)   | 1.405(10) | C(24)-C(25) | 1.377(11) |
| C(5)-C(21)  | 1.488(9)  | C(24)-C(27) | 1.517(10) |
| C(6)-C(7)   | 1.432(10) | C(25)-C(26) | 1.376(10) |
| C(7)-C(8)   | 1.344(10) | C(31)-C(32) | 1.372(10) |
| C(8)-C(9)   | 1.435(9)  | C(31)-C(36) | 1.385(10) |

|                  |           |                   |          |
|------------------|-----------|-------------------|----------|
| C(32)-C(33)      | 1.405(11) | C(20)-C(1)-C(2)   | 125.8(6) |
| C(33)-C(34)      | 1.362(13) | N(1)-C(1)-C(2)    | 109.5(6) |
| C(34)-C(35)      | 1.366(12) | C(3)-C(2)-C(1)    | 107.2(6) |
| C(34)-C(37)      | 1.529(12) | C(2)-C(3)-C(4)    | 108.3(6) |
| C(35)-C(36)      | 1.382(11) | C(5)-C(4)-N(1)    | 125.2(6) |
| C(41)-C(42)      | 1.373(11) | C(5)-C(4)-C(3)    | 126.0(6) |
| C(41)-C(46)      | 1.384(11) | N(1)-C(4)-C(3)    | 108.7(6) |
| C(42)-C(43)      | 1.370(11) | C(4)-C(5)-C(6)    | 124.4(6) |
| C(43)-C(44)      | 1.372(12) | C(4)-C(5)-C(21)   | 117.5(6) |
| C(44)-C(45)      | 1.387(13) | C(6)-C(5)-C(21)   | 118.1(6) |
| C(44)-C(47)      | 1.514(11) | N(2)-C(6)-C(5)    | 125.5(6) |
| C(45)-C(46)      | 1.368(11) | N(2)-C(6)-C(7)    | 109.4(6) |
| C(51)-C(52)      | 1.371(11) | C(5)-C(6)-C(7)    | 125.0(6) |
| C(51)-C(56)      | 1.382(10) | C(8)-C(7)-C(6)    | 107.2(6) |
| C(52)-C(53)      | 1.425(12) | C(7)-C(8)-C(9)    | 107.5(6) |
| C(53)-C(54)      | 1.362(13) | N(2)-C(9)-C(10)   | 124.8(6) |
| C(54)-C(55)      | 1.381(12) | N(2)-C(9)-C(8)    | 108.7(6) |
| C(54)-C(57)      | 1.515(11) | C(10)-C(9)-C(8)   | 126.0(6) |
| C(55)-C(56)      | 1.383(10) | C(11)-C(10)-C(9)  | 124.3(6) |
| C(61)-C(62)      | 1.453(12) | C(11)-C(10)-C(31) | 117.4(6) |
| C(61)-C(65)      | 1.479(12) | C(9)-C(10)-C(31)  | 118.3(6) |
| C(62)-C(63)      | 1.512(13) | N(3)-C(11)-C(10)  | 125.2(6) |
| C(63)-C(64)      | 1.518(14) | N(3)-C(11)-C(12)  | 109.1(6) |
| C(64)-C(65)      | 1.533(13) | C(10)-C(11)-C(12) | 125.6(6) |
| O(1)-C(71)       | 1.481(9)  | C(13)-C(12)-C(11) | 108.0(6) |
| C(71)-C(72)      | 1.587(9)  | C(12)-C(13)-C(14) | 107.7(6) |
|                  |           | N(3)-C(14)-C(15)  | 125.2(6) |
| N(4)-Rh(1)-N(1)  | 89.8(2)   | N(3)-C(14)-C(13)  | 108.8(6) |
| N(4)-Rh(1)-N(3)  | 90.3(2)   | C(15)-C(14)-C(13) | 126.1(6) |
| N(1)-Rh(1)-N(3)  | 179.8(2)  | C(16)-C(15)-C(14) | 124.2(7) |
| N(4)-Rh(1)-N(2)  | 172.2(2)  | C(16)-C(15)-C(41) | 118.6(6) |
| N(1)-Rh(1)-N(2)  | 90.3(2)   | C(14)-C(15)-C(41) | 117.2(6) |
| N(3)-Rh(1)-N(2)  | 89.6(2)   | N(4)-C(16)-C(15)  | 126.6(7) |
| N(4)-Rh(1)-C(61) | 91.6(3)   | N(4)-C(16)-C(17)  | 109.3(6) |
| N(1)-Rh(1)-C(61) | 92.5(3)   | C(15)-C(16)-C(17) | 124.1(7) |
| N(3)-Rh(1)-C(61) | 87.7(3)   | C(18)-C(17)-C(16) | 106.7(6) |
| N(2)-Rh(1)-C(61) | 96.1(3)   | C(17)-C(18)-C(19) | 107.8(7) |
| C(1)-N(1)-C(4)   | 106.3(5)  | N(4)-C(19)-C(20)  | 125.6(6) |
| C(1)-N(1)-Rh(1)  | 127.2(4)  | N(4)-C(19)-C(18)  | 109.6(6) |
| C(4)-N(1)-Rh(1)  | 125.6(4)  | C(20)-C(19)-C(18) | 124.8(7) |
| C(6)-N(2)-C(9)   | 106.9(5)  | C(1)-C(20)-C(19)  | 124.6(6) |
| C(6)-N(2)-Rh(1)  | 126.3(4)  | C(1)-C(20)-C(51)  | 118.5(6) |
| C(9)-N(2)-Rh(1)  | 126.7(4)  | C(19)-C(20)-C(51) | 116.9(6) |
| C(11)-N(3)-C(14) | 106.4(5)  | C(22)-C(21)-C(26) | 117.8(7) |
| C(11)-N(3)-Rh(1) | 126.1(4)  | C(22)-C(21)-C(5)  | 121.7(6) |
| C(14)-N(3)-Rh(1) | 126.4(5)  | C(26)-C(21)-C(5)  | 120.5(6) |
| C(16)-N(4)-C(19) | 106.6(6)  | C(21)-C(22)-C(23) | 120.9(7) |
| C(16)-N(4)-Rh(1) | 126.5(5)  | C(24)-C(23)-C(22) | 121.0(8) |
| C(19)-N(4)-Rh(1) | 126.9(5)  | C(25)-C(24)-C(23) | 117.6(7) |
| C(20)-C(1)-N(1)  | 124.7(6)  | C(25)-C(24)-C(27) | 121.5(8) |

|                   |          |                   |           |
|-------------------|----------|-------------------|-----------|
| C(23)-C(24)-C(27) | 120.9(8) | C(46)-C(45)-C(44) | 120.8(8)  |
| C(26)-C(25)-C(24) | 121.4(8) | C(45)-C(46)-C(41) | 121.7(8)  |
| C(25)-C(26)-C(21) | 121.3(7) | C(52)-C(51)-C(56) | 118.4(7)  |
| C(32)-C(31)-C(36) | 117.3(7) | C(52)-C(51)-C(20) | 120.4(7)  |
| C(32)-C(31)-C(10) | 121.0(6) | C(56)-C(51)-C(20) | 121.2(6)  |
| C(36)-C(31)-C(10) | 121.7(6) | C(51)-C(52)-C(53) | 120.2(8)  |
| C(31)-C(32)-C(33) | 120.9(7) |                   |           |
| C(34)-C(33)-C(32) | 120.9(8) | C(54)-C(53)-C(52) | 120.9(8)  |
| C(33)-C(34)-C(35) | 118.5(8) | C(53)-C(54)-C(55) | 118.3(7)  |
| C(33)-C(34)-C(37) | 120.4(9) | C(53)-C(54)-C(57) | 119.8(9)  |
| C(35)-C(34)-C(37) | 121.2(9) | C(55)-C(54)-C(57) | 121.8(9)  |
| C(34)-C(35)-C(36) | 121.1(8) | C(54)-C(55)-C(56) | 121.3(8)  |
| C(35)-C(36)-C(31) | 121.4(7) | C(51)-C(56)-C(55) | 121.0(7)  |
| C(42)-C(41)-C(46) | 117.1(7) | C(62)-C(61)-C(65) | 104.9(8)  |
| C(42)-C(41)-C(15) | 122.0(7) | C(62)-C(61)-Rh(1) | 117.5(6)  |
| C(46)-C(41)-C(15) | 120.8(7) | C(65)-C(61)-Rh(1) | 118.1(6)  |
| C(43)-C(42)-C(41) | 121.4(8) | C(61)-C(62)-C(63) | 105.5(8)  |
| C(42)-C(43)-C(44) | 121.7(8) | C(62)-C(63)-C(64) | 104.7(8)  |
| C(43)-C(44)-C(45) | 117.4(7) | C(63)-C(64)-C(65) | 105.9(8)  |
| C(43)-C(44)-C(47) | 122.0(9) | C(61)-C(65)-C(64) | 104.3(8)  |
| C(45)-C(44)-C(47) | 120.6(9) | O(1)-C(71)-C(72)  | 144.7(14) |

Table 4. Bond lengths [Å] and angles [deg] for Rh(ttp)(*n*-heptyl) **2e**.

|             |          |             |          |
|-------------|----------|-------------|----------|
| Rh(1)-N(3)  | 2.013(2) | C(10)-C(11) | 1.394(4) |
| Rh(1)-N(1)  | 2.015(2) | C(10)-C(31) | 1.503(4) |
| Rh(1)-N(4)  | 2.021(2) | C(11)-C(12) | 1.432(4) |
| Rh(1)-N(2)  | 2.026(2) | C(12)-C(13) | 1.340(4) |
| Rh(1)-C(61) | 2.048(3) | C(13)-C(14) | 1.435(4) |
| N(1)-C(1)   | 1.371(3) | C(14)-C(15) | 1.393(4) |
| N(1)-C(4)   | 1.381(3) | C(15)-C(16) | 1.393(4) |
| N(2)-C(6)   | 1.377(3) | C(15)-C(41) | 1.503(4) |
| N(2)-C(9)   | 1.377(3) | C(16)-C(17) | 1.431(4) |
| N(3)-C(14)  | 1.378(3) | C(17)-C(18) | 1.341(4) |
| N(3)-C(11)  | 1.380(3) | C(18)-C(19) | 1.433(4) |
| N(4)-C(19)  | 1.374(3) | C(19)-C(20) | 1.388(4) |
| N(4)-C(16)  | 1.379(3) | C(20)-C(51) | 1.505(4) |
| C(1)-C(20)  | 1.393(4) | C(21)-C(26) | 1.346(5) |
| C(1)-C(2)   | 1.439(4) | C(21)-C(22) | 1.353(5) |
| C(2)-C(3)   | 1.340(4) | C(22)-C(23) | 1.389(5) |
| C(3)-C(4)   | 1.437(4) | C(23)-C(24) | 1.358(6) |
| C(4)-C(5)   | 1.388(4) | C(24)-C(25) | 1.329(5) |
| C(5)-C(6)   | 1.399(4) | C(24)-C(27) | 1.514(4) |
| C(5)-C(21)  | 1.506(4) | C(25)-C(26) | 1.399(5) |
| C(6)-C(7)   | 1.432(4) | C(31)-C(36) | 1.383(5) |
| C(7)-C(8)   | 1.341(4) | C(31)-C(32) | 1.384(4) |
| C(8)-C(9)   | 1.440(4) | C(32)-C(33) | 1.387(5) |
| C(9)-C(10)  | 1.400(4) | C(33)-C(34) | 1.364(7) |

|                  |            |                   |          |
|------------------|------------|-------------------|----------|
| C(34)-C(35)      | 1.375(6)   | C(2)-C(3)-C(4)    | 108.2(3) |
| C(34)-C(37)      | 1.526(5)   | N(1)-C(4)-C(5)    | 125.6(2) |
| C(35)-C(36)      | 1.393(5)   | N(1)-C(4)-C(3)    | 108.5(2) |
| C(41)-C(42)      | 1.365(4)   | C(5)-C(4)-C(3)    | 125.6(3) |
| C(41)-C(46)      | 1.379(4)   | C(4)-C(5)-C(6)    | 125.0(2) |
| C(42)-C(43)      | 1.393(4)   | C(4)-C(5)-C(21)   | 116.7(3) |
| C(43)-C(44)      | 1.373(5)   | C(6)-C(5)-C(21)   | 118.3(2) |
| C(44)-C(45)      | 1.357(5)   | N(2)-C(6)-C(5)    | 124.9(2) |
| C(44)-C(47)      | 1.518(4)   | N(2)-C(6)-C(7)    | 108.9(2) |
| C(45)-C(46)      | 1.387(4)   | C(5)-C(6)-C(7)    | 126.2(3) |
| C(51)-C(56)      | 1.355(5)   | C(8)-C(7)-C(6)    | 107.8(2) |
| C(51)-C(52)      | 1.365(5)   | C(7)-C(8)-C(9)    | 107.7(2) |
| C(52)-C(53)      | 1.390(5)   | N(2)-C(9)-C(10)   | 125.1(2) |
| C(53)-C(54)      | 1.353(6)   | N(2)-C(9)-C(8)    | 108.5(2) |
| C(54)-C(55)      | 1.352(5)   | C(10)-C(9)-C(8)   | 126.2(2) |
| C(54)-C(57)      | 1.518(5)   | C(11)-C(10)-C(9)  | 123.9(2) |
| C(55)-C(56)      | 1.388(5)   | C(11)-C(10)-C(31) | 118.2(2) |
| C(61)-C(62)      | 1.329(6)   | C(9)-C(10)-C(31)  | 117.8(2) |
| C(62)-C(63)      | 1.519(6)   | N(3)-C(11)-C(10)  | 124.9(2) |
| C(63)-C(64)      | 1.383(10)  | N(3)-C(11)-C(12)  | 108.6(2) |
| C(64)-C(65)      | 1.396(10)  | C(10)-C(11)-C(12) | 126.2(2) |
| C(65)-C(66)      | 1.367(12)  | C(13)-C(12)-C(11) | 107.8(2) |
| C(66)-C(67)      | 1.384(11)  | C(12)-C(13)-C(14) | 107.7(2) |
|                  |            | N(3)-C(14)-C(15)  | 125.3(2) |
| N(3)-Rh(1)-N(1)  | 173.93(9)  | N(3)-C(14)-C(13)  | 108.7(2) |
| N(3)-Rh(1)-N(4)  | 90.31(8)   | C(15)-C(14)-C(13) | 125.9(2) |
| N(1)-Rh(1)-N(4)  | 89.88(9)   | C(16)-C(15)-C(14) | 124.7(2) |
| N(3)-Rh(1)-N(2)  | 89.49(9)   | C(16)-C(15)-C(41) | 117.6(2) |
| N(1)-Rh(1)-N(2)  | 90.49(9)   | C(14)-C(15)-C(41) | 117.6(2) |
| N(4)-Rh(1)-N(2)  | 178.36(9)  | N(4)-C(16)-C(15)  | 124.9(2) |
| N(3)-Rh(1)-C(61) | 91.73(12)  | N(4)-C(16)-C(17)  | 109.3(2) |
| N(1)-Rh(1)-C(61) | 94.34(12)  | C(15)-C(16)-C(17) | 125.7(3) |
| N(4)-Rh(1)-C(61) | 89.76(11)  | C(18)-C(17)-C(16) | 107.3(2) |
| N(2)-Rh(1)-C(61) | 88.62(11)  | C(17)-C(18)-C(19) | 107.9(2) |
| C(1)-N(1)-C(4)   | 106.8(2)   | N(4)-C(19)-C(20)  | 125.5(2) |
| C(1)-N(1)-Rh(1)  | 126.96(18) | N(4)-C(19)-C(18)  | 108.9(2) |
| C(4)-N(1)-Rh(1)  | 126.16(18) | C(20)-C(19)-C(18) | 125.5(2) |
| C(6)-N(2)-C(9)   | 107.0(2)   | C(19)-C(20)-C(1)  | 124.7(2) |
| C(6)-N(2)-Rh(1)  | 125.64(18) | C(19)-C(20)-C(51) | 117.8(2) |
| C(9)-N(2)-Rh(1)  | 125.97(18) | C(1)-C(20)-C(51)  | 117.4(2) |
| C(14)-N(3)-C(11) | 106.8(2)   | C(26)-C(21)-C(22) | 117.2(3) |
| C(14)-N(3)-Rh(1) | 126.06(17) | C(26)-C(21)-C(5)  | 120.6(3) |
| C(11)-N(3)-Rh(1) | 127.01(18) | C(22)-C(21)-C(5)  | 122.3(3) |
| C(19)-N(4)-C(16) | 106.6(2)   | C(21)-C(22)-C(23) | 121.5(4) |
| C(19)-N(4)-Rh(1) | 126.37(17) | C(24)-C(23)-C(22) | 121.4(4) |
| C(16)-N(4)-Rh(1) | 125.61(17) | C(25)-C(24)-C(23) | 116.7(3) |
| N(1)-C(1)-C(20)  | 125.5(2)   | C(25)-C(24)-C(27) | 122.5(4) |
| N(1)-C(1)-C(2)   | 109.4(2)   | C(23)-C(24)-C(27) | 120.9(4) |
| C(20)-C(1)-C(2)  | 125.0(3)   | C(24)-C(25)-C(26) | 122.6(4) |
| C(3)-C(2)-C(1)   | 107.0(3)   | C(21)-C(26)-C(25) | 120.6(4) |

|                   |          |                   |           |
|-------------------|----------|-------------------|-----------|
| C(36)-C(31)-C(32) | 117.8(3) | C(44)-C(45)-C(46) | 122.1(3)  |
| C(36)-C(31)-C(10) | 121.3(3) | C(41)-C(46)-C(45) | 120.4(3)  |
| C(32)-C(31)-C(10) | 120.9(3) | C(56)-C(51)-C(52) | 117.5(3)  |
| C(31)-C(32)-C(33) | 120.7(4) | C(56)-C(51)-C(20) | 121.8(3)  |
| C(34)-C(33)-C(32) | 121.6(4) | C(52)-C(51)-C(20) | 120.7(3)  |
| C(33)-C(34)-C(35) | 118.2(3) | C(51)-C(52)-C(53) | 120.8(3)  |
| C(33)-C(34)-C(37) | 121.6(5) | C(54)-C(53)-C(52) | 121.8(4)  |
| C(35)-C(34)-C(37) | 120.1(5) | C(55)-C(54)-C(53) | 116.9(3)  |
| C(34)-C(35)-C(36) | 120.9(4) | C(55)-C(54)-C(57) | 121.4(4)  |
| C(31)-C(36)-C(35) | 120.8(4) | C(53)-C(54)-C(57) | 121.7(4)  |
| C(42)-C(41)-C(46) | 118.1(3) | C(54)-C(55)-C(56) | 122.1(4)  |
| C(42)-C(41)-C(15) | 121.7(3) | C(51)-C(56)-C(55) | 120.8(3)  |
| C(46)-C(41)-C(15) | 120.2(3) | C(62)-C(61)-Rh(1) | 123.3(3)  |
| C(41)-C(42)-C(43) | 120.6(3) | C(61)-C(62)-C(63) | 120.9(5)  |
| C(44)-C(43)-C(42) | 121.5(3) | C(64)-C(63)-C(62) | 115.2(6)  |
| C(45)-C(44)-C(43) | 117.3(3) | C(63)-C(64)-C(65) | 130.4(10) |
| C(45)-C(44)-C(47) | 121.7(3) | C(66)-C(65)-C(64) | 132.0(12) |
| C(43)-C(44)-C(47) | 121.0(3) | C(65)-C(66)-C(67) | 122.5(11) |

Table 5. Bond lengths [Å] and angles [deg] for Rh(tp)(*c*-heptyl) **5a**.

|             |           |             |           |
|-------------|-----------|-------------|-----------|
| Rh(1)-N(2)  | 2.021(8)  | C(10)-C(11) | 1.372(14) |
| Rh(1)-N(1)  | 2.023(8)  | C(10)-C(31) | 1.508(13) |
| Rh(1)-N(3)  | 2.029(8)  | C(11)-C(12) | 1.458(13) |
| Rh(1)-N(4)  | 2.032(8)  | C(12)-C(13) | 1.324(15) |
| Rh(1)-C(61) | 2.125(14) | C(13)-C(14) | 1.458(15) |
| N(1)-C(1)   | 1.376(12) | C(14)-C(15) | 1.387(14) |
| N(1)-C(4)   | 1.406(12) | C(15)-C(16) | 1.413(15) |
| N(2)-C(6)   | 1.377(12) | C(15)-C(41) | 1.518(14) |
| N(2)-C(9)   | 1.403(12) | C(16)-C(17) | 1.425(14) |
| N(3)-C(11)  | 1.361(12) | C(17)-C(18) | 1.343(15) |
| N(3)-C(14)  | 1.379(12) | C(18)-C(19) | 1.447(14) |
| N(4)-C(16)  | 1.370(13) | C(19)-C(20) | 1.391(14) |
| N(4)-C(19)  | 1.377(13) | C(20)-C(51) | 1.517(14) |
| C(1)-C(20)  | 1.392(14) | C(21)-C(22) | 1.373(15) |
| C(1)-C(2)   | 1.431(14) | C(21)-C(26) | 1.396(15) |
| C(2)-C(3)   | 1.308(14) | C(22)-C(23) | 1.399(16) |
| C(3)-C(4)   | 1.413(14) | C(23)-C(24) | 1.362(17) |
| C(4)-C(5)   | 1.378(14) | C(24)-C(25) | 1.359(17) |
| C(5)-C(6)   | 1.411(14) | C(24)-C(27) | 1.549(16) |
| C(5)-C(21)  | 1.479(13) | C(25)-C(26) | 1.384(15) |
| C(6)-C(7)   | 1.427(13) | C(31)-C(36) | 1.364(16) |
| C(7)-C(8)   | 1.335(14) | C(31)-C(32) | 1.385(15) |
| C(8)-C(9)   | 1.415(13) | C(32)-C(33) | 1.408(15) |
| C(9)-C(10)  | 1.402(13) | C(33)-C(34) | 1.372(19) |

|                  |           |                   |           |
|------------------|-----------|-------------------|-----------|
| C(34)-C(35)      | 1.34(2)   | N(1)-C(1)-C(2)    | 108.3(9)  |
| C(34)-C(37)      | 1.471(18) | C(20)-C(1)-C(2)   | 127.4(10) |
| C(35)-C(36)      | 1.446(17) | C(3)-C(2)-C(1)    | 107.8(9)  |
| C(41)-C(42)      | 1.363(16) | C(2)-C(3)-C(4)    | 110.0(10) |
| C(41)-C(46)      | 1.368(16) | C(5)-C(4)-N(1)    | 124.9(9)  |
| C(42)-C(43)      | 1.398(17) | C(5)-C(4)-C(3)    | 127.9(9)  |
| C(43)-C(44)      | 1.381(19) | N(1)-C(4)-C(3)    | 107.0(8)  |
| C(44)-C(45)      | 1.343(18) | C(4)-C(5)-C(6)    | 125.6(9)  |
| C(44)-C(47)      | 1.513(16) | C(4)-C(5)-C(21)   | 117.8(9)  |
| C(45)-C(46)      | 1.403(16) | C(6)-C(5)-C(21)   | 116.6(9)  |
| C(51)-C(56)      | 1.354(15) | N(2)-C(6)-C(5)    | 123.8(9)  |
| C(51)-C(52)      | 1.368(17) | N(2)-C(6)-C(7)    | 109.4(8)  |
| C(52)-C(53)      | 1.373(19) | C(5)-C(6)-C(7)    | 126.4(9)  |
| C(53)-C(54)      | 1.38(2)   | C(8)-C(7)-C(6)    | 107.3(9)  |
| C(54)-C(55)      | 1.342(19) | C(7)-C(8)-C(9)    | 109.0(9)  |
| C(54)-C(57)      | 1.526(16) | C(10)-C(9)-N(2)   | 123.8(9)  |
| C(55)-C(56)      | 1.385(16) | C(10)-C(9)-C(8)   | 127.8(9)  |
| C(61)-C(67)      | 1.385(19) | N(2)-C(9)-C(8)    | 108.2(8)  |
| C(61)-C(62)      | 1.459(19) | C(11)-C(10)-C(9)  | 125.3(9)  |
| C(62)-C(63)      | 1.32(3)   | C(11)-C(10)-C(31) | 117.9(9)  |
| C(63)-C(64)      | 1.32(3)   | C(9)-C(10)-C(31)  | 116.8(9)  |
| C(64)-C(65)      | 1.40(3)   | N(3)-C(11)-C(10)  | 126.7(9)  |
| C(65)-C(66)      | 1.42(2)   | N(3)-C(11)-C(12)  | 108.0(9)  |
| C(66)-C(67)      | 1.47(2)   | C(10)-C(11)-C(12) | 125.0(9)  |
| Cl(1)-C(68)      | 1.784(10) | C(13)-C(12)-C(11) | 108.4(9)  |
| Cl(2)-C(68)      | 1.786(10) | C(12)-C(13)-C(14) | 107.2(9)  |
|                  |           | N(3)-C(14)-C(15)  | 126.8(9)  |
| N(2)-Rh(1)-N(1)  | 90.0(3)   | N(3)-C(14)-C(13)  | 108.2(9)  |
| N(2)-Rh(1)-N(3)  | 90.1(3)   | C(15)-C(14)-C(13) | 125.0(9)  |
| N(1)-Rh(1)-N(3)  | 171.0(3)  | C(14)-C(15)-C(16) | 124.7(9)  |
| N(2)-Rh(1)-N(4)  | 179.4(4)  | C(14)-C(15)-C(41) | 117.9(9)  |
| N(1)-Rh(1)-N(4)  | 89.6(3)   | C(16)-C(15)-C(41) | 117.4(9)  |
| N(3)-Rh(1)-N(4)  | 90.2(3)   | N(4)-C(16)-C(15)  | 124.8(9)  |
| N(2)-Rh(1)-C(61) | 91.6(5)   | N(4)-C(16)-C(17)  | 109.3(9)  |
| N(1)-Rh(1)-C(61) | 96.0(5)   | C(15)-C(16)-C(17) | 125.9(9)  |
| N(3)-Rh(1)-C(61) | 93.0(5)   | C(18)-C(17)-C(16) | 108.1(9)  |
| N(4)-Rh(1)-C(61) | 88.8(5)   | C(17)-C(18)-C(19) | 106.8(9)  |
| C(1)-N(1)-C(4)   | 106.5(8)  | N(4)-C(19)-C(20)  | 125.6(9)  |
| C(1)-N(1)-Rh(1)  | 127.4(7)  | N(4)-C(19)-C(18)  | 108.7(9)  |
| C(4)-N(1)-Rh(1)  | 126.0(6)  | C(20)-C(19)-C(18) | 125.5(9)  |
| C(6)-N(2)-C(9)   | 106.0(8)  | C(19)-C(20)-C(1)  | 125.2(9)  |
| C(6)-N(2)-Rh(1)  | 126.8(6)  | C(19)-C(20)-C(51) | 118.3(9)  |
| C(9)-N(2)-Rh(1)  | 126.0(7)  | C(1)-C(20)-C(51)  | 116.4(9)  |
| C(11)-N(3)-C(14) | 108.1(8)  | C(22)-C(21)-C(26) | 117.2(10) |
| C(11)-N(3)-Rh(1) | 126.2(6)  | C(22)-C(21)-C(5)  | 122.8(10) |
| C(14)-N(3)-Rh(1) | 125.7(7)  | C(26)-C(21)-C(5)  | 120.0(10) |
| C(16)-N(4)-C(19) | 106.9(9)  | C(21)-C(22)-C(23) | 120.5(11) |
| C(16)-N(4)-Rh(1) | 126.9(7)  | C(24)-C(23)-C(22) | 121.3(11) |
| C(19)-N(4)-Rh(1) | 125.3(7)  | C(25)-C(24)-C(23) | 118.9(11) |
| N(1)-C(1)-C(20)  | 123.9(10) | C(25)-C(24)-C(27) | 120.8(12) |

|                   |           |                   |           |
|-------------------|-----------|-------------------|-----------|
| C(23)-C(24)-C(27) | 120.3(12) | C(41)-C(46)-C(45) | 120.3(12) |
| C(24)-C(25)-C(26) | 120.6(12) | C(56)-C(51)-C(52) | 116.1(11) |
| C(25)-C(26)-C(21) | 121.4(11) | C(56)-C(51)-C(20) | 122.4(10) |
| C(36)-C(31)-C(32) | 118.7(10) | C(52)-C(51)-C(20) | 121.4(10) |
| C(36)-C(31)-C(10) | 119.7(10) | C(51)-C(52)-C(53) | 121.4(14) |
| C(32)-C(31)-C(10) | 121.6(9)  | C(52)-C(53)-C(54) | 121.4(15) |
| C(31)-C(32)-C(33) | 120.3(11) | C(55)-C(54)-C(53) | 116.6(12) |
| C(34)-C(33)-C(32) | 121.8(12) | C(55)-C(54)-C(57) | 122.1(14) |
| C(35)-C(34)-C(33) | 117.5(11) | C(53)-C(54)-C(57) | 121.3(15) |
| C(35)-C(34)-C(37) | 121.5(15) | C(54)-C(55)-C(56) | 121.1(12) |
| C(33)-C(34)-C(37) | 121.0(15) | C(51)-C(56)-C(55) | 122.4(12) |
| C(34)-C(35)-C(36) | 122.7(13) | C(67)-C(61)-C(62) | 124.0(14) |
| C(31)-C(36)-C(35) | 118.9(13) | C(67)-C(61)-Rh(1) | 116.5(10) |
| C(42)-C(41)-C(46) | 119.1(11) | C(62)-C(61)-Rh(1) | 115.4(9)  |
| C(42)-C(41)-C(15) | 119.6(11) | C(63)-C(62)-C(61) | 124.6(17) |
| C(46)-C(41)-C(15) | 121.3(11) | C(64)-C(63)-C(62) | 140(3)    |
| C(41)-C(42)-C(43) | 119.6(13) | C(63)-C(64)-C(65) | 121(2)    |
| C(44)-C(43)-C(42) | 121.9(13) | C(64)-C(65)-C(66) | 117(2)    |
| C(45)-C(44)-C(43) | 117.4(12) | C(65)-C(66)-C(67) | 123.8(16) |
| C(45)-C(44)-C(47) | 122.9(14) | C(61)-C(67)-C(66) | 123.8(14) |
| C(43)-C(44)-C(47) | 119.7(14) | Cl(1)-C(68)-Cl(2) | 111.2(14) |
| C(44)-C(45)-C(46) | 121.8(13) |                   |           |

Table 6. Bond lengths [Å] and angles [deg] for Rh(tp)(cycloheptatrienyl) 8.

|             |          |             |          |
|-------------|----------|-------------|----------|
| Rh(1)-N(2)  | 2.013(2) | C(6)-C(7)   | 1.448(4) |
| Rh(1)-N(4)  | 2.016(2) | C(7)-C(8)   | 1.343(4) |
| Rh(1)-N(3)  | 2.019(2) | C(8)-C(9)   | 1.436(4) |
| Rh(1)-N(1)  | 2.021(2) | C(9)-C(10)  | 1.396(4) |
| Rh(1)-C(61) | 2.104(3) | C(10)-C(11) | 1.399(4) |
| N(1)-C(1)   | 1.373(3) | C(10)-C(31) | 1.500(4) |
| N(1)-C(4)   | 1.382(3) | C(11)-C(12) | 1.432(4) |
| N(2)-C(6)   | 1.374(3) | C(12)-C(13) | 1.342(4) |
| N(2)-C(9)   | 1.386(4) | C(13)-C(14) | 1.435(4) |
| N(3)-C(11)  | 1.373(3) | C(14)-C(15) | 1.394(4) |
| N(3)-C(14)  | 1.381(3) | C(15)-C(16) | 1.396(4) |
| N(4)-C(16)  | 1.374(3) | C(15)-C(41) | 1.496(3) |
| N(4)-C(19)  | 1.382(3) | C(16)-C(17) | 1.439(4) |
| C(1)-C(20)  | 1.391(4) | C(17)-C(18) | 1.342(4) |
| C(1)-C(2)   | 1.439(4) | C(18)-C(19) | 1.433(4) |
| C(2)-C(3)   | 1.352(4) | C(19)-C(20) | 1.401(4) |
| C(3)-C(4)   | 1.434(4) | C(20)-C(51) | 1.502(3) |
| C(4)-C(5)   | 1.391(4) | C(21)-C(26) | 1.372(4) |
| C(5)-C(6)   | 1.387(4) | C(21)-C(22) | 1.385(4) |
| C(5)-C(21)  | 1.501(4) | C(22)-C(23) | 1.387(4) |

|                  |            |                   |            |
|------------------|------------|-------------------|------------|
| C(23)-C(24)      | 1.366(5)   | C(9)-N(2)-Rh(1)   | 126.29(18) |
| C(24)-C(25)      | 1.375(5)   | C(11)-N(3)-C(14)  | 106.5(2)   |
| C(24)-C(27)      | 1.511(4)   | C(11)-N(3)-Rh(1)  | 126.91(17) |
| C(25)-C(26)      | 1.389(4)   | C(14)-N(3)-Rh(1)  | 125.72(16) |
| C(31)-C(36)      | 1.377(4)   | C(16)-N(4)-C(19)  | 106.5(2)   |
| C(31)-C(32)      | 1.380(4)   | C(16)-N(4)-Rh(1)  | 126.56(17) |
| C(32)-C(33)      | 1.381(4)   | C(19)-N(4)-Rh(1)  | 126.86(17) |
| C(33)-C(34)      | 1.366(5)   | N(1)-C(1)-C(20)   | 125.6(2)   |
| C(34)-C(35)      | 1.374(6)   | N(1)-C(1)-C(2)    | 109.2(2)   |
| C(34)-C(37)      | 1.517(5)   | C(20)-C(1)-C(2)   | 125.1(2)   |
| C(35)-C(36)      | 1.380(5)   | C(3)-C(2)-C(1)    | 107.4(2)   |
| C(41)-C(46)      | 1.363(4)   | C(2)-C(3)-C(4)    | 107.3(2)   |
| C(41)-C(42)      | 1.381(4)   | N(1)-C(4)-C(5)    | 125.5(2)   |
| C(42)-C(43)      | 1.391(4)   | N(1)-C(4)-C(3)    | 109.2(2)   |
| C(43)-C(44)      | 1.376(5)   | C(5)-C(4)-C(3)    | 125.2(2)   |
| C(44)-C(45)      | 1.374(5)   | C(6)-C(5)-C(4)    | 124.3(2)   |
| C(44)-C(47)      | 1.510(4)   | C(6)-C(5)-C(21)   | 117.4(2)   |
| C(45)-C(46)      | 1.397(4)   | C(4)-C(5)-C(21)   | 118.2(2)   |
| C(51)-C(56)      | 1.371(4)   | N(2)-C(6)-C(5)    | 126.3(2)   |
| C(51)-C(52)      | 1.381(4)   | N(2)-C(6)-C(7)    | 108.8(2)   |
| C(52)-C(53)      | 1.394(5)   | C(5)-C(6)-C(7)    | 125.0(3)   |
| C(53)-C(54)      | 1.381(5)   | C(8)-C(7)-C(6)    | 107.6(3)   |
| C(54)-C(55)      | 1.349(5)   | C(7)-C(8)-C(9)    | 107.8(3)   |
| C(54)-C(57)      | 1.522(4)   | N(2)-C(9)-C(10)   | 125.9(2)   |
| C(55)-C(56)      | 1.384(4)   | N(2)-C(9)-C(8)    | 108.8(2)   |
| C(61)-C(67)      | 1.444(4)   | C(10)-C(9)-C(8)   | 125.0(3)   |
| C(61)-C(62)      | 1.458(4)   | C(9)-C(10)-C(11)  | 124.4(2)   |
| C(62)-C(63)      | 1.425(6)   | C(9)-C(10)-C(31)  | 117.3(2)   |
| C(62)-C(63')     | 1.447(7)   |                   |            |
| C(63)-C(64)      | 1.492(8)   | C(11)-C(10)-C(31) | 118.3(2)   |
| C(63')-C(64)     | 1.533(8)   | N(3)-C(11)-C(10)  | 125.0(2)   |
| C(64)-C(65)      | 1.442(6)   | N(3)-C(11)-C(12)  | 109.4(2)   |
| C(65)-C(66)      | 1.459(6)   | C(10)-C(11)-C(12) | 125.6(2)   |
| C(66)-C(67)      | 1.449(5)   | C(13)-C(12)-C(11) | 107.6(2)   |
|                  |            | C(12)-C(13)-C(14) | 107.5(2)   |
| N(2)-Rh(1)-N(4)  | 170.62(9)  | N(3)-C(14)-C(15)  | 125.2(2)   |
| N(2)-Rh(1)-N(3)  | 90.18(9)   | N(3)-C(14)-C(13)  | 109.0(2)   |
| N(4)-Rh(1)-N(3)  | 90.05(8)   | C(15)-C(14)-C(13) | 125.6(2)   |
| N(2)-Rh(1)-N(1)  | 89.94(9)   | C(14)-C(15)-C(16) | 124.4(2)   |
| N(4)-Rh(1)-N(1)  | 89.74(9)   | C(14)-C(15)-C(41) | 118.0(2)   |
| N(3)-Rh(1)-N(1)  | 179.39(9)  | C(16)-C(15)-C(41) | 117.6(2)   |
| N(2)-Rh(1)-C(61) | 92.42(12)  | N(4)-C(16)-C(15)  | 125.2(2)   |
| N(4)-Rh(1)-C(61) | 96.94(12)  | N(4)-C(16)-C(17)  | 108.9(2)   |
| N(3)-Rh(1)-C(61) | 91.85(15)  | C(15)-C(16)-C(17) | 125.6(2)   |
| N(1)-Rh(1)-C(61) | 88.75(15)  | C(18)-C(17)-C(16) | 107.6(2)   |
| C(1)-N(1)-C(4)   | 106.8(2)   | C(17)-C(18)-C(19) | 107.5(2)   |
| C(1)-N(1)-Rh(1)  | 125.87(17) | N(4)-C(19)-C(20)  | 124.4(2)   |
| C(4)-N(1)-Rh(1)  | 126.26(17) | N(4)-C(19)-C(18)  | 109.1(2)   |
| C(6)-N(2)-C(9)   | 107.0(2)   | C(20)-C(19)-C(18) | 126.0(2)   |
| C(6)-N(2)-Rh(1)  | 126.70(18) | C(1)-C(20)-C(19)  | 124.3(2)   |

|                   |          |                    |          |
|-------------------|----------|--------------------|----------|
| C(1)-C(20)-C(51)  | 117.7(2) | C(45)-C(44)-C(47)  | 120.4(3) |
| C(19)-C(20)-C(51) | 117.9(2) | C(43)-C(44)-C(47)  | 121.7(3) |
| C(26)-C(21)-C(22) | 118.0(3) | C(44)-C(45)-C(46)  | 120.9(3) |
| C(26)-C(21)-C(5)  | 121.4(3) | C(41)-C(46)-C(45)  | 121.2(3) |
| C(22)-C(21)-C(5)  | 120.5(3) | C(56)-C(51)-C(52)  | 118.2(3) |
| C(21)-C(22)-C(23) | 120.1(3) | C(56)-C(51)-C(20)  | 121.6(3) |
| C(24)-C(23)-C(22) | 122.1(3) | C(52)-C(51)-C(20)  | 120.2(3) |
| C(23)-C(24)-C(25) | 117.4(3) | C(51)-C(52)-C(53)  | 119.7(3) |
| C(23)-C(24)-C(27) | 120.9(3) | C(54)-C(53)-C(52)  | 121.7(3) |
| C(25)-C(24)-C(27) | 121.7(3) | C(55)-C(54)-C(53)  | 117.1(3) |
| C(24)-C(25)-C(26) | 121.3(3) | C(55)-C(54)-C(57)  | 121.4(4) |
| C(21)-C(26)-C(25) | 121.0(3) | C(53)-C(54)-C(57)  | 121.4(4) |
| C(36)-C(31)-C(32) | 118.1(3) | C(54)-C(55)-C(56)  | 122.2(3) |
| C(36)-C(31)-C(10) | 119.9(3) | C(51)-C(56)-C(55)  | 120.7(3) |
| C(32)-C(31)-C(10) | 122.0(2) | C(67)-C(61)-C(62)  | 123.8(3) |
| C(31)-C(32)-C(33) | 120.7(3) | C(67)-C(61)-Rh(1)  | 115.0(2) |
| C(34)-C(33)-C(32) | 121.5(3) | C(62)-C(61)-Rh(1)  | 116.6(2) |
| C(33)-C(34)-C(35) | 117.6(3) | C(63)-C(62)-C(63') | 52.1(6)  |
| C(33)-C(34)-C(37) | 121.4(4) | C(63)-C(62)-C(61)  | 126.5(5) |
| C(35)-C(34)-C(37) | 121.0(4) | C(63')-C(62)-C(61) | 118.9(6) |
| C(34)-C(35)-C(36) | 121.8(3) | C(62)-C(63)-C(64)  | 118.5(6) |
| C(31)-C(36)-C(35) | 120.4(3) | C(62)-C(63')-C(64) | 114.5(6) |
| C(46)-C(41)-C(42) | 118.1(3) | C(65)-C(64)-C(63)  | 122.2(6) |
| C(46)-C(41)-C(15) | 121.9(2) | C(65)-C(64)-C(63') | 114.1(6) |
| C(42)-C(41)-C(15) | 120.0(2) | C(63)-C(64)-C(63') | 49.3(6)  |
| C(41)-C(42)-C(43) | 120.9(3) | C(64)-C(65)-C(66)  | 120.9(5) |
| C(44)-C(43)-C(42) | 121.0(3) | C(67)-C(66)-C(65)  | 124.7(4) |
| C(45)-C(44)-C(43) | 117.9(3) | C(61)-C(67)-C(66)  | 123.8(4) |

Table 7. Bond lengths [Å] and angles [deg] for Rh(ttp)(*n*-octyl) **10b**.

|             |          |             |          |
|-------------|----------|-------------|----------|
| Rh(1)-N(1)  | 2.017(3) | C(2)-C(3)   | 1.341(5) |
| Rh(1)-N(3)  | 2.019(3) | C(3)-C(4)   | 1.436(5) |
| Rh(1)-N(2)  | 2.024(3) | C(4)-C(5)   | 1.395(5) |
| Rh(1)-N(4)  | 2.030(3) | C(5)-C(6)   | 1.397(5) |
| Rh(1)-C(61) | 2.031(4) | C(5)-C(21)  | 1.504(5) |
| N(1)-C(4)   | 1.373(4) | C(6)-C(7)   | 1.429(5) |
| N(1)-C(1)   | 1.383(4) | C(7)-C(8)   | 1.342(5) |
| N(2)-C(6)   | 1.374(4) | C(8)-C(9)   | 1.435(5) |
| N(2)-C(9)   | 1.382(4) | C(9)-C(10)  | 1.383(5) |
| N(3)-C(11)  | 1.377(4) | C(10)-C(11) | 1.396(5) |
| N(3)-C(14)  | 1.383(4) | C(10)-C(31) | 1.508(5) |
| N(4)-C(16)  | 1.378(4) | C(11)-C(12) | 1.439(5) |
| N(4)-C(19)  | 1.382(4) | C(12)-C(13) | 1.336(5) |
| C(1)-C(20)  | 1.388(5) | C(13)-C(14) | 1.439(5) |
| C(1)-C(2)   | 1.433(5) | C(14)-C(15) | 1.386(5) |

|                 |            |                   |            |
|-----------------|------------|-------------------|------------|
| C(15)-C(16)     | 1.403(5)   | N(1)-Rh(1)-N(4)   | 90.42(11)  |
| C(15)-C(41)     | 1.502(5)   | N(3)-Rh(1)-N(4)   | 89.54(11)  |
| C(16)-C(17)     | 1.443(5)   | N(2)-Rh(1)-N(4)   | 178.47(11) |
| C(17)-C(18)     | 1.347(5)   | N(1)-Rh(1)-C(61)  | 94.91(16)  |
| C(18)-C(19)     | 1.435(5)   | N(3)-Rh(1)-C(61)  | 91.25(16)  |
| C(19)-C(20)     | 1.395(5)   | N(2)-Rh(1)-C(61)  | 90.78(15)  |
| C(20)-C(51)     | 1.502(5)   | N(4)-Rh(1)-C(61)  | 87.71(15)  |
| C(21)-C(22)     | 1.359(6)   | C(4)-N(1)-C(1)    | 107.0(3)   |
| C(21)-C(26)     | 1.367(6)   | C(4)-N(1)-Rh(1)   | 126.8(2)   |
| C(22)-C(23)     | 1.397(6)   | C(1)-N(1)-Rh(1)   | 126.1(2)   |
| C(23)-C(24)     | 1.359(7)   | C(6)-N(2)-C(9)    | 106.6(3)   |
| C(24)-C(25)     | 1.361(7)   | C(6)-N(2)-Rh(1)   | 126.7(2)   |
| C(24)-C(27)     | 1.523(6)   | C(9)-N(2)-Rh(1)   | 125.4(2)   |
| C(25)-C(26)     | 1.386(6)   | C(11)-N(3)-C(14)  | 107.2(3)   |
| C(31)-C(32)     | 1.369(5)   | C(11)-N(3)-Rh(1)  | 125.9(2)   |
| C(31)-C(36)     | 1.383(5)   | C(14)-N(3)-Rh(1)  | 126.7(2)   |
| C(32)-C(33)     | 1.401(6)   | C(16)-N(4)-C(19)  | 107.2(3)   |
| C(33)-C(34)     | 1.368(6)   | C(16)-N(4)-Rh(1)  | 126.0(2)   |
| C(34)-C(35)     | 1.368(6)   | C(19)-N(4)-Rh(1)  | 125.5(2)   |
| C(34)-C(37)     | 1.527(6)   | N(1)-C(1)-C(20)   | 125.9(3)   |
| C(35)-C(36)     | 1.385(6)   | N(1)-C(1)-C(2)    | 108.4(3)   |
| C(41)-C(42)     | 1.379(6)   | C(20)-C(1)-C(2)   | 125.5(3)   |
| C(41)-C(46)     | 1.381(6)   | C(3)-C(2)-C(1)    | 108.1(3)   |
| C(42)-C(43)     | 1.399(6)   | C(2)-C(3)-C(4)    | 107.4(3)   |
| C(43)-C(44)     | 1.373(8)   | N(1)-C(4)-C(5)    | 125.6(3)   |
| C(44)-C(45)     | 1.370(8)   | N(1)-C(4)-C(3)    | 109.0(3)   |
| C(44)-C(47)     | 1.529(7)   | C(5)-C(4)-C(3)    | 125.3(3)   |
| C(45)-C(46)     | 1.381(6)   | C(4)-C(5)-C(6)    | 124.7(3)   |
| C(51)-C(56)     | 1.356(6)   | C(4)-C(5)-C(21)   | 117.5(3)   |
| C(51)-C(52)     | 1.364(6)   | C(6)-C(5)-C(21)   | 117.7(3)   |
| C(52)-C(53)     | 1.398(6)   | N(2)-C(6)-C(5)    | 125.2(3)   |
| C(53)-C(54)     | 1.357(7)   | N(2)-C(6)-C(7)    | 109.3(3)   |
| C(54)-C(55)     | 1.345(7)   | C(5)-C(6)-C(7)    | 125.5(3)   |
| C(54)-C(57)     | 1.513(6)   | C(8)-C(7)-C(6)    | 107.7(3)   |
| C(55)-C(56)     | 1.405(6)   | C(7)-C(8)-C(9)    | 107.6(3)   |
| C(61)-C(62)     | 1.5272(11) | N(2)-C(9)-C(10)   | 125.4(3)   |
| C(62)-C(63)     | 1.506(7)   | N(2)-C(9)-C(8)    | 108.8(3)   |
| C(63)-C(64)     | 1.498(10)  | C(10)-C(9)-C(8)   | 125.7(3)   |
| C(63)-C(64')    | 1.525(10)  | C(9)-C(10)-C(11)  | 124.6(3)   |
| C(64)-C(65)     | 1.526(10)  | C(9)-C(10)-C(31)  | 117.6(3)   |
| C(64)-C(65')    | 1.521(10)  | C(11)-C(10)-C(31) | 117.7(3)   |
| C(64)-C(66)     | 2.03(3)    | N(3)-C(11)-C(10)  | 125.3(3)   |
| C(65)-C(66)     | 1.501(10)  | N(3)-C(11)-C(12)  | 108.4(3)   |
| C(65)-C(66')    | 1.514(10)  | C(10)-C(11)-C(12) | 126.2(3)   |
| C(66)-C(67)     | 1.534(10)  | C(13)-C(12)-C(11) | 108.0(3)   |
| C(67)-C(68)     | 1.490(9)   | C(12)-C(13)-C(14) | 107.8(3)   |
|                 |            | N(3)-C(14)-C(15)  | 125.1(3)   |
| N(1)-Rh(1)-N(3) | 173.83(11) | N(3)-C(14)-C(13)  | 108.2(3)   |
| N(1)-Rh(1)-N(2) | 89.97(11)  | C(15)-C(14)-C(13) | 126.4(3)   |
| N(3)-Rh(1)-N(2) | 90.24(11)  | C(14)-C(15)-C(16) | 124.3(3)   |

|                   |          |                     |           |
|-------------------|----------|---------------------|-----------|
| C(14)-C(15)-C(41) | 118.5(3) | C(53)-C(54)-C(57)   | 121.1(5)  |
| C(16)-C(15)-C(41) | 117.2(3) | C(54)-C(55)-C(56)   | 121.9(5)  |
| N(4)-C(16)-C(15)  | 125.0(3) | C(51)-C(56)-C(55)   | 120.9(4)  |
| N(4)-C(16)-C(17)  | 108.5(3) | C(62)-C(61)-Rh(1)   | 120.3(3)  |
| C(15)-C(16)-C(17) | 126.5(3) | C(63)-C(62)-C(61)   | 110.8(5)  |
| C(18)-C(17)-C(16) | 107.7(3) | C(64)-C(63)-C(62)   | 110.6(11) |
| C(17)-C(18)-C(19) | 107.7(3) | C(64)-C(63)-C(64')  | 58.2(13)  |
| N(4)-C(19)-C(20)  | 125.1(3) | C(62)-C(63)-C(64')  | 108.4(9)  |
| N(4)-C(19)-C(18)  | 108.8(3) | C(63)-C(64)-C(65)   | 121.8(18) |
| C(20)-C(19)-C(18) | 126.1(3) | C(65')-C(64')-C(63) | 97.5(13)  |
| C(1)-C(20)-C(19)  | 124.8(3) | C(65')-C(64')-C(66) | 47.8(8)   |
| C(1)-C(20)-C(51)  | 117.0(3) | C(63)-C(64')-C(66)  | 138.0(13) |
| C(19)-C(20)-C(51) | 118.2(3) | C(66)-C(65)-C(64)   | 112(2)    |
| C(22)-C(21)-C(26) | 117.9(4) | C(66)-C(65')-C(64') | 84.2(16)  |
| C(22)-C(21)-C(5)  | 121.1(4) | C(65)-C(66)-C(65')  | 25.7(14)  |
| C(26)-C(21)-C(5)  | 121.0(3) | C(65)-C(66)-C(67)   | 87.2(15)  |
| C(21)-C(22)-C(23) | 121.0(4) | C(65')-C(66)-C(67)  | 101.2(16) |
| C(24)-C(23)-C(22) | 121.6(4) | C(65)-C(66)-C(64')  | 67.1(13)  |
| C(23)-C(24)-C(25) | 116.7(4) | C(65')-C(66)-C(64') | 48.1(8)   |
| C(23)-C(24)-C(27) | 121.8(5) | C(67)-C(66)-C(64')  | 148.2(16) |
| C(25)-C(24)-C(27) | 121.5(5) | C(68)-C(67)-C(66)   | 119.7(18) |
| C(24)-C(25)-C(26) | 122.6(4) |                     |           |
| C(21)-C(26)-C(25) | 120.3(4) |                     |           |
| C(32)-C(31)-C(36) | 118.2(3) |                     |           |
| C(32)-C(31)-C(10) | 121.6(3) |                     |           |
| C(36)-C(31)-C(10) | 120.1(3) |                     |           |
| C(31)-C(32)-C(33) | 120.5(4) |                     |           |
| C(34)-C(33)-C(32) | 121.5(4) |                     |           |
| C(35)-C(34)-C(33) | 117.3(4) |                     |           |
| C(35)-C(34)-C(37) | 121.5(4) |                     |           |
| C(33)-C(34)-C(37) | 121.2(4) |                     |           |
| C(34)-C(35)-C(36) | 122.2(4) |                     |           |
| C(31)-C(36)-C(35) | 120.3(4) |                     |           |
| C(42)-C(41)-C(46) | 117.5(4) |                     |           |
| C(42)-C(41)-C(15) | 121.4(4) |                     |           |
| C(46)-C(41)-C(15) | 121.1(4) |                     |           |
| C(41)-C(42)-C(43) | 120.7(5) |                     |           |
| C(44)-C(43)-C(42) | 121.1(5) |                     |           |
| C(45)-C(44)-C(43) | 117.9(4) |                     |           |
| C(45)-C(44)-C(47) | 122.4(6) |                     |           |
| C(43)-C(44)-C(47) | 119.7(7) |                     |           |
| C(44)-C(45)-C(46) | 121.4(5) |                     |           |
| C(45)-C(46)-C(41) | 121.3(5) |                     |           |
| C(56)-C(51)-C(52) | 117.6(4) |                     |           |
| C(56)-C(51)-C(20) | 120.5(3) |                     |           |
| C(52)-C(51)-C(20) | 122.0(4) |                     |           |
| C(51)-C(52)-C(53) | 120.6(4) |                     |           |
| C(54)-C(53)-C(52) | 121.9(4) |                     |           |
| C(55)-C(54)-C(53) | 117.0(4) |                     |           |
| C(55)-C(54)-C(57) | 121.8(5) |                     |           |

## GC-MS Spectra

*c*-Octane and benzene-*d*<sub>6</sub> had been found to be free of *n*-octane and 1-octene.

The GC-MS reports are attached as follow:

- i) Sample *c*-octane spiked with *n*-octane and 1-octene
- ii) Sample *c*-octane
- iii) Solvent benzene-*d*<sub>6</sub>

Details of Chemicals Used for GC-MS Analysis

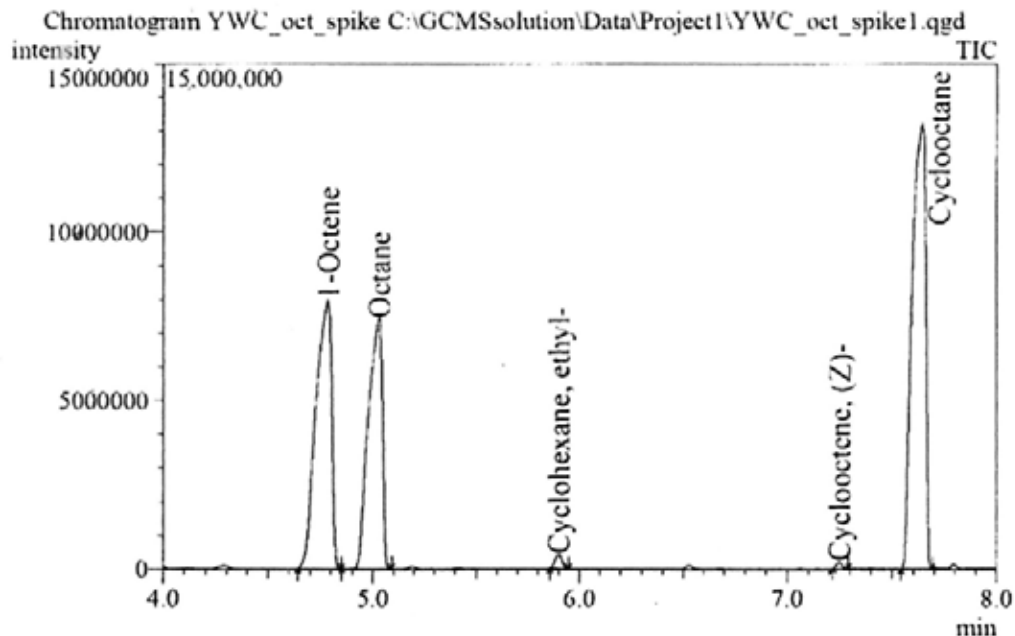
| Enrty | Chemical                       | Supplier          | Grade    |
|-------|--------------------------------|-------------------|----------|
| 1     | <i>c</i> -octane               | Aldrich           | 99+%     |
| 2     | <i>n</i> -octane               | Fluka             | >99%(GC) |
| 3     | 1-octene                       | Fluka             | 99%      |
| 4     | benzene- <i>d</i> <sub>6</sub> | Cambridge Isotope | 99.5%    |

i) GC-MS report of sample *c*-octane spiked with *n*-octane and 1-octene

## Sample Cyclooctane spiked with 1-Octene & n-Octane

Sample Information

Analyzed by : Admin  
 Analyzed : 4/7/2010 5:28:07 PM  
 Sample Type : Unknown  
 Level # : 1  
 Sample Name : YWC\_oct\_spike  
 Sample ID :  
 IS Amount : [1]=1  
 Sample Amount : 1  
 Dilution Factor : 1  
 Vial # : 9  
 Injection Volume : 1  
 Data File : C:\GCMSsolution\Data\Project1\YWC\_oct\_spike1.qgd  
 Org Data File : C:\GCMSsolution\Data\Project1\YWC\_oct\_spike1.qgd  
 Method File : C:\GCMSsolution\Data\Project1\Shmg\_1(4mm).qgd  
 Org Method File : C:\GCMSsolution\Data\Project1\Shmg\_1(4mm).qgd  
 Report File :  
 Tuning File : C:\GCMSsolution\System\Tune1\03032010.qd  
 Modified by : Admin  
 Modified : 4/8/2010 11:13:33 AM



Quantitative Result Table

| Name               | R Time | m/z   | Area    | Height  |
|--------------------|--------|-------|---------|---------|
| 1-Octene           | 4.783  | 55.00 | 8351875 | 1543069 |
| Octane             | 5.029  | 85.00 | 9302936 | 1952442 |
| Cyclohexane, ethyl | 5.900  | 83.00 | 312732  | 128068  |
| Cyclooctene, (Z)-  | 7.248  | 67.00 | 96065   | 47529   |
| Cyclooctane        | 7.644  | 56.00 | 8756382 | 1979570 |

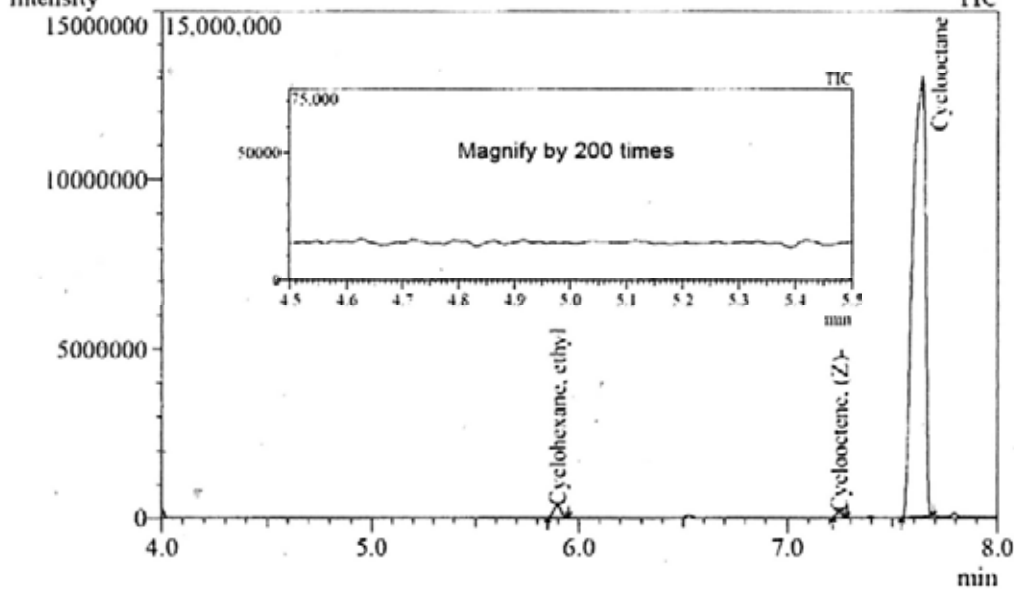
ii) GC-MS report of sample *c*-octane

## Sample Cyclooctane

### Sample Information

Analyzed by : Admin  
 Analyzed : 4/7/2010 5:57:58 PM  
 Sample Type : Unknown  
 Level # : 1  
 Sample Name : YWC\_oct\_nonspike  
 Sample ID :  
 IS Amount : [1]-1  
 Sample Amount : 1  
 Dilution Factor : 1  
 Vial # : 9  
 Injection Volume : 1  
 Data File : C:\GCMSsolution\Data\Project1\YWC\_oct\_nonspike.qgd  
 Orig Data File : C:\GCMSsolution\Data\Project1\YWC\_oct\_nonspike.qgd  
 Method File : C:\GCMSsolution\Data\Project1\Shing\_1(4min).qgd  
 Orig Method File : C:\GCMSsolution\Data\Project1\Shing\_1(4min).qgd  
 Report File :  
 Tuning File : C:\GCMSsolution\System\Tune1\03032010.qgd  
 Modified by : Admin  
 Modified : 4/8/2010 10:52:27 AM

Chromatogram YWC\_oct\_nonspike C:\GCMSsolution\Data\Project1\YWC\_oct\_nonspike.qgd



### Quantitative Result Table

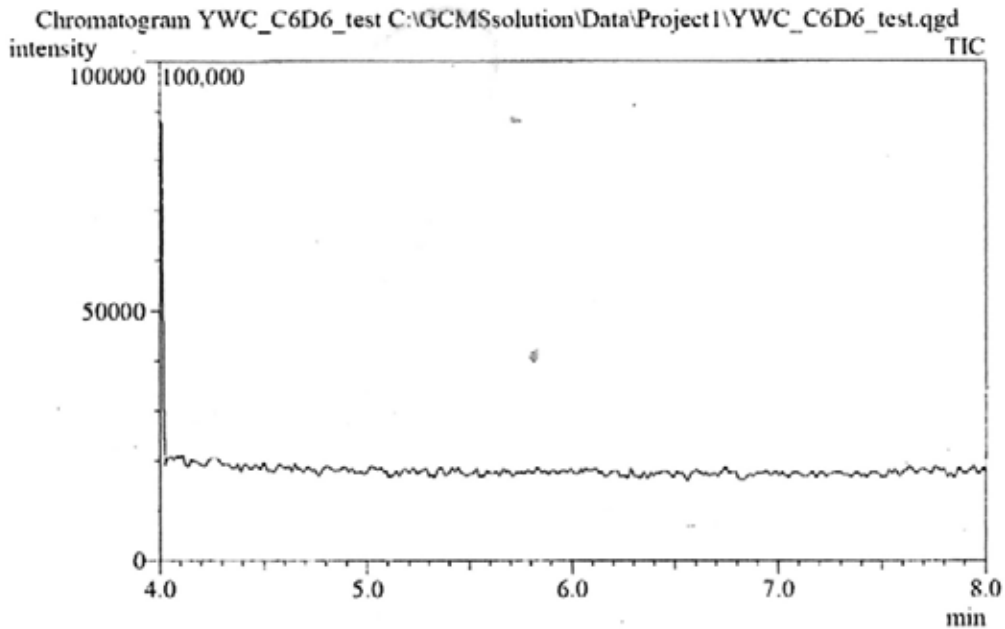
| Name               | R Time | m/z   | Area    | Height  |
|--------------------|--------|-------|---------|---------|
| Cyclohexane, ethyl | 5.896  | 83.00 | 279808  | 108316  |
| Cyclooctene, (Z)-  | 7.246  | 67.00 | 85941   | 41119   |
| Cyclooctane        | 7.639  | 56.00 | 8263485 | 1950977 |

iii) GC-MS report of solvent benzene-*d*<sub>6</sub>

## C6D6

### Sample Information:

Analyzed by : Admin  
Analyzed : 4/9/2010 10:07:18 AM  
Sample Type : Unknown  
Level # : 1  
Sample Name : YWC\_C6D6\_test  
Sample ID :  
IS Amount : [1]=1  
Sample Amount : 1  
Dilution Factor : 1  
Vial # : 9  
Injection Volume : 1  
Data File : C:\GCMSsolution\Data\Project1\YWC\_C6D6\_test.qgd  
Org Data File : C:\GCMSsolution\Data\Project1\YWC\_C6D6\_test.qgd  
Method File : C:\GCMSsolution\Data\Project1\Shing\_1(4min).qgm  
Org Method File : C:\GCMSsolution\Data\Project1\Shing\_1(4min).qgm  
Report File :  
Timing File : C:\GCMSsolution\System\Time1\03032010.qg  
Modified by : Admin  
Modified : 4/9/2010 10:27:18 AM



## List of Spectra

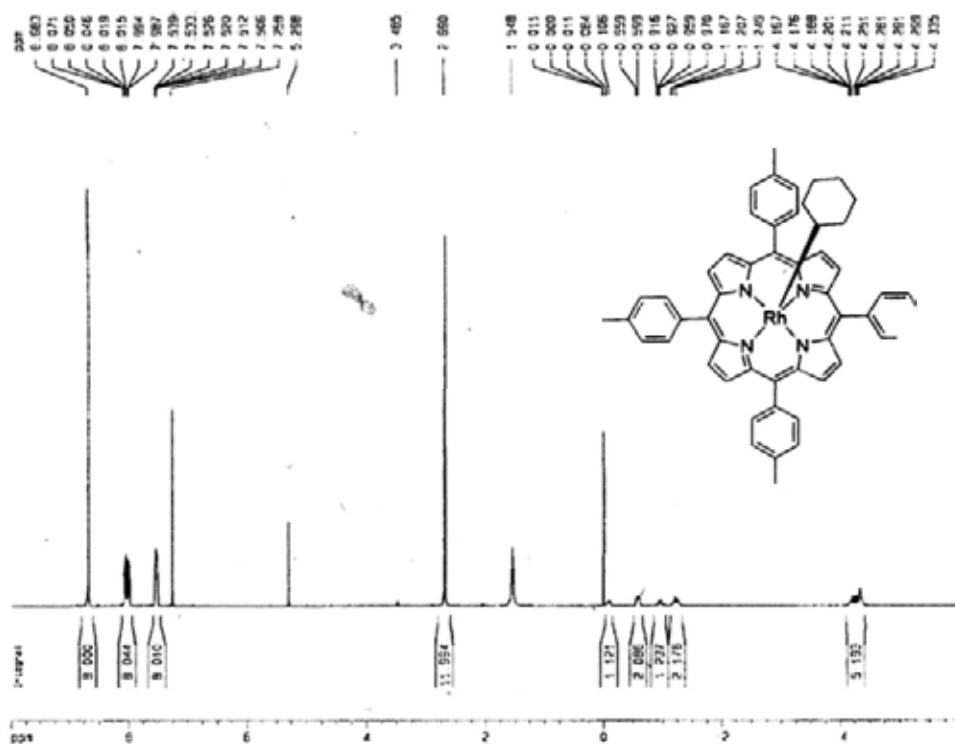
| No | Spectra   | Page |
|----|---|------|
| 1  | $^1\text{H}$ NMR Spectrum of $\text{Rh}(\text{ttp})(c\text{-hexyl})$ <b>2a</b>              | 215  |
| 2  | $^{13}\text{C}$ NMR Spectra of $\text{Rh}(\text{ttp})(c\text{-hexyl})$ <b>2a</b>            | 215  |
| 3  | $^1\text{H}$ NMR Spectrum of $\text{Rh}(\text{ttp})(c\text{-pentyl})$ <b>2b</b>             | 216  |
| 4  | $^{13}\text{C}$ NMR Spectra of $\text{Rh}(\text{ttp})(c\text{-pentyl})$ <b>2b</b>           | 216  |
| 5  | $^1\text{H}$ NMR Spectrum of $\text{Rh}(\text{ttp})(n\text{-pentyl})$ <b>2c</b>             | 217  |
| 6  | $^{13}\text{C}$ NMR Spectra of $\text{Rh}(\text{ttp})(n\text{-pentyl})$ <b>2c</b>           | 217  |
| 7  | $^1\text{H}$ NMR Spectrum of $\text{Rh}(\text{ttp})(n\text{-hexyl})$ <b>2d</b>              | 218  |
| 8  | $^{13}\text{C}$ NMR Spectra of $\text{Rh}(\text{ttp})(n\text{-hexyl})$ <b>2d</b>            | 218  |
| 9  | $^1\text{H}$ NMR Spectrum of $\text{Rh}(\text{ttp})(n\text{-heptyl})$ <b>2e</b>             | 219  |
| 10 | $^{13}\text{C}$ NMR Spectra of $\text{Rh}(\text{ttp})(n\text{-heptyl})$ <b>2e</b>           | 219  |
| 11 | $^1\text{H}$ NMR Spectrum of $\text{Rh}(\text{ttp})\text{Cl}(\text{PPh}_3)$ <b>2f</b>       | 220  |
| 12 | $^{13}\text{C}$ NMR Spectra of $\text{Rh}(\text{ttp})\text{Cl}(\text{PPh}_3)$ <b>2f</b>     | 220  |
| 13 | $^1\text{H}$ NMR Spectrum of $\text{Rh}(\text{tpp})(c\text{-hexyl})$ <b>4a</b>              | 221  |
| 14 | $^{13}\text{C}$ NMR Spectra of $\text{Rh}(\text{tpp})(c\text{-hexyl})$ <b>4a</b>            | 221  |
| 15 | $^1\text{H}$ NMR Spectrum of $\text{Rh}(\text{bocp})(c\text{-hexyl})$ <b>4b</b>             | 222  |
| 16 | $^{13}\text{C}$ NMR Spectra of $\text{Rh}(\text{bocp})(c\text{-hexyl})$ <b>4b</b>           | 222  |
| 17 | $^1\text{H}$ NMR Spectrum of $\text{Rh}(\text{ttp})(c\text{-heptyl})$ <b>5a</b>             | 223  |
| 18 | $^{13}\text{C}$ NMR Spectra of $\text{Rh}(\text{ttp})(c\text{-heptyl})$ <b>5a</b>           | 223  |
| 19 | $^1\text{H}$ NMR Spectrum of $\text{Rh}_2(\text{ttp})_2(\text{C}_7\text{H}_{12})$ <b>7a</b> | 224  |
| 20 | $^1\text{H}$ NMR Spectrum of $\text{Rh}(\text{ttp})(\text{cycloheptatrienyl})$ <b>8</b>     | 224  |
| 21 | $^{13}\text{C}$ NMR Spectra of $\text{Rh}(\text{ttp})(\text{cycloheptatrienyl})$ <b>8</b>   | 225  |
| 22 | $^1\text{H}$ NMR Spectrum of $\text{Rh}(\text{ttp})(c\text{-octyl})$ <b>10a</b>             | 225  |

|    |  |     |
|----|--|-----|
| 23 | $^{13}\text{C}$ NMR Spectra of Rh(tp)( <i>c</i> -octyl) <b>10a</b> | 226 |
| 24 | $^1\text{H}$ NMR Spectrum of Rh(tp)( <i>n</i> -octyl) <b>10b</b>   | 226 |
| 25 | $^{13}\text{C}$ NMR Spectra of Rh(tp)( <i>n</i> -octyl) <b>10b</b> | 227 |

---

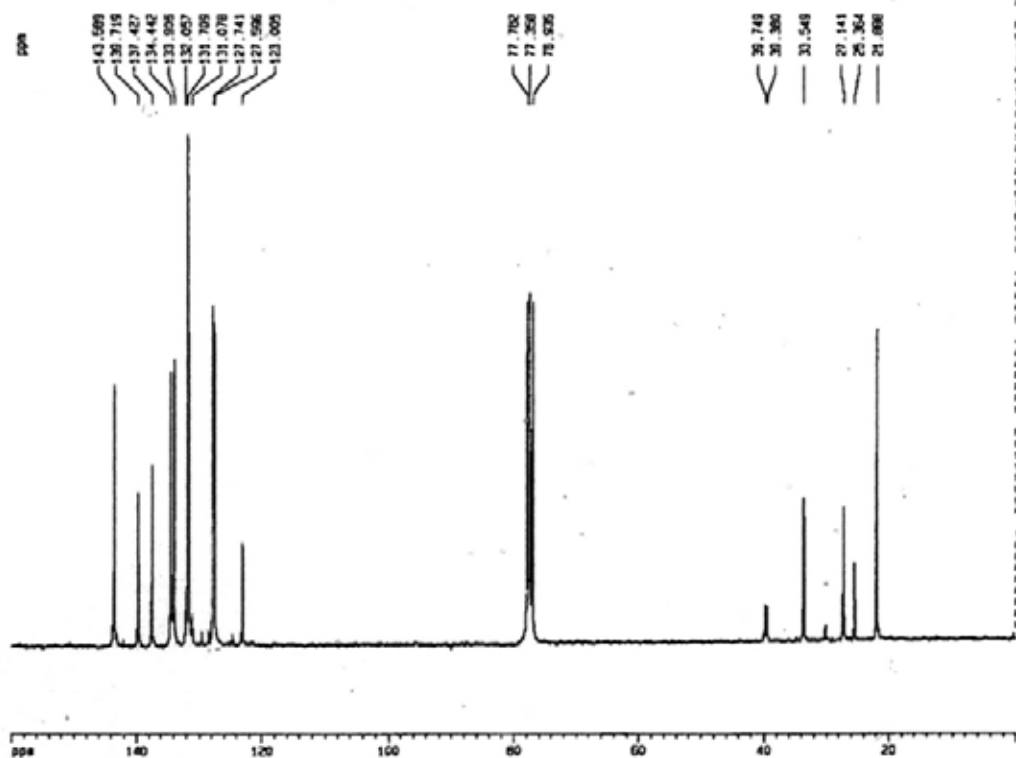
Rh(ttp)(c-hexyl) (2a)

<sup>1</sup>H NMR



Current Data Parameters  
 NAME: Rh(2a) 2011-12  
 EXPNO: 1  
 PROCNO: 1  
 F2 - Acquisition Parameters  
 Date\_: 20080115  
 Time: 9:18  
 INSTRUM: spect  
 PULPROG: zgpg30  
 FREQ: 300.135  
 SOLVENT: CDCl3  
 NS: 327  
 DS: 4  
 SWH: 6000.000 Hz  
 FIDRES: 0.274438 Hz  
 AQ: 1.821000 sec  
 RG: 445.1  
 DM: 55.820 Lines  
 DE: 79.42 Lines  
 TE: 300.2 K  
 D1: 3.0000000 sec  
 DCOffset: 0.0000000 sec  
 AQC: 0.0150000 sec  
 \*\*\*\*\* CHANNEL f1 \*\*\*\*\*  
 NUC1: 1H  
 P1: 9.00 Lines  
 PL1: -2.00 dB  
 SFO1: 300.131000 MHz  
 F2 - Processing parameters  
 SI: 327  
 SF: 300.1300000 MHz  
 WDW: EM  
 SSB: 0  
 LB: 0.30 Hz  
 GB: 0  
 PC: 1.00  
 G3 NMR list parameters  
 CH: 27.80 cm  
 CY: 10.00 cm  
 F1P: 10.000 cm  
 F1: 3001.30 Hz  
 F2P: 0.000 cm  
 F2: 1600.78 Hz  
 FWHM: 0.2777 Hz/Hz  
 JCH: 218.27637 Hz/Hz

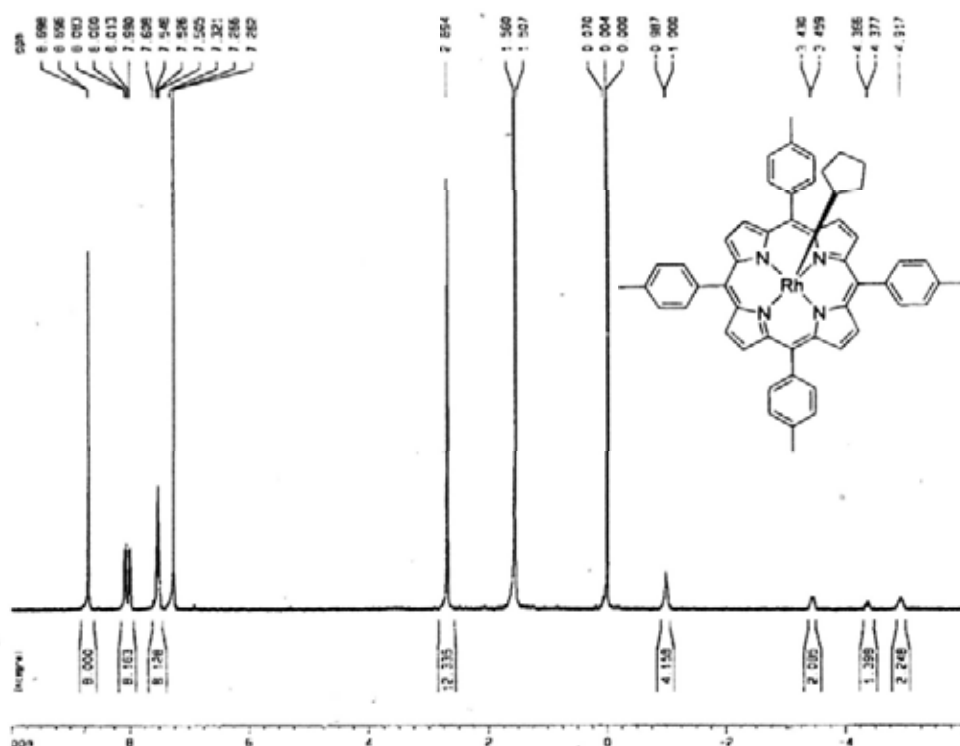
<sup>13</sup>C NMR



Current Data Parameters  
 NAME: Rh(2a) 2011-12  
 EXPNO: 2  
 PROCNO: 1  
 F2 - Acquisition Parameters  
 Date\_: 20080115  
 Time: 9:30  
 INSTRUM: spect  
 PULPROG: zgpg30  
 FREQ: 300.135  
 SOLVENT: CDCl3  
 NS: 400  
 DS: 4  
 SWH: 6000.000 Hz  
 FIDRES: 0.26804 Hz  
 AQ: 1.821000 sec  
 RG: 445.1  
 DM: 55.820 Lines  
 DE: 79.42 Lines  
 TE: 300.2 K  
 D1: 3.0000000 sec  
 DCOffset: 0.0000000 sec  
 AQC: 0.0150000 sec  
 \*\*\*\*\* CHANNEL f1 \*\*\*\*\*  
 NUC1: 13C  
 P1: 3.00 Lines  
 PL1: -2.00 dB  
 SFO1: 75.274111 MHz  
 \*\*\*\*\* CHANNEL f2 \*\*\*\*\*  
 NUC2: 1H  
 P2: 9.00 Lines  
 PL2: 10.00 dB  
 SFO2: 300.131000 MHz  
 F2 - Processing parameters  
 SI: 400  
 SF: 75.274111 MHz  
 WDW: EM  
 SSB: 0  
 LB: 0.30 Hz  
 GB: 0  
 PC: 1.00  
 G3 NMR list parameters  
 CH: 27.80 cm  
 CY: 10.00 cm  
 F1P: 10.000 cm  
 F1: 3001.30 Hz  
 F2P: 0.000 cm  
 F2: 1600.78 Hz  
 FWHM: 0.26804 Hz/Hz  
 JCH: 218.27637 Hz/Hz

Rh(tpp)(c-pentyl) (2b)

<sup>1</sup>H NMR



Current Data Parameters  
 NAME YAC302(2b)  
 EXPNO 1  
 PROCNO 1

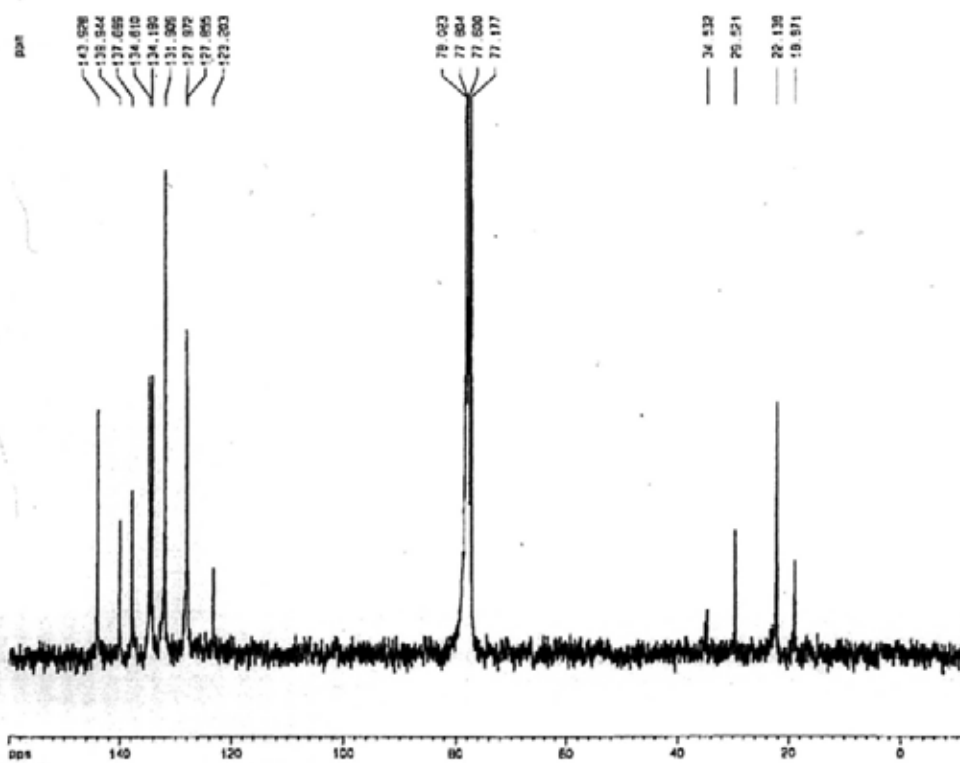
F2 - Acquisition Parameters  
 Date\_ 20080715  
 Time 8.14  
 INSTRUM spect  
 PROBHD 5 mm BBO BB-1H  
 PULPROG zgpg30  
 TO 10  
 SOLVENT CDCl3  
 NS 32  
 DS 0  
 SFO 800.136 MHz  
 FIDRES 0.274730 Hz  
 AQ 1.871800 sec  
 RG 182.5  
 DM 10.600 usec  
 DE 79.43 usec  
 TE 300.2 K  
 DT 1.0000000 sec  
 ACQRES 0.0000000 sec  
 NMRB 0.0100000 sec

===== CHANNEL f1 =====  
 NUC1 1H  
 P1 9.00 usec  
 PL1 2.00 dB  
 SFO1 300.1310000 MHz

F2 - Processing parameters  
 SI 32768  
 SF 300.1300043 MHz  
 NCM EM  
 SSB 0  
 LB 0.30 Hz  
 GB 0  
 PC 1.00

1D NMR plot parameters  
 EX 20.00 cm  
 CY 30.00 cm  
 F1P 10.000 usec  
 F1 300.130 MHz  
 F2P 6.000 usec  
 F2 -1800.00 Hz  
 PPMPP 0.72727 20A/1A  
 XCH 0.018 27037 Hz/cm

<sup>13</sup>C NMR



Current Data Parameters  
 NAME YAC302(2b)  
 EXPNO 1  
 PROCNO 1

F2 - Acquisition Parameters  
 Date\_ 20080715  
 Time 8.50  
 INSTRUM spect  
 PROBHD 5 mm BBO BB-1H  
 PULPROG zgpg30  
 TO 10  
 SOLVENT CDCl3  
 NS 3000  
 DS 0  
 SFO 101.626 MHz  
 FIDRES 0.346004 Hz  
 AQ 1.445180 sec  
 RG 8182  
 DM 20.070 usec  
 DE 8.00 usec  
 TE 300.2 K  
 DT 1.0000000 sec  
 ACQRES 0.0300000 sec  
 NMRB 0.0000000 sec  
 NMRB 0.0100000 sec

===== CHANNEL f1 =====  
 NUC1 13C  
 P1 3.00 usec  
 PL1 0.00 dB  
 SFO1 101.6260000 MHz

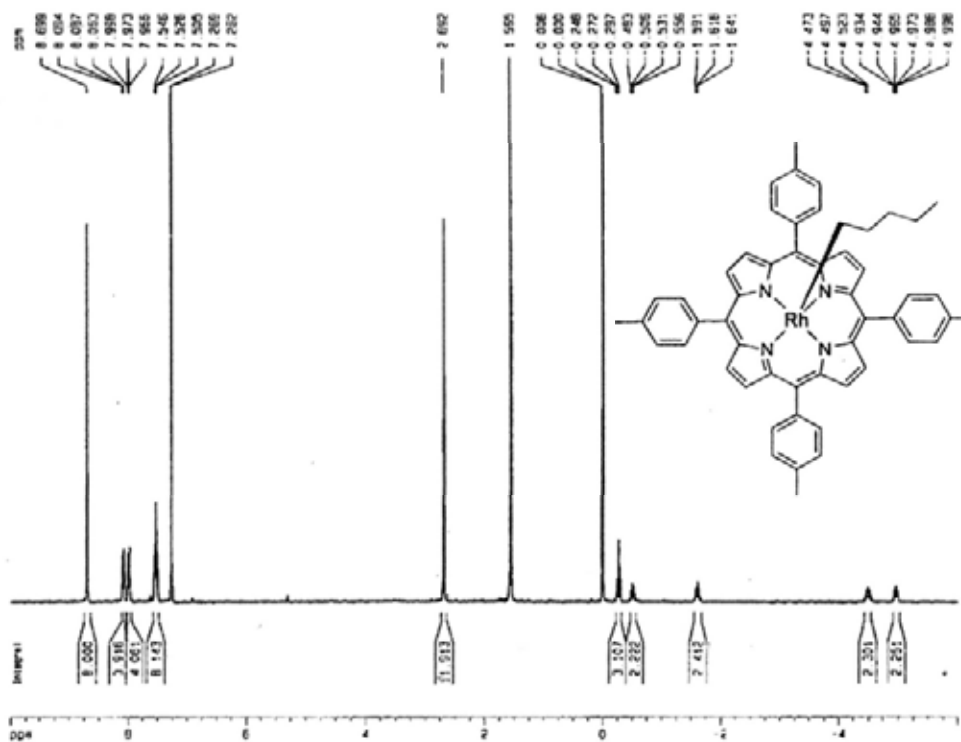
===== CHANNEL f2 =====  
 CPDPRG2 waltz16  
 NUC2 1H  
 PCPD2 100.00 usec  
 PL2 130.00 dB  
 PL12 19.00 dB  
 SFO2 300.1310000 MHz

F2 - Processing parameters  
 SI 85536  
 SF 101.6270253 MHz  
 NCM EM  
 SSB 0  
 LB 5.00 Hz  
 GB 0  
 PC 1.40

1D NMR plot parameters  
 EX 20.00 cm  
 CY 30.00 cm  
 F1P 100.000 usec  
 F1 100.626 MHz  
 F2P -20.000 usec  
 F2 -1500.00 Hz  
 PPMPP 7.82689 20A/1A  
 XCH 0.018 27037 Hz/cm

Rh(ttp)(*n*-pentyl) (2c)

<sup>1</sup>H NMR



Current Data Parameters  
 NAME: RHC24 (recr)  
 EXPNO: 1  
 PROCNO: 1

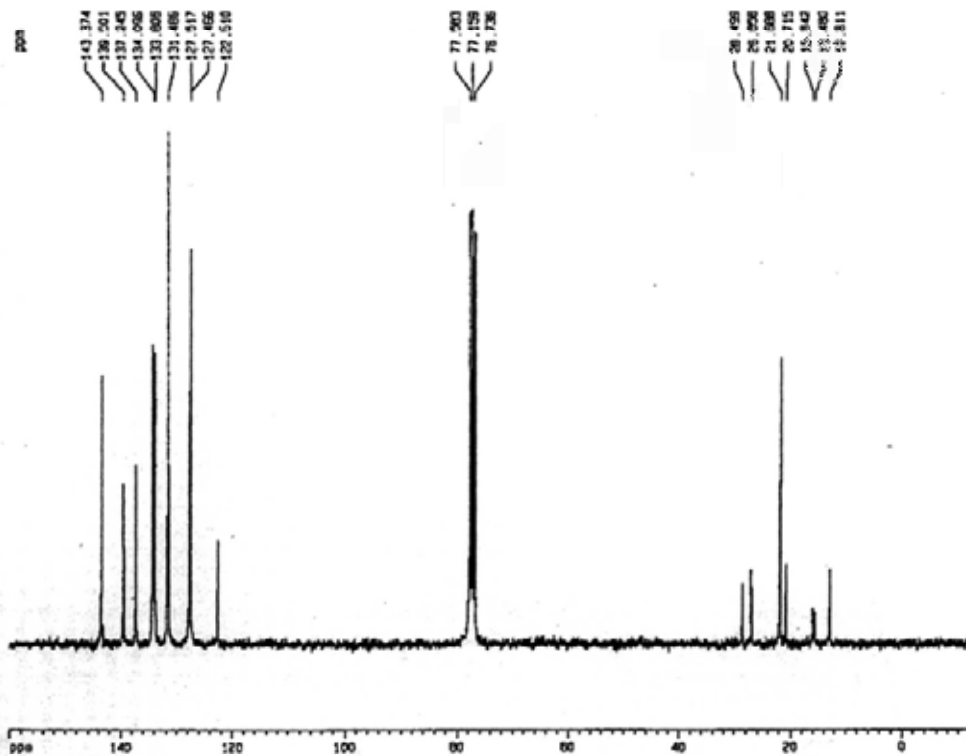
F2 - Acquisition Parameters  
 Date\_: 20060810  
 Time: 17.04  
 INSTRUM: spect  
 PROBMG: 5 mm BBO 80-1H  
 PULPROG: zgpg30  
 TD: 32768  
 SOLVENT: CDCl3  
 NS: 32  
 DS: 4  
 SWH: 8032.805 Hz  
 F2RES: 0.247438 Hz  
 AQ: 1.421368 sec  
 RG: 1142.4  
 CW: 56.800 MHz  
 DE: 78.43 MHz  
 TE: 300.2 K  
 D1: 1.0000000 sec  
 d11: 0.0000000 sec  
 MCHST: 0.0000000 sec  
 MCWID: 0.0100000 sec

----- CHANNEL f1 -----  
 NUC1: 1H  
 P1: 5.00 MHz  
 PL1: -2.00 dB  
 SFO1: 300.1372000 MHz

F2 - Processing parameters  
 SI: 32768  
 SF: 500.1360000 MHz  
 WFW: 1K  
 SSB: 0  
 LB: 0.30 Hz  
 GB: 0  
 PC: 1.00

1D NMR plot parameters  
 CX: 22.00 Hz  
 CY: 52.00 Hz  
 F1P: 10.000 MHz  
 F1: 300.137 Hz  
 F2P: -6.000 MHz  
 F2: -1800.78 Hz  
 WPCW: 7.7727 MHz  
 WCNH: 218.27637 MHz

<sup>13</sup>C NMR



Current Data Parameters  
 NAME: RHC24 (recr)  
 EXPNO: 1  
 PROCNO: 1

F2 - Acquisition Parameters  
 Date\_: 20060810  
 Time: 18.51  
 INSTRUM: spect  
 PROBMG: 5 mm BBO 80-1H  
 PULPROG: zgpg30  
 TD: 65536  
 SOLVENT: CDCl3  
 NS: 256  
 DS: 4  
 SWH: 30079.728 Hz  
 F2RES: 0.348004 Hz  
 AQ: 1.445138 sec  
 RG: 8000  
 CW: 57.800 MHz  
 DE: 8.00 MHz  
 TE: 300.2 K  
 D1: 1.0000000 sec  
 d11: 0.0000000 sec  
 MCHST: 0.0000000 sec  
 MCWID: 0.0100000 sec

----- CHANNEL f1 -----  
 NUC1: 13C  
 P1: 3.00 MHz  
 PL1: 6.00 dB  
 SFO1: 75.4745111 MHz

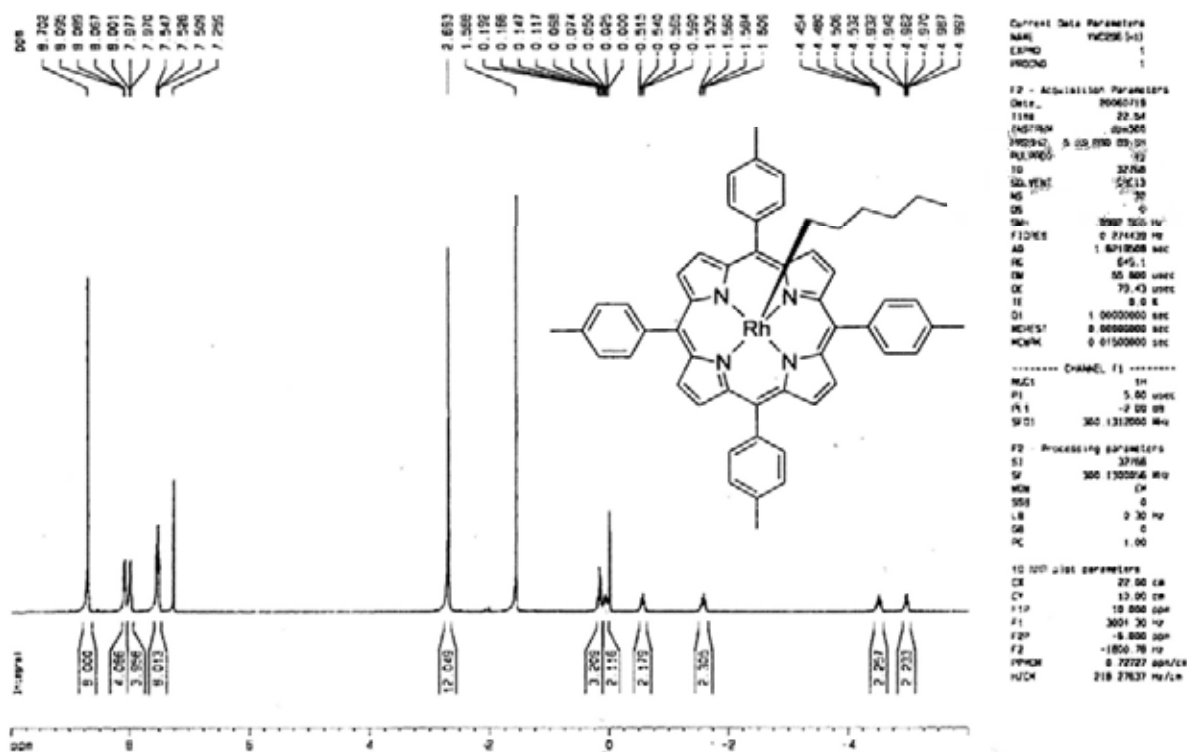
----- CHANNEL f2 -----  
 CPDPRG2: waltz16  
 NUC2: 1H  
 P2P2P: 180.00 MHz  
 PL2: 19.00 dB  
 PL12: 19.00 dB  
 SFO2: 500.1365837 MHz

F2 - Processing parameters  
 SI: 65536  
 SF: 75.4677395 MHz  
 WFW: 6K  
 SSB: 0  
 LB: 3.00 Hz  
 GB: 0  
 PC: 1.48

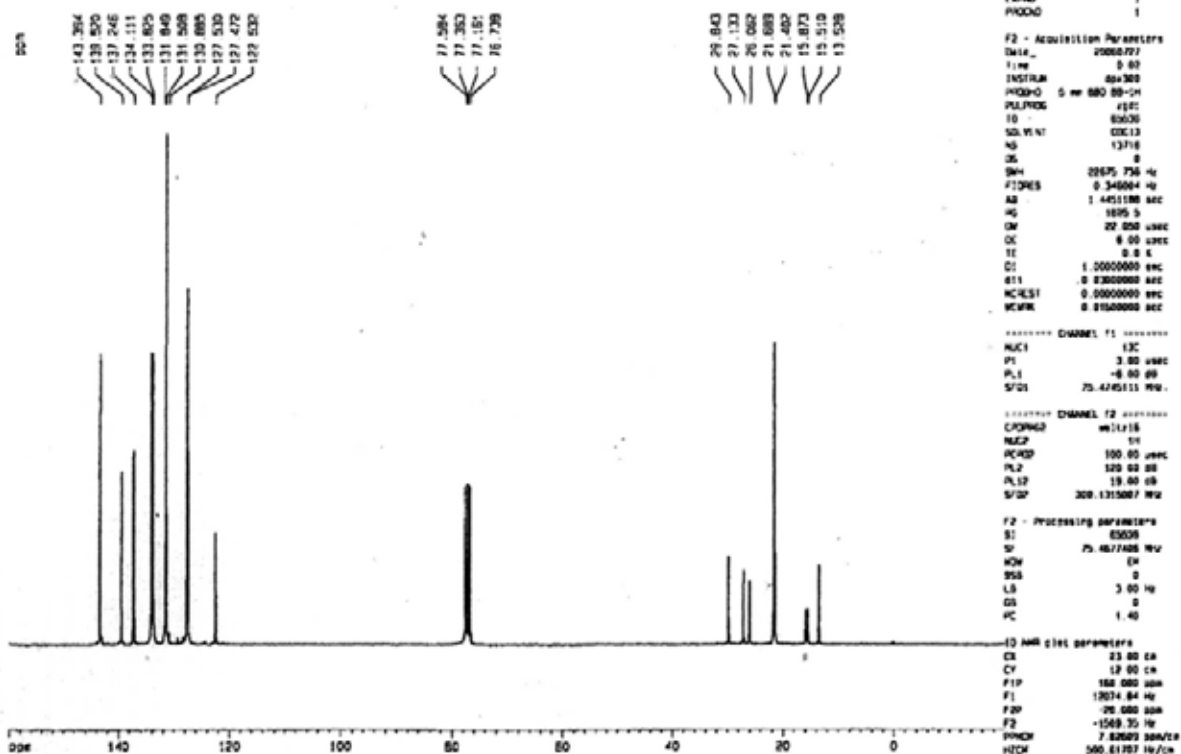
1D NMR plot parameters  
 CX: 22.00 Hz  
 CY: 52.00 Hz  
 F1P: 100.626 MHz  
 F1: 12074.84 Hz  
 F2P: -25.550 MHz  
 F2: -1000.26 Hz  
 WPCW: 7.62089 MHz  
 WCNH: 508.81367 MHz

Rh(ttp)(n-hexyl) (2d)

<sup>1</sup>H NMR



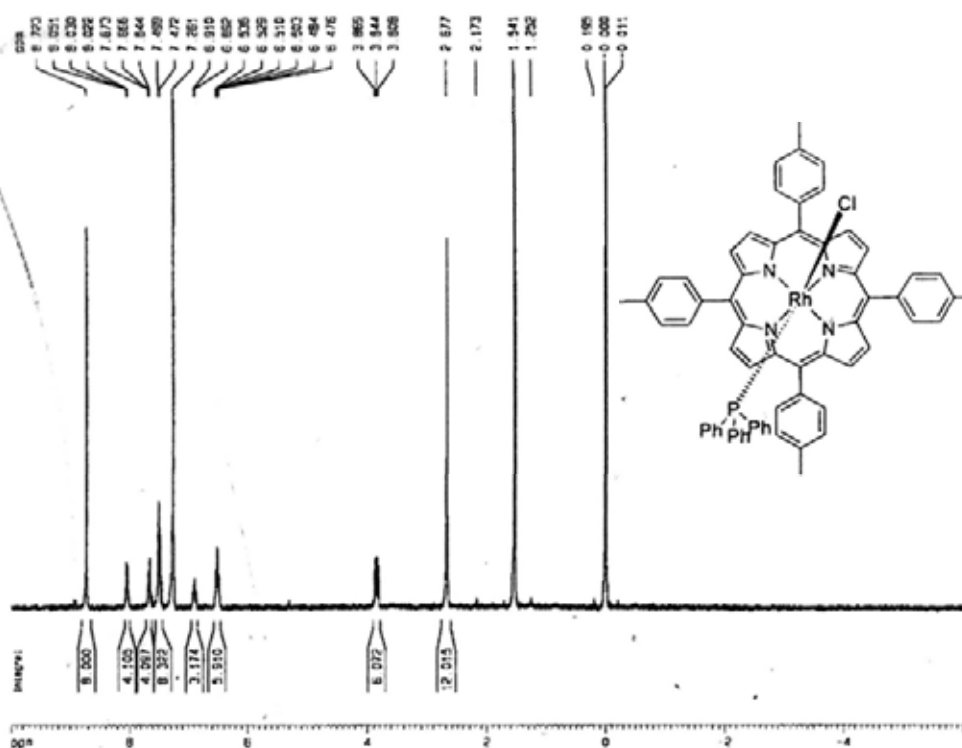
<sup>13</sup>C NMR





Rh(ttp)Cl(Ph<sub>3</sub>) (2f)

<sup>1</sup>H NMR



Current Data Parameters  
 NAME: rhc\_11001  
 EXPNO: 1  
 PROCNO: 1

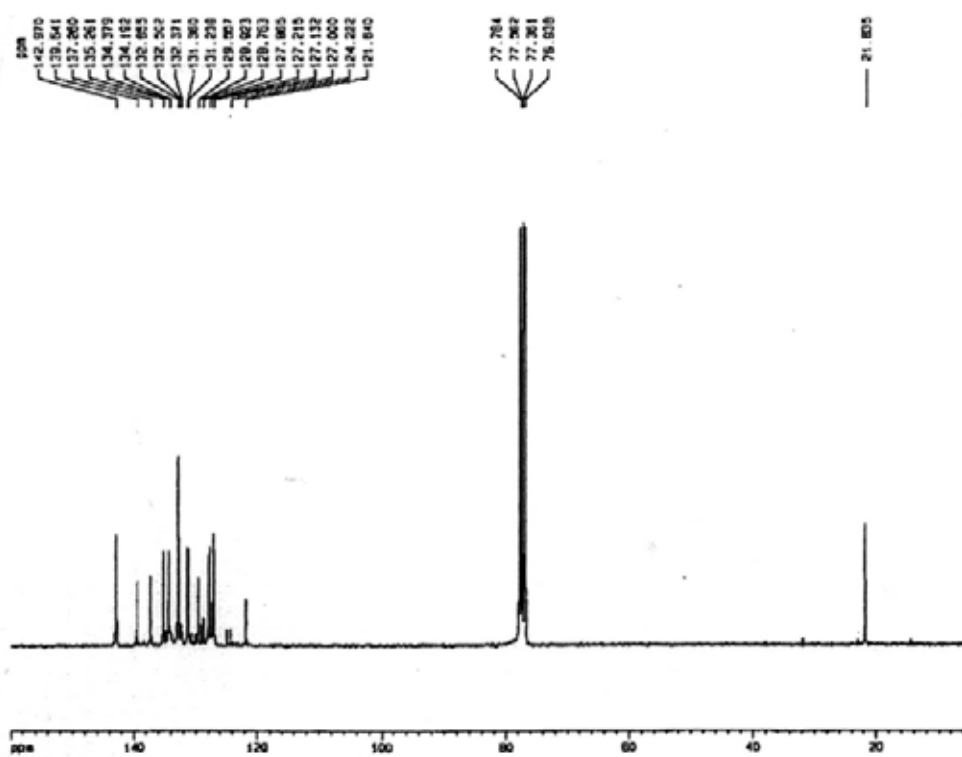
F2 - Acquisition Parameters  
 Date\_: 20070126  
 Time: 17:21  
 INSTRUM: csa300  
 PULPROG: zgpg30  
 SOLVENT: CDCl3  
 NS: 32768  
 DS: 4  
 SFO: 300.135060 MHz  
 FIDRES: 0.214230 Hz  
 AQ: 1.871000 sec  
 RG: 1824.6  
 CW: 50.500 MHz  
 CK: 79.43 MHz  
 IL: 0.0 K  
 O1: 1.0000000 sec  
 NUC1: 0.0000000 sec  
 NUC2: 0.0000000 sec

----- CHANNEL f1 -----  
 NUC1: 1H  
 P1: 0.00 MHz  
 PL1: 2.00 dB  
 SFO1: 300.135060 MHz

F2 - Processing parameters  
 SI: 300.135060 MHz  
 SF: 300.135060 MHz  
 WDW: EM  
 SSB: 0  
 LB: 0.30 Hz  
 GB: 0  
 PC: 1.00

1D NMR plot parameters  
 EX: 20.00 cm  
 CY: 30.00 cm  
 FID: 10.0000000  
 FI: 3001.70 Hz  
 F2: -0.5000000  
 F3: -1800.70 Hz  
 FWHM: 0.2272200 Hz  
 GC: 218.27837 Hz/cm

<sup>13</sup>C NMR



Current Data Parameters  
 NAME: rhc\_11001  
 EXPNO: 1  
 PROCNO: 1

F2 - Acquisition Parameters  
 Date\_: 20070126  
 Time: 17:21  
 INSTRUM: csa300  
 PULPROG: zgpg30  
 SOLVENT: CDCl3  
 NS: 32768  
 DS: 4  
 SFO: 300.135060 MHz  
 FIDRES: 0.214230 Hz  
 AQ: 1.871000 sec  
 RG: 1824.6  
 CW: 50.500 MHz  
 CK: 79.43 MHz  
 IL: 0.0 K  
 O1: 1.0000000 sec  
 NUC1: 0.0000000 sec  
 NUC2: 0.0000000 sec

----- CHANNEL f1 -----  
 NUC1: 13C  
 P1: 2.00 MHz  
 PL1: 2.00 dB  
 SFO1: 75.4740111 MHz

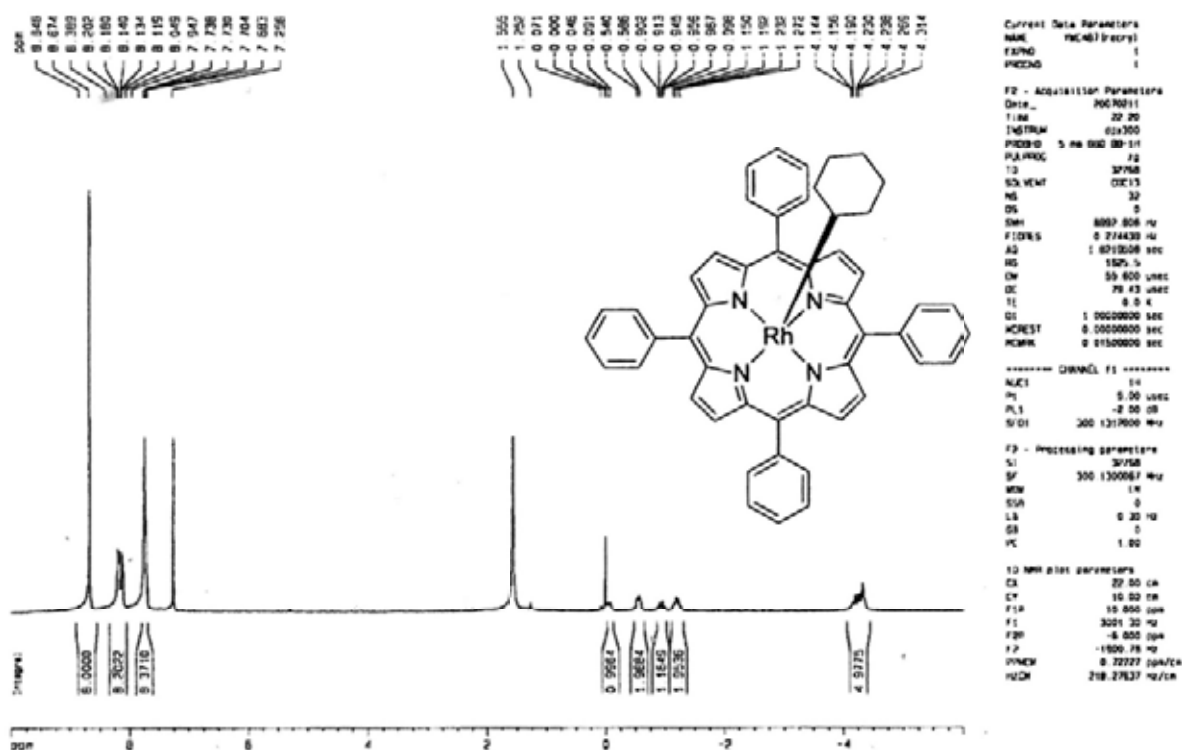
----- CHANNEL f2 -----  
 NUC2: 1H  
 P2: 0.00 MHz  
 PL2: 120.00 dB  
 PL12: 12.00 dB  
 SFO2: 300.135060 MHz

F2 - Processing parameters  
 SI: 300.135060 MHz  
 SF: 75.477040 MHz  
 WDW: EM  
 SSB: 0  
 LB: 3.00 Hz  
 GB: 0  
 PC: 1.00

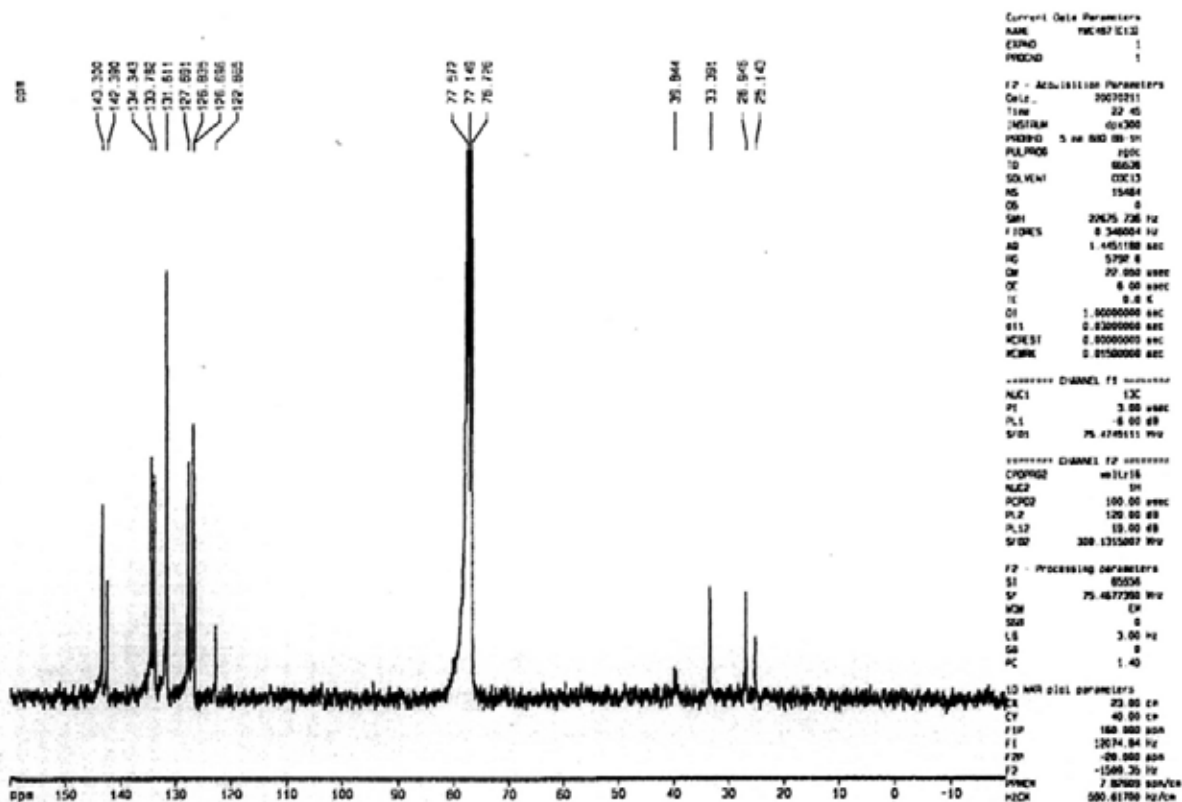
1D NMR plot parameters  
 EX: 20.00 cm  
 CY: 30.00 cm  
 FID: 10.0000000  
 FI: 12074.84 Hz  
 F2: -0.5000000  
 F3: -0.5000000  
 FWHM: 8.8586800 Hz/cm  
 GC: 524.92288 Hz/cm

Rh(tpp)(c-hexyl) (4a)

<sup>1</sup>H NMR

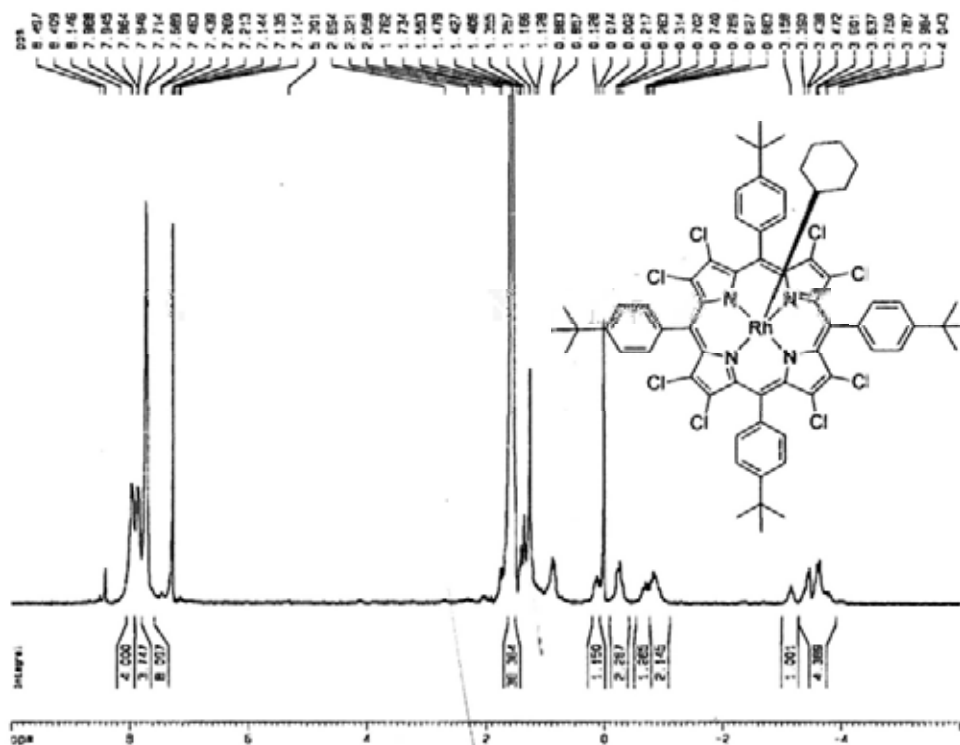


<sup>13</sup>C NMR



Rh(bocp)(c-hexyl) (4b)

<sup>1</sup>H NMR



Current Data Parameters  
 NAME: rhc 373 h1  
 EXPNO: 2  
 PROCNO: 1

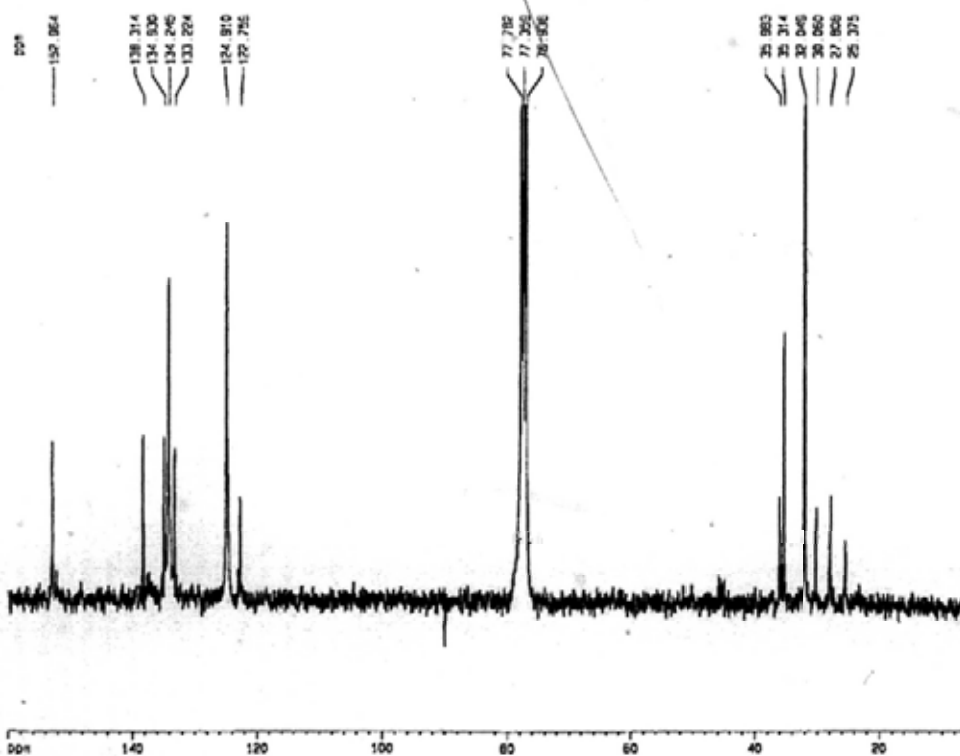
F2 - Acquisition Parameters  
 DATE\_: 20070117  
 TIME: 23 35  
 INSTRUM: spect  
 PROBRW: 6.44 500 98.14  
 PULPROG: zg  
 TD: 32768  
 SOLVENT: CDCl3  
 NS: 32  
 DS: 0  
 SWH: 6002.800 Hz  
 FIDRES: 0.21433 Hz  
 AQ: 1.871605 sec  
 RG: 656.1  
 RW: 50.000 usec  
 OR: 75.43 usec  
 TE: 300.2 K  
 UH: 1.0000000 sec  
 HCHW1: 0.0000000 sec  
 HCHW2: 0.0100000 sec

----- CHANNEL f1 -----  
 NUC1: 1H  
 P1: 9.00 usec  
 PL1: -2.00 dB  
 SFO1: 500.1318000 MHz

F2 - Processing parameters  
 SI: 32768  
 SF: 500.1306049 MHz  
 WHW: 1K  
 SSB: 0  
 LB: 0.30 Hz  
 GB: 0  
 PC: 1.00

1D NMR plot parameters  
 CA: 37.00 cm  
 CY: 80.00 cm  
 FXP: 10.000 cm  
 FI: 3001.30 Hz  
 FWH: 0.000 cm  
 FZ: -1500.38 Hz  
 HATCH: 4.72721 cm/Hz  
 HZCP: 218.2737 Hz/Hz

<sup>13</sup>C NMR



Current Data Parameters  
 NAME: rhc 373 c13  
 EXPNO: 2  
 PROCNO: 1

F2 - Acquisition Parameters  
 DATE\_: 20070117  
 TIME: 23 37  
 INSTRUM: spect  
 PROBRW: 6.44 500 98.14  
 PULPROG: zgpg  
 TD: 65536  
 SOLVENT: CDCl3  
 NS: 14096  
 DS: 0  
 SWH: 22675.726 Hz  
 FIDRES: 0.348204 Hz  
 AQ: 1.4451188 sec  
 RG: 7998.8  
 RW: 22.000 usec  
 OR: 8.00 usec  
 TE: 300.2 K  
 UH: 1.0000000 sec  
 HCHW1: 0.0000000 sec  
 HCHW2: 0.0100000 sec

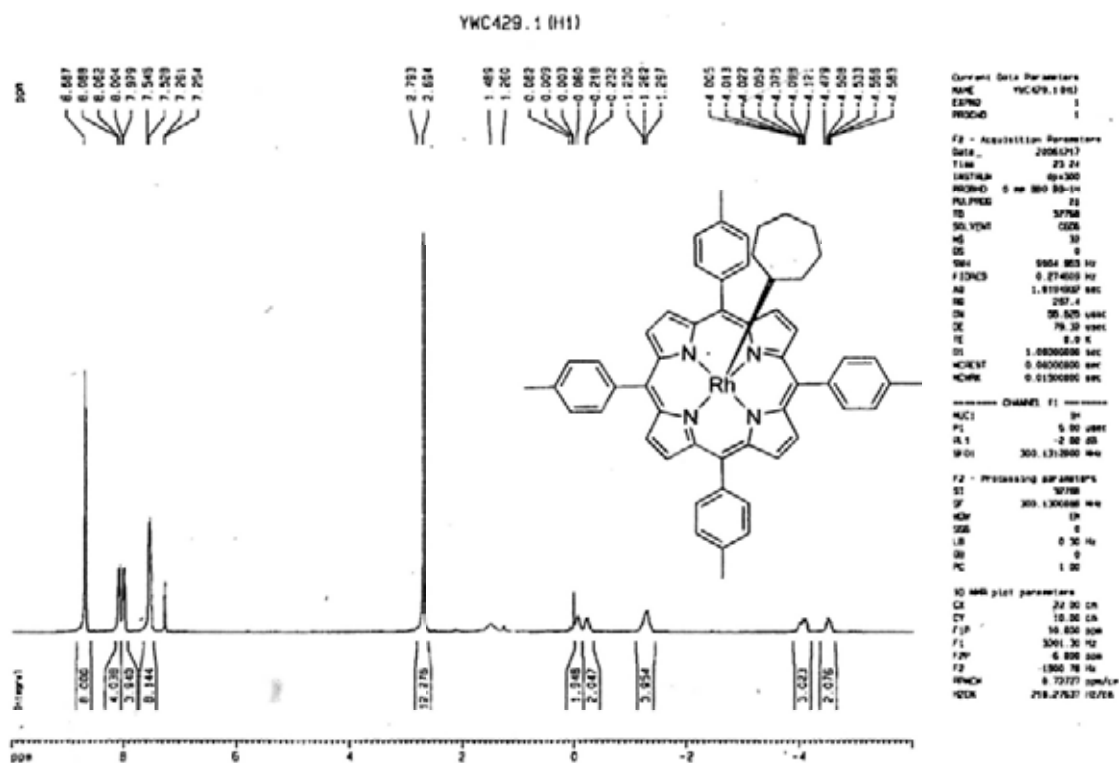
----- CHANNEL f1 -----  
 NUC1: 13C  
 P1: 3.00 usec  
 PL1: 0.00 dB  
 SFO1: 75.4746111 MHz

----- CHANNEL f2 -----  
 CPDPRG2: waltz16  
 NUC2: 1H  
 P2: 100.00 usec  
 PL2: 190.00 dB  
 PL12: 18.00 dB  
 SFO2: 500.1318007 MHz

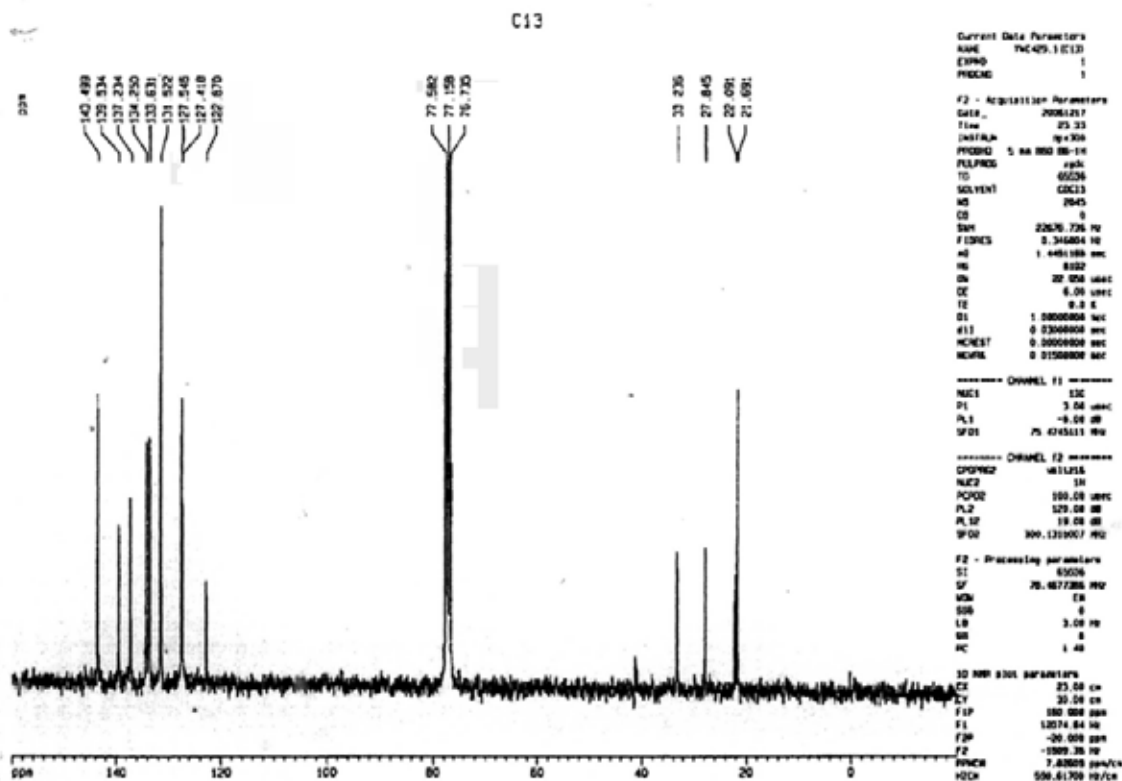
F2 - Processing parameters  
 SI: 65536  
 SF: 75.4677231 MHz  
 WHW: 1K  
 SSB: 0  
 LB: 3.00 Hz  
 GB: 0  
 PC: 1.40

1D NMR plot parameters  
 CA: 75.00 cm  
 CY: 50.00 cm  
 FXP: 100.000 cm  
 FI: 17074.83 Hz  
 FWH: -0.000 cm  
 FZ: 8.95667 cm/Hz  
 HATCH: 584.30084 Hz/Hz

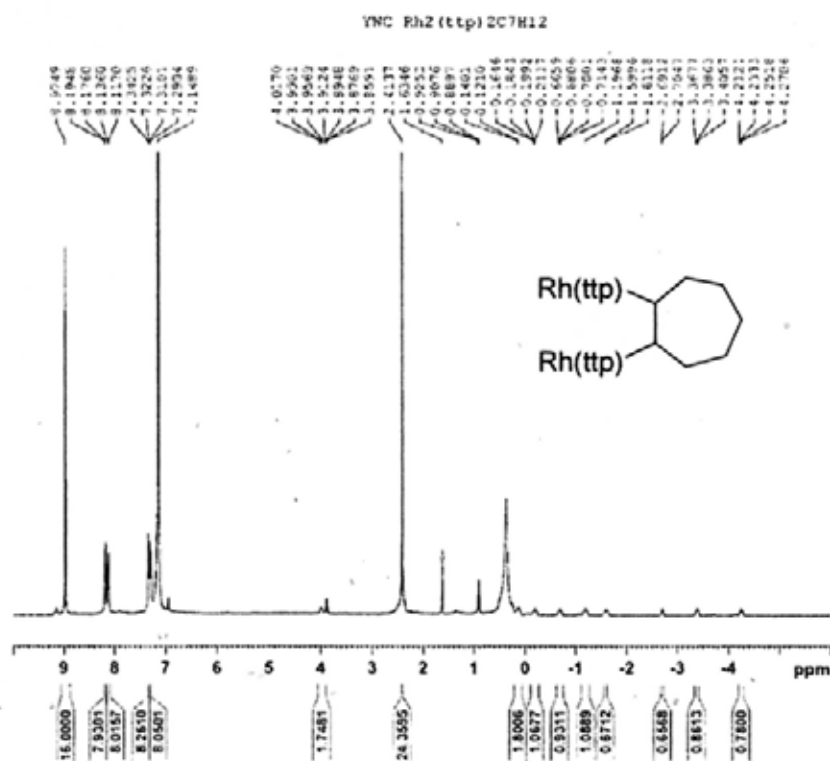
# Rh(tp)(c-heptyl) 5a <sup>1</sup>H NMR



# Rh(tp)(c-heptyl) 5a <sup>13</sup>C NMR



Rh<sub>2</sub>(ttp)<sub>2</sub>(C<sub>7</sub>H<sub>12</sub>) 7a <sup>1</sup>H NMR



```

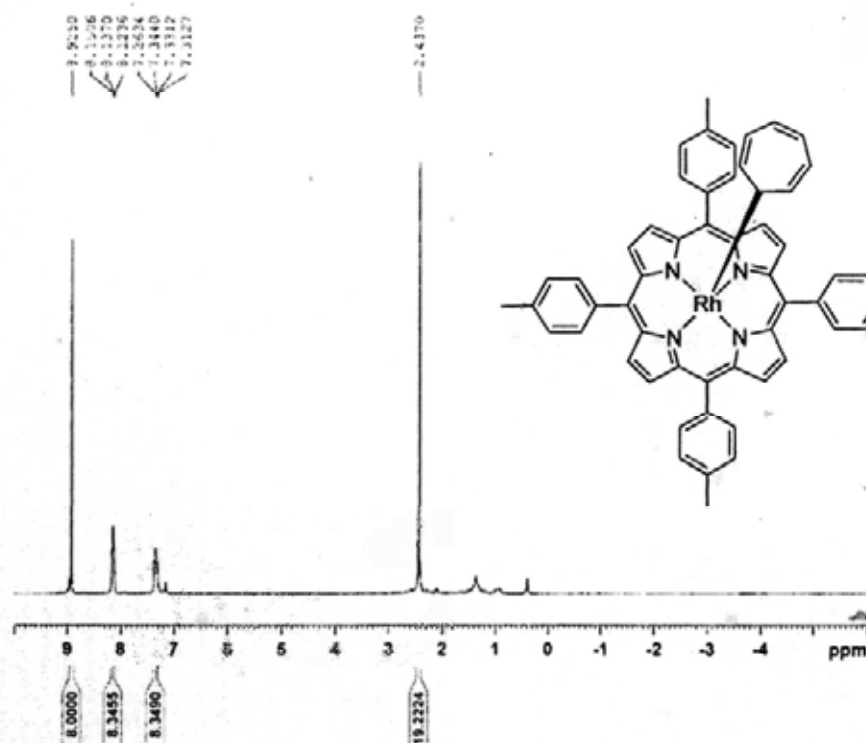
=====
Current Data Parameters
NAME      YMC Rh2(ttp)2C7H12 test1
EXPNO    2
PROCNO   1

PC - Acquisition Parameters
Date_    20090412
Time     7.56
INSTRUM  spect
PROBHD   5 mm QNP1H 13C
PULPROG  zgpg30
TD        65536
SOLVENT  CDCl3
NS        64
DS        4
SWH       39670.339 Hz
F2RES     0.455509 Hz
AQ         0.4259014 sec
RG         181
CW         12.400 usec
DE         6.50 usec
TE        473.1 K
SI         1.00000000 sec
TD0       1

===== CHANNEL f1 =====
NUC1      1H
P1         1.00
PL1        0 dB
PL12      -1.82000000 MHz
SFO1      400.1300000 MHz

PC - Processing parameters
SI         45536
SF         400.1300470 MHz
WDW        EM
SSB        0
LB         0.30 Hz
GB         0
PC         1.00
    
```

Rh(ttp)(cycloheptatrienyl) 8 <sup>1</sup>H NMR



```

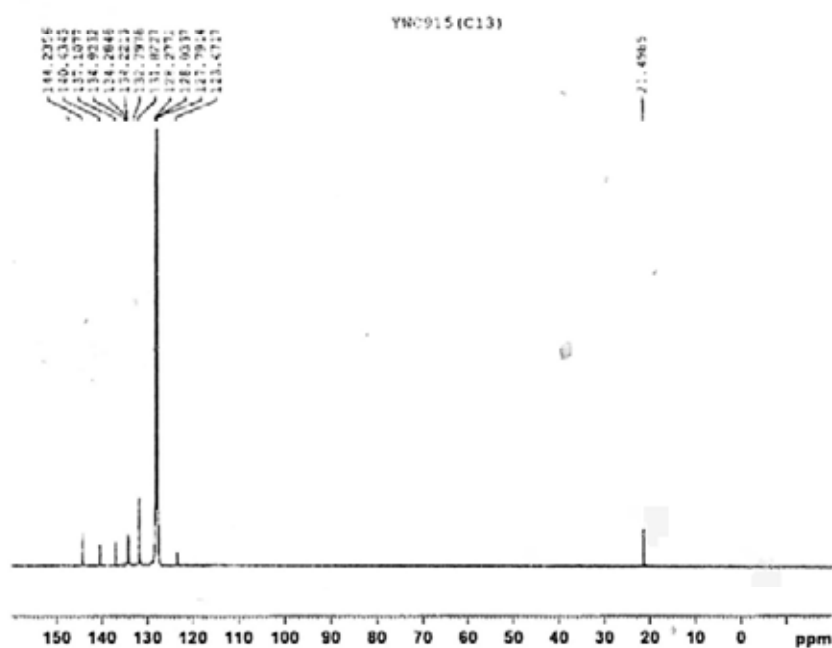
Current Data Parameters
NAME      YMC Rh2(ttp)2C7H12 test1
EXPNO    2
PROCNO   1

PC - Acquisition Parameters
Date_    20090412
Time     7.56
INSTRUM  spect
PROBHD   5 mm QNP1H 13C
PULPROG  zgpg30
TD        65536
SOLVENT  CDCl3
NS        64
DS        4
SWH       39670.339 Hz
F2RES     0.455509 Hz
AQ         0.4259014 sec
RG         181
CW         12.400 usec
DE         6.50 usec
TE        473.1 K
SI         1.00000000 sec
TD0       1

===== CHANNEL f1 =====
NUC1      1H
P1         1.00
PL1        0 dB
PL12      -1.82000000 MHz
SFO1      400.1300000 MHz

PC - Processing parameters
SI         45536
SF         400.1300470 MHz
WDW        EM
SSB        0
LB         0.30 Hz
GB         0
PC         1.00
    
```

# Rh(ttp)(cycloheptatrienyl) 8 <sup>13</sup>C NMR



```

Current Data Parameters
NAME      YWC915(C13)
EXPNO    1
PROCNO   1

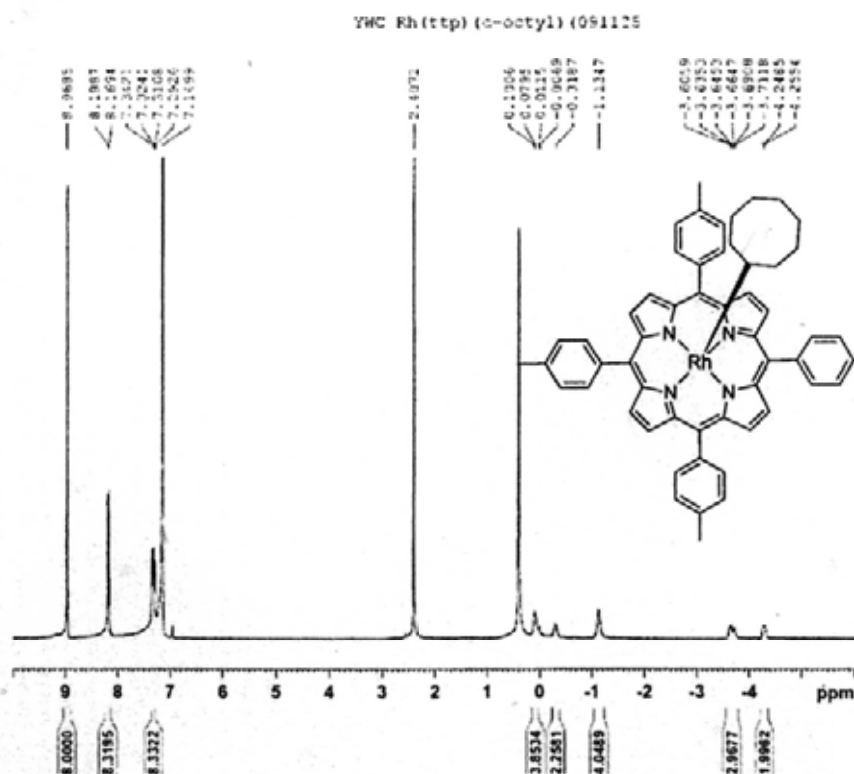
F2 - Acquisition Parameters
Date_    200601
Time     2.29
INSTRUM  spect
PROBHD   5 mm PABD1 1H/
PULPROG  zgpg30
TE       121.72
SOLVENT  CDCl3
NS       0
DS       0
SWH      24761.504 Hz
FIDRES   0.223665 Hz
AQ       2.202699 sec
RG       203
SM       16.610 cm/s
DE       6.50 mm/s
TE       294.8 K
D1       1.0000000 sec
d11      0.3300000 sec
TD0

===== CHANNEL f1 =====
NUC1     13C
P1       14.53 usec
PL1      -1.00 dB
PL12     -1.4000000 dB
PL1M     -1.4000000 dB
PL1W     100.0000000 Hz
PTC1     100.6205180 MHz

===== CHANNEL f2 =====
CPDPRG2  waltz16
NUC2     1H
PCPD2    00.00 usec
PL2      -2.00 dB
PL12     17.70 dB
PL1M     -1.4000000 dB
PL1W     100.0000000 Hz
PTC2     400.1320003 MHz

F2 - Processing parameters
SI       32768
SF       100.6205180 MHz
WDW      EM
SSB      0
LB       1.00 Hz
GB       0
PC       1.40
    
```

# Rh(ttp)(c-octyl) 10a <sup>1</sup>H NMR



```

Current Data Parameters
NAME      YWC Rh(ttp)(c-octyl) (091125)
EXPNO    1
PROCNO   1

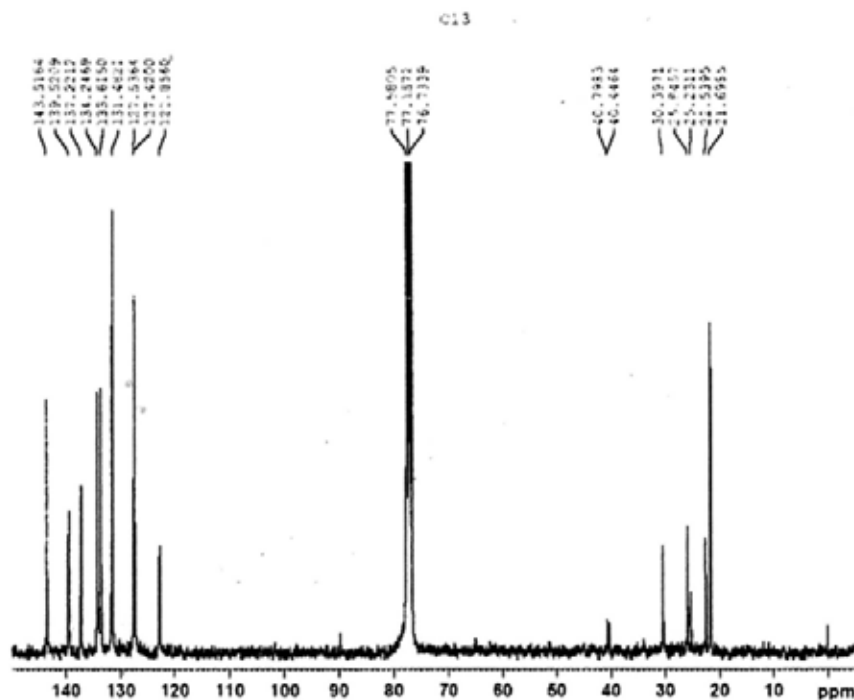
F2 - Acquisition Parameters
Date_    200611
Time     14.46
INSTRUM  spect
PROBHD   5 mm PABD1 1H/
PULPROG  zgpg30
TE       121.72
SOLVENT  CDCl3
NS       0
DS       0
SWH      12019.220 Hz
FIDRES   0.120989 Hz
AQ       2.714457 sec
RG       203
SM       16.610 cm/s
DE       6.50 mm/s
TE       297.5 K
D1       1.0000000 sec
d11      0.3300000 sec
TD0

===== CHANNEL f1 =====
NUC1     1H
P1       14.53 usec
PL1      -1.00 dB
PL12     -1.4000000 dB
PL1M     -1.4000000 dB
PL1W     100.0000000 Hz
PTC1     100.6205180 MHz

===== CHANNEL f2 =====
CPDPRG2  waltz16
NUC2     13C
PCPD2    00.00 usec
PL2      -2.00 dB
PL12     17.70 dB
PL1M     -1.4000000 dB
PL1W     100.0000000 Hz
PTC2     400.1320003 MHz

F2 - Processing parameters
SI       32768
SF       100.6205180 MHz
WDW      EM
SSB      0
LB       1.00 Hz
GB       0
PC       1.40
    
```

# Rh(ttp)(*c*-octyl) 10a <sup>13</sup>C NMR



```

Current Data Parameters
NAME      YWC116 (1.31)
EXPNO    2
PROCNO   1

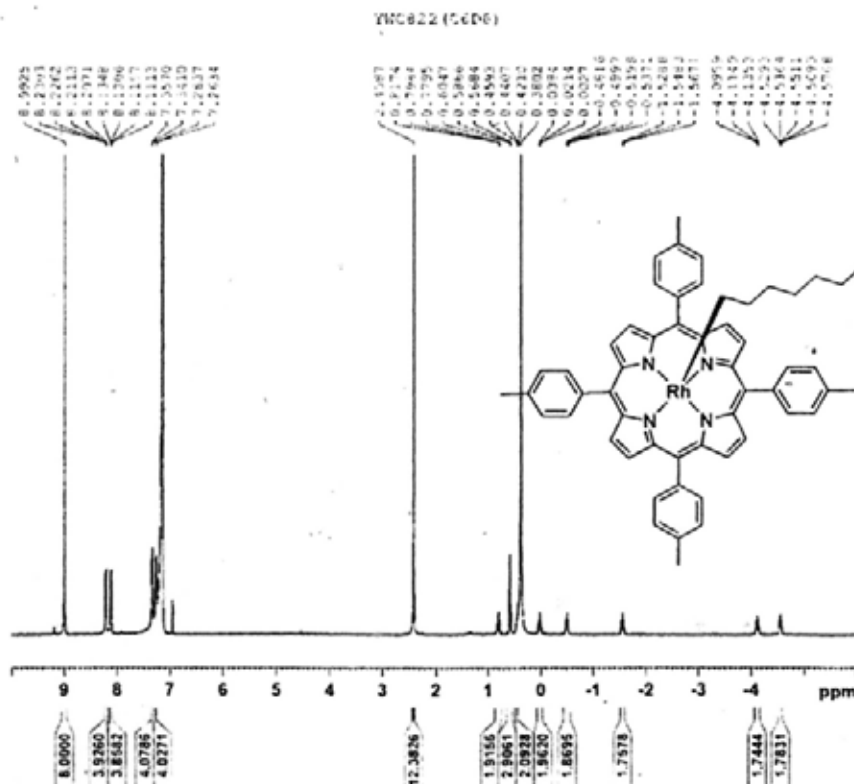
F2 - Acquisition Parameters
Date_    20011124
Time     1.12
INSTRUM  spect
PROBHD   5 mm BBO BB-1H
PULPROG  zgpg30
SOLVENT  CDCl3
NS       4096
DS       4
SWH      12812.293 Hz
FIDRES   0.207340 Hz
AQ       1.7500308 sec
RG       2894.3
RW       24.887 usec
DE       6.00 usec
TE       300.2 K
D1       1.00000000 sec
d11      0.03000000 sec
DELTA    0 sec
NUC1      13C
NUC2      1H
MAGNET   10.13500000 sec

----- CHANNEL f1 -----
NUC1      13C
P1       12.00 usec
PL1      0.00 dB
SFO1     101.625000 MHz

----- CHANNEL f2 -----
CPDPRG2  zgpg30
NUC2      1H
PCPD2    100.00 usec
PL2      19.00 dB
PL12     19.00 dB
SFO2     400.146000 MHz

F2 - Processing parameters
SI       65534
SF       400.146000 MHz
WDW      EM
SSB      0
LB       3.00 Hz
GB       0
PC       1.40
    
```

# Rh(ttp)(*n*-octyl) 10b <sup>1</sup>H NMR



```

Current Data Parameters
NAME      YWC822 (CDCl3)
EXPNO    1
PROCNO   1

F2 - Acquisition Parameters
Date_    20011124
Time     16.44
INSTRUM  spect
PROBHD   5 mm BBO BB-1H
PULPROG  zgpg30
SOLVENT  CDCl3
NS       32
DS       4
SWH      12812.293 Hz
FIDRES   0.207340 Hz
AQ       2.7500308 sec
RG       2894.3
RW       24.887 usec
DE       6.00 usec
TE       300.2 K
D1       1.00000000 sec
DELTA    0 sec
NUC1      1H
NUC2      13C
MAGNET   10.13500000 sec

----- CHANNEL f1 -----
NUC1      1H
P1       12.00 usec
PL1      0.00 dB
SFO1     400.146000 MHz

----- CHANNEL f2 -----
CPDPRG2  zgpg30
NUC2      13C
PCPD2    100.00 usec
PL2      19.00 dB
PL12     19.00 dB
SFO2     101.625000 MHz

F2 - Processing parameters
SI       65534
SF       400.146000 MHz
WDW      EM
SSB      0
LB       3.00 Hz
GB       0
PC       1.40
    
```

